

THESES
3
9004
57078074

This is to certify that the
dissertation entitled

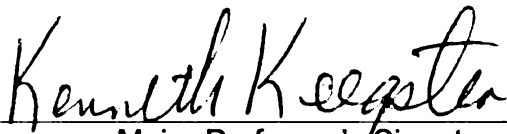
XYLOGLUCAN BIOSYNTHESIS: IDENTIFICATION AND
CHARACTERIZATION OF FUCOSYLTRANSFERASE AND
CELLULOSE SYNTHASE-LIKE GENES

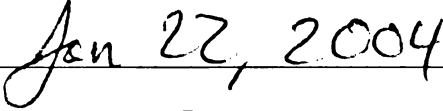
presented by

WEIQING ZENG

has been accepted towards fulfillment
of the requirements for the

Ph.D. degree in Cell and Molecular Biology


Major Professor's Signature


Date



PLACE IN RETURN BOX to remove this checkout from your record.
TO AVOID FINES return on or before date due.
MAY BE RECALLED with earlier due date if requested.

DATE DUE	DATE DUE	DATE DUE

**XYLOGLUCAN BIOSYNTHESIS: IDENTIFICATION AND CHARACTERIZATION
OF FUCOSYLTRANSFERASE AND CELLULOSE SYNTHASE-LIKE GENES**

By

Weiqing Zeng

A DISSERTATION

**Submitted to
Michigan State University
In partial fulfillment of the requirements
for the degree of**

DOCTOR OF PHILOSOPHY

Cell and Molecular Biology Program

2004

ABSTRACT

XYLOGLUCAN BIOSYNTHESIS: IDENTIFICATION AND CHARACTERIZATION OF FUCOSYLTRANSFERASE AND CELLULOSE SYNTHASE-LIKE GENES

By

Weiqing Zeng

Plant cell walls provide strength and shape to plant cells, and play a critical role in intra- and intercellular communications during plant growth and development.

Xyloglucan is the major hemicellulose in the primary wall of dicots and non-graminaceous monocots. XyG is composed of a β -(1,4)-glucan backbone that is usually decorated with α -(1,6)-xylose, β -(1,2)-galactose and α -(1,2)-fucose residues. Until very recently, none of the genes encoding xyloglucan synthetic enzymes had been identified. I am therefore interested in identification of these genes and in exploration of their expression patterns during plant growth and development.

Utilizing sequence information obtained from a partially purified xyloglucan fucosyltransferase enzyme from pea epicotyls, the full-length cDNAs encoding Arabidopsis and pea XyG fucosyltransferase, AtFut1 and PsFut1, were identified. The biochemical function of AtFUT1 was confirmed by the immunoprecipitation of XyG fucosyltransferase activities from Arabidopsis microsomes using antibodies against *E. coli*-expressed AtFUT1 proteins and, by the presence of XyG-specific fucosyltransferase activity in COS7 cells expressing the AtFut1 gene. The identity of the PsFUT1 was confirmed through sequence comparisons with the purified enzyme, its sequence similarity with AtFUT1, and its expression in COS7 cells. In young pea plants, the

expression level of PsFut1 was found to be highly correlated with the internode elongation rate of etiolated pea seedlings.

Cellulose synthase-like proteins of Arabidopsis show 7% to 46% identity with cellulose synthases and, therefore, have been hypothesized to be involved in the biosynthesis of wall matrix polysaccharides such as XyG. Expression profiling of AtCsl genes was performed by examining EST libraries, MPSS libraries and microarray databases, but did not reveal any strong candidate genes for encoding the xyloglucan backbone glucan synthase.

Among all AtCsl genes, those of the D subfamily have the highest level of identity to AtCesA genes. To distinguish whether AtCslD proteins might be isoforms of AtCesA proteins or enzymes involved in the biosynthesis of matrix polysaccharides, a polyclonal antibody against an AtCslD2 peptide was generated and utilized to locate the proteins at Golgi membranes using cellular membrane fractionation techniques such as sucrose density gradient and two-phase partitioning. Therefore AtCslD genes are likely to encode enzymes involved in the matrix polysaccharide biosynthesis instead of CesA proteins.

In another attempt to identify functions for AtCslD genes, transgenic plants containing RNAi constructs targeting AtCslD transcripts were generated. These plants showed deformed cotyledons, were dwarfed as adult plants, and had shortened roots with more branches. However, the transcript suppression of AtCslD genes was only clearly seen in cotyledons, and no clear alteration in cell wall sugar composition was detected. Therefore, the exact biochemical functions of AtCslD proteins still could not be determined.

ACKNOWLEDGMENTS

First and the most important, I would like to thank my thesis supervisor and mentor Dr. Ken Keegstra, for I have learned so much from his broad scientific knowledge, his logical scientific thinking and his personality. Ken has always been supportive and willing to help on trivial questions coming from everyday's bench work, on the design of experiments and projects, as well as on career development. I have therefore gained valuable experiences on how to develop and tackle scientific questions, how to think and communicate in a more scientific and more efficient way. Ken has been a role model for me not only as a successful and outstanding scientist, but also yet as a parent, a grand parent tending family matters.

I would also like to thank other members of my graduate committee, Dr. Christoph Benning, Dr. Hans Kende, Dr. Natasha Raikhel, Dr. Melvin Schindler, and Dr. Jonathan Walton. Their continuous support and supervision have helped tremendously to keep my thesis career alive and to reach this final stage. I also have learned a great deal from them about how to survive in a scientific career.

Members of the Keegstra lab have made my life in the last five years the most precious experience for me. Almost all of my techniques learned here were from these friendly people. They have been very supportive in both scientific matters and in daily life. Specially, Dr. Sigrun Reumann has showed me how to be organized and manage multiple gigantic experiments at the same time. Dr. Mitsuru Akita, Dr. Kentaro Inoue, and Dr. Teruko Konishi have been very generous sharing their expertise on protein and enzyme biochemistry. Dr. Lynda Fitzpatrick has always been a fun and caring colleague

and has made my lab life so delightful. Other current and past members including Dr. Aaron Liepman, Dr. John Frohlich, Dr. Ahmed Faik, Dr. Robyn Perrin, Dr. Dianne Jackson Constan, Dr. Curtis Wilkerson, Dr. Tanya Wagner, Sybil Myers, Linda Denhorf all have made my life in the lab much easier and full of fun with their assistance on my work and their companionship in the lab.

I would also have to thank the entire Plant Research Laboratory at Michigan State University. The people here have made PRL a scientifically challenging place, and as yet, have been constantly supportive and encouraging. Tremendous amount of help have come from the supporting staffs that have made my life so much easier over the years. Especially I want to thank Dr. Tony Sanderfoot and Dr. Jianping Yu for their constant help on my daily bench work as well as experiment designs. I am also grateful for my home department, the Cell and Molecular Biology Program, and its director Dr. Susan Conrad, its secretary Angie Zell, for taking care of many of trivial and important matters critical to a Ph.D student's maturation.

Finally I would like to thank my family for their understanding and support, especially my wife Qiong Wang for her patience, encouragement and her emotional support. Qiong's taking over of the entire house work has made the accomplishment of this thesis feasible.

TABLE OF CONTENTS

LIST OF TABLES.....	ix
LIST OF FIGURES.....	x
ABBREVIATIONS.....	xiii
CHAPTER1: The Plant Cell Wall, its Structure, Function, and Biosynthesis.....	1
Plant cell wall structure and function.....	2
Plant cell wall functions.....	2
Plant cell wall structures.....	3
Xyloglucan structure and function.....	10
Xyloglucan structures.....	10
Structural roles of xyloglucan.....	12
Xyloglucan's role during cell expansion.....	13
Functions of xyloglucan fragments.....	14
Xyloglucan as a reserve carbohydrate.....	15
Identification of genes involved in wall biosynthesis.....	17
Genes involved in xyloglucan biosynthesis.....	17
Genes involved in the biosynthesis of other wall polysaccharides.....	20
Functional studies of AtCsl genes.....	24
Regulation of cell wall metabolism.....	26
References.....	28
CHAPTER 2: Cloning and Expression Studies of Xyloglucan Fucosyltransferase.....	42
Abstract.....	43
Introduction.....	44
Materials and methods.....	48
Results.....	58
Isolation of full length cDNA clone encoding AtFUT1.....	58
Expression of AtFUT1 partial polypeptide in E. coli cells and the generation of antibodies against it.....	61
Cloning of full length coding region, intron and 5', 3' UTRs of PsFut1...67	
Sequence analysis of PsFut1.....	77
Specificity analysis of clone Ps5UTR as probe for Northern blotting.....79	
Internode elongation curve of etiolated seedlings.....	79
Expression of PsFut1 in three internodes of etiolated pea seedlings at 7 days old.....	82
Expression of PsFut1 in the third internode at different growth stages....84	
Discussion.....	88
References.....	93

CHAPTER 3: Sequence and Expression Pattern Analysis of Arabidopsis Cellulose Synthase-Like Genes.....	97
Preface.....	98
Abstract.....	99
Introduction.....	100
Materials and methods.....	105
Results.....	108
Sequence extraction, annotation and comparison analysis.....	108
Expression patterns of AtCsl genes revealed by EST abundance.....	124
Expression patterns of AtCsl genes revealed by MPSS database.....	127
Expression patterns of AtCsl genes revealed by tissue panel microarrays from Stanford Microarray Database.....	133
Regulated expressions of AtCsl genes revealed by microarray experiments.....	134
Discussion.....	138
References.....	141
CHAPTER 4: Localization Studies of AtCslD2 Proteins.....	144
Abstract.....	145
Introduction.....	146
Materials and methods.....	152
Results.....	160
Generation, purification and characterization of antibodies against AtCslD2.....	160
AtCslD2 is an integral membrane protein.....	166
AtCslD2 migrates differently from a plasma membrane marker PMA2 during linear sucrose gradient centrifugation.....	170
AtCslD2 is not a plasma membrane protein as revealed by two phase partition.....	173
AtCslD2 protein is localized at Golgi rich vesicles during floatation sucrose gradient centrifugation.....	173
Discussion.....	180
References.....	184
CHAPTER 5: Generation and Characterization of RNAi Transgenic Plants for AtCslD Genes.....	189
Abstract.....	190
Introduction.....	191
Materials and methods.....	197
Results.....	202
Generation of RNAi constructs.....	202
Generation of transgenic plants containing AtCsl RNAi constructs.....	210
RNAi transgenic plants containing construct D1235f3 or D23f2 showed deformed cotyledons and reduced adhesion of cotyledon cells...212	
D1235f3 transgenic plants showing deformed cotyledons have corresponding suppression of AtCslD gene transcripts218	

D1235f3 transgenic plants showing deformed cotyledons also showed dwarfed adult plants and shortened roots with more branching..	222
Cotyledon deformation is inheritable for D1235f3 transgenic plants but weakens when passed to the next generation.....	227
D1235f3 RNAi transgenic plants showed decreased glucose.....	236
Discussion.....	241
References.....	248

LIST OF TABLES

Table 2.1. Sequence alignment among the PsFut1-5UTR and its equivalents from all AtFut genes.....	80
Table 2.2. PsFUT1 activity during the elongation of third internode between day 7, 9 and 11.....	86
Table 3.1. Summary of reannotated AtCsl genes.....	112
Table 3.2. Characteristics of AtCsl proteins.....	120
Table 3.3. Summary of sequence identities among all AtCsl proteins.....	123
Table 3.4. Summary of ESTs identified in the dbEST for AtCsl genes.....	125
Table 3.5. EST abundance for AtCsl gene families.....	126
Table 3.6. Numbers of MPSS tags that found from five different Arabidopsis cDNA libraries for all AtCsl genes and AtFut1, AtGalT and AtXT1.....	128
Table 3.7. Tissue expression profile of AtCsl genes revealed by Stanford Microarray Database.....	135
Table 4.1. Specific activity of XyG fucosyltransferase and GSII for membrane vesicles present in each fraction from the sucrose step gradient (Figure 5.7).....	178
Table 5.1. Design of RNAi constructs targeting different AtCsl genes and primers used to create them.....	204
Table 5.2. Primers used for PCR reactions to confirm the existence of constructs in transgenic plants.....	205
Table 5.3. Primers used for RT-PCR reactions to confirm the suppression of transcripts.....	206
Table 5.4. Summary of the inheritance of cotyledon deformation phenotype from T1 to T2 generation for D1234f3 RNAi lines.....	232
Table 5.5. Inheritance and segregation of cotyledon deformation phenotype and Basta resistance marker for D1235f3 RNAi plants.....	233

LIST OF FIGURES

Figure 1.1. Structure of a typical xyloglucan building block.....	6
Figure 2.1. Cloning of full-length coding region of AtFut1	59
Figure 2.2. Expression of peptides AtFUT1-1.2 and AtFUT1-2.3 in BL21 (DE3)-pLysS cells.....	62
Figure 2.3. Anti-AtFUT1 polyclonal antibodies recognize an approximately 63-kDa polypeptide in solubilized membrane proteins of Arabidopsis.....	66
Figure 2.4. Isolation of PsFut1 fragment PsFut1-a.....	68
Figure 2.5. Second round of PCR reactions amplifying cDNA fragments toward the 5' and 3' of PsFut1-a.....	71
Figure 2.6. RACE reactions amplifying the 5' and 3' ends of PsFut1.....	73
Figure 2.7. DNA and protein sequences related to PsFut1 and PsFUT1, and the sequence and position of primers used for DNA fragment amplifications.....	74
Figure 2.8. PsFut1 specific DNA probe Ps5UTR.....	81
Figure 2.9. Growth curve of etiolated pea internodes.....	83
Figure 2.10. Expression of PsFut1 in etiolated pea internodes at day 7.....	85
Figure 2.11. Expression of PsFUT1 in the third internode of the etiolated pea at 7, 9 and 11 days old.....	87
Figure 3.1. Alignment of AtCslA proteins using sequences before (A) and after (B) manual re-annotation.....	109
Figure 3.2. Chromosomal locations of AtCsl genes.....	115
Figure 3.3. Predicted intron-exon structure of AtCsl genes according to the re-annotated sequences.....	116
Figure 3.4. A rooted phylogenetic tree of all AtCsl proteins.....	121
Figure 3.5. MPSS expression profile of all AtCsl genes and AtFut1, AtGalT, AtXT1.....	131
Figure 4.1. Expression and detection of peptides P2 and P3 in BL21 (DE3) cells.....	161

Figure 4.2. Specificity of AtCslD2 antibodies against Arabidopsis total protein extracts.....	164
Figure 4.3. Immunoblotting using purified AtCslD2 antibodies against Arabidopsis crude membranes (A) and purified Golgi complexes (B).....	167
Figure 4.4. Solubilization of AtCslD2 from Arabidopsis microsomal membranes using various reagents.....	168
Figure 4.5. Migration of AtCslD2 and selected marker proteins on a linear sucrose density gradient.....	171
Figure 4.6. Two phase partitioning of Arabidopsis microsomal membranes.....	174
Figure 4.7. Fractionation of microsomal vesicles by floatation centrifugation on a sucrose step gradient.....	177
Figure 5.1. Design of RNAi constructs for AtCsl genes.....	207
Figure 5.2. Sequence similarities between RNAi construct D1235f3, D23f2 and AtCslD genes.....	209
Figure 5.3. Transformation and screening of RNAi plants.....	211
Figure 5.4. Determination of the presence of RNAi constructs in transgenic plants....	213
Figure 5.5. Cotyledon deformation phenotype of transgenic plants carrying construct D1235f3 or D23f2.....	215
Figure 5.6. Abaxial side of cotyledons from T2 plant of control lines (Control) and D1235f3 lines (Normal, Inter I, Inter II and Strong).....	217
Figure 5.7. Cells within deformed cotyledons of D1235f3 plants showed less adherence.....	219
Figure 5.8. Transcript abundance of AtCslD genes in D1235f3 RNAi plants examined by two step RT-PCR reactions.....	220
Figure 5.9. Root length of T1 transgenic plants containing RNAi constructs.....	223
Figure 5.10. Root length of T1 plants containing construct D1235f3.....	224
Figure 5.11. T1 plants containing construct D1235f3 showing deformed cotyledons also showed more branched roots.....	225

Page 1
Page 2
Page 3
Page 4
Page 5

Figure 5.12. D1235f3 T1 plants had deformed cotyledons also yielded dwarfed adult plants.....	228
Figure 5.13. Adult T2 plants containing RNAi construct D1235f3 at 6 weeks old.....	230
Figure 5.14. Cell wall sugar composition of rosette leaves from T1 D1235f3 plants showing different cotyledon deformation.....	237
Figure 5.15. Sugar composition analysis of T2 plants of D1235f3 RNAi lines.....	238

2-D
AGP
Ara
asFut1
asGalT
asNT1
BSA
CIP
Cgl
DTT
EM
ER
Fac
GA
Gal
GAX
Gk
GRP
HGA
HRGP
Man
MPSS
NASC
NASC
PMSF
PRP
P-Fut.
RG I
RG II
Rha
SDS
SMD
TCA
TGN
UTR
VTH
VIG
VJ

ABBREVIATIONS

2,4-D	2,4-Dichlorophenoxyacetic acid
AGP	Arabinogalactan protein
Ara	Arabinose
AtFut1	Arabidopsis xyloglucan fucosyltransferase
AtGalT	Arabidopsis xyloglucan galactosyltransferase
AtXT1	Arabidopsis xyloglucan xylosyltransferase 1
BSA	Bovine serum albumin
CIP	Calf intestinal alkaline phosphatase
Csl	Cellulose synthase-like
DTT	Dithiothreitol
EM	Electron microscopy
ER	Endoplasmic reticulum
Fuc	Fucose
GA	Gibberellic acid
Gal	Galactose
GAX	Glucuronoarabinoxylan
Glc	Glucose
GRP	Glycine-rich protein
HGA	Homogalacturonic acid
HRGP	Hydroxyproline-rich glycoproteins
Man	Mannose
MPSS	Massively Parallel Signature Sequencing
NASCArrays	Nottingham Arabidopsis Stock Center's microarray database
PMSF	Phenylmethanesulfonyl fluoride
PRP	Proline-rich protein
PsFut1	Pea xyloglucan fucosyltransferase
RG I	Rhamnogalacturonan I
RG II	Rhamnogalacturonan II
Rha	Rhamnose
SDS	Sodium dodecyl sulfate
SMD	Stanford Microarray Database
TCA	Trichloroacetic acid
TGN	Trans-Golgi network
UTR	Untranslated region
XTH	Xyloglucan endotransglucosylase/hydrolase
XyG	Xyloglucan
Xyl	Xylose

* Images in this thesis are presented in color

CHAPTER 1

The Plant Cell Wall, its Structure, Function, and Biosynthesis

PLANT CELL WALL STRUCTURE AND FUNCTION

Plant cell wall functions

The presence of a cell wall is one of the unique features that distinguish plant cells from animal cells. The walls, on one hand, provide strength, shape and rigidity to plant cells and contribute to the structural integrity of plants. On the other hand, the walls also allow controlled flexibility to plant cells via a controlled weakening and loosening, thereby allowing cell expansion (Brett, 1983).

Plant cell walls limit the ability of macromolecules, such as large proteins or nucleic acids, to enter or leave cells. Walls are also involved in the apoplastic transport of small molecules and ions, including some small proteins and polysaccharides (Carpita et al., 1979). The movement through plant cell walls is also charge-dependent because the walls bear a net negative charge (Carpita et al., 1979).

Plants are constantly exposed to attacks from many microorganisms that are potentially pathogenic. Many plant defense mechanisms involve the cell wall. An intact cell wall is an effective physical barrier, protecting against pathogen penetration and spread (Stacey et al., 1992). In addition, the cross-linking of cell wall structural proteins strengthens the cell walls as a rapid response in the initial stages of the hypersensitive response before transcription-dependent defense mechanisms occur (Brisson et al., 1994). The formation of effective papillae at the site of infection provides further mechanical barriers to penetration (Israel et al., 1980). Another role for cell walls is the elicitation of phytoalexin production in response to pathogen attacks. Many endogenous elicitors of phytoalexin production are derivatives of degraded wall polysaccharides created by pathogen attack or abiotic stresses (Stacey et al., 1992). Oligosaccharide products derived

by degradation of wall polysaccharides may even diffuse to neighboring cells to trigger defense responses, or sometimes act as signal molecules regulating cell expansion and plant development (Aldington et al., 1991).

Plant cell wall structures

Electron microscopic examination showed that many plant cell walls consist of three layers, a middle lamella, a primary wall and sometimes a secondary wall (Brett and Waldron, 1996). The middle lamella is the first layer formed immediately after cell division and is derived from the cell plate. The primary wall is the next major layer deposited from daughter cells onto the middle lamella after cell division is completed (Brett and Waldron, 1996). The plant cells continue to deposit primary wall as long as the cell enlarges and its surface area grows (Brett and Waldron, 1996). The primary wall usually reaches a thickness of 50-100 nm and remains extensible for possible further growth (Kaczkowski, 2003). Many cells only have two layers of walls. For other cell types, a third layer of wall, the secondary wall, is deposited after cell expansion stops and differentiation begins. The thickness of the secondary wall is not as homogeneous as the primary wall and varies significantly even for different parts of a cell. This secondary cell wall contributes to many structurally and morphologically different cell types with unique functions (Preston, 1974; Bacic et al., 1988). For example, cells building up xylem elements or sclerenchyma have thick secondary walls and are mechanically more resistant (Kaczkowski, 2003). The deposition of secondary wall is usually accompanied by lignification to make the walls even stronger (Kaczkowski, 2003). Although a secondary wall is composed mostly of cellulose and lignin, other polysaccharides such as

xylans and glucomannans are also found in many cases to be deposited along with the cellulose (Fincher and Stone, 1982; Northcote, 1985; Gibeaut and Carpita, 1994).

Biochemically, the primary cell wall consists of two phases, a microfibrillar skeleton and a matrix (Carpita and Gibeaut, 1993). The microfibrillar phase has a high degree of crystallinity and is formed by microfibril structures that are composed solely of cellulose, a highly structured collection of β -1,4 glucan chains (Carpita and Gibeaut, 1993). The glucan chains are arranged in a crystalline lattice within each microfibril through intramolecular or intermolecular hydrogen bonding, thereby giving rise to the high tensile strength of the microfibrils (Carpita and Gibeaut, 1993).

The wall matrix phase is chemically complex and consists of many different polysaccharides, proteins and phenolic compounds (Brett and Waldron, 1996). There are two major categories of wall matrix polysaccharides, hemicellulose and pectin, characterized by their extractabilities by different reagents (Selvendran, 1985). Pectins are readily extracted by hot water with a chelating agent such as ammonium oxalate, EDTA, or dilute acid solution, whereas hemicelluloses are extracted only with alkaline solution (Selvendran, 1985).

Pectins are a mixture of variably branched and strongly hydrated polysaccharides that are rich in galacturonic acid, rhamnose, arabinose and galactose (Selvendran, 1985). The presence of pectins controls the wall porosity and charge. Pectic polysaccharides help cells adhere to form tissues, keep wall enzymes in position, and also keep tissues at proper hydration level (Kaczowski, 2003). Pectin polysaccharides also act as signal molecules in response of symbiotic organisms, pathogens, and insects (McNeil et al., 1984). The pectic polysaccharides comprise a group of acidic polysaccharides, including

homogalacturonan (HG), rhamnogalacturonan I (RG I), and rhamnogalacturonan II (RG II), as well as several neutral oligosaccharides and polysaccharides, including arabinan, galactan, and arabinogalactan that usually appear as side chains of the former three types (Bacic et al., 1988; Gibeaut and Carpita, 1994). RG I and RG II are extremely complex polysaccharides with numerous side-chain modifications of arabinans or galactans (Mohnen, 1999).

Overall, hemicelluloses generally have simpler side chains compared to pectic polysaccharides. Their backbones, on the other hand, are similar to β -glucan chains of cellulose so that hemicelluloses can form numerous hydrogen bonds with the cellulose molecules (Gibeaut and Carpita, 1994). This cross-linking ability of hemicelluloses is their main function and helps provide wall structural integrity. Major hemicelluloses include xyloglucan (XyG), β -(1,3)-(1,4) mixed-linkage glucan, glucuronoarabinoxylan (GAX), arabinoxylan, xylan, glucomannan, galactomannan, glucuronomannan, and mannan (Carpita and Gibeaut, 1993). The types of hemicellulose vary greatly in different plant species, as does the structure or amount of a particular hemicellulose (Carpita and Gibeaut, 1993).

XyG is the major hemicellulose in the primary cell wall of most dicot plants and consists of a backbone of a β -(1,4)-linked glucan chain that is modified with α -(1,6)-xylose, β -(1,2)-galactose, and sometimes α -(1,2)-fucose (Figure 1.1) (Hayashi, 1989). The mixed-linkage glucans are glucose chains with β -(1,3) and β -(1,4) linkages. Xylans and mannans are polymers of single sugar residues of β -(1,4)-xylose or β -(1,4)-mannose, respectively (Brett and Waldron, 1996). Other xylan- and mannan- derived hemicelluloses either have more than one sugar residue in their backbones

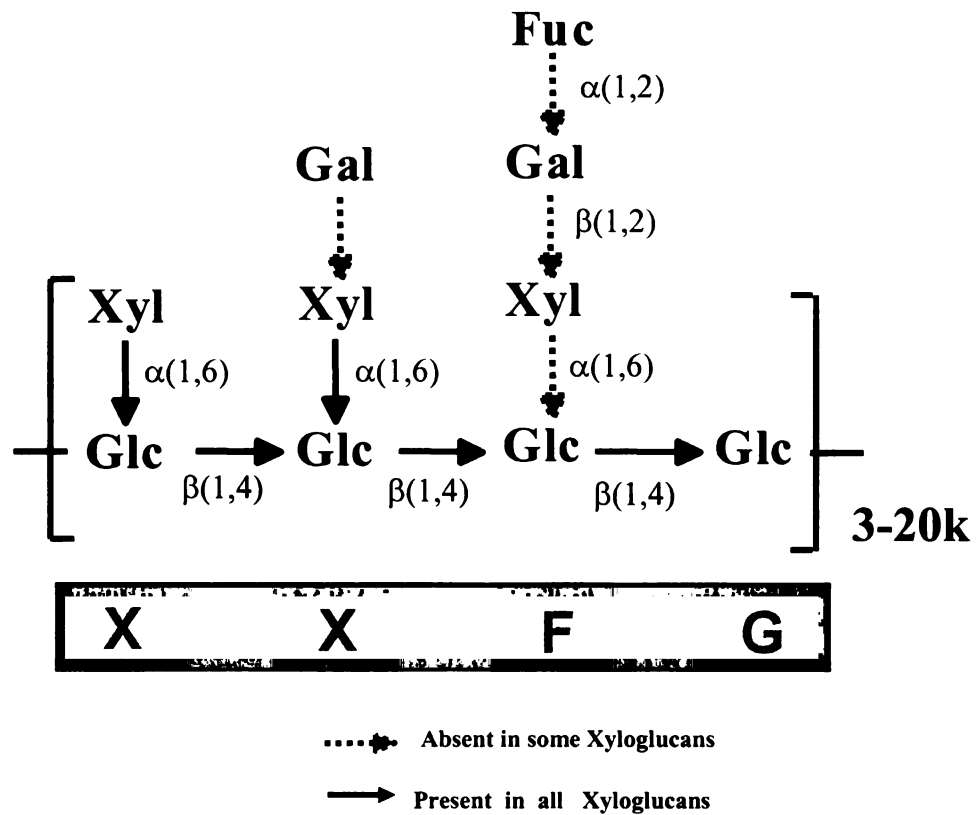


Figure 1.1: Structure of a typical xyloglucan building block. Adapted and modified from Hayashi, 1989 and Fry, 1989.

(glucomannan,), or have side chain modifications (galactomannan, arabinoxylan, GAX), or both (glucuronomannan) (Brett and Waldron, 1996).

Cell walls contain five major classes of structural proteins, hydroxyproline-rich glycoproteins (HRGPs) such as extensins, glycine-rich proteins (GRPs), proline-rich proteins (PRPs), solanaceous lectins, and arabinogalactan proteins (AGPs) (Showalter, 1993). There are also many enzymes associated with the walls such as peroxidases, phosphatases, invertases, proteases and many polysaccharide-degrading enzymes (Showalter, 1993).

The composition of the wall matrix varies significantly from plant to plant, cell to cell, and even at different developmental stages of the same cell type. Most of the compositional variation comes from differences in the categories, proportions, and structural modifications of the polysaccharides present in the wall matrix (McNeil et al., 1984). The primary walls of dicot plants all contain a high proportion of pectic polysaccharides and a smaller amount of XyGs (Bacic et al., 1988). Gymnosperms have a similar primary wall matrix with the presence of pectins and XyGs (Burke et al., 1974; Thomas et al., 1987). In the Poaceae plants, the primary walls usually contain highly substituted GAX as the major matrix polysaccharide as well as variable amounts of β -(1,3)-(1,4) mixed-linkage glucans. The pectic polysaccharides and XyGs are usually minor components (Bacic et al., 1988). Most non-graminaceous monocot plants have a cell wall matrix composition similar to that of dicot plants, while some of them showed similarity with graminaceous plants (Bacic et al., 1988).

Therefore, according to the different compositions, the primary walls in higher plants were classified into two distinct types (Carpita and Gibeaut, 1993). The type I wall

is representative of all Dicotyledonae and some Monocotyledonae. This type of wall has a wall skeleton structure of cellulose microfibrils cross-linked by the hemicellulose XyGs (Carpita and Gibeaut, 1993). Other non-cellulosic polysaccharides having similar inter-linking functions, such as glucomannan, galactomannan, glucuronomannan, β -(1,3)-glucans, and GAXs are also found in some type I walls but in very low amounts (Maltby et al., 1979; Darvill et al., 1980; Meier and Reid, 1982; Bacic et al., 1988). XyGs bind tightly to the surface of cellulose microfibrils through hydrogen bonds and connect different microfibrils (McCann and Roberts, 1992; Carpita and Gibeaut, 1993). Type I primary walls comprise three domains that are structurally different but interacting with each other (Carpita and Gibeaut, 1993). The first domain, cellulose-XyG network, is the basic wall structure framework that is embedded in a second domain of matrix pectin polysaccharides including mainly polygalacturonic acids (PGA) and RGs (Carpita and Gibeaut, 1993; Gibeaut and Carpita, 1994). Chains of PGA are cross-linked with Ca^{2+} to form junction zones for chain linkings. The size of junction zones and the size and frequency of side chains on RGs control the wall porosity (Brett and Waldron, 1996). The third wall structural domain consists of the structural proteins (Carpita and Gibeaut, 1993).

The type II wall is found only in Poaceae and closely related monocot families (Carpita and Gibeaut, 1993). Structurally the type II primary wall is based on the same cellulose microfibrils that are cross linked by GAXs instead of XyGs. The GAXs have a backbone of β -(1,4)-D-xylose residues that are modified with single arabinose residues at O-3 positions or glucuronosyl acid (GlcA) residues at the O-2 positions of the backbone xyloses (Gibeaut and Carpita, 1994). The degree of side chain modification varies greatly

among different plants. The variation determines the abilities of GAXs to bind with each other. The presence of high amount of side chains prevents the hydrogen bonding among themselves or with cellulose microfibrils (Carpita and Gibeaut, 1993). The type II walls not only have very little amount of pectins but also display a developmental preference for methyl esterified or unesterified pectins in specific cell types (Knox et al., 1990). The esterified PGAs are usually found in vascular tissues while the unesterified PGAs are usually found in the cortical cells of root tips and parenchyma cells of seedlings and coleoptiles (Knox et al., 1990).

XYLOGLUCAN STRUCTURE AND FUNCTION

Xyloglucan structures

XyGs have a cellulose-like backbone composed of β -(1,4) linked D-glucosyl residues (Figure 1.1). Some of the backbone glucosyl residues are decorated with α -D-xylosyl residues in 1,6 linkages in a regular pattern that varies depending upon the plant species. The combination of backbone glucosyl residues and their immediate xylose side chains constitute the core building blocks for each XyG molecule. Some of the xylose residues of XyGs are further substituted at the C-2 positions with mono-, or disaccharides containing β -D-galactose, α -L-arabinose, and α -L-fucose residues (Vierhuis et al., 2001). The constitution and distribution of side chains again is plant-species and tissue-type specific (Fry, 1989; York et al., 1996; Vincken et al., 1997; Pauly et al., 2001).

A concise nomenclature was developed to unambiguously designate XyG structures (Fry et al., 1993). XyG molecules are divided into segments consisting of only a single backbone glucosyl residue and its side chain residues attached. Each segment with a different overall structure is designated with a different code letter. The letter “G” refers to the unbranched backbone β -D-Glc, “X” refers to an α -D-Xyl-(1,6)- β -D-Glc disaccharide segment, “L” refers to the trisaccharide β -D-Gal-(1,2)- α -D-Xyl-(1,6)- β -D-Glc, and “F” refers to the tetrasaccharide α -L-Fuc-(1,2)- β -D-Gal-(1,2)- α -D-Xyl-(1,6)- β -D-Glc (Fry et al., 1993) (Figure 1.1). XyG from solanaceous plants usually contains terminal L-arabinose instead of fucose and is therefore designated as arabinoxyloglucan (Vincken et al., 1997; Vierhuis et al., 2001). The trisaccharide α -L-Ara-(1,2)- α -D-Xyl-(1,6)- β -D-Glc then is referred as “S”, and the tetrasaccharide β -L-Ara-(1,3)- α -L-Ara-(1,2)- α -D-Xyl-(1,6)- β -D-Glc is referred as “T” (Fry et al., 1993; Vincken et al., 1997).

Using this convenient nomenclature system, the two major core building blocks of XyG are named as XXXG and XXGG (Vincken et al., 1997). XXXG type of XyGs usually have 75% of the backbone glucoses substituted at their 6 positions with α -D-xylose at a regular pattern of three substituted residues followed by one unsubstituted residue (Figure 1.1). XXGG type of XyGs usually have clusters of two instead of three branched glucose residues alternating with a two glucose residues without any substituents (Vincken et al., 1996; York et al., 1996).

XXXG type of XyG is the major hemicellulose in the primary wall of dicotyledonous and non-graminaceous monocotyledonous plants (Pauly et al., 2001). They usually contain modifications of β -D-Gal or disaccharide α -L-Fuc-(1,2)- β -D-Gal on the xylose residues and yield structures of XXLG, XLLG, XXFG and XLFG (York et al., 1990; Hisamatsu et al., 1991). Furthermore the presence of fucose residues is regarded as a specific feature of dicotyledonous XyGs, as XyGs from graminaceous monocotyledonous plants generally lack the fucose residues. However some exceptions have been reported (Hayashi, 1989; McDougall and Fry, 1994).

The XXXG type of XyG is also found in seeds as storage polysaccharide, including seeds from *Tamarindus indica* (York et al., 1990), cyclamen (Braccini et al., 1995), *Tropaeolum majus* (McDougall and Fry, 1990), and *Detarium senegalense* (Wang et al., 1996). These XyGs rarely bear any other substituents except some β -D-galactose on some of the xylose residues, to give structures XXLG and XLLG.

The XXGG type of XyGs are usually found in solanaceous plants as well as Poaceae plants. One of the unique feature of this type of XyGs is the presence of terminal α -L-arabinose to form core structures XSOG (Hayashi, 1989; Vincken et al., 1996; York

et al., 1996). The presence of fucose has not yet been found in this type of XyGs (Vincken et al., 1997).

Structural roles of xyloglucan

XyG forms a load-bearing network with cellulose. It not only adheres to the surface of cellulose microfibrils, but also can connect different cellulose microfibrils at its two ends to contribute to wall plasticity and elasticity (Fry, 1989). The linkages between XyG and cellulose microfibrils are non-covalent hydrogen bonds (Thompson and Fry, 2000).

It was proposed many years ago that in dicot plants, XyGs and pectic polysaccharides, as well as the structural glycoproteins, are covalently joined together to form the wall matrix phase (Keegstra et al., 1973). Evidence obtained more recently further supports this hypothesis. XyG and pectic polysaccharides were repeatedly co-extracted from the wall and found to be inseparable from each other by ethanol precipitation, gel permeation chromatography, and ion exchange chromatography. (Chambat et al., 1984; Joseleau and Chambat, 1984; Selvendran, 1985; Selvendran et al., 1985; Femenia et al., 1999). Treatment of those XyG-pectin complexes with endo-glycosidases specific for a glycosyl linkage in one polymer would always cause molecular weight decrease of both XyG and pectic components, strongly indicating an association of XyG and pectic polysaccharides (Femenia et al., 1999; Watt et al., 1999; Thompson and Fry, 2000). It has been suggested that the covalent linkage between XyGs and pectic polysaccharides could be alkali-stable bonds of glycosidic or other forms (Keegstra et al., 1973; Thompson and Fry, 2000), alkali-labile ester bonds (Mueller et al.,

1976; Kim and Carpita, 1992; Brown and Fry, 1993; Brown and Fry, 1993), or through oxidatively coupled phenolics such as diferuloyl esters (Grabber et al., 1995; Parr et al., 1996).

Xyloglucan's role during cell expansion

The growing plant cell wall is a dynamic structure with constant metabolism of its constituent polysaccharides during cell growth and expansion. Apart from the usual degradation of existing molecules and the synthesis of new molecules, there is an additional key aspect of XyG metabolism. As one of the major components of the wall network connecting cellulose microfibrils and pectic polysaccharides, XyG constitutes 20-25% of the dry weight of the primary cell wall in dicot plants and contributes substantially to the mechanical strength of the cell wall fabric (Fry, 1989). Therefore XyG has to be disconnected from other polysaccharides in the wall or degraded to allow the loosening of the existing wall so that more newly synthesized wall materials can be incorporated during expansion. Two key enzymes, expansins and XyG endotransglucosylases/hydrolases (XTHs), are thought to be involved in these processes.

Expansins are cell wall-associated proteins that weaken the non-covalent binding, namely hydrogen bonds, between XyG and cellulose microfibrils, to allow turgor-driven polymer creep (Rayle and Cleland, 1992; Cosgrove, 2000). This reaction would then separate existing wall polysaccharides and allow new wall materials to be deposited and inserted among the previously existing ones.

XTH was first identified as an enzyme catalyzing the transglycosylation of XyGs (Fry et al., 1992; Nishitani and Tominaga, 1992). In contrast to expansins, which do not

possess hydrolytic activities, the XTHs cleave the glycosidic linkages in the backbone of XyG molecules. Instead of transferring the sugar to water, yielding hydrolysis of the glycosidic bond, XTHs transfer the cleavage product to another XyG molecule to form a new glycosidic linkage (McQueen-Mason, 1997). It is proposed that, by doing so, XTHs loosen the connections mediated by XyG molecules and allow temporary wall weakening. The rejoining between different existing XyG molecules or between newly deposited XyG molecules and old ones accomplish the expansion of walls as well as the incorporation of new wall materials, yet reconstitutes the wall network structure (Rose et al., 2002).

Functions of xyloglucan fragments

Oligosaccharin is a name for oligosaccharides derived from the degradation of fungal and plant cell wall polysaccharides that have the ability to modify plant growth or defense responses (Ozeretskovskaya and Romenskaya, 1996). The XyG degradation product, XXFG, is one of the earliest identified oligosaccharins. It was shown to have an effect on plant growth and development (York et al., 1984; McDougall and Fry, 1991).

In excised pea stem segments or whole shoots, the nonasaccharide XXFG at a concentration of 10^{-11} to 10^{-8} M can inhibit 2,4-dichlorophenoxyacetic acid (2,4-D)-induced elongation (York et al., 1984; McDougall and Fry, 1988; Emmerling and Seitz, 1990; Augur et al., 1992). At this concentration, XXFG also inhibits H^+ -induced growth (Lorences et al., 1990), gibberellic acid (GA_3)-induced growth (Warneck and Seitz, 1993) and endogenous growth (Warneck and Seitz, 1993). The growth inhibition effect of XXFG is dependent on the terminal α -L-fucose or the disaccharide α -L-fucose-(1,2)- β -

D-galactose, since neither XXLG nor XXXG showed similar growth inhibition abilities (McDougall and Fry, 1989). On the other hand the non-reducing terminal α -D-xylose and the reducing terminal D-glucose are not essential for the inhibition activity because the oligosaccharides GXFG and XXFGol are active growth inhibitors (Augur et al., 1992).

Interestingly, XXFG also shows a growth-promoting effect in pea stem segments when applied at a higher concentration of about 10^{-6} M and in the absence of exogenous phytohormones (McDougall and Fry, 1990; Warneck and Seitz, 1993; Cutillas and Lorences, 1997). This growth promotion ability is not dependent on the fucose-galactose side chains but requires a Xyl/Glc-rich backbone (Warneck et al., 1998). The mechanism and signal transduction pathway of the XyG oligosaccharin controlling plant growth and development are still poorly characterized.

Xyloglucan as a reserve carbohydrate

The seeds of plants have nutrition stored in the form of carbohydrate, lipid or protein. Those substances are mobilized during seed germination before the seedlings become self-sufficient, to allow for energy generation and to produce raw materials for building cells and tissues in the germinating seedlings (Mayer and Poljakoff-Mayber, 1975). The most common carbohydrate stored in seeds is starch. Other storage carbohydrates include fructan and cell wall polysaccharides such as galactomannans, XyGs and galactans (Buckeridge et al., 2000). These storage polysaccharides are normal components of the cell walls of other tissues but in much lower quantities.

XyG is the storage polysaccharide accumulated in the cotyledonary tissues of several dicot plants including tamarind (*Tamarindus indica*) (Kooiman, 1961), nasturtium

(*Tropaeolum majus*) (Edwards et al., 1985), *Hymenaea courbaril* (Buckeridge and Dietrich, 1990) and *Copaifera langsdorffii* (Buckeridge et al., 1992). Comparative studies of XyGs from seeds of these plants showed the same basic structural units XXXG, XLXG, XXLXG and XLLG (Buckeridge et al., 1992). It was also found that the ratios between these units changes depending on the fine structures shown by different species and different populations of the same species growing under different environmental conditions (Buckeridge et al., 1992). However all seed XyGs showed similar monosaccharides proportions, indicating that a similar degree of branching is preserved, but the distribution of blocks with different degree of galactosylation determines the fine structure of XyGs from different sources (Buckeridge et al., 2000).

Studies in *T. majus* (Edwards et al., 1985), *T. indica* (Reis et al., 1987), *C. langsdorffii* (Buckeridge et al., 1992), and *H. courbaril* (Tine et al., 2000) have shown that four degradative enzyme activities are involved in the mobilization of storage XyG. All four types of enzymes have been isolated from *T. majus*. They are a XyG-specific endo β -(1,4)-D-glucanase or XTH (Edwards et al., 1986; Fanutti et al., 1993), a β -galactosidase with high specificity for XyG (Edwards et al., 1988), a XyG-oligosaccharide specific α -xylosidase or oligoxyloglucan exo-xylohydrolase (Fanutti et al., 1991), and a transglycosylating β -glucosidase (Crombie et al., 1998).

IDENTIFICATION OF GENES INVOLVED IN WALL BIOSYNTHESIS

Genes involved in xyloglucan biosynthesis

According to the chemical structure of XyG one could predict the need for at least four different enzymes involved in its biosynthesis: a β -glucan synthase(s) to make the backbone, plus α -xylosyltransferase(s), β -galactosyltransferase(s) and α -fucosyltransferase to add the side chains. When I began my thesis work, none of the genes encoding these enzymes had been identified. I joined the first efforts to identify the gene encoding the XyG fucosyltransferase (Perrin et al., 1999). An enzyme activity assay for XyG fucosyltransferase was developed using the tamarind XyG, which naturally lacks the terminal fucose, as the acceptor substrate, and ^{14}C labeled GDP-fucose as the sugar donor (Farkas and Maclachlan, 1988). The XyG fucosyltransferase was purified from etiolated pea epicotyls through a GDP-affinity and size exclusion column with the XyG fucosyltransferase activity monitored at each step (Perrin et al., 1999). The peptide sequences obtained from the purified enzyme led to the identification of an Arabidopsis EST clone, which subsequently led to the identification of the full-length cDNA sequence for Arabidopsis XyG fucosyltransferase (AtFut1) (Perrin et al., 1999). The pea version of the XyG fucosyltransferase gene, PsFut1, was also identified from a cDNA library utilizing the peptide sequences identified from the purified enzyme (Faik et al., 2000). The identity of the AtFut1 was confirmed by the precipitation of XyG fucosyltransferase activity from detergent solubilized Arabidopsis microsomes with antibodies against an *E. coli*-expressed peptide encoded by AtFut1, and the detection of XyG fucosyltransferase activity from AtFUT1 proteins expressed in COS7 cells (Perrin et al., 1999).

An AtFut1 mutant *mur2*, was identified from a screen for altered monosaccharide **composition** in cell walls (Reiter et al., 1997). These mutants have a 50% reduction in **total cell wall** L-fucose content and showed a reduction in XyG fucosylation to about 1% **of wild type** due to the mutation in the *AtFut1* (Vanzin et al., 2002). Furthermore, XyG is **the only** polysaccharide affected in the *mur2* mutant plants (Vanzin et al., 2002). However, there is no visible phenotype observed for *mur2*, and its wall strength was **indistinguishable** from that of the wild-type plants (Vanzin et al., 2002). A total of nine DNA sequences that have significant sequence identity with AtFut1 have been identified in the Arabidopsis genome database (Sarria et al., 2001). Together with AtFUT1 and the PsFUT1, proteins encoded by these nine genes constitute a new glycosyltransferase family in the CAZY database (family 37, <http://afmb.cnrs-mrs.fr/~pedro/CAZY>) (Henrissat and Davies, 2000). AtFUT proteins other than AtFUT1 did not show XyG-specific fucosyltransferase activities when they were expressed in tobacco BY2 cell cultures (Sarria et al., 2001). These AtFUT proteins showed very low identity with fucosyltransferases involved in the biosynthesis of N-linked glycoproteins and were proposed to be fucosyltransferases forming fucose linkages present in cell wall carbohydrates other than XyG, namely, RG I, RG II and AGPs (Sarria et al., 2001).

The XyG galactosyltransferase was identified from a forward genetic approach. The *mur3* mutant was identified in the same screen that identified *mur2* (Reiter et al., 1997). The *mur3* plants also showed a 50% reduction in cell wall fucose content just as *mur2* plants do (Reiter et al., 1997). When the cell wall materials from *mur3* and wild-type plants were fractionated into pectin- and XyG- rich fractions, significant decreases of fucose and galactose contents in both 1 M KOH and 4 M KOH soluble fractions were

1876

مجلس

100

21

NSC

100

1997, 1998, 1999, 2000, 2001, 2002, 2003, 2004, 2005, 2006, 2007, 2008, 2009, 2010, 2011, 2012, 2013, 2014, 2015, 2016, 2017, 2018, 2019, 2020, 2021, 2022, 2023, 2024, 2025, 2026, 2027, 2028, 2029, 2030, 2031, 2032, 2033, 2034, 2035, 2036, 2037, 2038, 2039, 2040, 2041, 2042, 2043, 2044, 2045, 2046, 2047, 2048, 2049, 2050, 2051, 2052, 2053, 2054, 2055, 2056, 2057, 2058, 2059, 2060, 2061, 2062, 2063, 2064, 2065, 2066, 2067, 2068, 2069, 2070, 2071, 2072, 2073, 2074, 2075, 2076, 2077, 2078, 2079, 2080, 2081, 2082, 2083, 2084, 2085, 2086, 2087, 2088, 2089, 2090, 2091, 2092, 2093, 2094, 2095, 2096, 2097, 2098, 2099, 2100, 2101, 2102, 2103, 2104, 2105, 2106, 2107, 2108, 2109, 2110, 2111, 2112, 2113, 2114, 2115, 2116, 2117, 2118, 2119, 2120, 2121, 2122, 2123, 2124, 2125, 2126, 2127, 2128, 2129, 2130, 2131, 2132, 2133, 2134, 2135, 2136, 2137, 2138, 2139, 2140, 2141, 2142, 2143, 2144, 2145, 2146, 2147, 2148, 2149, 2150, 2151, 2152, 2153, 2154, 2155, 2156, 2157, 2158, 2159, 2160, 2161, 2162, 2163, 2164, 2165, 2166, 2167, 2168, 2169, 2170, 2171, 2172, 2173, 2174, 2175, 2176, 2177, 2178, 2179, 2180, 2181, 2182, 2183, 2184, 2185, 2186, 2187, 2188, 2189, 2190, 2191, 2192, 2193, 2194, 2195, 2196, 2197, 2198, 2199, 2200, 2201, 2202, 2203, 2204, 2205, 2206, 2207, 2208, 2209, 2210, 2211, 2212, 2213, 2214, 2215, 2216, 2217, 2218, 2219, 2220, 2221, 2222, 2223, 2224, 2225, 2226, 2227, 2228, 2229, 2230, 2231, 2232, 2233, 2234, 2235, 2236, 2237, 2238, 2239, 2240, 2241, 2242, 2243, 2244, 2245, 2246, 2247, 2248, 2249, 2250, 2251, 2252, 2253, 2254, 2255, 2256, 2257, 2258, 2259, 2260, 2261, 2262, 2263, 2264, 2265, 2266, 2267, 2268, 2269, 2270, 2271, 2272, 2273, 2274, 2275, 2276, 2277, 2278, 2279, 2280, 2281, 2282, 2283, 2284, 2285, 2286, 2287, 2288, 2289, 2290, 2291, 2292, 2293, 2294, 2295, 2296, 2297, 2298, 2299, 2300, 2301, 2302, 2303, 2304, 2305, 2306, 2307, 2308, 2309, 2310, 2311, 2312, 2313, 2314, 2315, 2316, 2317, 2318, 2319, 2320, 2321, 2322, 2323, 2324, 2325, 2326, 2327, 2328, 2329, 2330, 2331, 2332, 2333, 2334, 2335, 2336, 2337, 2338, 2339, 2340, 2341, 2342, 2343, 2344, 2345, 2346, 2347, 2348, 2349, 2350, 2351, 2352, 2353, 2354, 2355, 2356, 2357, 2358, 2359, 2360, 2361, 2362, 2363, 2364, 2365, 2366, 2367, 2368, 2369, 2370, 2371, 2372, 2373, 2374, 2375, 2376, 2377, 2378, 2379, 2380, 2381, 2382, 2383, 2384, 2385, 2386, 2387, 2388, 2389, 2390, 2391, 2392, 2393, 2394, 2395, 2396, 2397, 2398, 2399, 2400, 2401, 2402, 2403, 2404, 2405, 2406, 2407, 2408, 2409, 2410, 2411, 2412, 2413, 2414, 2415, 2416, 2417, 2418, 2419, 2420, 2421, 2422, 2423, 2424, 2425, 2426, 2427, 2428, 2429, 2430, 2431, 2432, 2433, 2434, 2435, 2436, 2437, 2438, 2439, 2440, 2441, 2442, 2443, 2444, 2445, 2446, 2447, 2448, 2449, 2450, 2451, 2452, 2453, 2454, 2455, 2456, 2457, 2458, 2459, 2460, 2461, 2462, 2463, 2464, 2465, 2466, 2467, 2468, 2469, 2470, 2471, 2472, 2473, 2474, 2475, 2476, 2477, 2478, 2479, 2480, 2481, 2482, 2483, 2484, 2485, 2486, 2487, 2488, 2489, 2490, 2491, 2492, 2493, 2494, 2495, 2496, 2497, 2498, 2499, 2500, 2501, 2502, 2503, 2504, 2505, 2506, 2507, 2508, 2509, 2510, 2511, 2512, 2513, 2514, 2515, 2516, 2517, 2518, 2519, 2520, 2521, 2522, 2523, 2524, 2525, 2526, 2527, 2528, 2529, 2530, 2531, 2532, 2533, 2534, 2535, 2536, 2537, 2538, 2539, 2540, 2541, 2542, 2543, 2544, 2545, 2546, 2547, 2548, 2549, 2550, 2551, 2552, 2553, 2554, 2555, 2556, 2557, 2558, 2559, 2560, 2561, 2562, 2563, 2564, 2565, 2566, 2567, 2568, 2569, 2570, 2571, 2572, 2573, 2574, 2575, 2576, 2577, 2578, 2579, 2580, 2581, 2582, 2583, 2584, 2585, 2586, 2587, 2588, 2589, 2590, 2591, 2592, 2593, 2594, 2595, 2596, 2597, 2598, 2599, 2600, 2601, 2602, 2603, 2604, 2605, 2606, 2607, 2608, 2609, 2610, 2611, 2612, 2613, 2614, 2615, 2616, 2617, 2618, 2619, 2620, 2621, 2622, 2623, 2624, 2625, 2626, 2627, 2628, 2629, 2630, 2631, 2632, 2633, 2634, 2635, 2636, 2637, 2638, 2639, 2640, 2641, 2642, 2643, 2644, 2645, 2646, 2647, 2648, 2649, 2650, 2651, 2652, 2653, 2654, 2655, 2656, 2657, 2658, 2659, 2660, 2661, 2662, 2663, 2664, 2665, 2666, 2667, 2668, 2669, 2670, 2671, 2672, 2673, 2674, 2675, 2676, 2677, 2678, 26

402

2000

2000

1

1998

257.

200

1997

44

55

10

10

12

observed, indicating the possibility that the disaccharide side chain α -L-fucose-(1,2)- β -D-galactose was missing (Madson et al., 2003). When the XyGs from *mur3* plants were digested with endo- β -D-glucanase, two of the normally seen XyG building blocks XXFG and XLFG were missing (Madson et al., 2003). The gene *mur3* was identified through positional cloning. When expressed in *Pichia pastoris*, MUR3 showed XyG-specific galactosyltransferase activity and therefore confirmed the identity of MUR3 to be a XyG galactosyltransferase (Madson et al., 2003).

The XyG xylosyltransferase was identified through a candidate gene approach. In XyG the α -D-xylose is added to the β -glucan backbone in a 1,6 linkage. This glycosidic reaction is very similar to the one catalyzed by the galactomannan-specific α -(1,6) galactosyltransferase (Faik et al., 2002). When the sequence of the galactomannan α -(1,6) galactosyltransferase gene from fenugreek (Edwards et al., 1999) was used to search the Arabidopsis genome database, a group of seven genes that share low sequence similarity with it was identified. When these genes were expressed in *Pichia pastoris*, one of them, AtXT1, showed XyG specific xylosyltransferase activity (Faik et al., 2002). This XyG-specific xylosyltransferase activity assay used cellopentose as substrate acceptor, and the product hydrolysis analysis indicated the xylose residue was added onto the second glucose residue from the non-reducing end (Faik et al., 2002). The other six homologs of AtXT1 did not show this XyG-specific xylosyltransferase activity during the same study, and their functions are still not known (Faik et al., 2002).

A gene encoding the XyG backbone glucan synthase has not yet been identified mainly due to the lack of a specific enzyme activity assay method. Currently, several groups, including ours, are working vigorously in trying to identify this gene by

developing the XyG glucan synthase assay and using reverse genetics and genomic candidate gene approaches. One attractive hypothesis is that one or more of the cellulose synthase-like genes encode(s) the XyG glucan synthases. Supporting evidence includes the **fact** that the chemical structures of cellulose and XyG backbone are exactly the same, and **the** fact that cellulose synthase-like genes share significant sequence identity with genes encoding cellulose synthases (Doblin et al., 2001).

Genes involved in the biosynthesis of other wall polysaccharides

The identification of genes encoding enzymes involved in plant cell wall polysaccharide biosynthesis began only in the mid-to-late 1990's with the identification of **the** first cellulose synthase from cotton (Pear et al., 1996). Even at the present time, **only** a few genes have been identified and functionally characterized even though **hundreds** of enzymes are predicted to participate in the biosynthesis of the various cell wall polysaccharides. Beside the genes that encode enzymes involved in XyG biosynthesis, as described above, other genes identified include those encoding the cellulose synthase catalytic subunits (Williamson et al., 2002), two genes encoding enzymes for the biosynthesis of galactomannan (Edwards et al., 1999) (Dhugga, personal communication), and two genes encoding enzymes involved in pectin polysaccharide biosynthesis (Bouton et al., 2002; Iwai et al., 2002).

The first cellulose synthase gene was identified through an effort of random sequencing of clones from a cDNA library constructed from developing cotton fiber at 21 days post anthesis, at which time cotton fibers make primarily cellulose in very high quantities (Pear et al., 1996). A full length clone identified showed sequence similarities

with the bacterial cellulose synthase, *celA*. When expressed in *E. coli* the proteins encoded by this cDNA specifically bound to UDP-glucose, the presumed substrate for cellulose synthase (Pear et al., 1996). An Arabidopsis mutant *rsw1* was identified later. The mutant plants grown at a restrictive temperature of 30°C contained only half the amount of cellulose present in wild type plants (Arioli et al., 1998). The mutant turned out to be defective in a gene encoding a glycosyltransferase closely related to the enzyme identified as cellulose synthase in cotton fibers (Arioli et al., 1998). Combining the protein sequence comparison analysis with bacterial cellulose synthases and the cellulose-deficient mutant analysis, the first Arabidopsis cellulose synthase gene was finally identified and designated as the cellulose synthase catalytic subunit, AtCesA1.

The Arabidopsis genome contains a cellulose synthase gene family of ten genes. Most of these ten genes have been linked to cellulose production by characterizing their corresponding mutant plants. AtCesA1 (Arioli et al., 1998), AtCesA3 (Burn et al., 2002), AtCesA4 (Fagard et al., 2000), AtCesA6 (Taylor et al., 1999), AtCesA7 (Zhong et al., 2003), and AtCesA8 (Taylor et al., 2000) all showed decreased cellulose production in their corresponding mutant or antisense plants. AtCesA3 and AtCesA6 mutations also resulted in resistance to isoxaben, a herbicide that selectively inhibits cellulose synthesis (Scheible et al., 2001; Desprez et al., 2002). Mutant plants for all these AtCesA genes, plus the antisense plant of AtCesA2 (Burn et al., 2002) all showed morphological phenotypes that are consistent with a cellulose deficiency. Therefore all ten AtCesA genes seem to have a function involved in cellulose synthesis.

Galactomannan is a hemicellulose that is synthesized as the major storage polysaccharide and deposited in large quantity in seed endosperm at a certain stage of

legume seed development (Reid and Meier, 1970; Meier and Reid, 1977; Edwards et al., 1992). Galactomannan has a β -(1,4)-mannan backbone decorated with α -(1,6) linked single galactose residues. A gene encoding the α -(1,6)-galactosyltransferase involved in the attachment of the galactose residues to galactomannan backbone was first identified from fenugreek (*Trigonella foenum-graecum* L) seed endosperm (Edwards et al., 1999). Microsomal membranes were prepared from developing fenugreek seed endosperm and solubilized with Triton X-100. With a combination of non-denaturing isoelectric focusing and SDS-PAGE, a protein band in the gel was identified to be associated with the galactosyltransferase activity (Edwards et al., 1999). This protein was subjected to sequencing and the peptide sequence information obtained allowed the isolation of a cDNA clone which, when expressed in *Pichia pastoris*, showed high activity of galactomannan specific galactosyltransferase (Edwards et al., 1999).

Very recently the gene encoding the enzyme involved in the backbone biosynthesis of galactomannan, the β -mannan synthase, was identified in guar seed (Kanwarpal S. Dhugga, personal communication). Again, the rapid deposition of galactomannan in large amounts in developing guar seeds was utilized as an advantage. An EST library was constructed from the developing seeds. One of the cDNA clones isolated, when expressed in soybean somatic embryos, showed high level of activity for β -mannan synthase (Kanwarpal S. Dhugga, personal communication). The hydrolysis analysis of the enzyme reaction product was also confirmed to be β -mannan (Kanwarpal S. Dhugga, personal communication).

A RG II-specific glucuronyltransferase gene (NpGUT1) was identified from *Nicotiana plumbaginifolia* through T-DNA tagging (Iwai et al., 2002). NpGUT1 is

similar to the gene encoding the catalytic domains of animal glucuronyltransferases involved in heparan sulfate synthesis (Iwai et al., 2002). When the expression of NpGUT1 was suppressed by an antisense gene, the glucuronic acid content level was remarkably reduced in the Na₂CO₃-soluble pectic fractions. In particular, the glucuronic acid in RG II of cell wall materials was totally missing, confirming a function involved in the formation of a rather specific sugar linkage (Iwai et al., 2002).

Another gene encoding an enzyme involved in pectic polysaccharide biosynthesis was identified through the characterization of an Arabidopsis T-DNA insertion mutant *QUASIMODO1* (*qual*) (Bouton et al., 2002). The *qual* plants were dwarfed and showed reduced cell adhesion (Bouton et al., 2002). The biosynthesis of homogalacturonic acid (HGA) in *qual* plants was affected since cell walls from the mutant plants had 25% less uronic acid and galacturonic acid, and a strong decrease of HGA backbone epitopes specifically recognizable by monoclonal antibodies JIM5 and JIM7 (Bouton et al., 2002). The cloned *qual* gene encodes a type II transmembrane protein that belongs to family 8 of glycosyltransferases (Bouton et al., 2002).

It is still a daunting task and a frustratingly slow process to identify all of the glycosyltransferases involved in the biosynthesis of wall matrix polysaccharides, given the large number of different sugar linkages present (Perrin et al., 2001). From these a few successful gene identifications described here, it is realized that the biochemical approach and the genomic candidate approach are both feasible and very efficient, especially when these two approaches are combined (Edwards et al., 1999; Perrin et al., 1999; Faik et al., 2002) (Kanwarpal S. Dhugga, personal communication). In addition, enzyme activity assays seem to be the most valuable tool and almost always a necessity

since the biochemical function of each glycosyltransferase needs to be confirmed individually. On the other hand, a wise choice of plant species and plant tissue is critical, especially for the success of the genomic candidate gene approach.

Functional studies of AtCsl genes

In an effort to identify genes encoding enzymes involved in wall matrix polysaccharide biosynthesis, genes showing significant sequence identity with known wall biosynthesis genes have drawn particular interest. The identification of AtCesA genes through genomic (Pear et al., 1996) and genetic approaches (Arioli et al., 1998) was a major breakthrough that allowed additional gene identification studies through comparative genomics (Cutler and Somerville, 1997; Richmond and Somerville, 2000; Saxena and Brown, 2000).

From the Arabidopsis genomic database, a Blast search using Arabidopsis cellulose synthase 1 (AtCesA1, AtRsw1) as query sequence identified a superfamily of 40 genes. Among them 10 cellulose synthase genes showed more than 50% identity with each other and are proposed to have similar functions. Most of these ten genes were later identified as encoding true cellulose synthases through mutant plant characterizations (Williamson et al., 2002). The other 30 homologs showed less than 50% identity with AtCesA and were named as Arabidopsis cellulose synthase-like (AtCsl) genes (Richmond and Somerville, 2000; Saxena and Brown, 2000). The proteins encoded by these AtCsl genes are sufficiently divergent from AtCesA proteins that they are not very likely cellulose synthase catalytic subunit isoforms (Richmond and Somerville, 2001). AtCsl proteins not only share identity with AtCesA proteins in the primary sequences, but

1000

1000

1000

1000

1000

1000

1000

1000

1000

1000

1000

1000

1000

1000

also contain a motif D..D...D..QxxRW that is indicative of β processive glycosyltransferases and thought to be important in the catalytic site of these enzymes (Saxena et al., 1995; Pear et al., 1996; Richmond and Somerville, 2001). Like CesA proteins, AtCsl proteins all appear to belong to family 2 of inverting nucleotide-diphospho-sugar glycosyltransferases (Campbell et al., 1997). These AtCsl proteins all contain multiple transmembrane domains organized in a way similar to AtCesA proteins with 1 or 2 transmembrane domains in the amino-terminal region and 3 to 6 of them in the carboxyl-terminal region (Richmond and Somerville, 2001).

Given their structural features, AtCsl proteins have been proposed to be enzymes involved in the biosynthesis of β -linked polysaccharide backbones, such as XyG, mannan, galactomannan, and GAX (Richmond and Somerville, 2001), or even cellulose (Doblin et al., 2001). Direct evidence supporting this hypothesis came from the recent observation that a guar CslA gene encodes the guar galactomannan-specific mannan synthase (Kanwarpal S. Dhugga, personal communication).

120

121

122

123

124

125

126

127

128

129

130

131

132

133

134

135

136

137

138

139

140

REGULATION OF CELL WALL METABOLISM

The plant cell wall, with its dynamic functions, not only maintains the integrity of **plant** cells but also participates in the regulation of cell growth. Consequently, wall **structure** is under frequent modulation by endogenous and external stimuli. The term “**cell** wall metabolism” used here describes the process of degradation of existing wall **materials**, synthesis and cross-linking of newly deposited wall materials, and also **changes** in individual wall polysaccharides including modification of their chemical **structure** and changes in the levels of individual polysaccharides.

The metabolism of cell walls is regulated during natural growth and **differentiation** (Bolwell, 1988; Stolle-Smits et al., 1999; Bush et al., 2001; Obel et al., 2002; Tokumoto et al., 2002). Among the factors that influence wall properties are **endogenous** or externally applied plant growth regulators such as auxin (Rubery and **Northcote**, 1970; Loescher and Nevins, 1972; Nishitani and Masuda, 1981; Masuda, 1985; **Talbott** and Ray, 1992), gibberellic acid (Fry, 1980; Potter and Fry, 1994; Nishitani, 1995), ethylene (Abeles and Forrence, 1970; Hayashi and Maclachlan, 1984), abscisic acid (Wu et al., 1994; Maheswari, 1999), jasmonic acid (Takahashi et al., 1995; Ueda et al., 1996; Moore et al., 2003), cytokinin (Robertson et al., 1999), salicylic acid (Nishimura et al., 2003), and brassinosteroid (Zurek and Clouse, 1994; Xu et al., 1995). **Environmental** stresses that induce plant responses often also induce changes in cell wall **metabolism**. Environmental signals that affect wall metabolism include light (Walton and **Ray**, 1982; Miyamoto et al., 1997; Shieh et al., 1997), temperature (Kubacka-Zebalska and **Kacperska**, 1999; Nakamura et al., 2003), drought (Gershenzon, 1984; Maheswari, 1999), osmotic stress (Boffey and Northcote, 1975; Singh et al., 1985; Talbott and Ray,

1992), mechanical stress (Jaffe et al., 1985), and wounding (Wu and Bradford, 2003).

Plant cell walls also participate actively in the pathogenesis process, including pathogen recognition, signal transduction, and the subsequent plant response (Bolwell, 1986; Esquerre-Tugaye et al., 2000). Fruit ripening is another process that involves significant wall metabolism, mostly degradation of cell wall polysaccharides (Wakabayashi, 2000).

Many genes encoding enzymes involved in the degradation or reorganization of cell wall polysaccharides have been identified. Consequently, antibodies have been generated against the proteins, and probes have been created for the genes. These reagents allowed the regulation of wall degradation and reorganization to be investigated. Examples include enzymes involved in wall degradation during fruit ripening (Redondo-Nevado et al., 2001; Tateishi et al., 2001; Tateishi et al., 2002; Chen and Paull, 2003), wall metabolism during auxin-induced rapid stem elongation (Inouhe and Nevins, 1991), as well as expansins and XTHs that are involved in wall reorganization (del Campillo and Lewis, 1992; Zurek and Clouse, 1994; Reidy et al., 2001; Lee et al., 2003). However, only a few genes involved in wall polysaccharide biosynthesis have been identified, and most of them have been identified very recently (Arioli et al., 1998; Edwards et al., 1999). Without the genes as molecular tools, very few studies on the regulation of wall biosynthetic enzymes have been performed. We are, therefore, interested in the identification of genes involved in XyG biosynthesis as the first step. In the second step we will generate necessary molecular tools such as gene-specific probes and enzyme-specific antibodies, and use them to explore the relationships between wall biosynthesis and plant growth and development.

REFERENCES

- Abeles, F. B. and Forrence, L. E.** (1970). "Temporal and hormonal control of beta-1,3-glucanase in *Phaseolus vulgaris* L." *Plant Physiol.* **45** (4): 395.
- Aldington, S., McDougall, G. J. and Fry, S. C.** (1991). "Structure-activity relationships of biologically-active oligosaccharides." *Plant Cell Env.* **14**: 625-636.
- Arioli, T., Peng, L., Betzner, A. S., Burn, J., Wittke, W., Herth, W., Camilleri, C., Hofte, H., Plazinski, J. and Birch, R.** (1998). "Molecular analysis of cellulose biosynthesis in Arabidopsis." *Science* **279**: 717-720.
- Augur, C., Yu, L., Sakai, K., Ogawa, T., Sinay, P., Darvill, A. G. and Albersheim, P.** (1992). "Further studies of the ability of xyloglucan oligosaccharides to inhibit auxin-stimulated growth." *Plant Physiol.* **99** (1): 180-185.
- Bacic, A., Harris, P. J. and Stone, B. A.** (1988). "Structure and function of plant cell walls". The Biochemistry of Plants. J. Preiss, New York, Academic Press. **14**: 297-371.
- Boffey, S. A. and Northcote, D. H.** (1975). "Pectin synthesis during wall regeneration of plasmolyzed tobacco leaf cells." *Biochem. J.* **150** (3): 433.
- Bolwell, G. P.** (1986). "Microsomal arabinosylation of polysaccharide and elicitor-induced carbohydrate-binding glycoprotein in french bean." *Phytochem.* **25** (8): 1807-1813.
- Bolwell, G. P.** (1988). "Synthesis of cell wall components: Aspects of control." *Phytochem.* **27** (5): 1235-1253.
- Bouton, S., Leboeuf, E., Mouille, G., Leydecker, M.-T., Talbotec, J., Granier, F., Lahaye, M., Hofte, H. and Truong, H.-N.** (2002). "*QUASIMODO1* encodes a putative membrane-bound glycosyltransferase required for normal pectin synthesis and cell adhesion in Arabidopsis." *Plant Cell* **14**: 2577-2590.
- Braccini, I., Du, P. C. H., Michon, V., Goldberg, R., Clochard, M., Jarvis, M. C., Huang, Z. H. and Gage, D. A.** (1995). "Structural analysis of cyclamen seed xyloglucan oligosaccharides using cellulase digestion and spectroscopic methods." *Carbohydr. Res.* **276** (1): 167-181.
- Brett, C. T.** (1983). "Cell walls do not a prison make." *New Scientist* **99**: 693-695.
- Brett, C. T. and Waldron, K. W.** (1996). Physiology and Biochemistry of Plant Cell Walls. Chapman & Hall.

Bro	1970	1971	1972	1973	1974	1975	1976	1977	1978	1979	1980	1981	1982	1983	1984	1985	1986	1987	1988	1989	1990	1991	1992	1993	1994	1995	1996	1997	1998	1999	2000	2001	2002	2003	2004	2005	2006	2007	2008	2009	2010	2011	2012	2013	2014	2015	2016	2017	2018	2019	2020	2021	2022	2023	2024	2025	2026	2027	2028	2029	2030	2031	2032	2033	2034	2035	2036	2037	2038	2039	2040	2041	2042	2043	2044	2045	2046	2047	2048	2049	2050	2051	2052	2053	2054	2055	2056	2057	2058	2059	2060	2061	2062	2063	2064	2065	2066	2067	2068	2069	2070	2071	2072	2073	2074	2075	2076	2077	2078	2079	2080	2081	2082	2083	2084	2085	2086	2087	2088	2089	2090	2091	2092	2093	2094	2095	2096	2097	2098	2099	2100	2101	2102	2103	2104	2105	2106	2107	2108	2109	2110	2111	2112	2113	2114	2115	2116	2117	2118	2119	2120	2121	2122	2123	2124	2125	2126	2127	2128	2129	2130	2131	2132	2133	2134	2135	2136	2137	2138	2139	2140	2141	2142	2143	2144	2145	2146	2147	2148	2149	2150	2151	2152	2153	2154	2155	2156	2157	2158	2159	2160	2161	2162	2163	2164	2165	2166	2167	2168	2169	2170	2171	2172	2173	2174	2175	2176	2177	2178	2179	2180	2181	2182	2183	2184	2185	2186	2187	2188	2189	2190	2191	2192	2193	2194	2195	2196	2197	2198	2199	2200	2201	2202	2203	2204	2205	2206	2207	2208	2209	2210	2211	2212	2213	2214	2215	2216	2217	2218	2219	2220	2221	2222	2223	2224	2225	2226	2227	2228	2229	2230	2231	2232	2233	2234	2235	2236	2237	2238	2239	2240	2241	2242	2243	2244	2245	2246	2247	2248	2249	2250	2251	2252	2253	2254	2255	2256	2257	2258	2259	2260	2261	2262	2263	2264	2265	2266	2267	2268	2269	2270	2271	2272	2273	2274	2275	2276	2277	2278	2279	2280	2281	2282	2283	2284	2285	2286	2287	2288	2289	2290	2291	2292	2293	2294	2295	2296	2297	2298	2299	2300	2301	2302	2303	2304	2305	2306	2307	2308	2309	2310	2311	2312	2313	2314	2315	2316	2317	2318	2319	2320	2321	2322	2323	2324	2325	2326	2327	2328	2329	2330	2331	2332	2333	2334	2335	2336	2337	2338	2339	2340	2341	2342	2343	2344	2345	2346	2347	2348	2349	2350	2351	2352	2353	2354	2355	2356	2357	2358	2359	2360	2361	2362	2363	2364	2365	2366	2367	2368	2369	2370	2371	2372	2373	2374	2375	2376	2377
-----	------	------	------	------	------	------	------	------	------	------	------	------	------	------	------	------	------	------	------	------	------	------	------	------	------	------	------	------	------	------	------	------	------	------	------	------	------	------	------	------	------	------	------	------	------	------	------	------	------	------	------	------	------	------	------	------	------	------	------	------	------	------	------	------	------	------	------	------	------	------	------	------	------	------	------	------	------	------	------	------	------	------	------	------	------	------	------	------	------	------	------	------	------	------	------	------	------	------	------	------	------	------	------	------	------	------	------	------	------	------	------	------	------	------	------	------	------	------	------	------	------	------	------	------	------	------	------	------	------	------	------	------	------	------	------	------	------	------	------	------	------	------	------	------	------	------	------	------	------	------	------	------	------	------	------	------	------	------	------	------	------	------	------	------	------	------	------	------	------	------	------	------	------	------	------	------	------	------	------	------	------	------	------	------	------	------	------	------	------	------	------	------	------	------	------	------	------	------	------	------	------	------	------	------	------	------	------	------	------	------	------	------	------	------	------	------	------	------	------	------	------	------	------	------	------	------	------	------	------	------	------	------	------	------	------	------	------	------	------	------	------	------	------	------	------	------	------	------	------	------	------	------	------	------	------	------	------	------	------	------	------	------	------	------	------	------	------	------	------	------	------	------	------	------	------	------	------	------	------	------	------	------	------	------	------	------	------	------	------	------	------	------	------	------	------	------	------	------	------	------	------	------	------	------	------	------	------	------	------	------	------	------	------	------	------	------	------	------	------	------	------	------	------	------	------	------	------	------	------	------	------	------	------	------	------	------	------	------	------	------	------	------	------	------	------	------	------	------	------	------	------	------	------	------	------	------	------	------	------	------	------	------	------	------	------	------	------	------	------	------	------	------	------	------	------	------	------	------	------	------	------	------	------	------	------	------	------	------	------	------	------	------	------	------	------	------	------	------	------	------	------	------	------	------	------	------	------	------

- Brisson, L. F., Tenhaken, R. and Lamb, C.** (1994). "Function of oxidative cross-linking of cell wall structural proteins in plant disease resistance." *Plant Cell* **6**: 1703-1712.
- Brown, J. A. and Fry, S. C.** (1993). "Novel O-D-galacturonoyl esters in the pectic polysaccharides of suspension-cultured plant cells." *Plant Physiol.* **103**: 993-999.
- Brown, J. A. and Fry, S. C.** (1993). "The preparation and susceptibility to hydrolysis of novel O-galacturonoyl derivatives of carbohydrates." *Carbohydr. Res.* **240**: 95-106.
- Buckeridge, M. S. and Dietrich, S. M. C.** (1990). "Galactomannans from Brazilian legume seeds." *Revta. Brasil. Bot.* **13**: 109-112.
- Buckeridge, M. S., Pessoa, d. S. H. and Tine, M. A. S.** (2000). "Mobilisation of storage cell wall polysaccharides in seeds." *Plant Physiol. Biochem.* **38** (1-2): 141-156.
- Buckeridge, M. S., Rocha, D. C., Reid, J. S. G. and Dietrich, S. M. C.** (1992). "Xyloglucan structure and post-germinative metabolism in seeds of *Copaifera langsdorfii* from savanna and forest populations." *Physiol. Plant.* **86** (1): 145-151.
- Burke, D., Kanfman, P., McNeil, M. and Albersheim, P.** (1974). "Structure of plant cell walls. 6. Survey of walls of suspension-cultured monocots." *Plant Physiol.* **54** (1): 109-115.
- Burn, J., Hocart, C. H., Birch, R. J., Cork, A. C. and Williamson, R. E.** (2002). "Functional analysis of the cellulose synthase genes *CesA1*, *CesA2*, *CesA3* in *Arabidopsis*." *Plant Physiol.* **129**: 797-807.
- Bush, M. S., Marry, M., Huxham, I. M., Jarvis, M. C. and McCann, M. C.** (2001). "Developmental regulation of pectic epitopes during potato tuberisation." *Planta* **213**: 869-880.
- Campbell, J. A., Davies, G. J., Bulone, V. and Henrissat, B.** (1997). "A classification of nucleotide-diphospho-sugar glycosyltransferases based on amino acid sequence similarities." *Biochem. J.* **326**: 929-939.
- Carpita, N., Sabulase, D., Montezumos, D. and Delmer, D. P.** (1979). "Determination of the pore size of cell walls of living plant cells." *Science* **205**: 1144-1147.
- Carpita, N. C. and Gibeaut, D. M.** (1993). "Structural models of primary cell walls in flowering plants: consistency of molecular structure with the physical properties of walls during growth." *Plant J.* **3**: 1-30.
- Chambat, G., Barnoud, F. and Joseleau, J. P.** (1984). "Structure of the primary cell walls of suspension cultured *Rosa glauca* cells 1. Polysaccharides associated with cellulose." *Plant Physiol.* **74** (3): 687-693.

- Chen, N. J. and Paull, R. E.** (2003). "Endoxylanase expressed during papaya fruit ripening: purification, cloning and characterization." *Funct. Plant Biol.* **30** (4): 433-441.
- Cosgrove, D. J.** (2000). "Loosening of plant cell walls by expansins." *Nature* **407**: 321-326.
- Crombie, H. J., Chengappa, S., Hellyer, A. and Reid, J. S. G.** (1998). "A xyloglucan oligosaccharide-active, transglycosylating beta-D-glucosidase from the cotyledons of nasturtium (*Tropaeolum majus* L.) seedlings-purification, properties and characterization of a cDNA clone." *Plant J.* **15** (1): 27-38.
- Cutillas, I. A. and Lorences, E. P.** (1997). "Effect of xyloglucan oligosaccharides on growth, viscoelastic properties, and long-term extension of pea shoots." *Plant Physiol.* **113** (1): 103-109.
- Cutler, S. and Somerville, C. R.** (1997). "Cellulose synthesis: *Cloning in silico*." *Curr. Biol.* **7**: R108-R111.
- Darvill, J. E., McNeil, M., Darvill, A. G. and Albersheim, P.** (1980). "Structure of plant cell walls XI. Glucuronoarabinoxylan, a second hemicellulose in primary cell walls of suspension-cultured sycamore cells." *Plant Physiol.* **66**: 1135-1139.
- del Campillo, E. and Lewis, L. N.** (1992). "Occurrence of 9.5 cellulase and other hydrolases in flower reproductive organs undergoing major cell wall disruption." *Plant Physiol.* **99** (1015-1020).
- Desprez, T., Vernhettes, S., Fagard, M., Refregier, G., Desnos, T., Aletti, E., Py, N., Pelletier, S. and Hofte, H.** (2002). "Resistance against herbicide isoxaben and cellulose deficiency caused by distinct mutations in same cellulose synthase isoform CESA6." *Plant Physiol.* **128**: 482-490.
- Doblin, M. S., Melis, L. D., Newbigin, E., Bacic, A. and Read, S. M.** (2001). "Pollen tubes of *Nicotiana glauca* express two genes from different beta-glucan synthase families." *Plant Physiol.* **125**: 2040-2052.
- Edwards, M., Bowman, Y. J. L., Dea, I. C. M. and Reid, J. S. G.** (1988). "A beta-D galactosidase from Nasturtium *Tropaeolum majus* L. cotyledons purification properties and demonstration that xyloglucan is the natural substrate." *J. Biol.Chem.* **263** (9): 4333-4337.
- Edwards, M., Dea, I. C. M., Bulpin, P. V. and Reid, J. S. G.** (1985). "Xyloglucan amyloid mobilization in the cotyledons of *Tropaeolum majus* seeds following germination." *Planta* **163** (1): 133-140.

Edwards, M., Dea, I. C. M., Bulpin, P. V. and Reid, J. S. G. (1986). "Purification and properties of a novel xyloglucan-specific endo-1-4-beta-D-glucanase from germinated Nasturtium seeds *Tropaeolum majus*." *J. Biol. Chem.* **261** (20): 9489-9494.

Edwards, M., Scott, C., Gidley, M. J. and Reid, J. S. G. (1992). "Control of mannose/galactose ratio during galactomannan formation in developing legume seeds." *Planta* **187** (67-74).

Edwards, M. E., Dickson, C. A., Chengappa, S., Sidebottom, C., Gidley, M. J. and Reid, J. S. G. (1999). "Molecular characterisation of a membrane-bound galactosyltransferase of plant cell wall matrix polysaccharide biosynthesis." *Plant J.* **19**: 691-697.

Emmerling, M. and Seitz, H. U. (1990). "Influence of a specific xyloglucan nonasaccharide derived from cell walls of suspension-cultured cells of *Daucus carota* L. on regenerating protoplasts." *Planta* **182**: 174-180.

Esquerre-Tugaye, M.-T., Boudart, G. and Dumas, B. (2000). "Cell wall degrading enzymes, inhibitory proteins, and oligosaccharides participate in the molecular dialogue between plants and pathogens." *Plant Physiol. Biochem.* **38** (1-2): 157-163.

Fagard, M., Desnos, T., Desprez, T., Goubet, F., Refregier, G., Mouille, G., McCann, M., Rayon, C., Vernhettes, S. and Hofte, H. (2000). "*PROCUSTE1* encodes a cellulose synthase required for normal cell elongation specifically in roots and dark-grown hypocotyls of Arabidopsis." *Plant Cell* **12**: 2409-2432.

Faik, A., Bar-Peled, M., DeRocher, A. E., Zeng, W., Perrin, R. M., Wilkerson, C., Raikhel, N. V. and Keegstra, K. (2000). "Biochemical characterization and molecular cloning of an alpha-1,2-fucosyltransferase that catalyzes the last step of cell wall xyloglucan biosynthesis in pea." *J. Biol. Chem.* **275** (20): 15082-15089.

Faik, A., Price, N. J., Raikhel, N. V. and Keegstra, K. (2002). "An Arabidopsis gene encoding an alpha-xylosyltransferase involved in xyloglucan biosynthesis." *Proc. Natl Acad. Sci. USA* **99** (11): 7797-7802.

Fanutti, C., Gidley, M. J. and Reid, J. S. G. (1991). "A xyloglucan oligosaccharide-specific alpha-D-xylosidase or exooligoxxyloglucan-alpha-xylohydrolase from germinated Nasturtium *Tropaeolum majus* L. seeds: Purification properties and its interaction with a xyloglucan-specific endo-1-4-beta-D glucanase and other hydrolases during storage xyloglucan mobilization." *Planta* **184** (1): 137-147.

Fanutti, C., Gidley, M. J. and Reid, J. S. G. (1993). "Action of a pure xyloglucan endo-transglycosylase (formerly called xyloglucan-specific endo-(1,4)-beta-D-glucanase) from the cotyledons of germinated nasturtium seeds." *Plant J.* **3**: 691-700.

Farkas, V. and Maclachlan, G. (1988). "Fucosylation of exogenous xyloglucans by pea microsomal membranes." *Arch. Biochem. Biophys.* **264** (1): 48-53.

Femenia, A., Rigby, N. M., Selvendran, R. R. and Waldron, K. W. (1999). "Investigation of the occurrence of pectic-xylan-xyloglucan complexes in the cell walls of cauliflower stem tissues." *Carbohydrate Polymers* **39** (2): 151-164.

Fincher, G. B. and Stone, B. A. (1982). "Metabolism of noncellulosic polysaccharides". Encyclopedia of Plant Physiology. W. Tanner and F. A. Loewus, Berlin, Springer-Verlag. **13B**: 68-132.

Fry, S. C. (1980). "Gibberellin-controlled pectinic acid and protein secretion in growing-cells." *Phytochemistry* **19** (5): 735-740.

Fry, S. C. (1989). "Cellulose, hemicellulose and auxin-stimulated growth: a possible relationship." *Physiol. Plant.* **75** (4): 532-536.

Fry, S. C. (1989). "The structure and functions of xyloglucan." *J. Exp. Bot.* **40** (210): 1-11.

Fry, S. C., Smith, R. C., Renwick, K. F., Martin, D. J., Hodge, S. K. and Matthews, K. J. (1992). "Xyloglucan endotransglycosylase: a new wall-loosening enzyme activity from plants." *Biochem. J.* **282** (3): 821-828.

Fry, S. C., York, W. S., Albersheim, P., Darvill, A., Hayashi, T., Joseleau, J. P., Kato, Y., Perez, L. E., Maclachlan, G. A. and et al. (1993). "An unambiguous nomenclature for xyloglucan-derived oligosaccharides." *Physiol. Plant.* **89** (1): 1-3.

Gershenzon, J. (1984). *Rec. Adv. Phytochem.* **18**: 274.

Gibeaut, D. M. and Carpita, N. C. (1994). "Biosynthesis of plant cell wall polysaccharides." *FASEB J.* **8** (12): 904-915.

Grabber, J. H., Hatfield, R. D., Ralph, J., Zon, J. and Amrhein, N. (1995). "Ferulate cross-linking in cell walls isolated from maize cell suspensions." *Phytochemistry* **40**: 1077-1082.

Hayashi, T. (1989). "Xyloglucans in the primary cell wall." *Ann. Rev. Plant Physiol. Plant Mol. Biol.* **40**: 139-168.

Hayashi, T. and Maclachlan, G. (1984). "Pea *Pisum sativum* cultivar Alaska xyloglucan and cellulose 3. Metabolism during lateral expansion of pea epicotyl cells." *Plant Physiol.* **76** (3): 739-742.

Henrissat, B. and Davies, G. J. (2000). "Glycoside hydrolases and glycosyltransferases: families, modules, and implications for genomics." *Plant Physiol.* **124**: 1515-1519.

- Hisamatsu, M., Impallomeni, G., York, W. S., Albersheim, P. and Darvill, A. G.** (1991). "A new undecasaccharide subunit of xyloglucans with two alpha-L-fucosyl residues." *Carbohydr. Res.* **211** (1): 117-130.
- Inouhe, M. and Nevins, D. J.** (1991). "Inhibition of auxin-induced cell elongation of maize coleoptiles by antibodies specific for cell wall glycanases." *Plant Physiol.* **96** (426-431).
- Israel, H. W., Wilson, R. G., Aist, J. R. and Kunoh, H.** (1980). "Cell wall appositions and plant disease resistance: Acoustic microscopy of Papillae that block fungal ingress." *Proc. Natl Acad. Sci. USA* **77**: 2046-2049.
- Iwai, H., Masaoka, N., Ishii, T. and Satoh, S.** (2002). "A pectin glucuronyltransferase gene is essential for intercellular attachment in the plant meristem." *Proc. Natl Acad. Sci. USA* **99** (25): 16319-16324.
- Jaffe, M. J., Wakefield, A. H., Telewski, F., Gulley, E. and Biro, R.** (1985). "Computer-assisted image-analysis of plant-growth, thigmomorphogenesis, and gravitropism." *Plant Physiol.* **77** (3): 722-730.
- Joseleau, J. P. and Chambat, G.** (1984). "Structure of the primary cell walls of suspension cultured *Rosa glauca* cells 2. Multiple forms of xyloglucans." *Plant Physiol.* **74** (3): 694-700.
- Kaczkowski, J.** (2003). "Structure, function and metabolism of plant cell wall." *Acta Physiol. Plant.* **25** (3): 287-305.
- Keegstra, K., Talmadge, K. W., Bauer, W. D. and Albersheim, P.** (1973). "The structure of plant cell walls. III. A model of the walls of suspension-cultured sycamore cells bases on the interconnections of the macromolecular components." *Plant Physiol.* **51**: 188-196.
- Kim, J. B. and Carpita, N. C.** (1992). "Changes in esterification of the uronic acid groups of cell wall polysaccharides during elongation of maize coleoptiles." *Plant Physiol.* **98**: 646-653.
- Knox, J. P., Linstead, P. J., King, J., Cooper, C. and Roberts, K.** (1990). "Pectin esterification is spatially regulated both within cell walls and between developing tissues of root apices." *Planta* **181**: 512-521.
- Kooiman, P.** (1961). "The constitution of *Tamarindus amyloid*." *Rev. Trav. Chim.* **80**: 849-865.

Kuba
mid
class

Lee
EVA
27

Loes
telev

Lore
high
Rural

Mad
Carp
Wife
Rural

Mah
VET

Malt
Ben
Spoke

Mas
man

May
Press

McC
Cyte

McD
Sam

McD
Shag

McD
and a
B. J.

- Kubacka-Zebalska, M. and Kacperska, A.** (1999). "Low temperature-induced modifications of cell wall content and polysaccharide composition in leaves of winter oilseed rape (*Brassica napus* L. var. *oleifera* L.)." *Plant Sci.* **148**: 59-67.
- Lee, D.-K., Ahn, J. H., Song, S.-K., Choi, Y. D. and Lee, J. S.** (2003). "Expression of an expansin gene is correlated with root elongation in soybean." *Plant Physiol.* **131**: 985-997.
- Loescher, W. H. and Nevins, D. J.** (1972). "Auxin-induced changes in *Avena* coleoptile cell wall composition." *Plant Physiol.* **50**: 556-563.
- Lorences, E. P., McDougall, G. J. and Fry, S. C.** (1990). "Xyloglucan and cello-oligosaccharides antagonists of the growth-promoting effect of hydrogen ion." *Physiol. Plant.* **80** (1): 109-113.
- Madson, M., Dunand, C., Li, X., Verma, R., Vanzin, G. F., Caplan, J., Shoue, D. A., Carpita, N. C. and Reiter, W.-D.** (2003). "The MUR3 gene of *Arabidopsis* encodes a xyloglucan galactosyltransferase that is evolutionarily related to animal exostosins." *Plant Cell* **15**: 1662-1670.
- Maheswari, M.** (1999). "Effect of GA, ABA and water stress on leaf elongation and XET activity in barley *Hordeum vulgare* L." *Indian J. Exp. Biol.* **37** (10): 1001-1004.
- Maltby, D., Carpita, N. C., Montezinos, D., Kulow, C. and Delmer, D. P.** (1979). "Beta-1,3-glucan in developing cotton fibers. Structure, localization, and relationship of synthesis to that of secondary wall cellulose." *Plant Physiol.* **63**: 1158-1164.
- Masuda, Y.** (1985). "Cell-wall modifications during auxin-induced cell extension in monocotyledonous and dicotyledonous plants." *Biol. Plant.* **27** (2-3): 119-124.
- Mayer, A. M. and Poljakoff-Mayber, A.** (1975). *The Germination of Seeds*. Pergamon Press.
- McCann, M. C. and Roberts, K.** (1992). "Architecture of the primary cell wall". *The Cytoskeletal Basis of Plant Growth and Form*. C. W. Lloyd, London, Academic: 109-129.
- McDougall, G. J. and Fry, S. C.** (1988). "Inhibition of auxin-stimulated growth of pea stem segments by a specific nonasaccharide of xyloglucan." *Planta* **175** (3): 412-416.
- McDougall, G. J. and Fry, S. C.** (1989). "Structure-activity relationships for xyloglucan oligosaccharides with antiauxin activity." *Plant Physiol.* **89** (3): 883-887.
- McDougall, G. J. and Fry, S. C.** (1990). "Xyloglucan oligosaccharides promote growth and activate cellulase evidence for a role of cellulase in cell expansion." *Plant Physiol.* **93** (3): 1042-1048.

- McDougall, G. J. and Fry, S. C.** (1991). "Xyloglucan nonasaccharide a naturally-occurring oligosaccharin arises in-vivo by polysaccharide breakdown." *J. Plant Physiol.* **137** (3): 332-336.
- McDougall, G. J. and Fry, S. C.** (1994). "Fucosylated xyloglucan in suspension-cultured cells of the graminaceous monocotyledon *Festuca arundinacea*." *J. Plant Physiol.* **143** (6): 591-595.
- McNeil, M., Darvill, A. G., Fry, S. C. and Albersheim, P.** (1984). "Structure and function of the primary cell walls of plants." *Ann. Rev. Biochem.* **53**: 652-683.
- McQueen-Mason, S.** (1997). "Plant cell wall and the control of growth." *Biochemical Society Transactions* **25**: 204-214.
- Meier, H. and Reid, J. S. G.** (1977). "Morphological aspects of the galactomannan formation in the endosperm of *Trigonella foenum-graecum* L. (*Leguminosae*)." *Planta* **133**: 243-248.
- Meier, H. and Reid, J. S. G.** (1982). "Reserve polysaccharides other than starch in higher plants". Encyclopedia of Plant Physiology. F. A. Loewus and W. Tanner, Berlin, Springer-Verlag. **13A**: 418-471.
- Miyamoto, K., Mitani, Y., Soga, K., Ueda, J., Wakabayashi, K., Hoson, T., Kamisaka, S. and Masuda, Y.** (1997). "Modification of chemical properties of cell wall polysaccharides in the inner tissues by white light in relation to the decrease in tissue tension in *Pisum sativum* epicotyls." *Physiol. Plant.* **101** (1): 38-44.
- Mohnen, D.** (1999). "Biosynthesis of pectins and galactomannans". Carbohydrates and Their Derivatives Including Tannins, Cellulose, and Related Lignins. B. M. Pinto, Elsevier Science LTD, Oxford. **3**: 497-527.
- Moore, J. P., Paul, N. D., Whittaker, J. B. and Taylor, J. E.** (2003). "Exogenous jasmonic acid mimics herbivore-induced systemic increase in cell wall bound peroxidase activity and reduction in leaf expansion." *Funct. Ecol.* **17** (4): 549-554.
- Mueller, S. C., Brown, R. M. J. and Scott, T. K.** (1976). "Cellulosic microfibrils: nascent stages of synthesis in a higher plant cell." *Science* **194**: 949-951.
- Nakamura, Y., Wakabayashi, K. and Hoson, T.** (2003). "Temperature modulates the cell wall mechanical properties of rice coleoptiles by altering the molecular mass of hemicellulosic polysaccharides." *Physiol. Plant.* **118**: 597-604.
- Nishimura, M. T., Stein, M., Hou, B.-H., Vogel, J. P., Edwards, H. and Somerville, S. C.** (2003). "Loss of a callose synthase results in salicylic acid-dependent disease resistance." *Science* **301**: 969-972.

- Nishitani, K.** (1995). "Endo-xyloglucan transferase, a new class of transferase involved in cell wall construction." *J. Plant Res.* **108** (1089): 137-148.
- Nishitani, K. and Masuda, Y.** (1981). "Auxin-induced changes in the cell wall structure: changes in the sugar compositions, intrinsic viscosity and molecular weight distributions of matrix polysaccharides of the epicotyl cell wall of *Vigna angularis*." *Physiol. Plant.* **52**: 482-494.
- Nishitani, K. and Tominaga, R.** (1992). "Endoxyloglucan transferase, a novel class of glycosyltransferase that catalyzes transfer of a segment of xyloglucan molecule to another xyloglucan molecule." *J. Biol. Chem.* **267** (29): 21058-21064.
- Northcote, D. H.** (1985). "Cell organelles and their function in biosynthesis of cell wall components: control of wall assembly during differentiation". Biosynthesis and Degradation of Wood Components. T. Higuchi, Orlando, Florida, Academic: 87-108.
- Obel, N., Porchia, A. C. and Scheller, H. V.** (2002). "Dynamic changes in cell wall polysaccharides during wheat seedling development." *Phytochem.* **60**: 603-610.
- Ozeretskovskaya, O. L. and Romenskaya, I. G.** (1996). "Oligosaccharins as regulatory molecules of plants." *Russian J. Plant. Physiol.* **43** (3): 648-655.
- Parr, A. J., Waldron, K. W., Ng, A. and Parker, M. L.** (1996). "The wall-bound phenolics of Chinese water chestnut (*Eleocharis dulcis*)." *J. Sci Food Agric* **71**: 501-507.
- Pauly, M., Qin, Q., Greene, H., Albersheim, P., Darvill, A. and York, W. S.** (2001). "Changes in the structure of xyloglucan during cell elongation." *Planta* **212** (5-6): 842-850.
- Pear, J. R., Kawagoe, Y., Schreckengost, W. E., Delmer, D. P. and Stalker, D. M.** (1996). "Higher plants contain homologs of the bacterial celA genes encoding the catalytic subunit of cellulose synthase." *Proc. Natl. Acad. Sci. USA* **93**: 12637-12642.
- Perrin, R., Wilkerson, C. and Keegstra, K.** (2001). "Golgi enzymes that synthesize plant cell wall polysaccharides: finding and evaluating candidates in the genome era." *Plant Mol. Biol.* **47**: 115-130.
- Perrin, R. M., DeRocher, A. E., Bar-Peled, M., Zeng, W., Norambuena, L., Orellana, A., Raikhel, N. V. and Keegstra, K.** (1999). "Xyloglucan fucosyltransferase, an enzyme involved in plant cell wall biosynthesis." *Science* **284** (5422): 1976-1979.
- Potter, I. and Fry, S. C.** (1994). "Changes in xyloglucan endotransglycosylase (XET) activity during hormone-induced growth in lettuce and cucumber hypocotyls and spinach cell suspension cultures." *J. Exp. Bot.* **45** (280 SPEC. ISSUE): 1703-1710.

Preston, R. D. (1974). "Plant cell walls". Dynamic Aspects of Plant Ultrastructure. A. W. Robards, Maidenhead, McGraw-Hill: 256-309.

Rayle, D. L. and Cleland, R. E. (1992). "The acid growth theory of auxin-induced cell elongation is alive and well." *Plant Physiol.* **99**: 1271-1274.

Redondo-Nevado, J., Moyano, E., Medina-Escobar, N., Caballero, J. L. and Munoz-Blanco, J. (2001). "A fruit-specific and developmentally regulated endopolygalacturonase gene from strawberry (*Fragaria x ananassa* cv. Chandler)." *J. Exp. Bot.* **52** (362): 1941-1945.

Reid, J. S. G. and Meier, H. (1970). "Formation of reserve galactomannan in the seeds of *Trigonella foenum-graecum*." *Phytochem.* **9**: 513-520.

Reidy, B., McQueen, M. S., Nosberger, J. and Fleming, A. (2001). "Differential expression of alpha- and beta-expansin genes in the elongating leaf of *Festuca pratensis*." *Plant Mol. Biol.* **46** (4): 491-504.

Reis, D., Vian, B., Darzens, D. and Roland, J. C. (1987). "Sequential patterns of intramural digestion of galactoxyloglucan in tamarind seedlings." *Planta* **170** (1): 60-73.

Reiter, W. D., Chapple, C. and Somerville, C. R. (1997). "Mutants of *Arabidopsis thaliana* with altered cell wall polysaccharide composition." *Plant J.* **12** (2): 335-345.

Richmond, T. A. and Somerville, C. R. (2000). "The cellulose synthase superfamily." *Plant Physiol.* **124**: 495-498.

Richmond, T. A. and Somerville, C. R. (2001). "Integrative approaches to determining Csl function." *Plant Mol. Biol.* **47**: 131-143.

Robertson, D., Wojtaszek, P. and Bolwell, G. P. (1999). "Stimulation of cell wall biosynthesis and structural changes in response to cytokinin- and elicitor-treatments of suspension-cultured *Phaseolus vulgaris* cells." *Plant Physiol. Biochem.* **37** (7-8): 611-622.

Rose, J. K. C., Braam, J., Fry, S. C. and Nishitani, K. (2002). "The XTH family of enzymes involved in xyloglucan endotransglucosylation and endohydrolysis: Current perspectives and a new unifying nomenclature." *Plant Cell Physiol.* **43** (12): 1421-1435.

Rubery, P. H. and Northcote, D. H. (1970). "Effect of Auxin (2,4-Dichlorophenoxyacetic acid) on synthesis of cell wall polysaccharides in cultured sycamore cells." *Biochim. Biophys. Acta.* **222** (1): 95.

Sarria, R., Wagner, T. A., O, N. M. A., Faik, A., Wilkerson, C. G., Keegstra, K. and Raikhel, N. V. (2001). "Characterization of a family of Arabidopsis genes related to xyloglucan fucosyltransferase1." *Plant Physiol.* **127** (4): 1595-1606.

Saven
277

Saven
278
279

Schei
279
280
281

Selve
282

Selve
283
C. T.

Shieh
284
285

Show
5-9-2

Singh
286
287

Stace
288

Stoil
Der
289

Tak
290
291

Talb
292
293

Saxena, I. M. and Brown, R. M. J. (2000). "Cellulose synthases and related enzymes." *Curr. Opin. Plant Biol.* **3**: 523-531.

Saxena, I. M., Brown, R. M. J., Fevre, M., Geremia, R. A. and Henrissat, B. (1995). "Multidomain architecture of beta-glycosyltransferases: implications for mechanism of action." *J. Bacteriol.* **177**: 1419-1424.

Scheible, W.-R., Eshed, R., Richmond, T. A., Delmer, D. and Somerville, C. R. (2001). "Modifications of cellulose synthase confer resistance to isoxaben and thiazolidinone herbicides in *Arabidopsis lxr1* mutants." *Proc. Natl Acad. Sci. USA* **98** (18): 10079-10084.

Selvendran, R. R. (1985). "Developments in the chemistry and biochemistry of pectic and hemicellulosic polymers." *J. Cell Sci. Suppl.* **2**: 51-88.

Selvendran, R. R., Stevens, B. J. H. and O' Neill, M. A. (1985). "Developments in the isolation and analysis of cell walls from edible plants". Biochemistry of plant cell walls. C. T. Brett and J. R. Hillman, Cambridge University Press: 39-78.

Shieh, M. W., Shi, J. and Cosgrove, D. J. (1997). "Developmental, hormonal and light regulation of the transcript for the cell wall loosening protein expansin." *Plant Physiol.* **114** (3): 341. Suppl. S.

Showalter, A. M. (1993). "Structure and function of plant cell wall proteins." *Plant Cell* **5**: 9-23.

Singh, N. K., Handa, A. K., Hasegawa, P. M. and Bressan, R. A. (1985). "Proteins associated with adaptation of cultured tobacco cells to NaCl." *Plant Physiol.* **79** (1): 126-137.

Stacey, G., Greshoff, P. M. and Keen, N. T. (1992). "Friends and foes: new insights into plant-microbe interactions." *Plant Cell* **4**: 1173-1179.

Stolle-Smits, T., Beekhuizen, J. G., Kok, M. T. C., Pijnenburg, M., Recourt, K., Derksen, J. and Voragen, A. G. J. (1999). "Changes in cell wall polysaccharides of green bean pods during development." *Plant Physiol.* **121**: 363-372.

Takahashi, K., Fujino, K., Kikuta, Y. and Koda, Y. (1995). "Involvement of the accumulation of sucrose and the synthesis of cell-wall polysaccharides in the expansion of potato cells in response to jasmonic acid." *Plant Sci.* **111** (1): 11-18.

Talbott, L. D. and Ray, P. M. (1992). "Changes in molecular size of previously deposited and newly synthesized pea cell wall matrix polysaccharides effects of auxin and turgor." *Plant Physiol.* **98** (1): 369-379.

- Tateishi, A., Inoue, H., Shiba, H. and Yamaki, S.** (2001). "Molecular cloning of beta-galactosidase from Japanese pear (*Pyrus pyrifolia*) and its gene expression with fruit ripening." *Plant Cell Physiol.* **42** (5): 492-498.
- Tateishi, A., Inoue, H. and Yamaki, S.** (2002). "Cloning and expression of beta-galactosidase cDNA related to softening of avocado (*Persea americana*) fruit." *J. Jpn. Soc. Hortic. Sci.* **71** (1): 48-55.
- Taylor, N. G., Laurie, S. and Truner, S. R.** (2000). "Multiple cellulose synthase catalytic subunits are required for cellulose synthesis in Arabidopsis." *Plant Cell* **12**: 2529-2539.
- Taylor, N. G., Scheible, W.-R., Cutler, S., Somerville, C. R. and Turner, S. R.** (1999). "The irregular xylem3 locus of Arabidopsis encodes a cellulose synthase required for secondary cell wall synthesis." *Plant Cell* **11**: 769-779.
- Thomas, J. R., McNeil, M., Darvill, A. G. and Albersheim, P.** (1987). "Structure of plant cell walls XIX. Isolation and characterization of wall polysaccharides from suspension-cultured Douglas fir cells." *Plant Physiol.* **83** (3): 659-671.
- Thompson, J. E. and Fry, S. C.** (2000). "Evidence for covalent linkage between xyloglucan and acidic pectins in suspension-cultured rose cells." *Planta* **211** (2): 275-286.
- Tine, M. A. S., Cortelazzo, A. L. and Buckeridge, M. S.** (2000). "Xyloglucan mobilisation in cotyledons of developing plantlets of *Hymenaea courbaril* L. (*Leguminosae-Caesalpinoideae*)." *Plant Sci.* **154** (2): 117-126.
- Tokumoto, H., Wakabayashi, K., Kamisaka, S. and Hoson, T.** (2002). "Changes in the sugar composition and molecular mass distribution of matrix polysaccharides during cotton fiber development." *Plant Cell Physiol.* **43** (4): 411-418.
- Ueda, J., Miyamoto, K. and Hashimoto, M.** (1996). "Jasmonates promote abscission in bean petiole explants: Its relationship to the metabolism of cell wall polysaccharides and cellulase activity." *J. Plant Growth Regul.* **15** (4): 189-195.
- Vanzin, G. F., Madson, M., Carpita, N. C., Raikhel, N. V., Keegstra, K. and Reiter, W. D.** (2002). "The *mur2* mutant of Arabidopsis thaliana lacks fucosylated xyloglucan because of a lesion in fucosyltransferase AtFUT1." *Proc. Natl Acad. Sci. USA* **99** (5): 3340-3345.
- Vierhuis, E., York, W. S., Kolli, V. S. K., Vincken, J. P., Schols, H. A., Van, A. G. J. W. M. and Voragen, A. G. J.** (2001). "Structural analyses of two arabinose containing oligosaccharides derived from olive fruit xyloglucan: XXSG and XLSG." *Carbohydr. Res.* **332** (3): 285-297.

- Vincken, J. P., Wijsman, A. J. M., Beldman, G., Niessen, W. M. A. and Voragen, A. G. J.** (1996). "Potato xyloglucan is built from XXGG-type subunits." *Carbohydr. Res.* **288** (0): 219-232.
- Vincken, J. P., York, W. S., Beldman, G. and Voragen, A. G. J.** (1997). "Two general branching patterns of xyloglucan, XXXG and XXGG." *Plant Physiol.* **114** (1): 9-13.
- Wakabayashi, K.** (2000). "Changes in cell wall polysaccharides during fruit ripening." *J. of Plant Res.* **113** (1111): 231-237.
- Walton, J. D. and Ray, P. M.** (1982). "Inhibition by light of growth and Golgi-localized glucan synthetase in the maize mesocotyl." *Planta* **156**: 302-308.
- Wang, Q., Ellis, P. R., Ross, M. S. B. and Reid, J. S. G.** (1996). "A new polysaccharide from a traditional Nigerian plant food: *Detarium senegalense* Gmelin." *Carbohydr. Res.* **284** (2): 229-239.
- Warneck, H. and Seitz, H. U.** (1993). "Inhibition of gibberellic acid-induced elongation-growth of pea epicotyls by xyloglucan oligosaccharides." *J. Exp. Bot.* **44** (264): 1105-1109.
- Warneck, H. M., Fulton, D. C., Seitz, H. U. and Fry, S. C.** (1998). "Transport, degradation and cell wall-integration of XXFGol, a growth-regulating nonasaccharide of xyloglucan, in pea stems." *Planta* **204** (1): 78-85.
- Watt, D. K., Brasch, D. J., Larsen, D. S. and Melton, L. D.** (1999). "Isolation, characterisation, and NMR study of xyloglucan from enzymatically depectinised and non-depectinised apple pomace." *Carbohydr. Polymers* **39** (2): 165-180.
- Williamson, R. E., Burn, J. E. and Hocart, C. H.** (2002). "Towards mechanism of cellulose synthesis." *Trends Plant Sci.* **7** (10): 461-467.
- Wu, C. T. and Bradford, K. J.** (2003). "Class I chitinase and beta-1,3-glucanase are differentially regulated by wounding, methyl jasmonate, ethylene, and gibberellin in tomato seeds and leaves." *Plant Physiol.* **133** (1): 263-273.
- Wu, Y., Spollen, W. G., Sharp, R. E., Hetherington, P. R. and Fry, S. C.** (1994). "Root growth maintenance at low water potentials: Increased activity of xyloglucan endotransglycosylase and its possible regulation by abscisic acid." *Plant Physiol.* **106** (2): 607-615.
- Xu, W., Purugganan, M. M., Polisensky, D. H., Antosiewicz, D. M., Fry, S. C. and Braam, J.** (1995). "Arabidopsis TCH4, regulated by hormones and the environment, encodes a xyloglucan endotransglycosylase." *Plant Cell* **7** (10): 1555-1567.

York, W. S., Darvill, A. G. and Albersheim, P. (1984). "Inhibition of 2,4-D stimulated elongation of pea stem segments by a xyloglucan oligosaccharide." *Plant Physiol.* **75** (2): 295-297.

York, W. S., Kolli, V. S. K., Orlando, R., Albersheim, P. and Darvill, A. G. (1996). "The structures of arabinoxyloglucans produced by solanaceous plants." *Carbohydr. Res.* **285** (0): 99-128.

York, W. S., Van Halbeek, H., Darvill, A. G. and Albersheim, P. (1990). "Structural analysis of xyloglucan oligosaccharides by proton NMR spectroscopy and fast-atom-bombardment mass spectrometry." *Carbohydr. Res.* **200**: 9-32.

Zhong, R., Morrison III, W. H., Freshour, G. D., Hahn, M. G. and Ye, Z.-H. (2003). "Expression of a mutant form of cellulose synthase AtCesA7 causes dominant negative effect on cellulose biosynthesis." *Plant Physiol.* **132**: 786-795.

Zurek, D. M. and Clouse, S. D. (1994). "Molecular cloning and characterization of a brassinosteroid-regulated gene from elongating soybean (*Glycine max* L.) epicotyls." *Plant Physiol.* **104** (1): 161-170.

CHAPTER 2

Cloning and Expression Studies of Xyloglucan Fucosyltransferase

Part of the work presented in this chapter has been published:

Perrin, R. M., DeRocher, A. E., Bar-Peled, M., Zeng, W., Norambuena, L., Orellana, A.,

Raikhel, N. V. and Keegstra, K. (1999). *Science* 284 (5422): 1976-1979.

Faik, A., Bar-Peled, M., DeRocher, A. E., Zeng, W., Perrin, R. M., Wilkerson, C.,

Raikhel, N. V. and Keegstra, K (2000). *J. Biol. Chem.* 275 (20): 15082-15089.

ABSTRACT

XyG is the major hemicellulose in the primary cell wall of dicot and nongraminaceous monocot plants. However, the genes involved in its biosynthesis are still largely unknown. In our previous effort to identify genes involved in XyG biosynthesis, XyG fucosyltransferase was purified from etiolated pea epicotyls, and a partial-length cDNA clone was identified from Arabidopsis using the protein sequence information obtained. The first part of this chapter describes the identification of a full-length cDNA encoding the Arabidopsis XyG fucosyltransferase, using sequence information obtained from a genomic BAC clone, T18E12. Part of the polypeptide encoded by this cDNA was expressed in *E. coli* cells, and a polyclonal antibody against it was generated. This antibody was used to immunoprecipitate XyG fucosyltransferase activity from detergent-solubilized Arabidopsis membrane proteins. Heterologous expression of this cDNA in mammalian COS7 cells or tobacco BY2 cells produced XyG fucosyltransferase activity, thereby confirming the identity of this cDNA clone. Furthermore, the tryptic peptide sequence information obtained from the purified pea XyG fucosyltransferase protein led to the isolation of a full-length pea cDNA encoding this enzyme. Sequence comparison revealed that pea XyG fucosyltransferase and its Arabidopsis equivalent are very close orthologs. The second part of this chapter describes the rapid elongation of the internodes of etiolated pea seedlings at early growth stages and the expression of pea XyG fucosyltransferase during the growth process. The data presented here have established a correlation between the internode elongation rate and XyG fucosyltransferase expression.

المشقة

56

23

10

10

10

2

100

•

3

•

1

22

2

10



4

1.

Introduction

XyG has the same β -(1,4)-glucan backbone as cellulose, but with side chain decorations of L-Fuc-(1,2)-D-Gal-(1,2)-D-Xyl-(1,6); D-Gal-(1,2)-D-Xyl-(1,6); and D-Xyl-(1,6) (Figure 1.1) (Kato and Matsuda, 1980; Fry, 1989). The terminal fucose residue is thought to have an important function in stabilizing a planar configuration of the XyG backbone that is essential for cellulose binding as determined by molecular modeling and in vitro binding studies (Hayashi et al., 1994; Cosgrove, 1997; Levy et al., 1997), although contradictory evidence has also been presented (Whitney et al., 1995). The terminal fucose has also been suggested to be involved in signal transduction during plant growth and development. Some oligosaccharides produced by partial digestion of XyG influence the growth rate of intact plant tissue at very low concentrations (Darvill et al., 1992; Aldington and Fry, 1993). One oligosaccharide, XXFG, is able to antagonize the growth promoting effect of auxin at a concentration of 10^{-9} M (York et al., 1984), but loses its effectiveness when the terminal fucose is absent (McDougall and Fry, 1989). Therefore the fucose was hypothesized to determine the ability of XyG oligosaccharides to act as signaling molecules in vivo (McDougall and Fry, 1989).

GDP-fucose:XyG 1,2- α -L-fucosyltransferase is the enzyme responsible for the attachment of fucose onto galactose of the XyG sidechains. Given the importance that the terminal fucose might have, we sought to identify the gene encoding the enzyme that adds it to XyG. A biochemical approach was used to purify the enzyme while monitoring its activity using an in vitro assay developed by Maclachlan's group (Farkas and Maclachlan, 1988). This assay uses radiolabeled GDP-fucose as donor and tamarind seed XG that naturally lacks the terminal fucose as acceptor (Farkas and Maclachlan, 1988;

Hanna et al., 1991; Desveaux et al., 1998). The enzyme activity of XyG fucosyltransferase has been partially purified from pea epicotyl microsomal membranes (Hanna et al., 1991; Desveaux et al., 1998). The activity co-migrated with a 150 kD peptide observed on a nondenaturing gel (Hanna et al., 1991). However, previous attempts to purify the protein to homogeneity or to clone the XyG fucosyltransferase gene had not been successful. Neither had any other genes encoding enzymes involved in XyG biosynthesis been cloned.

Etiolated pea epicotyls contain significant amount of XyG fucosyltransferase activity (Farkas and Maclachlan, 1988; Hanna et al., 1991; Maclachlan et al., 1992). Consequently this tissue was used by Drs. Amy E. DeRocher and Maor Bar-Peled in our group to successfully purify this enzyme, utilizing a combination of GDP affinity and anion exchange chromatography (Perrin et al., 1999). Information from the purified protein led to the identification of a partial cDNA clone from Arabidopsis. The first half of this chapter describes the cloning of the full-length coding region of the Arabidopsis XyG fucosyltransferase (AtFut1) and its pea equivalent (PsFut1) based on peptide sequence information obtained from the purified enzyme.

For the work on the identification of Arabidopsis XyG fucosyltransferase (Perrin et al., 1999), my role was the isolation of a full-length coding region of AtFut1, and the generation and characterization of a polyclonal antibody against *E. coli*-expressed AtFUT peptide. For the work on pea (Faik et al., 2000), my role was the isolation of a full-length coding region of PsFut1, as well a genomic clone with the intron and the untranslated regions (UTR).

With the identification of XyG fucosyltransferase genes (Perrin et al., 1999; Faik et al., 2000), it is feasible to study for the first time the relationship between plant growth and development and XyG biosynthesis at the molecular level. At the time this work was done, XyG fucosyltransferase was the only molecular tool available with its gene cloned and with an in vitro enzyme assay.

The process of cell growth often involves up to a thousand fold increase in cell volume (Pennell, 1998). The cell enlargement is brought about by a process of relaxation of existing cell walls, the synthesis and deposition of new cell wall polysaccharides, and the cross linking of new and old wall materials. Therefore enzymes involved in these three aspects of cell wall growth, wall degradation, wall modification, and wall biosynthesis, are all thought to be delicately regulated during plant growth.

XyG plays a key role in controlling cell wall expansion by providing mechanical strength and physical integrity to cell walls via cross-linking the cellulose microfibrils (Cosgrove, 2000). As the major hemicellulose of the primary cell wall for dicot and nongraminaceous plants, XyG undergoes rapid synthesis and also turnover during plant growth and development (Pauly et al., 2001). An α -xylosidase that degrades XyG oligosaccharides isolated from *Arabidopsis* showed higher enzyme activity and messenger RNA abundance in younger leaves, where XyG turnover is higher (Sampedro et al., 2001). XyG endotransglycosylase (XET) and expansin are two additional types of wall modifying proteins. XET cleaves XyG mid-chain and then transfers the cleaved XyG molecule to the non-reducing end of another XyG chain (Sulova et al., 1998; Steele and Fry, 1999). Expansins are thought to loosen the polysaccharide associations, mainly cellulose – XyG association or XyG – XyG association, to allow slippage or the

100

101

102

103

104

105

106

107

108

109

110

111

112

113

114

115

116

117

118

119

120

121

deposition of new wall materials (Cosgrove, 2000). More XET mRNAs were detected in elongating stems, during phytohormone-induced plant growth and during fruit softening (Steele et al., 2001). A root-specific soybean expansin, GmEXP1, also shows higher transcript abundance during root rapid elongation (Lee et al., 2003). Even though there are clear indications that enzyme activities involved in XyG biosynthesis (XyG synthase and XyG fucosyltransferase) are regulated during plant development and primary wall biosynthesis (Hayashi and Matsuda, 1981; Pauly et al., 2001), there has never been any molecular studies on the regulation of gene expression, because none of the genes involved in XyG biosynthesis had been cloned. I tried to address this question in the second part of this chapter utilizing the molecular tool of pea XyG fucosyltransferase.

Many scientists have used etiolated pea as a model system to study the expression of enzymes involved in cell wall biosynthesis, including the development of enzyme activity assays and the partial purification of XyG fucosyltransferase (Camirand and Maclachlan, 1986; Farkas and Maclachlan, 1988; Hanna et al., 1991; Maclachlan et al., 1992). Etiolated pea seedlings have a relatively simple morphology and large amount of rapidly growing tissue. At a young stage of growth etiolated pea seedlings contain both fast growing and non-growing tissues. Seedling growth occurs in a visible manner. Its XyG oligosaccharides were also well characterized (Hayashi and Maclachlan, 1984; Guillen et al., 1995). This plant has therefore become an attractive model for both biochemists and molecular biologist (Labavitch and Ray, 1974; Talbott and Ray, 1992), and In the second half of this chapter, etiolated pea seedlings were used to correlate the expression patterns of the XyG fucosyltransferase with plant growth stages.

MATERIALS AND METHOD

Plant material

Pisum sativum cv. Alaska seeds were sterilized with 10% bleach at room temperature for 15 min and rinsed 4 to 5 times with running water before being imbibed overnight (~12 hr) with aeration. Seeds were planted in coarse vermiculite and grown in the dark at 25°C. Internode length was measured in the dark under green safe light with a ruler. Pea tissues were also collected in the dark under safe light and stored on ice until used.

Preparation of pea microsomes

Pea seedling samples were cut into small pieces and homogenized in extraction buffer (40 mM Hepes-KOH, pH6.5, 0.2 M sucrose, 1 mM dithiothreitol [DTT], 1 mM MgCl₂, 0.2 mM phenylmethanesulfonyl fluoride [PMSF]) with a Polytron for 15 seconds four times on ice. The homogenate was filtered through a double layer of miracloth and centrifuged at 10,000×g for 10 minutes at 4°C. The supernatant was collected as the S10 fraction and centrifuged again at 100,000×g for 1 hour at 4°C. The pellet, labeled P100, was resuspended in extraction buffer using an ice-cold Dounce homogenizer. The protein concentration of P100 microsomes was determined with the BCA protein assay reagent (PIERCE, Rockford, Illinois).

Oligonucleotide primer synthesis and PCR product sequencing

All oligonucleotide primers were synthesized at the Macromolecular Sequencing and Synthesis Facility in the Department of Biochemistry, Michigan State University. All

PCR reactions were carried out in a Peltier thermal cycler-200 (MJ Research). PCR products were all purified from low melting point agarose gel and cloned into pGEM-T Easy vector (Promega, Madison, WI) for sequencing. Sequence alignments were carried out using the software package DNASTAR version 4.0 (Madison, WI) and GCG programs (Madison, WI). DNA sequencing was done either at the Genomics Technology Support Facility at Michigan State University or the W. M. Keck Biotechnology Resource Lab, Yale University.

RNA isolation, gel electrophoresis and Northern blotting

Total RNA from pea seedlings was isolated according to a standard protocol (Houdebine and Puissant, 1990). Messenger RNA was isolated from total RNA in the same way as for mRNAs used for RACE reactions. RNA separation by formaldehyde gel electrophoresis, RNA blotting to N⁺ Hybrid-bond Nylon membrane, and Northern hybridization all followed standard protocols (Sambrook et al., 1989) except that the hybridization buffer used was 0.25 M Na₂HPO₄, 7% sodium dodecyl sulfate (SDS), 1 mM EDTA, pH 7.6.

Preparation of E. coli competent cells

A single colony of DH5α or BL21 (pLysS) was picked from a fresh LB plate and inoculated in 10 ml LB for overnight culturing at 37°C. On the second day, 3 ml of the mini culture was inoculated into 300 ml of new LB medium (at 1:100 dilution) and allowed to grow at 30°C with brisk shaking (≥ 250 rpm) until the OD₆₀₀ reached 0.3 to 0.6. The bacterial culture was chilled on ice for 10 to 15 minutes and all following steps

were carried out on ice. Cells were collected by centrifugation at 1,000×g for 15 minutes at 4°C and resuspended by swirling in 100 ml (1/3 of the starting culture volume) of RF1 buffer (100 mM RbCl, 50 mM MnCl₂, 30 mM KOAc-pH7.5, 10 mM CaCl₂, 15% glycerol, pH 6.0 with acetic acid, filter sterilized) that was pre-chilled on ice. The cell suspension in RF1 buffer was incubated on ice for 0.5 to 2 hours. Cells were then pelleted again under the same conditions and resuspended again in 24 ml (1/12.5 to 1/20 of the starting culture volume, depending on the OD600 value when the cells were collected) of pre-chilled RF2 buffer (10 mM MOPS-pH6.8, 10 mM RbCl, 75 mM CaCl₂ and 15% glycerol, filter sterilized) by swirling and incubated on ice for 15 minutes up to 12 hours. Cells were then divided into aliquots and placed into pre-chilled eppendorf tubes on ice in the cold room and quickly frozen by dropping them into liquid nitrogen. Competent cells were stored at -80°C for up to four years.

5'and 3' RACE

Poly(A)⁺ RNA was isolated from total RNA using the polyATtract mRNA Isolation System IV (Promega). RACE reactions were carried out using the 5'-RACE System, version 2.0 (Life Technologies, Inc.) according to the manufacturer's instructions. For 5'-RACE, kee258 (5'-ACTCCCGGGTCAACTAGTAGAA-3') was used for cDNA synthesis, and kee305 (5'-GGCTGACTGATACCTGCTGAGACAAGATTTTT-3') or kee304 (5'-GTTTGTGTCGGGCTTCATATT-3') were used as the nested primers. For 3'-RACE, poly (dT) primer was used for cDNA synthesis, and kee302 (5'-CCAAAAAGCCTGGGCAGAAAT-3') was the nested primer. For both reactions 1.5 µg mRNA were used for reverse transcription.

Construction of plasmid pBS-AtFut1

Oligonucleotide primers kee213 (5'-GATCCAGAGTCTCCCTCAAGAGCAATCCATGGATCAG-3') and kee214 (5'-AATTCTGATCCATGGATTGCTCTTGAGGGAGACTCTG-3') were designed to contain the missing sequence of the partial Arabidopsis XyG fucosyltransferase cDNA clone 6-1B1 (Perrin et al., 1999) and to contain restriction sites BamHI and EcoRI at their ends and a NcoI site in the middle (Figure 2.1A). About 2 µg of each primer were vacuum dried and redissolved separately in polynucleotide kinase (PNK) buffer (Boehringer Mannheim) containing 1 mM ATP in a total volume of 20 µl each. Primers were phosphorylated at 37°C for 15 minutes by 10 units of PNK followed by 15 minutes incubation at 70°C to inactivate the enzyme. Phosphorylated primers were mixed together and denatured at 95°C for 30 seconds, then transferred to a water bath at 90°C. The primer mixture in the water bath then was allowed to air cool to 30°C on a lab bench. The annealed oligonucleotide primers were inserted into vector pBlueScript SK (+) via restriction enzymes BamHI and EcoRI. A positive clone was selected by restriction digestion of plasmids with NcoI and named as pBS-AtFut1-NcoI. Its identity was further confirmed by sequencing.

Plasmid DNA of pBS-AtFut1-NcoI was linearized with EcoRI digestion, dephosphorylated with calf intestinal alkaline phosphatase (CIP) and purified via low melting point agarose gel. The insert released from cDNA clone 6-1B1 by EcoRI digestion was purified the same way and ligated into the treated pBS-AtFut1-NcoI vector, giving rise to the construct of pBS-AtFut1 containing the full coding region for AtFut1.

Construct pBS-AtFut1 was screened by double digestion with NcoI and BglII. After digestion the construct with insert in the right direction gave rise to two fragments of 1.2 kb and 3.52 kb while constructs containing the insert in the opposite direction gave rise to two fragments of 0.56 kb and 4.16 kb.

Construction of expression plasmids pET-AtFut1-1.2 and pET-AtFut1-2.3

DNA fragments of AtFut1-1.2 and AtFut1-2.3 were amplified by PCR reactions using primers kee176 (5'-AACTACTACCATATGAAGTATCTCAGCT-3', NdeI site underlined) and kee178 (5'-CACAAGAATTCATACTAGCTTAAGTC-3', EcoRI site underlined), or primers kee177 (5'-TAAATTGGCATATGGTTTCGCCGAA-3', NdeI site underlined) and kee178, and plasmid DNA of pBS-AtFut1 as template. Gel purified PCR products were inserted into expression vector plasmid pET28a through restriction sites NdeI and EcoRI to give rise to the expression plasmids pET-AtFut1-1.2 and pET-AtFut1-2.3. Positive clones were screened by a combination of digestions using BglII alone, XhoI alone, NdeI plus EcoRI, or KpnI plus SacI. Positive clones selected were sequenced to confirm their identities.

Expression of pET-AtFut1-1.2 and pET-AtFut1-2.3

Expression plasmids pET-AtFut1-1.2, pET-AtFut1-2.3, and vector control pET28a were transformed into *E. coli* expression strain BL21 (DE3)-pLysS. One colony was picked up for each construct for protein expression and inoculated in 10 ml LB with 50 µg/ml kanamycin for overnight culture at 37°C. On the second day new cultures of 200 ml were inoculated with 2 ml overnight culture. Cells were induced with 1 mM IPTG

at 37°C when their OD600 value reached 0.4 to 0.6. One milliliter of cell culture was collected before induction and every hour after induction for 4 hr. After measuring the OD600 value, cells were collected and resuspended in adequate amount of 2× SDS-polyacrylamide gel electrophoresis (PAGE) loading buffer. The volumes of the loading buffer used were adjusted according to the OD600 values of individual cell culture so that the final concentration of the cells roughly equaled to each other. Total proteins from equal amount of cells collected from different induction time points were resolved by SDS-PAGE and visualized by Commassie staining or western blotting with antibodies against the 6×His tag. SDS-PAGE loading buffer contained 62.5 mM Tris·HCl (pH6.8), 2% SDS, 10% glycerol, 5% β-mercaptoethanol and 0.01% bromphenol blue.

Solubility test of peptide AtFUT1-2.3

After being induced for 4 hr, a 2 ml culture of cells containing pET-AtFut1-2.3 was collected and washed once with PBS buffer and resuspended in 200 µl PBS buffer. After sonication at a 10 seconds duration for a total of 1 min in an output of 50% on ice, an aliquot of 20 µl was taken out as total protein. The sonicated solution was spun at 4°C for 5 minutes at 10,000×g. The pellet was resuspended in 180 µl PBS buffer by sonication and designated as the P10 fraction. The supernatant was saved as the S10 fraction. After removing an aliquot of 20 µl, the S10 fraction was centrifuged again at 100,000×g for 30 minutes at 4°C. This time the supernatant was saved as S100, and the pellet was resuspended in 160 µl PBS buffer by sonication and designated as P100. Aliquots of 20 µl from each fraction was used for SDS-PAGE.

Purification of peptide AtFUT1-2.3

A colony that showed high expression of peptide AtFUT1-2.3 was inoculated into 1 liter of LB medium at 37°C and induced with 1 mM IPTG when the OD₆₀₀ reached 0.47. After 5 hr, the cells were collected and washed once with 50mM Tris·HCl (pH7.8) buffer containing 5 mM MgCl₂, and resuspended in 20 ml of the same buffer. Cells were lysed by adding lysozyme to a final concentration of 100 µg/ml and DNase I to a final concentration of 10 U/ml followed by sonication on ice for 1 min at 50% output. The protein inclusion bodies were pelleted at 10,000×g for 10 min and washed four times with 1% Triton X-100 and four times with H₂O. This protein pellet was then solubilized in 12 ml of 6 M guanidine hydrochloride buffer and precipitated with trichloroacetic acid (TCA). The pellet was resuspended in 2 ml of 6 M guanidine hydrochloride and analyzed on SDS-PAGE with bovine serum albumin (BSA) as standard.

Generation of polyclonal antibodies against purified AtFUT1-2.3 peptide

About 600 µg of protein in 6 M guanidine hydrochloride buffer were emulsified with Titermax adjuvant (CytRx Corporation, Norcross GA) and injected into two New Zealand White rabbits (MSU Clinical Center Animal Service) No. 61 and No. 86. The rabbits were each boosted with 50 µg protein two weeks after the first bleed and the second bleed was collected after two more weeks. All blood samples were allowed to clot at 37°C for 30 minutes. The clots stuck to the wall of tubes were scraped down with Pasteur pipette. The clotted blood was allowed to sit at 4°C overnight and then spun for 10 min at 1800×g in a Sorvall RT 6000D centrifuge. The supernatant was collected as

serum and sodium azide was added to a final concentration of 0.02%. Sera were stored at -20°C for long term and 4°C for short term use.

Isolation of full-length coding region and genomic clone of PsFut1

All five tryptic peptide sequences obtained from purified pea XyG fucosyltransferase were conceptually reverse translated into nucleotide sequences. After analyzing the degenerate rate of each nucleotide sequence and the length of possible PCR amplification products from using each two of them as primers, two of these five peptides P5 and P2 were chosen for the design of degenerate primers. Part of the P5 peptide sequence (ADGFDEK) was used to design the upstream degenerate primer kee230 (5'-GCIGAYGGITTYGAYGARAA-3'; I = inosine; R = purines, A or G; Y = pyrimidines, C or T), and part of the P2 peptide sequence (HPTNNVWG) was used to design the downstream degenerate primer kee232 (5'-ICCCCAIACRTTTRTTIGTIGGRTG-3'). The template used for fragment PsFut1-a amplification is a plasmid cDNA library derived from apical hooks of 4-hour-auxin-treated etiolated pea seedlings in vector pBluescript SK (+) and was kindly provided by Dr. Hans Kende (Department of Energy Plant Research Laboratory, Michigan State University). In a PCR reaction of 50 µl, 0.1 µl of cDNA library template and 50 pmol of each primer were used. A discontinuous touchdown PCR program was designed with the reaction carried for 3 cycles at annealing temperature of 60°C, then 10 cycles at 55 °C, and then 50 °C for 25 cycles. Taq polymerase, and dNTPs were added after the denaturing step during the first amplification cycle to hot start the reaction.

Second round PCR reactions were performed under the same conditions using PsFut1-a specific primers (kee257: 5'-TTCTACTAGTTGACCCGGGAGT-3'; kee258: 5'-ACTCCCGGGTCAACTAGTAGAA-3') and the cDNA library vector specific primers (REV: 5'-TCAGGAAACAGCTATGACCATG-3'; DIR: 5'-GTAATACGACTCACTATAGGGC-3'). Primers kee257 and kee258 were designed from a 21 bp region from PsFut1-a that bears unique restriction digestion sites for HincII, Aval, XmaI, HapII, MspI and SmaI. Primers REV and DIR were derived from the sequences outside the polylinker area of the vector plasmid pBluescript SK (+) in which the template cDNA library was constructed. The same parameters and template were used as for the amplification of fragment PsFut1-a with the program being slightly modified to 10 cycles of amplification at an annealing temperature of 65°C, 20 cycles at 60°C and 10 cycles at 55°C.

The full-length cDNA coding region of PsFut1 was amplified using Pwo polymerase (Roche Molecular Biochemicals), end-specific primers (kee322: 5'-AATGAATATGCTGATAAAGAGAGTC-3' and kee323: 5'-CTAATTGTCTACGAGCTTAAGGC-3', start and stop codons are bolded), and the same cDNA library as template under the same PCR conditions for PsFut1-a amplification. Clone PsFut1-geno was amplified by the same reaction using 300 ng pea genomic DNA as template. Clone PsFut1-5UTR was amplified with primers kee324 (5'-ACGAGACATTCGTTCTAATTTACG-3') and kee325 (5'-CAAAGTCAAAGGGCATGTTGTAC-3') with 300 ng genomic DNA as template.

Xyloglucan fucosyltransferase enzyme activity assay

Microsomal membrane samples were solubilized with 1% Triton X-100 for 15 minutes on ice immediately before enzyme assays were performed. In a fucosyltransferase activity assay reaction of 50 μ l, 10 μ l of solubilized P100 membranes (9 μ l P100 sample plus 1 μ l 10% Triton X-100) was added with 20 μ l of 2.5 \times Reaction Buffer (100 mM HEPES·KOH pH6.8, 0.5 M Sucrose, 2.5 mM DTT, 2.5 mM MgCl₂), 10 μ l of 1% tamarind seed XyG and 2.5 μ l (diluted to 10 μ l with H₂O before use) of GDP ¹⁴C-fucose (10 μ Ci/ml and 271 mCi/mmol) (NEN Life Science Products, Inc.). Reactions were carried out at room temperature and stopped with 1 ml of 70% ethanol. Products of the enzyme assays were precipitated at 4°C or room temperature for at least 2 hours and washed three times with 70% ethanol. After the last washing, the pellet was briefly air dried and resuspended in 200 μ l H₂O for scintillation counting.

Images in this thesis are presented in color

RESULTS

Isolation of full length cDNA clone encoding AtFUT1

XyG fucosyltransferase was purified from microsomes derived from the epicotyls of etiolated pea (*Pisum Sativum* var. Alaska) seedlings by Drs. Amy DeRocher and Maor Bar-Peled. Although a 1400× enrichment over microsomal membranes was achieved, two proteins were present in the final preparation. Tryptic peptides derived from each purified protein were subjected to sequencing (Perrin et al., 1999). One of the proteins was identified as a homolog of Hsp70 and therefore was not pursued further. Database searches using the resulting sequence information from the other protein led to the identification of an Arabidopsis clone from the PRL-2 EST library that encoded four of the six tryptic peptides. Screening of a size-fractionated Arabidopsis cDNA library (Kieber et al., 1993) with this EST sequence yielded cDNA clone 6-1B1 (Perrin et al., 1999).

The sequence of this cDNA was compared with that of a newly deposited BAC, T18E12. An open reading frame (ORF) from T18E12 contained all the sequence of 6-1B1 plus regions encoding three amino acids at the N-terminus, and a region before that presumably to be the 5' untranslated region. I began working on the project at about this time and participated in generating a full-length clone for the gene we identified as described here. A pair of complementary oligonucleotide primers designed to contain sequences encoding the missing first three amino acids (Figure 2.1A) were annealed and inserted into vector plasmid pBluescript SK (+). The AtFut1 coding region from clone 6-1B1 was then inserted into the same plasmid vector right after the annealed primers, giving rise to the full-length clone pBS-AtFut1 (Figure 2.1B). The full-length clone pBS-

Figure 2.1: Cloning of full-length coding region of AtFut1. **A.** Complementary primers containing the sequence encoding the missing first three amino acids (in bold) of AtFut1. Restriction enzyme recognition sites are italic. **B.** Cloning procedure for pBS-AtFut1. Primers kee213 and kee214 were annealed and inserted into pBluescript through BamHI and EcoRI to form intermediate plasmid pBS-AtFut1-NcoI. The fragment of AtFut1 released from clone 6-1B1 was inserted behind the annealed primers on pBS-AtFut1-NcoI through restriction site EcoRI to form the construct pBS-AtFut1. When digested with NcoI and BglII, pBS-AtFut1 gave rise to two fragments of 1.2 kb and 3.52 kb. The construct containing an opposite insert yielded two fragments of 0.56 kb and 4.16 kb when digested with the same enzymes.

A

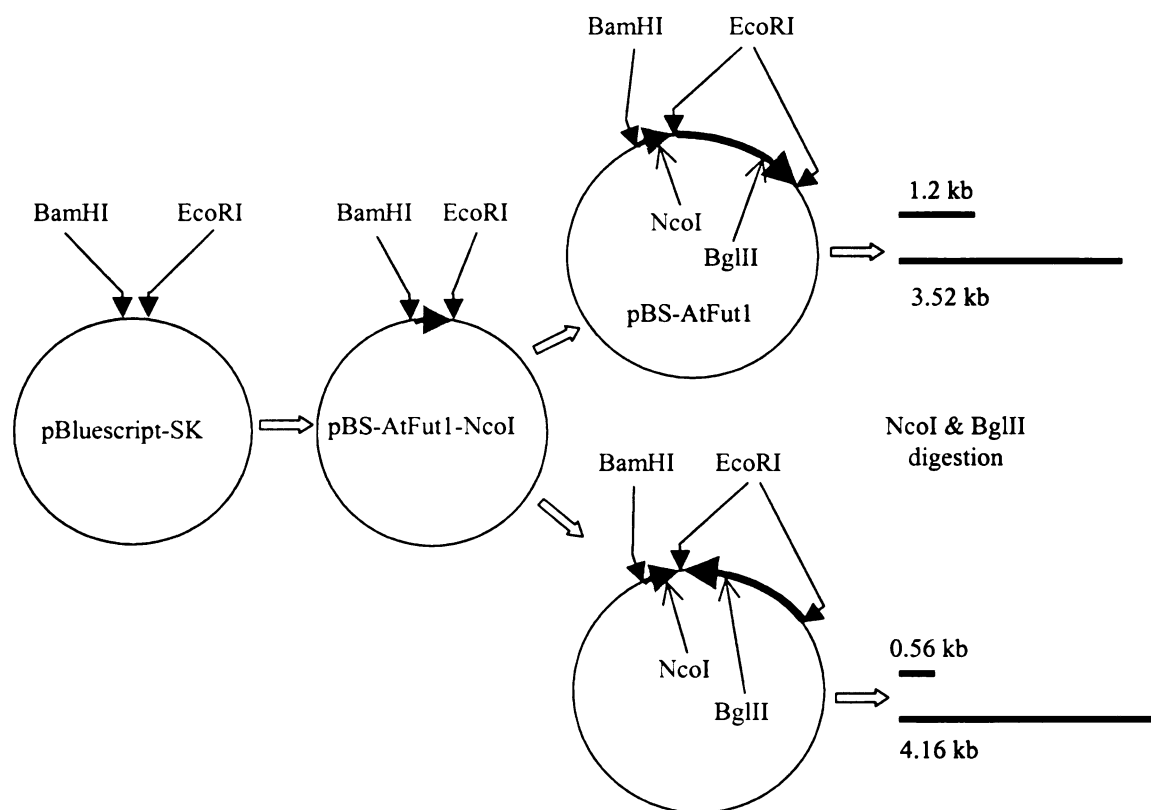
KEE213: 5' GATCCAGAGTCTCCCTCAAGAGCAATCC**ATGGATCAG** 3'
 KEE214: 3' GTCTCAGAGGGAGTTCTCGTTAGG**TACCTAGTC**TTAA 5'

BamHI

NcoI

EcoRI

B



➡ : annealed primers kee213 and kee214

↪ : EcoRI fragment released from clone 6-1B1

AtFut1 was expressed in both COS-7 cell lines (Perrin et al., 1999) and tobacco BY2 cell lines (Sarria et al., 2001). In both cases, the expressed proteins were able to transfer fucose from GDP-fucose to tamarind XyG, thereby confirming the identity of this clone as XyG fucosyltransferase.

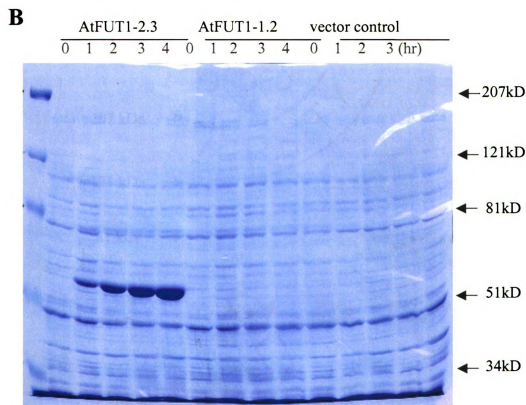
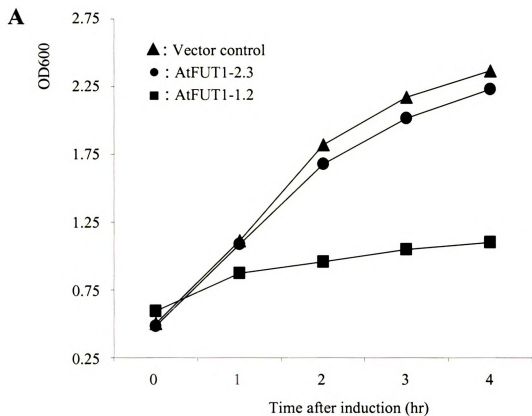
Expression of AtFUT1 partial polypeptide in E. coli cells and the generation of antibodies against it

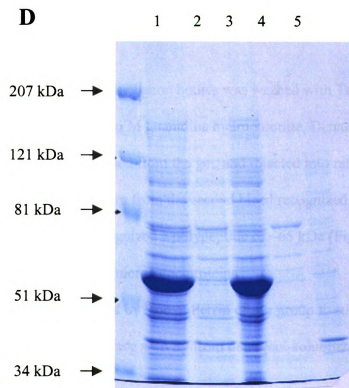
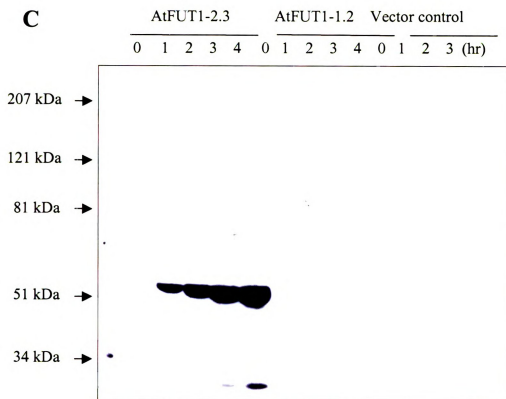
To further confirm the identity of the cDNA clone of AtFut1 and explore its expression patterns during plant growth, a polyclonal antibody was generated against an AtFUT1 polypeptide expressed in *E. coli* cells.

Two DNA fragments of AtFut1, AtFut1-1.2 and AtFut1-2.3, were amplified by PCR reactions and inserted into vector pET28a behind a 6×His tag. Clone pET-AtFut1-1.2 encoded a peptide starting from Met 31 until the end of AtFUT1 and contained the putative transmembrane domain that is predicted for the region between residues 45 and 62. Clone pET-AtFut1-2.3 encoded a peptide starting from Met 73 until the end of AtFUT1 and did not contain the transmembrane domain.

Peptide AtFUT1-2.3 was expressed in large quantity after IPTG induction and was detected easily with both Commassie stained SDS-PAGE gel (Figure 2.2B) and antibodies against the 6×His tag (Figure 2.2C). However the majority of the expressed polypeptide was detected in inclusion bodies (Figure 2.2D). Attempts to prevent the formation of inclusion bodies by lowering the induction temperature, shortening the culture time after induction, or using lower concentration of the inducing reagent IPTG

Figure 2.2: Expression of peptides AtFUT1-1.2 and AtFUT1-2.3 in BL21 (DE3)-pLysS cells. **A:** Growth curve after IPTG induction of BL21 cells containing plasmids pET-AtFut1-2.3, pET-AtFut1-1.2 and vector control pET28a. **B:** Commassie Blue stained 10% SDS-PAGE showing the induction time course of AtFUT1-2.3, AtFUT1-1.2 and vector control (1 mM IPTG at 37°C). **C:** Western blot of the same gel as in **B** using antibodies against 6×His Tag (PIERCE). **D:** The solubility test of overexpressed peptides AtFUT1-2.3 (1. Total protein after 4 hour induction; 2. 10,000×g supernatant after sonication; 3. 10,000×g pellet after sonication; 4. 100,000×g supernatant from sample 2; 5. 100,000×g pellet from sample 2).





all yielded negative results. XyG fucosyltransferase activity was not detected from either the soluble protein fractions or the inclusion bodies.

Peptide AtFUT1-1.2 with the transmembrane domain was not expressed when the plasmid was introduced into BL21 (DE3)-pLysS cells (Figure 2.2B). After induction with IPTG the growth of the cell culture expressing construct pET-AtFut1-1.2 was highly suppressed as its OD600 value had only very limited increase during the incubation time (Figure 2.2A). No protein of the expected size could be detected by either coomassie staining of SDS-PAGE gel (Figure 2.2B) or by immunoblotting with antibodies against the 6×His tag (Figure 2.2C). Different colonies containing plasmid pET-AtFut1-1.2 in BL21 (DE3)-pLysS were tried for induction but yielded similar results. Efforts to induce the expression of peptide AtFUT1-1.2 under lower culture temperature or with lower IPTG concentration or under both conditions yielded no recombinant protein. This toxicity seemed to be due to the presence of the transmembrane domain of the peptide since peptide AtFUT1-2.3 lacking the transmembrane domain was expressed in *E. coli* cells (Figure 2.2).

Peptide AtFUT1-2.3 in the inclusion bodies was washed with Triton X-100 and water three times and denatured in 6 M guanidine hydrochloride. Denatured peptides were resolved in SDS-PAGE, excised from the gel, and injected into rabbits to generate polyclonal antibodies. The antiserum from the second bleed recognized the *E. coli* antigen very strongly and also recognized a polypeptide of ~65 kDa (Figure 2.3) from detergent-solubilized Arabidopsis microsome proteins.

This antibody was then used by Robyn Perrin of our group to successfully precipitate the XyG fucosyltransferase activity from detergent-solubilized Arabidopsis

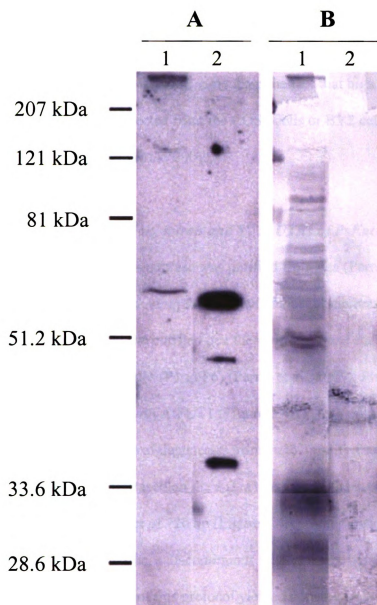


Figure 2.3: Anti-AtFUT1 polyclonal antibodies recognize an approximately 63 kDa polypeptide in solubilized membrane proteins of Arabidopsis. A. Immunoblotting using antibodies against *E. coli* expressed AtFUT1-2.3 peptides. **B.** Coomassie blue stained immunoblot PVDF membrane used in A. Lane 1 is Arabidopsis carbonate-washed, detergent-solubilized membrane proteins and lane 2 is antigen (80 ng).

microsome membranes (Perrin et al., 1999), and therefore confirmed that the cDNA identified indeed encodes the XyG fucosyltransferase. Another piece of evidence confirming the identity of this cDNA clone came from the fact that high XyG fucosyltransferase activity was detected from the COS7 cells or BY2 cells expressing AtFut1 (Perrin et al., 1999; Sarria et al., 2001).

Cloning of full-length coding region, intron and 5', 3' UTRs of PsFut1

Because the XyG fucosyltransferase was purified from pea (Perrin et al., 1999), we decided to isolate the cDNA encoding the pea XyG fucosyltransferase. Analysis of the tryptic peptides derived from the purified pea fucosyltransferase enzyme yielded sequence information for six peptides (P1 to P6) (Perrin et al., 1999). Five of them showed high sequence similarity with AtFUT1 (Figure 2.4A). Two of the peptides, P2 and P5, were chosen for the design of degenerate primers to amplify fragments from a pea cDNA library (Figure 2.4B). Based on the AtFut1 sequence, these two primers were expected to generate a PCR product of 726 bp (Figure 2.4A). After unsuccessful trials with commonly used PCR programs, a discontinuous touchdown program with hot start was developed (Figure 2.4C). Use of this protocol yielded a single band of about 700 bp; controls with single primer or no primer showed no clear bands (Figure 2.4D). This PCR product was designated as PsFut1-a. The sequence of PsFut1-a has 67% identity with the corresponding region of AtFut1 at the nucleotide level and the peptide it encodes has 61.6% identity with the corresponding region of AtFUT1 protein. The peptide encoded by PsFut1-a also contains the amino acid sequence of tryptic peptide P1. A further round of PCR reactions were designed to amplify cDNA fragments toward the 5' and 3' ends of

Figure 2.4: Isolation of PsFut1 fragment PsFut1-a. **A.** Sequences of tryptic peptides derived from purified pea XyG fucosyltransferase and the deduced sequences of comparable regions from Arabidopsis. **B.** Degenerate primers kee230 and kee232 used for the amplification of PsFut1-a were designed according to the sequences of peptides P5 and P2. Their relative positions on the cDNA were predicted according to the positions of their comparable regions on AtFut1 cDNA. **C.** The discontinuous touchdown PCR program with hot start used for the amplification of fragment PsFut1-a. The amplification reaction was first carried out at an annealing temperature of 60°C for three cycles, then 55°C for 10 cycles, followed by 50°C for 26 cycles. Taq polymerase was added immediately after the denaturing step of the first amplification cycle for the hot start. **D.** PCR reactions for the amplification of PsFut1-a with primers kee230 and kee232 (1); with primer kee230 alone (2); with primer kee232 alone; and with no primer added (4).

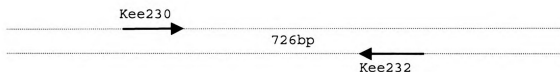
A

	Pea Peptide	Arabidopsis Peptide	Identity
P1	VFGFLGR	VFHHLGR	86%
P2	YLLHPTNNVWGLVVR	YLFHPTNQVWGLVTR	80%
P3	AVLITSLSSGYFEK	AVLVTSLNAGYAEN	64%
P4	YYDAYLAK	YYEAYLSH	63%
P5	LLGGLLADGFDEK	LLGGLLASGFDED	85%
P6	ESILPDVNR	EKLLPEVDT	44%

B

P5: A D G F D E K
 Kee230: 5' G C I G A Y G G I T T Y G A Y G A R A A 3'

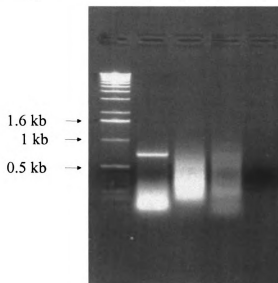
P2: H P T N N V W G
 5' C A Y C C I A C I A A Y A A Y G T I T G G G G I 3'
 Kee232: 3' G T R G G I T G I T T R T T R C A I A C C C C I 5'

**D****C**

94°C 3'
 94°C 1'
 60°C 1'
 72°C 2'
 94°C 1'
 55°C 1'
 72°C 2'
 94°C 1'
 50°C 1'
 72°C 2'
 72°C 10'

3x
 10x
 26x

1 2 3 4

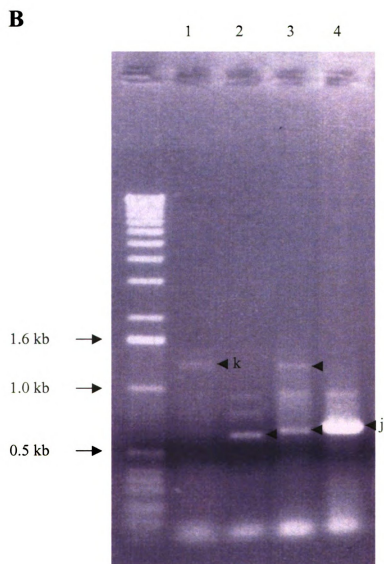
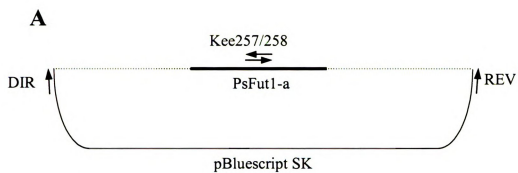


this gene from the same cDNA library using primers derived from the fragment of PsFut1-a and regions derived from the plasmid vector (Figure 2.5). Among five major PCR products generated and sequenced (Figure 2.5B), PsFut1-j and PsFut1-k revealed the longest unknown sequences 5' and 3' to the fragment PsFut1-a, respectively. Because one of the primers used for the amplification of both PsFut1-j and PsFut1-k came from the same region of PsFut1-a, the combined sequence of PsFut1-j and PsFut1-k encompassed the entire sequence of PsFut1-a. The combined sequence encoded all six peptide sequences previously obtained from the purified enzyme (Perrin et al., 1999) with one amino acid change in peptide P1 (Figure 2.7B), indicating these sequences were indeed part of the cDNA clone encoding the pea XyG fucosyltransferase.

However, the sequence combined from cDNA fragments PsFut1-j, PsFut1-a and PsFut1-k still lacked the 5' end as compared with the sequence of AtFut1 cDNA. Primers were then designed according to the sequence of fragment PsFut1-j and PsFut1-k to amplify the missing ends of PsFut1 and possibly the 5' and 3' UTR regions. Five 5' RACE products were generated using primers at different locations (Figure 2.6). These products were sequenced. One of the fragments PsFut1-5R33 showed the longest previously-unidentified sequence containing 73 bp of coding region and 194 bp of 5'UTR region. At the same time, one of the 3' RACE products, PsFut1-3Ra1, was sequenced and showed a perfect match with fragment PsFut1-k plus about 90 bp sequence after the stop codon. The combined sequence of cDNA fragments PsFut1-5R33, PsFut1-j, PsFut1-a, PsFut1-k yielded the full coding region for PsFut1 compared with AtFut1 (Figure 2.7A).

A full-length cDNA coding region was amplified with primers specific for the ends of the predicted gene (PsFut1, Figure 2.7B). The same reaction was also performed

Figure 2.5: Second round of PCR reactions amplifying cDNA fragments toward the 5' and 3' of PsFut1-a. **A.** Location of primers used for the PCR reactions on the plasmid from the cDNA library template. Broken line indicates the cDNA inserts in the library constructed on vector pBluescript. Solid line on top of the broken line is the cloned fragment PsFut1-a. Primers kee 257 and kee 258 were derived from PsFut1-a. DIR and REV are primers derived from the vector plasmid pBluescript SK; **B.** PCR reactions with primers kee257 and REV (1), kee258 and REV (2), kee257 and DIR (3), and kee258 and DIR (4). Five major PCR products (indicated by arrows) were cloned onto pGEM-T easy vector (Promega) and subjected to sequencing. Fragment j and k showed the longest unknown sequences 5' and 3' to fragment PsFut1-a.



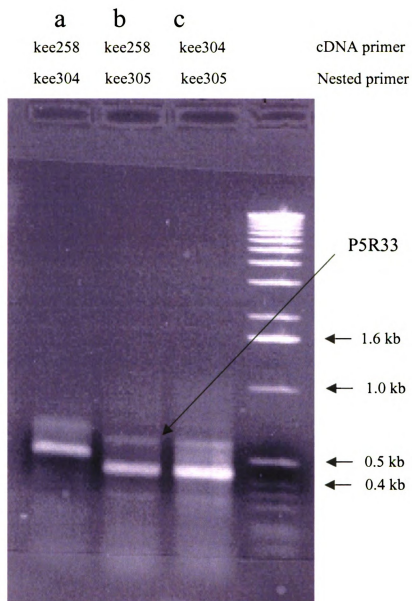


Figure 2.6: RACE reactions amplifying the 5' and 3' ends of PsFut1. Primers used include kee258 and kee304 (a); kee258 and kee305 (b); kee304 and kee305 (c). Five major PCR products were cloned into pGEM-T easy for sequencing. Fragment PsFut1-5R33 showed the longest unknown sequence and is marked with arrow. Primer sequences and their positions on the cDNA were as indicated in Figure 2.7.

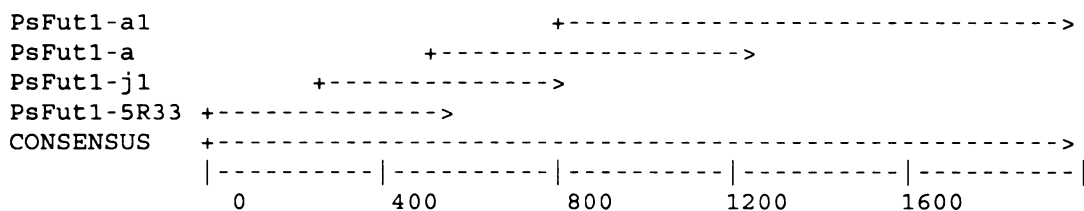
Figure 2.7: DNA and protein sequences related to PsFut1 and PsFUT1, and the sequence and positions of primers used for DNA fragment amplifications. A.

Sequence alignment of cDNA fragments PsFut1-a1, PsFut1-j1, PsFut1-a and PsFut1-

5R33 by Pileup of GCG program. **B.** Sequence of PsFut1 including cDNA coding region, intron, and 5' and 3' UTR. Peptide sequence is underneath the cDNA coding region.

Primers used for cDNA fragments amplification are marked with lines above or underneath the specific nucleotide sequences. Primers kee230 and kee232 were used for the amplification of the first PCR fragment PsFut1-a. Kee257 and kee258 were used for the second round PCR reactions. Primers kee258, kee304 and kee305 were used for 5' RACE while kee302 was used for 3'RACE. Primers kee322 and kee323 were used for the amplification of full length cDNA coding region PsFut1 and the genomic clone PsFut1-geno. Kee324 and kee325 were used for the amplification of clone PsFut1-5UTR. Peptide sequences obtained from purified enzyme are underlined and marked as P1~6, with one mismatch for P1 indicated in parenthesis. The sequence motif found in all α -1,2-fucosyltransferases and α -1,6-fucosyltransferases is in bold and green, and a putative transmembrane domain is in bold and italic. Asparagines that are possibly N-glycosylated are marked with # underneath.

A



B

Kee324		
1	ACGAGACATTTCGTTCTAATTTACAGTAGTGAATCAAATGACAAAGTGCCACATCAATTTA	60
61	CCGTGGCCACAGCATCACTGTACCAGGCAGTCACACACTCAGAGTCGGTGGTTGAAAGTTT	120
121	TGAAGTACCATTGGAAGTACCACTCTCTCTACTCTCAACTAGAAATCAATCGTTGTGCA	180
Kee322		
181	TCTGTGGCAATGAATATGCTGATAAAGAGAGTCATTGCAATCAAGAATCCAAGGGGTGAT	240
1	M N M L I K R V I A I K N P R G D	17
241	GATAATAATAATAATAAACTCTCAGATTTGGAAACCCCTACCGACAAATGTACAACATGC	300
18	D N N N N K L S D L E T L T D K C T T C	37
Kee325		
301	CCTTTGACTTTGATGCGTGTAATGGCTTTCTTCGTCGTTTCTTTCATGCTCTTCTCCGTT	360
38	P L T L M R V M A F F V V S F M L F S V	57
361	CTCTTCTCACTCTCCGTCGTTCTTCGAGACCCTCCCTCTGATGCCGCTATTTTCATCTACA	420
58	L F S L S V V L R D P P S D A A I S S T	77
421	ACTACTCTCTTCCAACTCAATCAGGGTATGTTCCCTCTTTTCCAAAACATATTCCTTTTC	480
78	T T L F Q L N Q G	86
481	TCAATTCAGTTTACCTAACTTCATGAATAAGATTGTAGATCGGGATCAGCATCGGTGGAA	540
541	ATCTATCTAGTCATTTTTGTCTAATTAATTACAAATTTAACTAAAGGTTTGTAGTTTTTG	600
601	ACAAACAACGGGCTTGTTTAGAATCTGTATTCTTAAATTTGTTAGCTTTAGTTAGAAAAA	660
661	AGATGATATTTGCTTTTCTTGCAACTGCATCTCATTGCAGAGTTATGGAATTCATCTTC	720
721	TCTGACTTGTTACTTGTAGGTTTGGGCAGTGATGACTTTGATTCTGTGGAGTTGCTAAAT	780
87	L G S D D F D S V E L L N	99
Kee230		
781	GATAAACTGCTCGGTGGCCTTCTCGCTGATGGATTTGACGAAAAATCTTGTTCTCAGCAGG	840
100	D K L L G G L L A D G F D E K S C L S R	119
P5		
841	TATCAGTCAGCCATTTTCGGCAAAGGACTATCAGGAAAACCTTCTTCTTACCTTATTTCT	900
120	Y Q S A I F G K G L S G K P S S Y L I S	139
Kee304		
901	AGACTGAGAAAAATATGAAGCCCGACACAAACAATGTGGACCTTATACTGAATCTTATAAC	960
140	R L R K Y E A R H K Q C G P Y T E S Y N	159
#		
961	AAAACGGTGAAAGAACTCGGTTCTGGTCAATTCTCTGAGTCCGTGGATTGTAAATATGTA	1020
160	K T V K E L G S G Q F S E S V D C K Y V	179
1021	GTATGGATTTTCGTTTGTAGTGGGTTAGGAAATAGGATATTGACCCTAGTTTCAGCATTTCTT	1080
180	V W I S F S G L G N R I L T L V S A F L	199
Kee257		
1081	TACGCTCTCCTCACTGATCGTGTCTTCTACTAGTTGACCCGGGAGTCGATATGACTGATCTT	1140
200	Y A L L T D R V L L V D P G V D M T D L	219
Kee258		

1141 TTTTGTGAACCATTTCTCTGACGCTTCCTGGTTTGTCCCTCCTGATTTTCTCTTAACAGT 1200
220 F C E P F P D A S W F V P P D F P L N S 239

1201 CATTTGAATAATTTCAACCAGGAATCGAATCAGTGTACGGGAAAATACTGAAAAACAAAA 1260
240 H L N N F N Q E S N Q C H G K I L K T K 259

1261 TCAATCACAAATTCCACTGTGCCATCTTTTGTATTATCTTCATCTAGCCCATGATTACGAT 1320
260 S I T N S T V P S F V Y L H L A H D Y D 279

1321 GATCATGACAAGCTTTTCTTCTGTGATGAAGAGCAACTTTTTCTCCAAAATGTACCTTTG 1380
280 D H D K L F F C D E E Q L F L Q N V P L 299

1381 TTGATTATGAAAACCGATAATTATTTTCATCCCATCTCTGTTCTTGATGCCATCTTTTGAG 1440
300 L I M K T D N Y F I P S L F L M P S F E 319

1441 CAGGAGTTGAATGATCTCTTCCCAAAGAAAGAAAAAGTTTTCCATTTCTTGGGTAGATAT 1500
320 Q E L N D L F P K K E K V F H F L G R Y 339
(G) P1
1501 CTGTTACACCCCAACAAATGTGTGGGGACTTGTGCGTCAGATACTATGATGCATACTTA 1560
340 L L H P T N N V W G L V V R Y Y D A Y L 359
P2 P4
1561 GCTAAAGTTGATGAAAGAATAGGCATACAAATCAGAGTATTTGACACCGATCCCGGTCCA 1620
360 A K V D E R I G I Q I R V F D T D P G P 379

1621 TTTCAACATGTACTCGATCAGGTCTTAGCTTGTACTTTGAAGGAGAGTATTTTGCCTGAT 1680
380 F Q H V L D Q V L A C T L K E S I L P D 399
P6
1681 GTAAACCGCGAGCAGAACATTAATAGTTCATCAGGAACACCAAAGTCAAAAGCTGTACTG 1740
400 V N R E Q N I N S S S G T P K S K A V L 419

1741 ATAACATCGTTAAGTTCTGGTTATTTTCGAAAAGGTAAGAGACATGTATTGGGAATTTCT 1800
420 I T S L S S G Y F E K V R D M Y W E F P 439
P3
1801 ACAGAAACAGGAGAAGTGGTTGGCATTATATCAGCCAAGCCATGAAGGTTATCAACAAACT 1860
440 T E T G E V V G I Y Q P S H E G Y Q Q T 459

1861 CAGAAGCAATTTACAAACCAAAAAGCCTGGGCAGAAATGTATCTCTTAAGCTTAACTGAT 1920
460 Q K Q F H N Q K A W A E M Y L L S L T D 479
Kee302
1921 GTGCTAGTTACTAGCTCATGGTCTACTTTTGGATACGTGGCTCAGGGGCTTGGAGGGTTG 1980
480 V L V T S S W S T F G Y V A Q G L G G L 499

1981 AAACCATGGATACTCTACAAACCAGAGAATCGAACGGCCCCAAATCCGCCTTGTC AACGT 2040
500 K P W I L Y K P E N R T A P N P P C Q R 519

2041 GCCATGTCAATGGAGCCATGTTTTCATGCTCCTCCTTTTTATGACTGCAAGGCTAAGAGA 2100
520 A M S M E P C F H A P P F Y D C K A K R 539

2101 GGAAGTGCACACTGGTGCACCTTGTTCACATGTAAGGCACTGTGAGGATATGAGTTGGGGC 2160
540 G T D T G A L V P H V R H C E D M S W G 559

2161 CTTAAGCTCGTAGACAATTAGTTTTATCTAGATAGCTATGGCTTATGCTACTGTAAGTGT 2220
560 L K L V D N * 566

2221 TAAAACTTGCGAAGTGTGCAAATTTTGTGTACAATAGATTGAGTAATTCCTCGTAAAA 2280
2281 AAAAAAAAAA 2290

using gDNA

Figure 2.7

The deduc

Sequence

Th

5'UTR of

acid resid

5.91 as de

an identit

The high

other che

Berger, 1

by the tr

Figure 2.7

transmem

glycosyl

A

with PsF

gene was

Figure 2.7

sequence

AtFut1 (fr

using genomic DNA as template to amplify the coding region plus introns (PsFut1-geno, Figure 2.7B). PsFut1-geno contains all the sequences of PsFut1, plus an intron of 294 bp. The deduced amino acid sequence of PsFUT1 is shown in Figure 2.7B.

Sequence analysis of PsFut1

The cDNA clone obtained for PsFut1 contains a coding region of 1695 bp, a 5'UTR of 190 bp, and a 3'UTR of 110 bp. The deduced translation product is 565 amino acid residues long, has a predicted molecular mass of 64 kDa, and a theoretical pI of 5.91 as determined by DNASTAR (Madison, WI). The coding region of PsFut1 showed an identity of 62.3% at the amino acid level and 63.8% at the nucleotide level to AtFut1. The highest similarity was observed at the COOH terminus, which has been postulated in other characterized fucosyltransferases to contain the catalytic domain (Kleene and Berger, 1993). A single transmembrane domain from amino acids 43 to 65 was predicted by the transmembrane helices prediction server TMHMM V. 2.0 (<http://www.cbs.dtu.dk/services/TMHMM>) (Figure 2.7B). The single N-terminal transmembrane domain is consistent with the observation that Golgi-localized glycosyltransferases are typically type II integral membrane proteins.

An intron of 294 bp was found in PsFut1-geno when its sequence was compared with PsFut1 (Figure 2.7B). The same region was predicted to be an intron when PsFut1-geno was subjected to a web-based gene prediction program BCM Gene Finder (<http://dot.imgen.bcm.tmc.edu:9331/gene-finder/gf.html>). PsFut1 shows not only a high sequence identity with AtFut1, but also similar gene structure. The genomic sequence of AtFut1 (from Arabidopsis BAC clone T18E12) has two exons of 277 bp and 1400 bp

with an intron of 276 bp in between. The genomic sequence of PsFut1 (PsFut1-geno) has exons of 258 bp and 1440 bp with an intron of 294 bp. The sequence similarity mostly lies in the second exon with an identity of 67% while the first exon shares only 40% identity. The first exon encodes for the very N-terminus, the transmembrane domain and the stem region, and therefore it is more variable compared with the region coded by the second exon, which contains conserved motifs for α -1,2; 1,6 fucosyltransferases and the catalytic domain. The introns from these two genes are located at similar position on their respective genomic clones and also share a 47% identity, even higher than the identity shared by the first exon. It seems likely that the intron was already present in the gene before evolutionary divergence of peas and Arabidopsis.

Four N-glycosylation sites were predicted by the GCG program (Madison, Wisconsin) (Figure 2.7B). This program also predicted a cAMP/cGMP-dependent protein kinase phosphorylation site at position 538-541, five casein kinase II phosphorylation sites, a glycosaminoglycan attachment site at position 185-188, four N-myristoylation sites, and seven protein kinase C phosphorylation sites. However all these predictions need experimental confirmation to determine whether any of these posttranslational modifications actually occur.

Although AtFUT1 and PsFUT1 proteins have very low overall sequence similarity with other known fucosyltransferases (less than 20% identity), three conserved motifs were found using the PATTERNFIND program (http://hits.isb-sib.ch/cgi-bin/hits_patsearch) (Faik et al., 2000). Among five motifs that were previously identified (Oriol et al., 1999) to be present in all known α -1,2- and α -1,6-fucosyltransferases, three

of them were found in both PsFUT1 and AtFUT1 (Faik et al., 2000).

Specificity analysis of clone Ps5UTR as probe for Northern blotting

A DNA fragment named PsFut1-5UTR containing 189 bp of 5'UTR sequence and 124 bp of 5' end coding region of PsFut1 was amplified from pea genomic DNA (Figure 2.7B) and used as a probe for northern studies. To determine whether this region is gene specific, the counterpart regions from all AtFut genes were identified from their corresponding BAC clones and aligned by MultiAlign (DNASar), a computer program using ClustalW. Among the ten AtFut genes, this part of the sequence from AtFut1 shared only very low identity with other AtFut genes (5.1 to 16.3%) (Table 2.1). At this low identity level it was very unlikely that the probe region from AtFut1 would recognize other AtFut genes. Therefore we postulated that PsFut1-5UTR would also be specific for PsFut1 when used as probe for northern blotting in peas. This assessment was further tested by probing pea genomic DNA digested with EcoRV and HindIII using PsFut1-5UTR as probe (Figure 2.8). There are only one EcoRV restriction site and two HindIII restriction sites in the PsFut1 genomic clone (Figure 2.8A). All three restriction sites were in exon II (Fig2.8A). Therefore when PsFut1-5UTR was used as probe for southern blotting, only one band was expected for both digestions. That was exactly what was observed (Fig2.8B), supporting the conclusion that PsFut1-5UTR is a gene-specific probe for PsFut1.

Internode elongation curve of etiolated pea seedlings

Table 2.1: Sequence alignment among Pst⁺St⁺IR and its equivalents from all AdFut genes. DNA fragment (Pst⁺St⁺IR) is aligned with the Pst⁺St⁺IR from the Pst⁺St⁺IR gene. The alignment is shown in the table below.

Table 2.1: Sequence alignment among PsFut1-5UTR and its equivalents from all AtFut genes. DNA fragment PsFut1-5UTR contains 189 bp of 5' UTR and 124 bp of 5' end coding region of PsFut1. The same regions for all AtFut genes were extracted from their corresponding BAC clones and aligned by MultiAlign (DNASar), a ClustalW method. Numbers are percent similarities.

AtFut1	AtFut10	AtFut2	AtFut3	AtFut4	AtFut5	AtFut6	AtFut7	AtFut8	AtFut9	Ps5UTR	
***	5.8	8.6	8.9	16.3	7.7	5.1	16.0	7.7	5.4	6.4	AtFut1
	***	4.5	6.7	6.7	5.1	3.8	3.5	5.4	6.4	5.8	AtFut10
		***	7.3	8.9	6.4	9.3	11.2	5.1	8.9	4.5	AtFut2
			***	13.1	10.2	6.4	7.7	6.4	8.9	6.4	AtFut3
				***	23.3	4.8	17.3	6.7	16.0	4.5	AtFut4
					***	26.6	59.6	9.9	14.4	7.0	AtFut5
						***	28.5	29.8	26.0	17.6	AtFut6
							***	15.4	13.5	6.1	AtFut7
								***	24.6	11.5	AtFut8
									***	5.1	AtFut9
										***	Ps5UTR

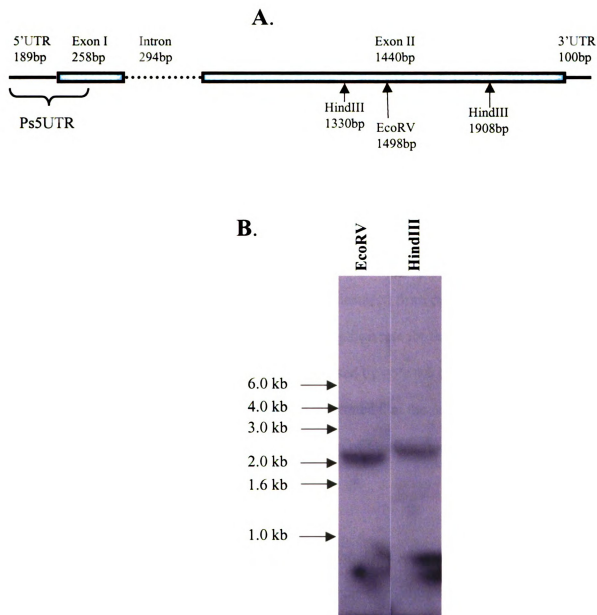


Figure 2.8: PsFut1 specific DNA probe Ps5UTR. **A.** The organization of clone PsFUTgeno. Recognition sites for HindIII and EcoRV are indicated. Clone Ps5UTR contains 189bp of 5' UTR and 124bp of 5' end coding region; **B.** Southern analysis of pea genomic DNA using Ps5UTR as probe. Fifteen μ g of genomic DNA was used for each digestion. The signals below the 1.0 kb marker are non-specific irregular spots.

I examined the expression of PsFut1 during growth of etiolated pea in terms of enzyme activity and messenger RNA abundance. The growth of etiolated pea seedlings was monitored by measuring the internode length daily from day 6 until day 11 (Figure 2.9A). At day 6 the first internode had already accomplished its elongation as very little additional length increase was seen in the following days (Figure 2.9). The second internode elongated slightly from day 6 to day 7 with an increase of 1.1 cm, and stopped its elongation thereafter (Figure 2.9). However the third internode showed dramatic elongation between days 6 and 11, showing an increase in length of more than 10 fold. The most rapid elongation for the third internode occurred from day 7 to day 8 when the length increased by 5.0 cm (Figure 2.9). The elongation rate for the third internode then decreased daily after this time point until it increased by only 0.6 cm from day 10 to day 11 (Figure 2.9B). Collectively, the results demonstrated that the third internode had the highest elongation rate at day 7 and that elongation of this internode was nearly complete at day 11.

Expression of PsFut1 in three internodes of etiolated pea seedlings at 7 days old

To correlate the expression of PsFut1 with the elongation of etiolated pea internodes, microsomal membranes were isolated from the three internodes of etiolated seedlings at 7 days old and examined for XyG fucosyltransferase activity. Total RNA was also isolated from the same tissues and examined for PsFut1 messenger RNA abundance. PsFut1-5UTR was used as probe for the northern blotting. As indicated in Figure 2.9, only the third internode showed dramatic elongation at day 7. Accordingly, the specific activity of PsFUT1 from the third internode was found to be nearly 6 times

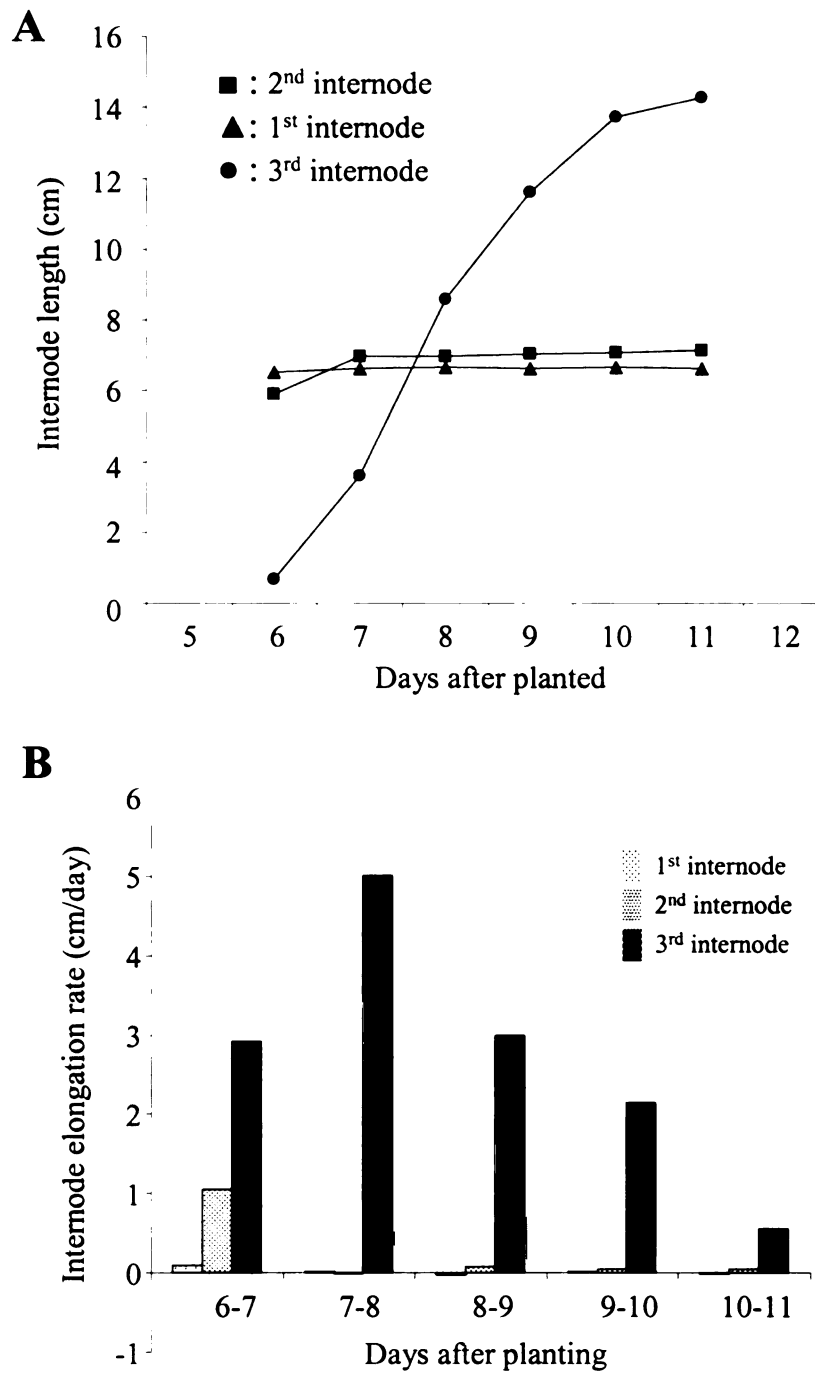


Figure 2.9: Growth curve of etiolated pea internodes. All lengths were measured in the dark under safe light, and were averages of 40 seedlings. **A**, internode length of etiolated pea seedlings from day 6 to day 11; **B**, elongation rate of etiolated pea internodes expressed as increased length (cm) per day comparing two consecutive days.

that from the first internode and 3 times that from the second internode (Figure 2.10A). While the second internode didn't show much increase of PsFut1 messenger RNA compared with the first internode at day 7, the third internode had dramatically higher expression of PsFut1 as measured by northern blotting (Figure 2.10B). This experiment demonstrated a good correlation between pea internode elongation rate and the expression of PsFut1.

Expression of PsFut1 in the third internode at different growth stages

From day 7 to day 11, the elongation rate of the third internode decreased almost 8-fold, although the absolute length increased almost 3-fold (Figure 2.9). There was a 223% increase in internode length from day 7 to day 9 compared with only 75% increase from day 9 to day 11 (Table 2.2). Accordingly, the elongation rate decreased dramatically from 5.0 cm/day at day 7 to 0.6 cm/day at day 11 (Figure 2.9). The PsFUT1 activity also decreased during this time (Figure 2.11A). From day 7 to day 9, the specific activity of PsFUT1 decreased 48% while from day 9 to day 11, it further decreased by 22.5% (Table 2). Thus a correlation between the decrease of elongation rate and the decrease of PsFUT1 enzyme activity was observed. At the same time the PsFut1 transcripts also showed a dramatic decrease between day 7 and day 9, and a further, but smaller, decrease between day 9 and day 11 (Figure 2.11B). This again demonstrated a correlation between the internode elongation rate and PsFut1 expression.

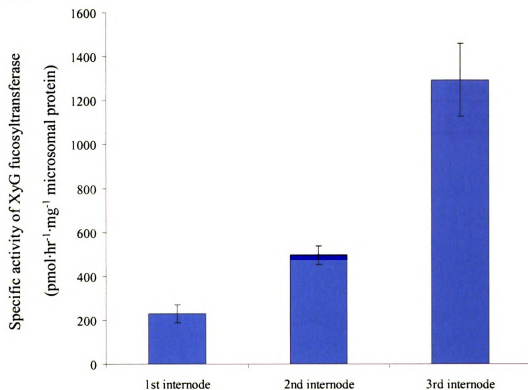
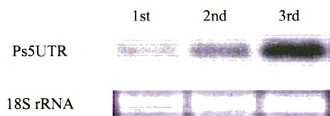
A**B**

Figure 2.10: Expression of PsFut1 in etiolated pea internodes at day 7. A, Specific activity of XyG fucosyltransferase; **B,** northern blotting using Ps5UTR as probe.

Table 2.2: PsFUT1 activity decreases during the elongation of third internode between day 7, 9 and 11.

After planted	Internode length (cm)		Spec. act. (pmol·hr ⁻¹ ·mg ⁻¹ micros. pro.)	
7 days	3.59	increase	1686.4	decrease
9 days	11.6	223%	873.6	48.2%
11 days	14.29	75%	494.2	22.5%

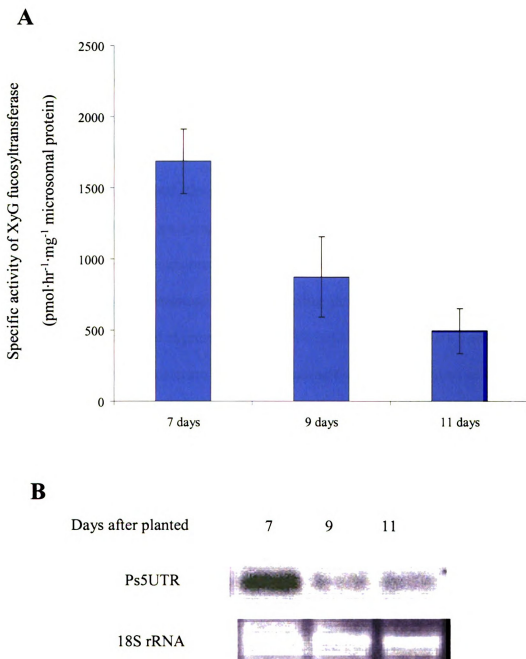


Figure 2.11: Expression of PsFUT1 in the third internode of the etiolated pea at 7, 9 and 11 days old. A, Specific activity of PsFUT1; B, Northern blotting using Ps5UTR as probe.

DISCUSSION

Isolation of cDNAs encoding the XyG fucosyltransferase

Identifying genes involved in the biosynthesis of plant cell wall polysaccharides is the first step to understand the mechanism of plant growth and development. Only a few genes with proven cell wall biosynthesis functions have been identified. Through the efforts described in this chapter, the gene encoding the XyG fucosyltransferase was identified from both Arabidopsis and pea. The identity of AtFut1 was confirmed in two ways. The first involved immunoprecipitation of XyG fucosyltransferase activity from solubilized Arabidopsis microsomal membranes using antibodies against part of AtFUT1 protein. The second involved expression of AtFUT1 in COS7 cells and BY2 cells and detection of XyG fucosyltransferase activities in extracts of the transformed cells. The identity of PsFut1 was confirmed by the fact that the protein encoded by PsFut1 contains the sequences of all six peptides that we obtained from the microsequencing of the purified PsFUT1.

The complete Arabidopsis genome has revealed the presence of a fucosyltransferase family with nine additional AtFut genes in addition to AtFut1. AtFut1, however, is the only AtFut gene for which the function of the gene product has been determined, i.e., adding a fucose residue to the side chain galactose of XyG in an α -1,2 glycosidic bond. All of the AtFut genes were placed into the same CAZy family 37 according to the sequence comparison of the proteins they encode. The other AtFUT proteins showed less sequence identity with PsFUT1 compared with AtFUT1, and are not likely XyG fucosyltransferases. Indeed XyG fucosyltransferase activity was not detected

in the BY2 cells expressing AtFUT3, 4 and 5 using non-fucosylated XyG as substrate (Sarria et al., 2001).

The Kyte-Doolittle hydrophilicity plots suggested the presence of a transmembrane domain at the NH₂ terminus for both AtFUT1 and PsFUT1. Based on this, it is likely that both AtFUT1 and PsFUT1 are type II membrane proteins (Singer, 1990). The catalytic domains of AtFUT1 and PsFUT1 are likely to be facing the lumen and similar to all other fucosyltransferases described to date. This conclusion is further supported by the fact that Triton X-100 solubilization of microsomes from both pea and Arabidopsis could stimulate the XyG fucosyltransferase many times (Wulff et al., 2000).

An Arabidopsis mutant line *mur2* was identified to carry a point mutation on the XyG fucosyltransferase gene *AtFut1* (Vanzin et al., 2002). XyG isolated from leaves, stems, flowers and roots of *mur2* plants all contained only 2% of the wild-type amount of fucose, while the fucose content of pectins and glycoproteins in *mur2* plants are very similar to that of the wild type plants (Vanzin et al., 2002). The mutant copy of *AtFUT1* expressed in mammalian cells also lost its ability to transfer fucose from GDP-fucose onto the galactose residue of tamarind XyG (Vanzin et al., 2002). A T-DNA insertion mutant line of *AtFut1* was also identified from the Arabidopsis Knockout Facility (Madison, WI) (Perrin et al., 2003). This *AtFut1* mutant showed 50% - 75% less fucose than wild type in mature rosette leaves, expanding leaves, and flowers (Perrin et al., 2003). While the fucose content in RGI and RGII of *AtFut1* mutant is comparable with that of the wild type plants, no fucose was detected from the 4 M KOH-soluble XyG fraction isolated from the mutant plants (Perrin et al., 2003). The characterizations of

AtFut1 mutants further confirmed that AtFut1 encodes for the enzyme responsible for the attachment of the terminal fucose onto XyG.

The discontinuous touchdown PCR program (Figure 2.4C) developed for the amplification of PsFut1-a is a powerful and effective program that easily amplifies low-abundance targets, especially low copy number templates from cDNA libraries where traditional PCR programs do not always work (Dr. Qin Du, personal communication). This program was also used successfully to amplify target DNA fragments from non-traditional organisms or from unpurified DNA samples contaminated with lipids and proteins. One example was the successful utilization of this PCR program to amplify various prokaryotic 16s rRNA fragments from the house fly intestinal extracts containing various bacteria, where a various of traditional PCR programs didn't work (Dr. Yunling Xu, Dr. Edward Walker, personal communication). This PCR program starts with high annealing temperature at 60°C for a small number of cycles to ensure the fidelity of the initial amplification products. The product from the first few amplification cycles therefore becomes part of the perfect match template pool for later cycles. Later cycles using lower annealing temperature at 55°C or 50°C ensured that enough products would be generated. This combination of different annealing temperatures therefore highly increases the probability that the amplification product from the true template become the dominant product at the end of the PCR reactions.

Expression of PsFut1 is correlated with internode elongation rate

The growth and development of plants requires a series of biochemical processes, including the biosynthesis and degradation of cell wall polysaccharides. Changes in the

plant cell wall occur in response to many developmental and environmental stimuli to coordinate cell expansion and maturation. These changes are thought to occur by regulating the expression of enzymes responsible for the metabolism of cell wall polysaccharides. In this chapter I utilized the fast-growing internodes from etiolated pea seedlings during their early growth stages to correlate the expression of XyG fucosyltransferase with internode elongation rate. More XyG fucosyltransferase activity and PsFut1 transcripts were detected in the third internode at 7 days old that showed the highest elongation rates, compared with either the first and second internodes of the same age, or the third internode at 9 or 11 days old.

Since XyG is one of the major structural components of the primary cell walls, its metabolism plays a major role during wall expansion in plant development and growth (Talbot and Ray, 1992). During auxin-induced rapid elongation of pea epicotyls, XyGs are partially solubilized and their molecular weight decrease (Labavitch and Ray, 1974; Hayashi and MacLachlan, 1984; Hoson, 1990; Talbot and Ray, 1992). The metabolism of XyG consists of its degradation, biosynthesis and crosslinking into the wall. The regulation of these three processes are all mediated by the regulated expressions of corresponding enzymes. Endoglucanases (EGs) (Verma et al., 1975), α -fucosidase (Augur et al., 1995) and α -xylosidase (Sampedro et al., 2001) are examples of XyG degradation enzymes that show a higher expression in fast growing tissues or at fast growing stages. XyG endotransglycosylases (XETs) and expansins are enzymes involved in the incorporation of new polysaccharide molecules into cell walls. They also have been shown to be up-regulated during the elongation of plant cells (Polisensky and Braam, 1996; Steele et al., 2001; Lee et al., 2003). Therefore the incorporation of XyG into the

expanding walls would be a net result of actions from enzymes involved in XyG degradation, biosynthesis and reorganization.

REFERENCES

- Aldington, S. and Fry, S. C.** (1993). "Oligosaccharins." *Adv. Bot. Res.* **19**: 1-101.
- Augur, C., Stiefel, V., Darvill, A., Albersheim, P. and Puigdomenech, P.** (1995). "Molecular cloning and pattern of expression of an alpha-L-fucosidase gene from pea seedlings." *J. Biol. Chem.* **270** (42): 24839-24843.
- Camirand, A. and MacLachlan, G.** (1986). "Biosynthesis of the fucose-containing xyloglucan nonasaccharide by pea *Pisum sativum* cultivar Alaska microsomal membranes." *Plant Physiol.* **82** (2): 379-383.
- Cosgrove, D. J.** (1997). "Assembly and enlargement of the primary cell wall in plants." *Annu. Rev. Cell Dev. Biol.* **13**: 171-201.
- Cosgrove, D. J.** (2000). "Expansive growth of plant cell walls." *Plant Physiol. Biochem.* **38** (1-2): 109-124.
- Darvill, A. G., Augur, C., Bergmann, C., Carlson, R. W., Cheong, J.-J., Eberhard, S., Hahn, M. G., Lo, V.-M., Marfa, V., Meyer, B., Mohnen, D., O' Neill, M. A., Spiro, M. D., Van Halbeek, H., York, W. S. and Albersheim, P.** (1992). "Oligosaccharins-oligosaccharides that regulate growth, development and defence responses in plants." *Glycobiology* **2**: 181-198.
- Desveaux, D., Faik, A. and MacLachlan, G.** (1998). "Fucosyltransferase and the biosynthesis of storage and structural xyloglucan in developing nasturtium fruits." *Plant Physiol.* **118** (3): 885-894.
- Faik, A., Bar-Peled, M., DeRocher, A. E., Zeng, W., Perrin, R. M., Wilkerson, C., Raikhel, N. V. and Keegstra, K.** (2000). "Biochemical characterization and molecular cloning of an alpha-1,2-fucosyltransferase that catalyzes the last step of cell wall xyloglucan biosynthesis in pea." *J. Biol. Chem.* **275** (20): 15082-15089.
- Farkas, V. and MacLachlan, G.** (1988). "Fucosylation of exogenous xyloglucans by pea microsomal membranes." *Arch. Biochem. Biophys.* **264** (1): 48-53.
- Fry, S. C.** (1989). "The structure and functions of xyloglucan." *J. Exp. Bot.* **40** (210): 1-11.
- Guillen, R., York, W. S., Pauly, M., An, J., Impallomeni, G., Albersheim, P. and Darvill, A. G.** (1995). "Metabolism of xyloglucan generates xylose-deficient oligosaccharide subunits of this polysaccharide in etiolated peas." *Carbohydr. Res.* **277** (2): 291-311.
- Hanna, R., Brummell, D. A., Camirand, A., Hensel, A., Russell, E. F. and MacLachlan, G. A.** (1991). "Solubilization and properties of GDP-fucose xyloglucan 1,2-

alpha-L-fucosyltransferase from pea epicotyl membranes." *Arch. Biochem. Biophys.* **290** (1): 7-13.

Hayashi, T. and Maclachlan, G. (1984). "Pea *Pisum sativum* cultivar Alaska xyloglucan and cellulose 1. Macromolecular organization." *Plant Physiol.* **75** (3): 596-604.

Hayashi, T. and Maclachlan, G. (1984). "Pea *Pisum sativum* cultivar Alaska xyloglucan and cellulose 3. Metabolism during lateral expansion of pea epicotyl cells." *Plant Physiol.* **76** (3): 739-742.

Hayashi, T. and Matsuda, K. (1981). "Biosynthesis of xyloglucan in suspension cultured soybean cells: Occurrence and some properties of xyloglucan 4-beta-D-glucosyltransferase and 6-alpha-D-xylosyltransferase." *J. Biol. Chem.* **256** (21): 11117-11122.

Hayashi, T., Ogawa, K. and Mitsuishi, Y. (1994). "Characterization of the adsorption of xyloglucan to cellulose." *Plant Cell Physiol.* **35** (8): 1199-1205.

Hoson, T. (1990). "Effect of auxin on autolysis of cell walls in Azuki bean epicotyls." *Plant Cell Physiol.* **31**: 281-287.

Houdebine, L.-M. and Puissant, C. (1990). "An improvement of the single-step method of RNA isolation." *BioTechniques* **8** (2): 148-149.

Kato, Y. and Matsuda, K. (1980). "Structure of oligosaccharides obtained by controlled degradation of mung bean xyloglucan with acid and *Aspergillus oryzae* enzyme preparation." *Agric. Biol. Chem.* **44** (8): 1751-1758.

Kieber, J. J., Rothenberg, M., Roman, G., Feldmann, K. A. and Ecker, J. R. (1993). "CTR1, a negative regulator of the ethylene response pathway in Arabidopsis, encodes a member of the RAF family of protein-kinase." *Cell* **72** (3): 427-441.

Kleene, R. and Berger, E. G. (1993). "The molecular and cell biology of glycosyltransferases." *Biochim. Biophys. Acta.* **1154** (3-4): 283-325.

Labavitch, J. M. and Ray, P. M. (1974). "Relationship between promotion of xyloglucan metabolism and induction of elongation by indoleacetic acid." *Plant Physiol.* **54**: 499-502.

Lee, D.-K., Ahn, J. H., Song, S.-K., Choi, Y. D. and Lee, J. S. (2003). "Expression of an expansin gene is correlated with root elongation in soybean." *Plant Physiol.* **131**: 985-997.

Levy, S., Maclachlan, G. and Staehelin, L. A. (1997). "Xyloglucan sidechains modulate binding to cellulose during in vitro binding assays as predicted by conformational dynamics simulations." *Plant J.* **11** (3): 373-386.

Maclachlan, G., Levy, B. and Farkas, V. (1992). "Acceptor requirements for GDP-fucose xyloglucan 1, 2- α -L-fucosyltransferase activity solubilized from pea epicotyl membranes." *Arch. Biochem. Biophys.* **294** (1): 200-205.

McDougall, G. J. and Fry, S. C. (1989). "Anti-auxin activity of xyloglucan oligosaccharides. The role of groups other than the terminal α -L-fucose residue." *J. Exp. Bot.* **20** (211): 233-238.

McDougall, G. J. and Fry, S. C. (1989). "Structure-activity relationships for xyloglucan oligosaccharides with antiauxin activity." *Plant Physiol.* **89** (3): 883-887.

Oriol, R., Mollicone, R., Cailleau, A., Balanzino, L. and Breton, C. (1999). "Divergent evolution of fucosyltransferase genes from vertebrates, invertebrates, and bacteria." *Glycobiology* **9**: 323-334.

Pauly, M., Qin, Q., Greene, H., Albersheim, P., Darvill, A. and York, W. S. (2001). "Changes in the structure of xyloglucan during cell elongation." *Planta* **212** (5-6): 842-850.

Pennell, R. (1998). "Cell walls: structures and signals." *Curr. Opin. Plant Biol.* **1**: 504-510.

Perrin, R. M., DeRocher, A. E., Bar-Peled, M., Zeng, W., Norambuena, L., Orellana, A., Raikhel, N. V. and Keegstra, K. (1999). "Xyloglucan fucosyltransferase, an enzyme involved in plant cell wall biosynthesis." *Science* **284** (5422): 1976-1979.

Perrin, R. M., Jia, Z., Wagner, T. A., O'Neill, M. A., Sarria, R., York, W. S., Raikhel, N. V. and Keegstra, K. (2003). "Analysis of xyloglucan fucosylation in Arabidopsis." *Plant Physiol.* **132**: 1-11.

Polisensky, D. H. and Braam, J. (1996). "Cold-shock regulation of the Arabidopsis TCH genes and the effects modulating intracellular calcium levels." *Plant Physiol.* **111** (4): 1271-1279.

Sambrook, J., Fritsch, E. F. and Maniatis, T. (1989). *Molecular Cloning, a Laboratory Manual*. Cold Spring Harbor Laboratory Press.

Sampedro, J., Sieiro, C., Revilla, G., Gonzalez, V. T. and Zarra, I. (2001). "Cloning and expression pattern of a gene encoding an α -xylosidase active against xyloglucan oligosaccharides from Arabidopsis." *Plant Physiol.* **126** (2): 910-920.

Sarria, R., Wagner, T. A., O'Neill, M. A., Faik, A., Wilkerson, C. G., Keegstra, K. and Raikhel, N. V. (2001). "Characterization of a family of Arabidopsis genes related to xyloglucan fucosyltransferase1." *Plant Physiol.* **127** (4): 1595-1606.

- Singer, S. J.** (1990). "The structure and insertion of integral proteins in membranes." *Annu. Rev. Cell Biol.* **6**: 247-296.
- Steele, N. M. and Fry, S. C.** (1999). "Purification of xyloglucan endotransglycosylases (XETs): A generally applicable and simple method based on reversible formation of an enzyme-substrate complex." *Biochem. J.* **340** (1): 207-211.
- Steele, N. M., Sulova, Z., Campbell, P., Braam, J., Farkas, V. and Fry, S. C.** (2001). "Ten isoenzymes of xyloglucan endotransglycosylase from plant cell walls select and cleave the donor substrate stochastically." *Biochem. J.* **355** (3): 671-679.
- Sulova, Z., Takacova, M., Steele, N. M., Fry, S. C. and Farkas, V.** (1998). "Xyloglucan endotransglycosylase: Evidence for the existence of a relatively stable glycosyl-enzyme intermediate." *Biochem. J.* **330** (3): 1475-1480.
- Talbott, L. D. and Ray, P. M.** (1992). "Changes in molecular size of previously deposited and newly synthesized pea cell wall matrix polysaccharides effects of auxin and turgor." *Plant Physiol.* **98** (1): 369-379.
- Vanzin, G. F., Madson, M., Carpita, N. C., Raikhel, N. V., Keegstra, K. and Reiter, W. D.** (2002). "The *mur2* mutant of *Arabidopsis thaliana* lacks fucosylated xyloglucan because of a lesion in fucosyltransferase AtFUT1." *Proc. Natl Acad. Sci. USA* **99** (5): 3340-3345.
- Verma, D. P. S., Maclachlan, G., Byrne, H. and Ewings, D.** (1975). "Regulation and in vitro translation of messenger ribonucleic acid for cellulase from auxin-treated pea epicotyls." *J. Biol. Chem.* **250** (1019-1026).
- Whitney, S. E. C., Brigham, J. E., Drake, A. H., Reid, J. S. G. and Gidley, M. J.** (1995). "In vitro assembly of cellulose/xyloglucan networks: Ultrastructural and molecular aspects." *Plant J.* **8** (4): 491-504.
- Wulff, C., Norambuena, L. and Orellana, A.** (2000). "GDP-fucose uptake into the Golgi apparatus during xyloglucan biosynthesis requires the activity of a transporter-like protein other than the UDP-glucose transporter." *Plant Physiol.* **122** (3): 867-877.
- York, W. S., Darvill, A. G. and Albersheim, P.** (1984). "Inhibition of 2,4-D stimulated elongation of pea stem segments by a xyloglucan oligosaccharide." *Plant Physiol.* **75** (2): 295-297.

CHAPTER 3

Sequence and Expression Pattern Analysis of Arabidopsis

Cellulose Synthase-Like Genes

At

XyG bio

product

enzymes

After the

divided

decided

synthase

of XyG.

PREFACE

My research focus has shifted from XyG fucosyltransferase to another aspect of XyG biosynthesis, i.e., efforts to identify the genes encoding the glucan synthase(s) that produce(s) the glucan backbone of XyG. The effort to identify the genes encoding enzymes involved in XyG biosynthesis began, and continue to operate, as a group project. After the initial identification of fucosyltransferase genes, research efforts have been divided into smaller new projects for different individuals involving new directions. I decided to test the hypothesis that one or more members of the Arabidopsis cellulose synthase-like gene families might be involved in the biosynthesis of the glucan backbone of XyG.

ABSTRACT

Arabidopsis cellulose synthase-like genes are a group of 30 gene encoding proteins that share identities ranging from 7% to 46% with Arabidopsis cellulose synthase proteins. It has been hypothesized that the cellulose synthase-like genes may encode proteins involved in the synthesis of other polysaccharides, such as the glucan backbone of XyG. I started to evaluate this hypothesis by analyzing the sequences of AtCsl genes and the proteins they encode. The automated annotation in the public database resulted in unusual protein sequence alignments that most likely derived from annotation mistakes. Therefore, the beginning of this chapter focuses on a manual re-annotation and sequence analysis of AtCsl genes. We sought to investigate the possibility that genes involved in the biosynthesis of the same polysaccharide might show similar expression profiles. Therefore the expression profiles of AtCsl genes were compared with genes known to be involved in cell wall biosynthesis. The dbEST and, Arabidopsis MPSS databases, and the microarray data from Stanford Microarray Database and the Nottingham Arabidopsis Stock Center Microarray Database were all utilized for the gene expression analysis. Even though the expression studies did not reveal a tight link between AtCsl genes and XyG fucosyltransferase, xylosyltransferase or galactosyltransferase, several interesting observations were recorded. Specifically, some AtCsl genes showed strong tissue expression preferences, and the expression of some AtCsl genes changed in response to environmental signals. These sequence analyses and gene expression profiling could be used in future studies on the functions of AtCsl genes and the changes in wall biosynthesis in response to environmental signals.

INTRODUCTION

XyG is the major hemicellulose for dicot and nongraminaceous monocot plants. Its most common structure is a β -(1,4)-glucan backbone modified with side chains composed of α -(1,6)-xylose, β -(1,2)-galactose, and α -(1,2)-fucose residues (Figure 1.1) (Hayashi and Maclachlan, 1984). XyG is proposed to be synthesized through the action of at least four different enzymes, i.e., β -(1,4)-glucan synthase, α -(1,6)-xylosyltransferase, β -(1,2)-galactosyltransferase and α -(1,2)-fucosyltransferase (Camirand and Maclachlan, 1986; Camirand et al., 1987). XyG fucosyltransferase has already been identified through earlier efforts of our group (Perrin et al., 1999; Faik et al., 2000). Other studies were also being carried out by Dr. Ahmed Faik in our group for the identification of xylosyltransferase (Faik et al., 2002) and Dr. Wolf Dieter Reiter's group for the identification of galactosyltransferase (Madson et al., 2003). Therefore my effort was focused on the identification of the glucan synthase that is responsible for the biosynthesis of the XyG backbone.

XyG backbone has the same chemical structure as cellulose, a rigid, straight chain polymer of β -(1,4)-linked D-glucose residues (Kato and Matsuda, 1980; Fry, 1989). It is reasonable to postulate that the glucan synthase responsible for the synthesis of XyG backbone will have significant sequence similarity to cellulose synthase, because it recognizes the same donor substrate, i.e. UDP-glucose, and produces a similar product. This was proved by the synthesis of XyG when UDP-glucose and UDP-xylose were added into suspension cultured soybean cells at the same time (Hayashi and Matsuda, 1981). However, due to the existence of the sidechain sugar moieties on XyG, the enzyme responsible for the backbone synthesis should also have some unique features.

Moreover, the XyG glucan synthase is hypothesized to operate in the Golgi complex whereas cellulose synthase forms its product at the plasma membrane (Delmer and Stone, 1988). Initial attempts to identify homologs of cellulose synthase in *Arabidopsis* identified a cellulose synthase-like (AtCsl) gene family (Cutler and Somerville, 1997), encoding proteins of only about 30% identity to the cotton cellulose synthase encoded by GhCesA1, which was the first cellulose synthase gene cloned in plants (Pear et al., 1996).

As sequencing of the *Arabidopsis* genome progressed, additional sequence data allowed a more detailed and complete computational analysis of AtCsl genes. Richmond and Somerville (2000) identified 30 AtCsl genes in the *Arabidopsis* genome through blast searches (Richmond, <http://cellwall.stanford.edu/cesa/index.shtml>). All *Arabidopsis* cellulose synthase (AtCesA) genes and Csl genes were placed in a large cellulose synthase superfamily. AtCsl genes were grouped into six families, namely AtCslA, AtCslB, AtCslC, AtCslD, AtCslE, and AtCslG, according to the distances among sequences within the phylogenetic tree (Richmond, 2000; Richmond and Somerville, 2000; Saxena and Brown, 2000). Proteins encoded by the various Csl genes have become the most prominent candidates for the synthesis of XyG backbone. It was postulated that some of them might also function in the synthesis of other polysaccharide backbones such as xylan, galactans, or mannans that are constructed with β -glycosidic linkages (Cutler and Somerville, 1997). This chapter describes some efforts to explore this hypothesis as it relates to the XyG glucan backbone.

When we began our work at the early stages in the *Arabidopsis* genome sequencing project, many gene annotations were not accurate. When the sequences of AtCsl genes were extracted from the GenBank and aligned, many of them showed

missing S

Conclusion

my first ef

possible. A

or cDNA

compare

K

lead to in

of the pr

usually e

different

morpho

during e

cDNA

and the

condit

libran

(White

analys

within

abund

missing 5' or 3' coding regions or missing domains in the middle of the gene.

Conclusions from those sequence comparisons many times were misleading. Therefore my first effort was to re-annotate the AtCsl gene sequences in the database as much as possible. Most of the re-annotated sequences were confirmed to be correct by EST clones or cDNA clones identified later on. The re-annotated sequences then were analyzed and compared for gene or protein specific features and features common for each family.

Knowledge about where, when and to what extent a gene is expressed can often lead to insights about the function of the gene and an understanding of the biological role of the protein it encodes (Lockhart and Winzler, 2000). Different tissues or cell types usually express different sets of genes or the same genes to different extents. The differences in gene expression determine the different cellular phenotypes and plant morphologies. Transcriptional profiling therefore has become an important approach during efforts to investigate the function of genes that are known only by their sequences.

The expressed sequence tags (ESTs) derived from large-scale sequencing of cDNA libraries provide valuable information for the annotation of genomic sequences and the gene expression profiles associated with specific tissues under specific growth conditions. The frequency of the appearance of ESTs recovered from specific cDNA libraries have often been used to estimate the expression pattern of individual genes (White et al., 2000; Fernandes et al., 2002).

MPSS (Massively Parallel Signature Sequencing) is another gene expression analysis technique, generating gene-specific short sequence tags from a defined position within a particular mRNA (Brenner et al., 2000; Brenner et al., 2000). The relative abundance of these tags for a particular gene in a given library represents a quantitative

estimate of expression of that gene. An Arabidopsis MPSS database was built up by the Meyers lab (<http://dbixs001.dbi.udel.edu/MPSS4/java.html>), which includes 12.3 million MPSS tags of 17 bp from five different libraries constructed from callus (1.96 million), inflorescence (1.79 million), shoot (2.89 million), root (3.65 million) and silique (2.02 million). More than 95% of all Arabidopsis genes could be identified with unique MPSS tags using these five MPSS libraries (<http://dbixs001.dbi.udel.edu/MPSS4/java.html>).

Microarray analysis has been a powerful method for evaluating transcript abundance on a genome scale. The expression profiles of genes of interest can be examined at the same time for any given tissue under a given growth condition. Changes in gene expression under various growth conditions or environmental stresses also can be detected with microarray techniques. The Stanford Microarray Database (SMD, <http://genome-www.stanford.edu/microarray>) contains data from over 3500 microarrays from various experiments involving different model organisms including Arabidopsis (Gollub et al., 2003). The Nottingham Arabidopsis Stock Center's microarray database (NASCArrays) is another database containing large amounts of data from many Arabidopsis-related experiments using Affymetrix microarray chips (<http://ssbdjc2.nottingham.ac.uk/narrays/experimentbrowse.pl>). These two databases therefore are a rich source of gene expression profiles.

To investigate the hypothesis that one or more AtCsl genes might encode the XyG glucan synthase, the expression patterns of AtCsl genes were compared with genes encoding known XyG glycosyltransferases, i.e. fucosyltransferase (AtFut1), galactosyltransferase (AtGalT) and xylosyltransferase (AtXT1). Assuming that genes that cooperate during the biosynthesis of the same cell wall polysaccharides might show

similar expression patterns, any AtCsl genes that show similar expression patterns with those encoding XyG glycosyltransferases would be very likely encoding XyG backbone glucan synthase. For this purpose the tissue expression profiles of AtCsl genes were analyzed by examining their corresponding EST clones from the dbEST and the frequency of their specific MPSS signatures from the Arabidopsis MPSS database. The relative expression levels among different tissues of Arabidopsis were also examined by analyzing Arabidopsis tissue comparison data from the Stanford Microarray Database. Finally, data from microarray experiments carried under conditions that might have physiological effects on cell wall metabolism from both the SMD and the NASCArrays were analyzed. The behaviors of all AtCsl genes appeared on those microarrays were examined for their possible co-regulation with known cell wall biosynthesis-related genes.

MATERIALS AND METHODS

Sequence extraction and annotation

Sequences for all AtCsl genes were obtained in May of 2000 from a BlastN search against the NCBI database using the sequence of AtCesA1 (AtRsw1-1) as query. The BAC clone IDs obtained from the blast search were compared with Dr. Todd Richmond's collection for the designation of each AtCsl gene. All cDNA sequences thus obtained were translated into protein sequences using the EditSeq program of DNASTAR (Madison, WI). Protein sequences were aligned by Multalin with default parameters (<http://prodes.toulouse.inra.fr/multalin/multalin.html>). For proteins that showed obvious N-terminal, C-terminal or internal deletions, or out-of-place sequence insertions, the equivalent region from its BAC clone was identified and translated into six frames with the Map program of GCG (Madison, WI). The possible amino acid sequences were then examined against the protein sequences of other members of the same AtCsl family, searching for new intron-exon boundaries. Re-annotated sequences were translated and subjected to multiple alignments again.

EST database search

All AtCsl genes were searched using BlastN against the NCBI EST database-others in July 2001 and updated a year later. Sequence alignments of AtCsl genes with their EST clones were carried out with Multalin and manually examined. EST clones showing more than 90% overall identity and those containing mismatches only in a single region were selected as being derived from a particular gene. All EST clones found for

one particular AtCsl gene were aligned to make sure they all contain the same sequence at either the 5' or 3' end.

Arabidopsis MPSS database search

A custom-made java script (Qiong Wang, Ribosome Database Center, Michigan State University) was used to search all AtCsl genes, AtCesA genes, AtFut1, AtXT1 and AtGalT against the Arabidopsis MPSS database (<http://mpss.ucdavis.edu/nonjava.html>) in February of 2003. All related information about the MPSS signatures for each gene query were extracted and input into a Microsoft Access database. The sequence and position of each MPSS signature were manually examined, and only the true ones were picked up according to instructions from the database website.

Microarray data retrieval and analysis

A custom-made S+ script (Rodrigo A Gutierrez, Department of Biochemistry, Michigan State University) was used to search all AtCsl genes, AtCesA genes, AtFut1, AtXT1 and AtGalT against a custom microarray database made from the SMD (<http://genome-www.stanford.edu/microarray>) raw data (Gutierrez, 2003). The custom microarray database was constructed by selecting data only from good quality microarray hybridizations considering the spatial bias of slides, R-square value of hybridizations, data integrity, spot quality parameters, and reproducibility (Gutierrez, 2003). Data from tissue expression profile arrays were analyzed separately. Data from experiments with no hybridization repeats, and experiments comparing gene expression profiles of mutant

(non-cell wall related) and wild type plants were not selected. Only data from those experiments with repeat arrays or reverse control arrays were kept and analyzed.

Data from microarray experiments involving environmental stress, pathogen attack or possible cell wall metabolism were retrieved from NASCArray at August of 2003 (<http://ssbdjc2.nottingham.ac.uk/narrays/experimentbrowse.pl>). Hybridization signals and information of microarray chips were downloaded as cvs files and incorporated into a Microsoft Access database for each selected microarray experiment (Qiong Wang, Ribosome Database Center, Michigan State University). Hybridization signals and chip information of AtCsl and related genes then were extracted, and the log₂ ratios of signals from microarray chip pairs were calculated. However, only data with a D Call of “1” were used.

Sequenc

A

non-redu

informat

Comp. c

clones to

encoded

many m

fragme

AtCsl-

was m

and 1:

occur

AtC

into

the

Se

se

se

and

sho

RESULTS

Sequence extraction, annotation and comparison analysis

All AtCesA and AtCsl genes were identified through a Blast search against the non-redundant GenBank database using AtCesA1 (AtRsw1-1) as query and using information supplied by Dr. Todd Richmond at his website (<http://cellwall.stanford.edu/cesa/index.shtml>), mainly the identification numbers of BAC clones that bear one or more AtCsl genes. A simple alignment of the protein sequences encoded by these cDNA sequences within the same individual AtCsl family showed many missed N- or C-terminal regions, or missed internal and out-of-place sequence fragments. An example is shown in Figure 3.1 for the manual sequence re-annotation of AtCslA genes. The initial protein sequence alignment showed that the 5' end of the gene was missing for AtCslA1, 11 and 15; internal sequence was missing from AtCslA10, 11 and 15; internal insertions were present in AtCslA7 and A11; internal mis-annotation occurred for AtCslA7 (Figure 3.1A). The genomic sequences from BAC clones of those AtCsl genes were therefore re-examined for intron-exon boundaries and again translated into protein sequences for alignment. After several rounds of careful manual annotation, the alignment of AtCslA proteins showed a much improved consistency (Figure 3.1B). Sequences of other AtCsl families were re-annotated the same way. The re-annotated sequences of AtCslD3 and AtCslA9 matched perfectly with their cloned cDNA sequences, respectively (Favery et al., 2001; Zhu et al., 2003) and, therefore, the re-annotated sequences seemed to be much more accurate and reliable.

Information of the re-annotated AtCsl genes are summarized in Table 3.1, showing the gene ID and the clone ID of the BAC clones where the AtCsl genes were

Figure 3.1: Alignment of AtCslA proteins using sequences before (A) and after (B) manual re-annotation. Sequences were extracted from the public GenBank database based on their identity with AtCesA1 (AtRsw1-1), and named according to Todd Richmond's classification (<http://cellwall.stanford.edu/cesa/index.shtml>). Protein sequences were aligned using MultAlin (<http://prodes.toulouse.inra.fr/multalin/multalin.html>) with default parameter settings. Amino acids showed high consensus value of more than 90% are in red, amino acids showed low consensus value of 50%-90% are in blue.

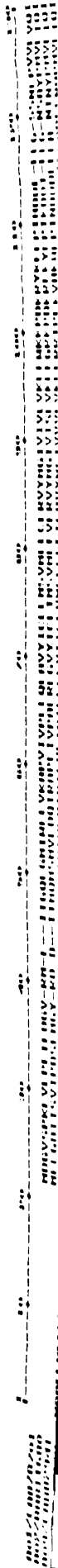


Table 3.1: Summary of re-annotated AtCsl gene. The gene ID, BAC clone ID were found, and the match with corresponding cDNA clones found in the NCBI database and the RIKEN cDNA database are shown. “M”: match; “nM”: not match; “no”: no cDNA clone available at this time. All information was extracted from the public database. Protein sequences encoded by the corresponding cDNAs were aligned to examine the sequence match. Protein sequence alignments were carried out with the MultAlin program (<http://prodes.toulouse.inra.fr/multalin/multalin.html>) using default parameters.

Gene	Gene_ID	BAC_ID	NCBI	RIKEN
AtCslA1	At4g16590	dl4320w	nM	M
AtCslA2	At5g22740	MDJ22.16	M	M
AtCslA3	At1g23480	F28C11.11	nM	M
AtCslA7	At2g35650	T20F21.16	M	M
AtCslA9	At5g03760	F17C15.180	M	M
AtCslA10	At1g24070	T23E23.23	M	no
AtCslA11	At5g16190	T21H19.110	nM	no
AtCslA14	At3g56000	F27K19.180	M	M
AtCslA15	At4g13410	T9E8.150	nM	no
AtCslC4	At3g28180	MIG10.8	M	M
AtCslC5	At4g31590	F28M20.220	M	M
AtCslC6	At3g07330	F21O3.4	M	M
AtCslC8	At2g24630	F25P17.7	M	no
AtCslC12	At4g07960	F1K3.3	M	M
AtCslB1	At2g32610	T26B15.17	nM	no
AtCslB2	At2g32620	T26B15.18	M	no
AtCslB3	At2g32530	T26B15.9	M	M
AtCslB4	At2g32540	T26B15.10	M	no
AtCslB5	At4g15290	FCAALL.256	nM	M
AtCslB6	At4g15320	FCAALL.268	nM	no
AtCslD1	At2g33100	F25I18.16	M	no
AtCslD2	At5g16910	F2K13.60	M	no
AtCslD3	At3g03050	T17B22.26	M	M
AtCslD4	At4g38190	F20D10.310	M	nM
AtCslD5	At1g02730	F22D16.26	M	no
AtCslD6	At1g32180	F3C3.4	M	no
AtCslE1	At1g55850	F14J16.9	M	M
AtCslG1	At4g24010	T19F6.17	nM	no
AtCslG2	At4g24000	T19F6.18	M	M
AtCslG3	At4g23990	T19F6.19	nM	no

four

for

(for

and

NO

(Te

in t

ma

but

exc

ad

(Fig

the

on. E

gene

inter

cons

chro

with

dis

cons

found. The corresponding cDNA clones available for AtCsl genes were also identified from the NCBI database and the RIKEN Arabidopsis Full Length cDNA database (http://pfgweb.gsc.riken.go.jp/pub_data/index.html). The alignments of protein sequences encoded by the re-annotated AtCsl cDNA coding regions with their counterparts from the NCBI and RIKEN database indicated that most of the re-annotations were accurate (Table 3.1). Even at the present time, there are still many mis-annotations for AtCsl genes in the NCBI database. For example, the re-annotated sequence of AtCslA1 and AtCslA3 matched with the corresponding cDNA sequences from the RIKEN database perfectly, but their sequences from the NCBI database still show missing domains (Table 3.1).

Genes within the same family showed random chromosome locations with the exception of AtCslB and AtCslG families (Figure 3.2). AtCslB1 and B2 were found adjacent to each other. The same was true for AtCslB3 and B4 and for AtCslB5 and B6 (Figure 3.2). Furthermore AtCslB1 and B2 are very close to AtCslB3 and B4, located on the same BAC clone T26B15 (Figure 3.2). All three AtCslG genes were found together on BAC clone T19F6 as a tandem array (Figure 3.2). This phenomenon could be due to gene duplication events late in the gene evolution pathway. AtCslD genes showed a very interesting pattern in that AtCslD5 and D6 were found on chromosome I, but at a considerable distance apart, and the four other AtCslD genes were each on a different chromosome (Figure 3.2). This predicts that it should be relatively easy to obtain plants with multiple AtCslD genes knocked out by crossing plants bearing single AtCslD gene disruptions.

The intron-exon structures of genes within the same AtCsl family were highly conserved (Figure 3.3). This was easily seen for genes of family G, B and C. AtCslG1,

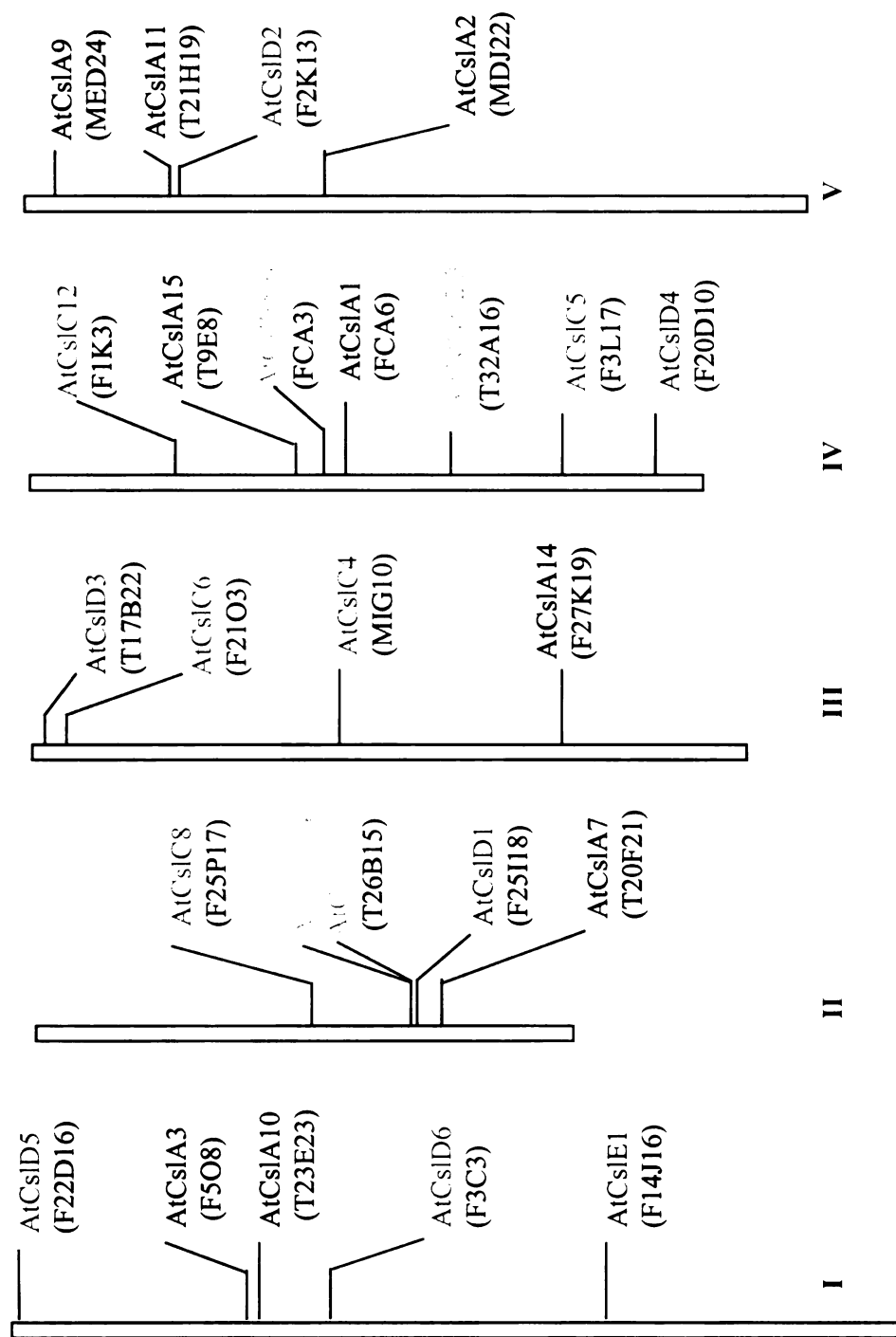
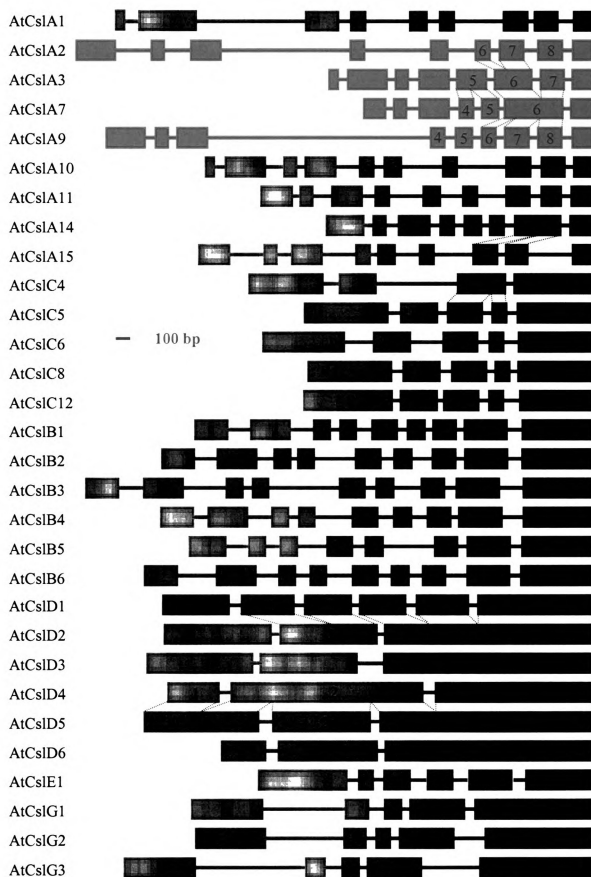


Figure 3.2: Chromosomal locations of *AtCsl* genes. The approximate position of each *AtCsl* gene was marked according to the chromosomal locations of the BAC clones containing them. The position of BAC clones were adapted from MIPS website.

Figure 3.3: Predicted intron-exon structure of AtCsl genes according to the re-annotated sequences. Some exons were numbered and linked with each other to indicate their sequence equivalences as described in the text.



G2 and G3 all contained five exons, and both the length and sequence of each exon were very similar through out the family. The same phenomenon was observed for AtCslB and AtCslC families except that AtCslB5 was missing the first exon found at the 5' end of other AtCslB genes, and the third exon of AtCslC4 was the fusion of exon 3 and 4 of other AtCslC genes (Figure 3.3). The intron-exon structures of genes from AtCslD and AtCslA families were more complicated. After careful analysis, it was found that AtCslD2, D3, D5 and D6 seemed to have the most straightforward structure, containing three exons, with the 5' end of the first exon of AtCslD6 missing (Figure 3.3). AtCslD1, however, had 6 exons, but its exon 2 and 3 was the equivalent of the second exon of AtCslD2, 3, 5, 6; and its exon 4, 5 and 6 were equivalent of the third exon of AtCslD2, 3, 5, 6 genes (Figure 3.3). AtCsl D4 also only showed three exons, but was more complicated in that its second exon could be considered as three pieces with the first piece as the equivalent of the 3' part of the first exon of AtCslD2, 3, 5, 6; the middle piece as the equivalent of the second exon of AtCslD2, 3, 5, 6; and the 3' piece when fused with the third exon became the equivalent of the third exon of AtCslD2, 3, 5, 6 (Figure 3.3). The intron-exon structure for AtCslA family was even more complicated. As indicated in Figure 3.3, exon 5 of AtCslA3 was the equivalent of the fusion of exon 5 and 6 of AtCslA10, and the fusion of exon 4 and 5 of all other AtCslA genes. Exon 6 of AtCslA3 was equivalent to the fusion of exon 6 and 7 of AtCslA1, 2, 9, 11, 14 and 15, or exon 7 and 8 of AtCslA10 (Figure 3.3). Exon 7 of AtCslA14 was equivalent to the fusion of exon 7 and 8 of AtCslA1, 2, 9, 11, and 15, or exon 8 and 9 of AtCslA10 (Figure 3.3). The diversity of the intron-exon structures of genes from AtCslA and AtCslD family, combined with their dispersed chromosome locations, strongly suggested that AtCslA

and AtCslD were more ancient gene families and they have gone through more evolutionary modifications.

The intron-exon structures of most of the re-annotated AtCsl genes matched with Dr. Todd Richmond's observations (<http://cellwall.stanford.edu/cesa/index.shtml>). Exceptions were noted from this database for AtCslA1, A3, A10 and B5. Compared with the re-annotated sequences described here, AtCslA1 showed a size discrepancy in exons 3 and 4, AtCslA3 was missing the first exon and part of the 5' end of the second exon, AtCslA10 was missing the first exon, and AtCslB05 had an extra exon in the 5' end. Because the sequences described here for AtCslA1, 3, and B5 all matched with the cDNA sequences from the RIKEN database, and sequence for AtCslA10 matched with the cDNA sequence from the NCBI database (Table 3.1), the annotations presented here for these four genes seemed more accurate.

The re-annotated cDNA sequences of AtCsl genes were translated into protein sequences. The protein length and GenBank ID are summarized in Table 3.2. All AtCsl proteins were predicted to have multiple transmembrane domains, with 1-3 near the N-terminus and 3-6 close to the C-terminus (Table 3.2). A phylogenetic tree was constructed for all AtCsl proteins (Figure 3.4). AtCslA and AtCslC grouped together whereas all other AtCsl proteins were grouped into another major clad. With all the corrections of the gene annotations, the assignment of proteins to a family were still the same as that done earlier (Richmond and Somerville, 2000; Richmond and Somerville, 2001). The relationships within each family were also mostly the same, except that among the re-annotated sequences AtCslA15 was the closest relative of AtCslA10 (Figure 3.4) instead of AtCslA11 as shown before by Richmond and Somerville (2000,

Table 3.2: Characteristics of AtCsl proteins. Protein ID, predicted length, and the predicted number and locations of transmembrane domains are included. All information was extracted from the public database with manual annotation. Transmembrane domain were predicted with server TMHMM (<http://www.cbs.dtu.dk/services/TMHMM/>) with default parameters.

Protein	Length	Protein_ID	Transmembrane Domain [number (position)]
AtCslA1	553aa	CAB78701.1	4 (70-92, 389-411, 431-453, 513-535)
AtCslA2	534aa	BAB11680.1	4 (34-56,356-385,404-426,509-531)
AtCslA3	556aa	AAF79586.1	5 (57-79,386-408,427-449,509-531)
AtCslA7	556aa	AAD15455.1	5 (72-94, 389-411, 426-448, 500-522, 527-549)
AtCslA9	533aa	CAB82941.1	5 (35-57,363-385,404-426,481-503,507-529)
AtCslA10	553aa	AAF87149.1	5 (70-92,394-415,430-452,511-529,533-551)
AtCslA11	500aa	CAC01860.1	5 (12-34,332-354,380-402,458-476,480-498)
AtCslA14	535aa	CAB87854.1	4 (43-65,361-383,402-424,502-524)
AtCslA15	503aa	CAB40776.1	4 (19-41,332-354,380-402,464-486)
AtCslC4	673aa	BAB01433.1	4 (469-487,494-512,531-553,628-650)
AtCslC5	692aa	CAA19764.1	6 (67-85,105-127,178-200,488-510,522-540,647-669)
AtCslC6	682aa	AAF02144.1	6 (67-85,106-128,171-193,485-507,516-534,637-659)
AtCslC8	690aa	AAD23884.1	6 (67-85,105-127,178-200,491-513,522-540,645-667)
AtCslC12	699aa	AAD15482.1	5 (122-144,192-214,502-524,536-554,673-695)
AtCslB1	757aa	T02560	8 (15-37,49-71,525-547,560-578,597-619,662-684,699-721,728-746)
AtCslB2	757aa	T02561	8 (20-38,47-69,533-555,570-592,605-627,671-693,706-724,733-755)
AtCslB3	755aa	T02552	6 (7-25,491-513,526-544,628-650,657-679,688-710)
AtCslB4	755aa	T02553	8 (20-42,51-69,531-553,572-594,614-636,671-693,700-722,731-753)
AtCslB5	664aa	CAB78571.1	3 (622-644,655-677,686-708)
AtCslB6	759aa	CAB78574.1	8 (24-42,49-71,108-126,264-282,316-338,620-642,657-679,686-708)
AtCslD1	1037aa	AAC04910.1	8 (179-201,208-230,815-837,848-866,885-903,936-958,962-984,1004-1022)
AtCslD2	1145aa	CAC01704.1	8 (288-310,323-341,923-945,952-974,993-1015,1046-1064,1079-1097,1110-1128)
AtCslD3	1145aa	AAF26119.1	8 (285-307,320-338,923-945,952-974,993-1015,1046-1064,1079-1097,1110-1128)
AtCslD4	1111aa	CAB37559.1	8 (263-285,298-316,884-906,913-935,954-976,1009-1031,1040-1058,1071-1089)
AtCslD5	1181aa	AAF02892.1	5 (958-980,992-1010,1081-1103,1116-1134,1144-1166)
AtCslD6	979aa	AAG23436.1	7 (118-140,147-166,752-774,787-809,880-902,915-934,944-966)
AtCslE1	730aa	AAF79313.1	6 (29-51, 64-83, 511-533, 553-575, 645-667, 677-699)
AtCslG1	771aa	AAB63622.1	6 (28-50,537-559,566-584,603-625,659-681,693-711)
AtCslG2	730aa	AAB63623.1	7 (21-39,51-69,520-542,554-576,641-663,675-697,710-728)
AtCslG3	747aa	AAB63624.1	8 (29-51,55-77,531-553,572-594,607-625,664-686,693-715,727-745)

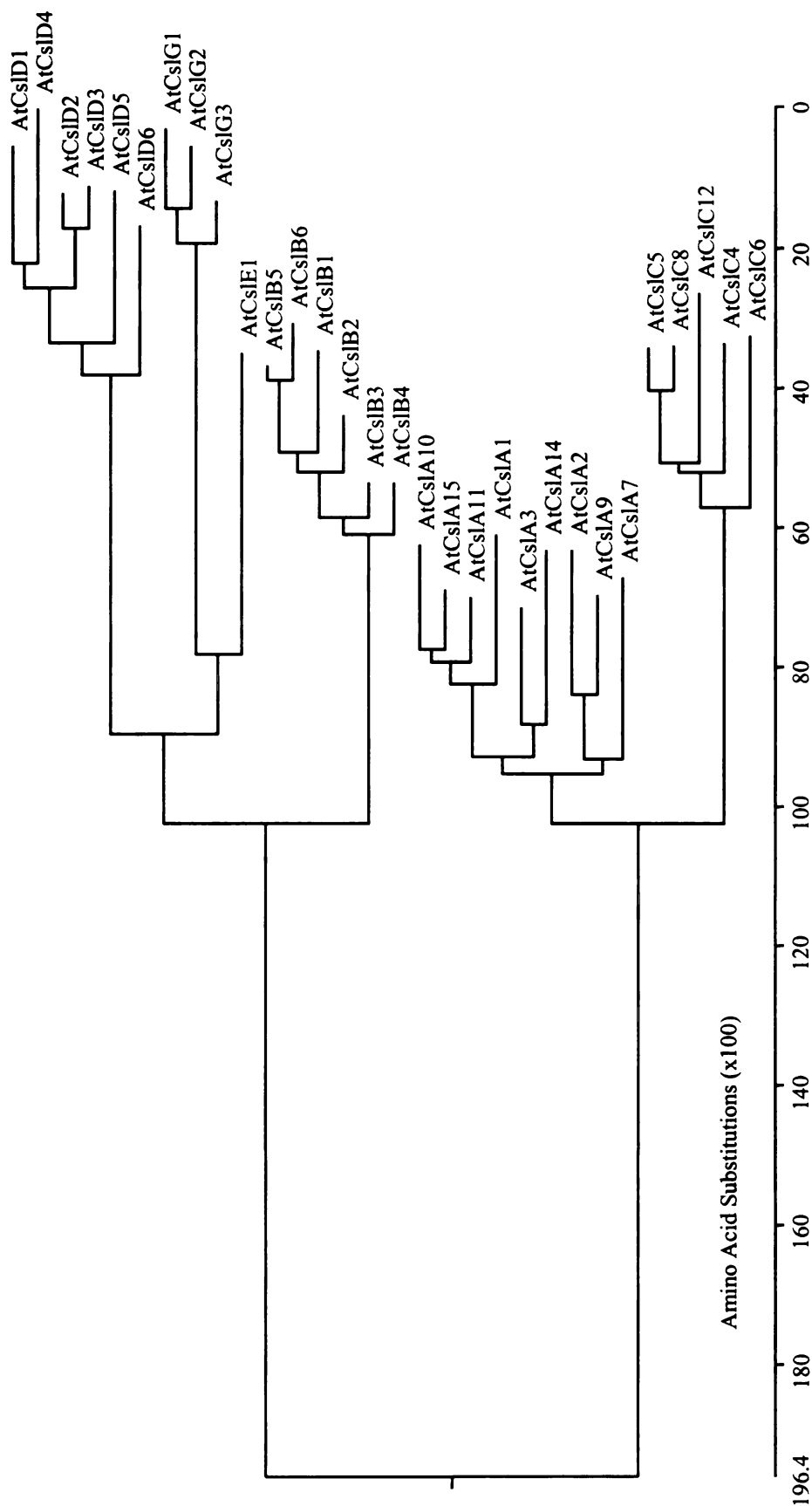


Figure 3.4: A rooted phylogenetic tree of AtCsl proteins. Proteins are encoded by the re-annotated cDNA sequences and aligned using the DNASTar program MegAlign (ClustalV, PAM250). The length of each pair of branches represents the distance between sequence pairs, while the units at the bottom of the tree indicate the number of substitution events.

2001). Another multiple alignment including AtCesA proteins showed that AtCslD family had the closest relationship to AtCesA showing sequence identity of 39.1-45.9%, while AtCslC family was the most distantly related with AtCesA proteins, showing sequence identities of only 7.3-12% (Table 3.3). The highest sequence identities shared among AtCsl protein families is between AtCslA and AtCslC families at 36.3-43.5% (Table 3.3).

Two interesting genes were found during the Blast searches for AtCsl genes, a β -(1, 3)-glucosyltransferase from *Bradyrhizobium japonicum* (AAC62210) and a secondary xylem cellulose synthase from *Populus tremuloides* (AAD03417). When the β -(1, 3)-glucosyltransferase was used as the query for a Blast search against the non redundant database, all AtCslC and AtCslA genes were found in the hit list with E values ranging from $2e-22$ to $4e-16$ but none of the members from other AtCsl gene families showed any significant similarity. When the secondary xylem cellulose synthase was used as query for the Blast search, all AtCslD, AtCslB, AtCslG and AtCslE genes were found in the hit list with E value ranging from 0 to $2e-61$, but none of the AtCslA and AtCslC genes were found. Based on this analysis, AtCsl genes can be grouped into two categories, with AtCslA and AtCslC in one group and AtCslD, B, E and G in another. This observation leads to the prediction that the two categories may have distinct functions, but further work will be needed to confirm this prediction. The sequence divergence showed from the phylogenetic tree (Figure 3.3) fits this assessment well. Proteins encoded by AtCslD, B, G, E genes might synthesize β -(1, 4)-glycosidic bonds or using UDP-glucose as substrate as AtCesA proteins do. The *Bradyrhizobium japonicum* β -(1, 3)-glucosyltransferase encodes an enzyme responsible for the synthesis of a β -(1,3)- (1,6)-glucan polymer, suggesting AtCslA and C proteins on the other hand might encode

Table 3.3: Summary of sequence identities among all AtCsl proteins. Re-annotated cDNA sequences of AtCsl genes were translated into protein sequences and aligned with the MegAlign program of DNASTar (Clustal W). The highest and lowest number of protein identities from the comparisons of different proteins within the same family or between two families were selected as the upper and lower range.

	AtCesA	AtCslA	AtCslB	AtCslC	AtCslD	AtCslE	AtCslG
AtCesA	61.1-90.8	8.4-14.9	29.4-33.2	7.3-12.0	39.1-45.9	31.9-33.7	29.3-32.7
AtCslA		53.2-79.6	6.5-14.9	36.3-43.5	7.0-15.9	8.6-14.4	7.0-13.5
AtCslB			73.8-89.5	6.5-11.4	26.4-30.6	29.6-31.2	24.8-30.8
AtCslC				59.8-88.1	6.4-12.9	7.4-10.8	7.3-10.1
AtCslD					59.0-87.9	29.9-32.3	25.9-30.2
AtCslE						---	35.5-36.3
AtCslG							79.7-80.7

enzymes responsible for sugar linkages different from β -(1,4) or using nucleotide sugar substrate different from UDP-glucose.

Expression patterns of AtCsl genes revealed by EST abundance

While the functions of all AtCsl genes remain unknown, the expression patterns of these genes were examined in different tissues, hoping that this information will shed some light on their functions. The EST database was searched for the expression of AtCsl genes associated with specific tissues or growth conditions. All EST clones available at the time (July, 2002) for AtCsl genes were manually examined and only those with more than 90% overall identity and no multiple mismatches were selected. AtCsl genes were found to be expressed in a wide range of tissues such as siliques, flowers, roots, rosette leaves, developing seeds, soil grown or liquid grown seedlings etc (Table 3.4). AtCsl genes within the same family showed different numbers of EST clones derived from them. Those EST clones also come from a wide range of different tissues (Table 3.4). AtCslA1, AtCslC4 and C6, AtCslD2 and D3, AtCslE1 all showed more than 9 EST clones in the database, indicating that these AtCsl genes might be expressed more abundantly than other AtCsl genes (Table 3.4). Sequence alignments of EST clones with AtCsl genes also confirmed the accuracy of many re-annotations of AtCsl gene ends (data not shown).

Altogether there are 106 EST clones identified for all AtCsl genes. AtCslC and D family have the most EST clones with 31 for each. AtCslB and G have the least, only 2 and 4 respectively (Table 3.5). When the number of genes within each family is considered, there are 3.5 EST clones on average for each AtCsl gene when all 30 AtCsl

Table 3.4: Summary of ESTs identified in the dbEST for AtCsl genes. Numbers of EST clones and tissues where they are derived from. AtCsl genes not listed were not represented by any EST clones, including AtCslA15, B1, 2, 4, 6, D6, G1, 2.

Gene	EST clones	Source of EST clones
AtCslA1	9	green siliques, flower buds, seedlings
AtCslA2	6	roots, rosettes and other
AtCslA3	4	seedlings, and other
AtCslA7	3	seedlings
AtCslA9	1	green siliques
AtCslA10	1	siliques and flower
AtCslA11	3	flower buds and others
AtCslA14	1	roots
AtCslB3	1	rosettes
AtCslB5	1	roots
AtCslC4	10	above ground organs 2-6 weeks, green siliques, roots, leaves, hypocotyls, seedlings
AtCslC5	6	above ground organs 2-6 weeks, developing seeds, rosettes, seedlings
AtCslC6	12	above ground organs 2-6 weeks, flower buds, green siliques, roots, seedlings
AtCslC8	2	rosettes, developing seeds
AtCslC12	1	developing seeds
AtCslD1	1	flower buds
AtCslD2	11	above ground organs 2-6 weeks, developing seeds, roots, rosettes
AtCslD3	15	above ground organs 2-6 weeks, roots, green siliques, developing seeds, rosettes, seedlings
AtCslD4	1	siliques and flowers
AtCslD5	3	roots, liquid-cultured seedlings
AtCslE1	10	above ground organs 2-6 weeks, green siliques, flower buds, roots
AtCslG3	4	above ground organs 2-6 weeks, seedlings

Table 3.5: EST abundance for AtCsl gene families. Numbers of EST clones for each AtCsl family are summarized from Table 3.4. Percentage of EST clones is calculated as the percentage of EST clones for each AtCsl family out of the total EST clones for all AtCsl genes.

Gene family	Number of genes	Number of EST clones	Percentage of EST clones	Average EST clones per gene
AtCslA	9	28	26.4%	3.1
AtCslB	6	2	1.9%	0.3
AtCslC	5	31	29.2%	6.2
AtCslD	6	31	29.2%	5.2
AtCslE	1	10	9.4%	10
AtCslG	3	4	3.8%	1.3
Total	30	106	100%	3.5

genes are included (Table 3.5). AtCslE family showed the highest expression as it has 10 EST clones per gene. AtCslC family follows it with 6.2 EST clones per gene, and AtCslB family showed the least expression with only 0.3 EST clones per gene (Table 3.5). Therefore AtCslE, C and D family genes showed relatively high expression among AtCsl genes indicated from the EST clones identified, while AtCslB and G genes showed extremely low expression that were even difficult to detect by RT-PCR reactions (data not shown).

Expression patterns of AtCsl genes revealed by MPSS database

The Arabidopsis MPSS database was searched for the expression of all AtCsl genes, together with AtCesA genes, AtFut1, AtXT1 and AtGalT genes. The comparison of expression patterns of AtCsl genes with that of these genes that are known to be involved in cellulose and XyG biosynthesis might yield some clues about the functions of AtCsl genes. Most AtCesA genes showed reasonable expression with appearance of their gene-specific MPSS tags ranging from 50 PPM (parts per million) to 250 PPM, while AtCesA3 showed the highest expression, especially in flowers, at 1225 PPM (Table 3.6). AtCesA1, 3, 5 and 6 all showed significantly more MPSS signature hits than AtCesA4, 7 and 8 (Table 3.6). Considering the fact that all five MPSS libraries were made from vigorously growing tissues where primary wall is still the main wall biosynthesis event (<http://dbixs001.dbi.udel.edu/MPSS4/java.html>, actively growing 10 weeks old callus, mixed-stage buds and immature flowers, 14-day-old leaves, 14-day-old roots and siliques one to two days post fertilization), this different expression pattern for different AtCesA genes is consistent with the observation that AtCesA1, 3, 5, 6 are cellulose synthase for

Table 3.6: Numbers of MPSS tags that found from five different Arabidopsis cDNA libraries for all AtCsl genes and AtFut1, AtGalT and AtXT1. Numbers are in PPM (parts per million) and were normalized according to the MPSS database (<http://dbixs001.dbi.udel.edu/MPSS4/java.html>). All MPSS tags were manually examined for their accuracy (Materials and Methods). Note that the tags for AtCslB5 and B6 could not be differentiated. Also AtCslD2 showed two different tags that both seemed valid according to criteria from the database, and therefore were both retained and named as AtCslD2 and AtCslD2'.

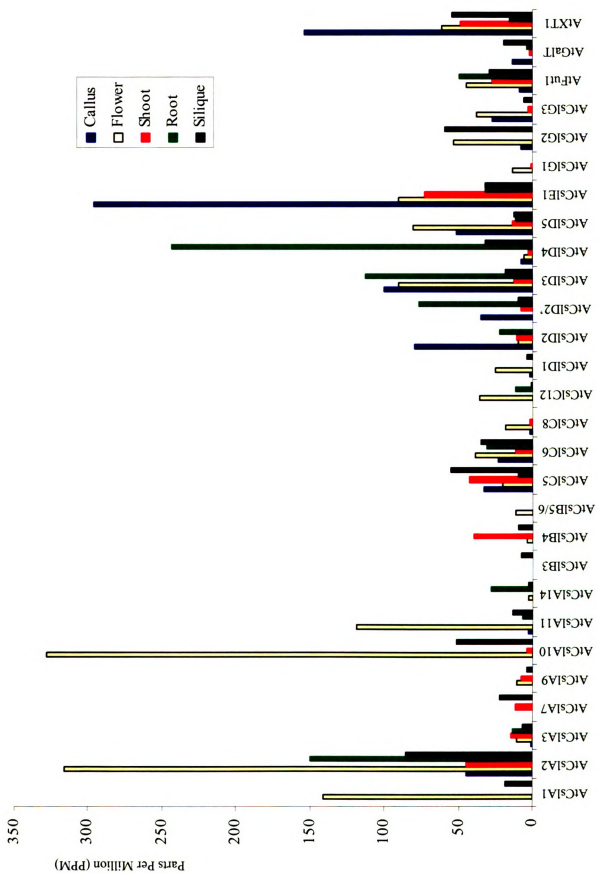
Gene_name	Callus	Flower	Shoot	Root	Silique
AtCesA1	184	238	262	146	128
AtCesA2	4	120	64	48	34
AtCesA3	237	1225	366	604	451
AtCesA4	0	104	8	61	28
AtCesA5	38	190	153	75	61
AtCesA6	42	23	144	156	80
AtCesA7	10	9	5	47	38
AtCesA8	0	46	4	32	39
AtCesA9	0	24	3	2	2
AtCslA1	0	141	0	0	18
AtCslA2	45	316	45	150	86
AtCslA3	1	11	15	14	7
AtCslA7	0	0	12	0	22
AtCsl09	0	11	8	0	4
AtCslA10	0	328	4	0	52
AtCslA11	3	119	0	7	14
AtCslA14	0	3	0	28	3
AtCslB3	0	0	0	0	8
AtCslB4	0	4	40	0	10
AtCslB5/B6	0	12	0	0	0
AtCslC5	33	20	43	10	55
AtCslC6	23	39	12	31	35
AtCslC8	2	18	2	0	0
AtCslC12	0	36	0	12	1
AtCslD1	2	25	0	0	4
AtCslD2	80	10	11	22	0
AtCslD2'	35	0	8	77	10
AtCslD3	100	90	13	113	18
AtCslD4	8	6	3	243	32
AtCslD5	52	81	14	12	13
AtCslE1	296	90	73	32	32
AtCslG1	0	14	1	0	0
AtCslG2	8	53	0	0	59
AtCslG3	27	38	3	0	6
AtFut1	9	45	27	50	29
AtGalT	14	0	2	4	19
AtXT1	154	61	49	16	54

primary walls expressed in expanding tissues, while AtCesA4, 7 and 8 are cellulose **synthases** for the secondary walls expressed in developing vascular tissue (Williamson et al., 2002).

The overall expression of AtCsl genes is generally lower than that of AtCesA **genes** as seen from the frequency of appearance of their gene-specific MPSS tags (Table 3.6; Figure 3.5). AtCslA2 showed the highest overall expression with 316 PPM in **flowers** and 150 PPM in roots (Table 3.6; Figure 3.5). AtCslA1, 10 and 11 also showed **moderate** expression in flowers, at 141 PPM, 328 PPM and 119 PPM respectively (Table 3.6; Figure 3.5). Among other AtCsl genes, only AtCslD3 in callus and roots, D4 in roots and AtCslE1 in callus showed an expression level of more than 100 PPM (Table 3.6; Figure 3.5). AtCslB genes showed the lowest expression with a maximum value of 40 PPM in shoot for AtCslB4 (Table 3.6), which is consistent with the difficulties accounted during the amplification of AtCslB transcripts by RT-PCR (data not shown). The MPSS **data** also supported a root-preference expression of AtCslD genes, including D2, D3 and D4 (Table 3.6; Figure 3.5). AtCslD2 and D3 also showed good expression levels in the **callus**, indicating that they are responsive to environmental stimuli (Table 3.6; Figure 3.5)., since callus is a tissue type develops as a response to injury caused by physical or **chemical** means and contains cells that are differentiated but unorganized (<http://www.agls.uidaho.edu/plsc202/pdf/02notes-8.pdf>).

AtCslD proteins are the closest paralogs of AtCesA proteins within the AtCesA **superfamily**, but their sequence identities with AtCesA proteins are lower than the **identities** shared among different AtCesA proteins. Since XyG has the same backbone **chemical** structure as cellulose, AtCslD proteins are good candidates for encoding the

Figure 3.5: MPSS expression profile of all AtCsl genes and AtFut1, AtGalT, AtXT1. Data is summarized from Table 3.5. Noting that there were two signature tags for AtCslD2 and represent AtCslD2 twice. Signature tags for AtCslB5 and B6 could not be differentiated from each other and were combined to represent both.



XyG β -(1, 4)-glucan synthase. Therefore the expression of AtCslD genes were compared with that of genes involved in XyG biosynthesis, AtFut1, AtGalT and AtXT1. However, no obvious common expression profile was observed (Figure 3.5). This did not invalidate the hypothesis though, since gene redundancy brings in complexity when gene expression patterns are compared among gene families.

Two MPSS signature tags were recorded for AtCslD2, one is 27 bp upstream of the stop codon, and the other one is 143 bp downstream of the stop codon into the 3'UTR. After careful analysis, no criteria could be used to eliminate either one of them as a technical error. On the other hand, alternative splicing is always a possibility to generate two different transcripts from the same gene. Without further experimental investigation, both signatures were retained.

Expression patterns of AtCsl genes revealed by tissue panel microarrays from Stanford Microarray Database

Genes involved in the biosynthesis of the same plant cell wall polysaccharide might have similar expression patterns in different tissues. Any AtCsl gene encoding the XyG glucan synthase might have similar expression profile with others involved in XyG biosynthesis, i.e. AtFut1, AtGalT and AtXT1. Therefore the expression profiles of AtFut1, AtGalT, AtXT1, AtCesA genes and all AtCsl genes were examined by analyzing available microarray data comparing gene expression in different Arabidopsis tissues.

AtCsl gene expression data were extracted from microarray experiments comparing gene expression levels among different tissues of Arabidopsis from the Stanford Microarray Database (SMD). Only statistically significant and repeatable data

were selected (Table 3.7) after considering array quality, reproducibility and statistical analysis (Gutierrez, 2003). Five AtCesA genes, AtCesA1, 3, 5, 6 and 7, showed a strong expression bias in stems (Table 3.7). AtCesA1 and 7 also showed higher expression in siliques (Table 3.7). This observation is consistent with the concept that stems contain large amounts of cellulose compared to other tissues. Whether the same is true for siliques still remain to be seen. AtCesA2, however, showed an opposite trend with less expression in siliques and roots compared with whole seedlings (Table 3.7). This suggests that AtCesA2 has tissue specific expressions different from most other AtCesA genes.

Among the expression profiles of AtCsl genes, a few tissue specific expressions were noted (Table 3.7). Firstly AtCslA1 and C5 showed higher expression in flowers (Table 3.7). Secondly AtCslE1 was expressed higher in both flowers and stems (Table 3.7). Finally AtCslA1 and D2 showed higher expression in roots while the expression of G3 was lower in roots (Table 3.7). These observations might suggest the existence of gene redundancy of AtCsl genes, and different members within the same AtCsl family might have different tissue preference of expression.

The expression of AtFut1 and AtGalT, however, did not show very strong tissue expression preferences, with maybe slightly higher expression of AtFut1 in flowers and AtGalT in siliques and stems (Table 3.7). This made it rather difficult to compare the expression pattern of AtCsl genes with them and therefore no conclusions regarding AtCsl function can be drawn from this analysis of tissue expression profiles.

Regulated expressions of AtCsl genes revealed by microarray experiments

Table 3.7: Tissue expression profile of AtCsl genes revealed by Stanford Microarray Database. All data were normalized

(Materials and Methods) log2 ratio of signals detected from microarray chip sets. Numbers showing more than 2 fold signal change (log2 ratio is bigger than 1, or smaller than -1) in both forward and reverse hybridizations are shaded.

	silique- vs-ref	ref-vs- silique	stem- vs-ref	stem- ref	ref-vs- stem	leaf- ref	leaf- vs-ref	ref-vs- leaf	flower- ref	flower- vs-ref	root- ref	root- vs-ref	ref-vs- root	leaf- ref	leaf- vs-ref	flower- ref	flower- vs-ref
AtCesA1	-1.12	1.10	-1.25	1.64	0.74	-0.34	0.56	-0.11	0.33	-0.01	-0.44	0.10					
AtCesA2	1.11	-1.19	0.43	-0.55	-0.35	-0.30	-0.66	0.35	1.34	-1.44							
AtCesA3	-1.13	0.97	-1.76	1.79	0.28	-0.53	0.26	0.00	0.03	0.22	-0.25	0.41					
AtCesA4	-0.74	0.81	-0.94	1.25		-0.73	-0.30	0.40	0.35								
AtCesA5	-1.06	0.81	-1.22	1.30	1.08	-0.69	0.92	-0.22	0.69	-0.41	-0.63	0.65					
AtCesA6	-0.91	0.82	-1.49	1.59	0.74	-0.70	0.78	-0.53	-0.07	0.29	-0.60	0.45					
AtCesA7	-1.96	1.99	-2.31	3.29							-1.15	0.89					
AtCslA1	-0.13	-0.13	0.82	-0.59	0.50	-0.45	2.85	-1.77	-1.97	2.44	-3.53	3.50					
AtCslA3	0.44	-0.56	0.14	-0.36	0.07	-0.58	0.31	-0.74	0.31		-0.81	0.64					
AtCslA7	-0.13	0.33	0.45	-0.32	0.54	-0.62	0.37	-0.23	0.08	-0.42							
AtCslC4	0.24	-0.46	-0.51	0.59	0.24	-0.93	-0.78	0.46	-0.79	0.68	0.37	0.07					
AtCslC5	-0.62	0.82	-0.04	-0.07	1.08	-0.79	0.77	-1.10	-0.51	-0.03	-1.87	1.84					
AtCslD2	-0.51	0.30	-0.35	0.41	0.66	0.08	0.99	-0.10	-1.57	1.63							
AtCslD3	-0.62	0.52	-0.69	0.73	0.74	-0.13	0.47	-0.33	-1.37	0.92	-0.55	-0.01					
AtCslE1	-1.34	0.90	-1.28	1.05	-0.24	-0.10	1.28	-1.43	-0.58	0.26	-0.39	0.28					
AtCslG1	0.18	-0.28	-0.18	0.30	-0.09	-0.33	-1.07	0.75	-1.22	0.84	0.28	-0.69					
AtCslG3	0.53	-0.15	0.44	-0.48	0.07	0.48	0.17	0.59	1.56	-1.01	-0.61	0.99					
AtFut1	-0.71	0.58	-0.12	0.07	0.45	0.17	0.58	-0.79	-0.33	0.30	-0.88	1.22					
AtGalT	-1.02	0.91	-0.71	1.00	0.65	-0.33			0.20	0.05	-0.19	0.57					

In order to see if any of the AtCsl genes showed similar regulated expression profile with genes involved in XyG biosynthesis, AtFut1, AtGalT and AtXT1, under various internal or environmental conditions, the microarray data from the SMD and NASCArray were examined for the expression patterns of AtCesA, AtCsl, AtFut1, AtGalT and AtXT1 genes. There are 688 microarray hybridizations available at the time (January 2002) from the Stanford Microarray Database. After discarding hybridizations that correspond to technical experiments, analysis of other organisms, or did not meet various quality control criteria (Gutierrez, 2003), data from 338 microarray hybridizations were selected. Similarly data of 25 microarray hybridizations from the Nottingham Arabidopsis Stock Center's microarray database were retrieved and incorporated with the ones from the SMD.

The expression of detectable AtCesA, AtCsl and AtFut1, AtGalT, and AtXT1 genes from these microarray hybridizations were selected and analyzed with hierarchical clustering - Gene Cluster (<http://rana.lbl.gov/EisenSoftware.htm>). The relationships among genes and experiments were seen through Treeview (<http://rana.lbl.gov/EisenSoftware.htm>). However, the microarray data clustering analysis of those selected data didn't reveal any significant expression pattern linkage either among AtCsl genes, or between AtCsl genes and genes of known functions (data not shown). Part of the reason was that well-designed experiments with high quality repeatable array chips and consistent signal detections are rare; and the signals of many AtCsl genes detected on microarray chips were not significant due to their extremely low expression. Furthermore, none of the AtCsl genes showed similar expression profile with

any of the AtCesA genes throughout these microarray experiments, consistent with the hypothesis that AtCsl proteins have different function from cellulose synthase.

However, based on some well-designed and repeatable microarray experiments, the expression of some AtCsl genes showed more alterations than others under a series of environmental stress conditions (data not shown). If confirmed by RNA blottings or RT-PCR, these AtCsl genes could well serve as links to connect different environmental signal with plant cell wall metabolism.

DISCUSSION

Accurate gene annotation is essential for cloning genes via PCR, RT-PCR reactions, and expressing genes for the production of active proteins. The sequencing of the complete Arabidopsis genome was accomplished in 2001 and has become a rich source for gene expression and gene functional studies for plant research (<http://www.arabidopsis.org/>). However, inaccuracies of gene annotation have hampered many research projects. The first part of this chapter described the re-annotation of AtCsl genes from the Arabidopsis whole genome database. Many of the corrected sequences were confirmed by comparison with cloned AtCsl cDNA sequences or EST clone sequences. Among the 30 AtCsl genes, 9 of them from the NCBI database still show mis-annotations compared with the sequences described in this chapter (Table 3.1). The sequences of three of these 9 AtCsl genes were confirmed by the RIKEN cDNA clones. The other 6 genes showed much improved sequence alignment when compared with their corresponding homologs, but their annotations have still not been confirmed by comparison with cDNA sequences available from any database.

The sequence alignment and structural analysis of AtCsl proteins indicated that the substrate structure and catalytic mechanism for AtCslB, D, E and G proteins might be more closely related to AtCesA proteins than that of AtCslA and C proteins (Table 3.3). In other words, AtCslB, D, E, G proteins are more likely to use UDP-glucose as substrate and form β -1,4 glycosidic bonds than the AtCslA and C proteins. Among them AtCslD proteins have the highest probabilities to have these enzymatic properties as they showed the highest protein identity with AtCesA.

Several investigators have noted that all AtCsl proteins contain the conserved aspartic acid residues and the QxxRW motif that are characteristic of processive β -glycosyltransferases (Richmond and Somerville, 2000; Saxena and Brown, 2000; Doblin et al., 2001). All AtCsl proteins described here showed the D,D,D and QxxRW motifs even before re-annotation. It is therefore quite possible that all AtCsl proteins are involved in the synthesis of different β linked polysaccharide backbones such as the backbones of callose, XyG, GAX, mixed-linkage glucan, glucomannan, galactomannan or galactoglucomannan. Doblin et al (2001) proposed that CslD proteins are involved in cellulose biosynthesis based on gene expression studies in pollen. However, activity assays and product analysis to support this conclusion are still lacking.

The second part of this chapter explored the relative expression levels and tissue expression preferences of AtCsl genes revealed by digital northern approaches examining EST clone abundance, the MPSS signature abundance, and microarray experiment analysis. These efforts did not reveal any expression profile similarity between any AtCsl genes and genes with known cell wall-related functions such as AtCesA, AtFut1, AtGalT and AtXT1. Therefore, no immediate candidate can be identified as encoding the XyG glucan synthase. We also could not make any new functional suggestions for AtCsl genes based on the analysis shown here. However, because of the low expression of AtFut1, AtGalT, AtXT1, and most of the AtCsl genes, it is possible that the expression of some of them may often not be detected. At the same time, because of the existence of family members sharing high sequence identities, the expression of AtCsl genes may be misrepresented by their close homologs. Techniques like real-time RT-PCR and RNA blotting may reveal more meaningful expression patterns for AtCslD genes.

A guar (*Cyamopsis tetragonoloba*) homolog of AtCslA9 gene was recently found to encode a β -mannan synthase (Kanwarpal S. Dhugga, personal communications). Guar seeds contain 37% galactomannan as cell wall storage polysaccharide (<http://www.polygal.ch/poly/ENGLISH/ROHSTO.HTM>). A cDNA clone was isolated from a guar seed EST database and showed sequence similarity with cellulose synthase-like genes from other organisms (Kanwarpal S. Dhugga, personal communications). This gene, when expressed in a soybean somatic embryo system, showed high level of activity for β -mannan synthase (Kanwarpal S. Dhugga, personal communications). This study is the first to provide experimental evidence for the speculation that Csl genes encode glycan synthases or glycosyltransferases involved in cell wall polysaccharide biosynthesis. While this provides a function for one gene in guar, it leaves unresolved the functions of the Arabidopsis genes. It will be interesting to determine whether the Arabidopsis homolog of the guar gene also encodes a mannan synthase.

REFERENCE

- Brenner, S., Johnson, M., Bridgham, J., Golda, G., Lloyd, D. H., Johnson, D., Luo, S., McCurdy, S., Foy, M., Ewan, M., Roth, R., George, D., Eletr, S., Albrecht, G., Vermaas, E., Williams, S. R., Moon, K., Burcham, T., Pallas, M., DuBridge, R. B., Kirchner, J., Fearon, K., Mao, J.-i. and Corcoran, K.** (2000). "Gene expression analysis by massively parallel signature sequencing (MPSS) on microbead arrays." *Nat. Biotechnol.* **18**: 630-634.
- Brenner, S., Williams, S. R., Vermaas, E. H., Storck, T., Moon, K., McCollum, C., Mao, J.-i., Luo, S., Kirchner, J., Eletr, S., DuBridge, R. B., Burcham, T. and Albrecht, G.** (2000). "In vitro cloning of complex mixtures of DNA on microbeads: Physical separation of differentially expressed cDNAs." *Proc. Natl Acad. Sci. USA* **97**: 1665-1670.
- Camirand, A., Brummell, D. and Maclachlan, G.** (1987). "Fucosylation of xyloglucan localization of the transferase in dictyosomes of pea stem cells." *Plant Physiol.* **84** (3): 753-756.
- Camirand, A. and Maclachlan, G.** (1986). "Biosynthesis of the fucose-containing xyloglucan nonasaccharide by pea *Pisum sativum* cultivar Alaska microsomal membranes." *Plant Physiol.* **82** (2): 379-383.
- Cutler, S. and Somerville, C. R.** (1997). "Cellulose synthesis: *Cloning in silico*." *Curr. Biol.* **7**: R108-R111.
- Delmer, D. P. and Stone, B. A.** (1988). "Biosynthesis of plant cell walls." *The Biochemistry of Plants*. J. Priess, New York, Academic Press Inc. **14**: 373-421.
- Doblin, M. S., Melis, L. D., Newbigin, E., Bacic, A. and Read, S. M.** (2001). "Pollen tubes of *Nicotiana glauca* express two genes from different beta-glucan synthase families." *Plant Physiol.* **125**: 2040-2052.
- Faik, A., Bar-Peled, M., DeRocher, A. E., Zeng, W., Perrin, R. M., Wilkerson, C., Raikhel, N. V. and Keegstra, K.** (2000). "Biochemical characterization and molecular cloning of an alpha-1,2-fucosyltransferase that catalyzes the last step of cell wall xyloglucan biosynthesis in pea." *J. Biol. Chem.* **275** (20): 15082-15089.
- Faik, A., Price, N. J., Raikhel, N. V. and Keegstra, K.** (2002). "An Arabidopsis gene encoding an alpha-xylosyltransferase involved in xyloglucan biosynthesis." *Proc. Natl Acad. Sci. USA* **99** (11): 7797-7802.
- Favery, B., Ryan, E., Foreman, J., Linstead, P., Boudonck, K., Steer, M., Shaw, P. and Dolan, L.** (2001). "KOJAK encodes a cellulose synthase-like protein required for root hair cell morphogenesis in *Arabidopsis*." *Gene. Dev.* **15**: 79-89.

Fernandes, J., Brendel, V., Gai, X., Lal, S., Chandler, V. L., Elumalai, R. P., Galbraith, D. W., Pierson, E. A. and Walbot, V. (2002). "Comparison of RNA expression profiles based on maize expressed sequence tag frequency analysis and micro-array hybridization." *Plant Physiol* **128**: 896-910.

Fry, S. C. (1989). "The structure and functions of xyloglucan." *J. Exp. Bot.* **40** (210): 1-11.

Gollub, J., Ball, C. A., Binkley, G., Demeter, J., Finkelstein, D. B., Hebert, J. M., Hernandez-Boussard, T., Jin, H., Kaloper, M., Matese, J. C., Schroeder, M., Brown, P. O., Botstein, D. and Sherlock, G. (2003). "The Stanford Microarray Database: data access and quality assessment tools." *Nucleic Acids Res.* **31** (1): 94-96.

Gutierrez, R. A. (2003). Inherent and regulated mRNA stability in *A. thaliana*. Ph.D. Thesis. Department of Biochemistry and Molecular Biology, Michigan State University.

Hayashi, T. and Maclachlan, G. (1984). "Pea *Pisum sativum* cultivar Alaska xyloglucan and cellulose 1. Macromolecular organization." *Plant Physiol.* **75** (3): 596-604.

Hayashi, T. and Matsuda, K. (1981). "Biosynthesis of xyloglucan in suspension cultured soybean *Glycine max* cells. Synthesis of xyloglucan from UDP-glucose and UDP-xylose in the cell-free system." *Plant Cell Physiol.* **22** (3): 517-524.

Kato, Y. and Matsuda, K. (1980). "Structure of oligosaccharides obtained by controlled degradation of mung bean xyloglucan with acid and *Aspergillus oryzae* enzyme preparation." *Agric. Biol. Chem.* **44** (8): 1751-1758.

Lockhart, D. J. and Winzeler, E. A. (2000). "Genomics, gene expression and DNA arrays." *Nature* **405**: 827-836.

Madson, M., Dunand, C., Li, X., Verma, R., Vanzin, G. F., Caplan, J., Shoue, D. A., Carpita, N. C. and Reiter, W.-D. (2003). "The MUR3 gene of Arabidopsis encodes a xyloglucan galactosyltransferase that is evolutionarily related to animal exostosins." *Plant Cell* **15**: 1662-1670.

Pear, J. R., Kawagoe, Y., Schreckengost, W. E., Delmer, D. P. and Stalker, D. M. (1996). "Higher plants contain homologs of the bacterial celA genes encoding the catalytic subunit of cellulose synthase." *Proc. Natl. Acad. Sci. USA* **93**: 12637-12642.

Perrin, R. M., DeRocher, A. E., Bar-Peled, M., Zeng, W., Norambuena, L., Orellana, A., Raikhel, N. V. and Keegstra, K. (1999). "Xyloglucan fucosyltransferase, an enzyme involved in plant cell wall biosynthesis." *Science* **284** (5422): 1976-1979.

Richmond, T. A. (2000). "Higher plant cellulose synthases." *Genome Biology* **1** (4): 3001.1-5.

Richmond, T. A. and Somerville, C. R. (2000). "The cellulose synthase superfamily." *Plant Physiol.* **124**: 495-498.

Richmond, T. A. and Somerville, C. R. (2001). "Integrative approaches to determining Csl function." *Plant Mol. Biol.* **47**: 131-143.

Saxena, I. M. and Brown, R. M. J. (2000). "Cellulose synthases and related enzymes." *Curr. Opin. Plant Biol.* **3**: 523-531.

White, J. A., Todd, J., Newman, T., Focks, N., Girke, T., Martinez de Ilarduya, O., Jaworski, J. G., Ohlrogge, J. B. and Benning, C. (2000). "A new set of Arabidopsis expressed sequence tags from developing seeds. The metabolic pathway from carbohydrates to seed oil." *Plant Physiol* **124**: 1582-1594.

Williamson, R. E., Burn, J. E. and Hocart, C. H. (2002). "Towards mechanism of cellulose synthesis." *Trends Plant Sci.* **7** (10): 461-467.

Zhu, Y., Nam, J., Humara, J. M., Mysore, K. S., Lee, L. Y., Cao, H., Valentine, L., Li, J., Kaiser, A. D., Kopecky, A. L., Hwang, H. H., Bhattacharjee, S., Rao, P. K., Tzfira, T., Rajagopal, J., Yi, H., Veena, Yadav, B. S., Crane, Y. M., Lin, K., Larcher, Y., Gelvin, M. J., Knue, M., Ramos, C., Zhao, X., Davis, S. J., Kim, S. I., Ranjith-Kumar, C. T., Choi, Y. J., Hallan, V. K., Chattopadhyay, S., Sui, X., Ziemienowicz, A., Matthyse, A. G., Citovsky, V., Hohn, B. and Gelvin, S. B. (2003). "Identification of Arabidopsis *rat* mutants." *Plant Physiol.* **132** (2): 494-505.

CHAPTER 4

Localization Studies of AtCslD2 Proteins

ABSTRACT

Among the subfamilies of the AtCesA superfamily of genes, the AtCslD subfamily has the highest level of sequence identity to the cellulose synthase subfamily. AtCslD proteins not only share significant sequence identity with AtCesA proteins but also contain the β processive glycosyltransferase motifs conserved for AtCesA proteins. However, the function of AtCslD proteins is still not known. The two major hypotheses are that they are involved in cellulose biosynthesis or the formation of matrix polysaccharides that are similar in structure to cellulose, such as xyloglucan. In some cases, unique tissue-specific expression of AtCslD genes were observed, with high level of expression in pollen tubes or roots. These observations led to the hypothesis that AtCslD proteins were isoforms of AtCesA proteins expressed in specific tissues. Among the cell wall polysaccharides, only cellulose and callose are synthesized at the plasma membrane while all other polysaccharides are synthesized in the Golgi complex. To test this hypothesis and, thereby, shed some light on the functions of AtCslD proteins, antibodies against AtCslD2 were generated and purified. Utilizing techniques of endomembrane purification such as two-phase partitioning or sucrose density gradient centrifugation, combined with localization of antibodies against marker enzymes for different organelles, AtCslD2 was localized in the Golgi complex. This observation made it unlikely that AtCslD proteins are involved in cellulose synthesis and more likely that they are responsible for the synthesis of a matrix polysaccharide backbone.

INTRODUCTION

Plant cell walls consist of cellulose microfibrils embedded in a matrix of polysaccharides. While cellulose microfibrils contain only β -(1, 4)-glucan chains, the cell wall matrix is a heterogeneous complex including neutral polysaccharides such as xyloglucan, mannan, galactomannan, and xylan, and acidic pectic polysaccharides such as PGA, RG I and RG II (Staehelin and Moore, 1995). Another polysaccharide of plant cell walls is callose, consisting of β -(1,3)-glucan chains.

A definitive feature that distinguishes enzymes involved in the biosynthesis of cellulose and callose from those involved in the biosynthesis of other matrix polysaccharides is their localization within the cell. Cellulose and callose are synthesized at the plasma membrane and then incorporated into the wall while other matrix polysaccharides are synthesized in Golgi complexes and then transported to the cell surface for their incorporation into the cell wall (Delmer and Stone, 1988).

Cellulose synthase was first visualized as an organized macromolecular complex (the terminal complex) using freeze–fracture techniques to examine the synthesis of cellulose microfibrils in the plasma membrane of a green alga *Oocystis apiculata* (Brown and Montezinos, 1976). The cellulose synthase terminal complex structure has been observed at the plasma membrane using the same technique in many other organisms, such as bacteria (Zaar, 1979), mosses and ferns (Rudolph et al., 1989), various algae (Hotchkiss, 1989; Mizuta and Brown, 1992), and higher plants (Mueller et al., 1976; Mueller and Brown, 1980). One of the latest localization studies of the cellulose synthase rosette terminal complexes on the plasma membrane was done in the vascular plant *Vigna angularis* (Kimura et al., 1999). Authors of this study utilized an antibody against

an *E. coli*-expressed conserved region of the catalytic subunit CelA of cotton cellulose synthase, combined with the freeze–fracture technique, to localize the terminal complexes on the P-fracture face, i.e., the cytoplasmic side of the plasma membrane (Kimura et al., 1999).

Callose is not a universal component of the cell wall matrix. It is often only seen at limited locations such as cell plates of dividing cells, plasmodesmata, and sieve plates (Northcote et al., 1989). It is also rapidly synthesized during wounding, pathogen attack, and mechanical stress (Kauss, 1987; Bolwell, 1993; Benhamou, 1995). Callose synthase activity has long been used as a classical marker for the plant plasma membrane (Larsson et al., 1987; Widell and Larsson, 1990). This activity has been localized in plasma membranes purified by linear sucrose density gradients from *Nicotiana alata* (Turner et al., 1998) and by two-phase partitioning from *Brassica oleracea* (Fredrikson et al., 1991). Using specific antibodies against (1,3)- β -glucan, the product itself, callose synthase activity was also localized on cell walls of the yeasts *Saccharomyces rouxii* and *Schizosaccharomyces pombe*, of the fungus *Conidiobolus obscurus* (Horisberger and Rouvet-Vauthey, 1985; Horisberger et al., 1985; Latge et al., 1986), the roots of bean (*Phaseolus vulgaris*) (Northcote et al., 1989), and *Nicotiana alata* pollen tubes (Meikle et al., 1991).

It has been estimated that the biosynthesis of cell wall matrix polysaccharides requires the activity of more than a hundred glycan synthases and glycosyltransferases (Perrin et al., 2001). However, only a few genes encoding them have been identified and characterized (Edwards et al., 1999; Perrin et al., 1999; Faik et al., 2000; Faik et al., 2002; Madson et al., 2003). There are still no immunochemical studies utilizing antibodies

against specific enzymes to localize them to Golgi membranes. These glycan synthases and glycosyltransferases have traditionally been localized to the Golgi complex by localizing epitopes carried on their specific polysaccharides products. Polyclonal antibodies against PGA/RG-I and XyG were generated and used to localize the complex pectic polysaccharides PGA/RG-1 to cis- and medial cisternae of the Golgi complexes, and XyG to the trans cisternae and the transgolgi network (TGN). Well-studied examples include the localization of these matrix polysaccharides in clover root tip cortical parenchyma cells (Moore et al., 1991; Lynch and Staehelin, 1992) and suspension-cultured sycamore maple (*Acer pseudoplatanus* L.) cells (Zhang and Staehelin, 1992). Monoclonal antibody JIM5 specifically recognizes unesterified PGA, while JIM7 recognizes methyl-esterified PGA, and CCRC-M1 recognizes the terminal fucose residue of XyG. These monoclonal antibodies were utilized to localize the corresponding wall matrix polysaccharides to both the Golgi complex and secretory vesicles in winter vetch (*Vicia villosa* Roth) (Sherrier and Vandenbosch, 1994) and sycamore maple cells (Zhang and Staehelin, 1992). Recently another type of hemicellulose, mannan, was also localized to the Golgi-rich vesicles from Arabidopsis callus using polyclonal antibodies against mannans (Handford et al., 2003).

On the other hand, the activities of many glycan synthases and glycosyltransferases have been detected in membrane vesicles derived from the Golgi complexes. The presence of these activities in Golgi-rich fractions was used as evidence to support a Golgi localization of these enzymes. Examples include XyG fucosyltransferase, XyG galactosyltransferase, galactan galactosyltransferase from pea

(Brummell et al., 1990; Baydoun et al., 2001), and the arabinosyltransferase involved in arabinoxytan synthesis from wheat (Porchia et al., 2002).

We are interested in identifying functions of AtCsl proteins as some of them might be XyG glucan synthases (see chapter 3). The localization of AtCsl proteins becomes critical for determining if they are glycosyltransferases involved in the matrix polysaccharide biosynthesis or just cellulose synthases. The AtCslD family has the highest sequence similarity to AtCesA proteins within the AtCesA superfamily, showing sequence identities of around 40~45% (see chapter 3). They are also very similar in size and have a similar number and organization of predicted transmembrane domains (see chapter 3). Moreover, AtCslD and AtCesA proteins share structural features that have been proposed to be indicative of processive glycosyltransferases (Saxena et al., 1995), such as the D,D,D,QxxRW motif proposed to define the nucleotide-sugar binding domain and the catalytic site (Richmond and Somerville, 2000). They both belong to family 2 of inverting nucleotide-diphospho-sugar glycosyltransferases that synthesize repeating β -glycosyl unit structures (Campbell et al., 1997; Richmond and Somerville, 2001).

Doblin et al. (2001) provided evidence that led them to postulate that CslD genes encode a specialized cellulose synthase activity. RT-PCR studies using primers designed from conserved regions of AtCesA superfamily from *Nicotiana alata* pollen tubes amplified NaCslD1 as a major product and NaCesA1 as a minor product (Doblin et al., 2001). Expression studies revealed that NaCslD1 was expressed abundantly in male gametophyte tissues after pollen mitosis, and NaCesA1 was expressed at a low level in a range of floral and vegetative tissues, but not in the male gametophyte (pollen or anthers) (Doblin et al., 2001). Given the fact that cellulose is a major component of pollen tube

cell walls, the authors hypothesized that the gene(s) encoding cellulose synthase in pollen should have a relatively high expression. Since NaCslD1 and NaCesA1 are the only members of the AtCesA superfamily found in pollen tubes, the authors proposed that CslD proteins were actually isoforms of CesA proteins and that NaCslD1 was responsible for the deposition of cellulose in *Nicotiana alata* pollen tubes (Doblin et al., 2001). If this prediction is correct, CslD proteins should be localized at the plasma membrane.

However in another study, AtCslD3 was localized in the endoplasmic reticulum. In this case, a AtCslD3-GFP fusion protein under the constitutive 35S promoter was transiently expressed in *Nicotiana benthamiana* leaf cells (Favery et al., 2001). GFP fluorescence was only observed in the endoplasmic reticulum present in the thin layer of cytoplasm between the plasma membrane and vacuole (Favery et al., 2001). Therefore localization studies of AtCslD proteins will be an important part of the attempt to clarify the contradictory conclusions currently present in the literature.

Whether the AtCslD proteins are localized at the Golgi complexes is critical for understanding their functions. A convincing localization of AtCslD proteins at the plasma membrane would clearly support the hypothesis that they are cellulose synthases. On the other hand, AtCslD proteins are more likely to be enzymes involved in matrix polysaccharides biosynthesis if they are located at the Golgi complex. Therefore, antibodies against AtCslD proteins were generated and used to detect those proteins in *Arabidopsis* intracellular membrane organelles.

Sedimentation by centrifugation through sucrose density gradients has frequently been used to separate intracellular membrane organelles including the plasma membrane, ER, Golgi, mitochondria, chloroplast etc. An organelle purification protocol has been

developed in maize (Buckeridge et al., 1999) and pea (Teruko Konishi, personal communication) to isolate relatively pure Golgi vesicles using sucrose floatation gradient centrifugation. Two-phase partitioning is another technique used for plasma membrane purification from other endomembrane systems in many organisms (Albertsson, 1977; Larsson et al., 1987; Buckeridge et al., 1999; Lu and Hrabak, 2002).

This chapter describes the generation and characterization of a polyclonal antibody against AtCslD2 and the utilization of this antibody to localize AtCslD2 proteins in fractions enriched in membrane vesicles derived from Golgi complexes.

MATERIALS AND METHODS

Plant materials

Arabidopsis plants were grown under non-sterile hydroponic conditions (Gibeaut et al., 1997) in environmentally controlled growth chamber on a 18-h day period and day/night temperature of 22°C/20°C. Arabidopsis (ecotype Columbia) embryonic suspension cell line T87-C33 (Axelos et al., 1992) were maintained in the dark at 25°C in suspension culture medium (20 g L⁻¹ sucrose, 4.3 g L⁻¹ Murashige-Skoog salts [GIBCO-BRL], 0.5 g L⁻¹ MES, 0.1 g L⁻¹ myo-inositol, 1 mg L⁻¹ thiamine-HCl, 1 µM 2,4-D, and 1 mM K₂HPO₄, pH 5.7).

Preparation of total protein fraction and microsomal membranes from Arabidopsis plants

Different tissues from 5-week-old hydroponically grown Arabidopsis plants were cut, weighed and frozen in liquid nitrogen. Tissues were then ground in liquid nitrogen and the resulting powder was resuspended in extraction buffer (150 mM Tris·HCl at pH6.8, 3% SDS, 7.5% 2-mercaptoethanol) at 2 ml per gram fresh weight. The extracts were boiled in a water bath for 15 minutes and centrifuged for 15 minutes at 10,000×g. The supernatants were saved as total protein fractions.

For microsomal membrane preparation, every 20 g tissues from 5-week-old Arabidopsis plants were cut into small pieces with a Comfort Food Chopper (Zyliss, Switzerland) and ground in 40 ml extraction buffer (50mM Hepes·KOH, pH6.5, 10mM potassium acetate, 2.5mM EDTA, 0.4M sucrose, 1 mM DTT, 0.2mM PMSF, 1% Protease Inhibitors [Sigma]) with mortar and pestle on ice. After passage through a

double layer of miracloth, extracts were centrifuged at $10,000\times g$ for 10 minutes at 4°C . The pellet was called the P10 fraction. The supernatant S10 fraction was subjected to further centrifugation at $100,000\times g$ for 1 hour at 4°C . The supernatant from this step was saved as the S100 fraction, and the pellet was resuspended in extraction buffer and labeled as the P100 fraction.

Preparation of S10 protein fraction and microsomal membranes from Arabidopsis cell suspension cultures

Arabidopsis cells cultured for 4 to 5 days after inoculation were collected on miracloth using vacuum filtration. Usually 20 g of Cells were suspended at a concentration of 1 g per 3 ml of extraction buffer (50mM Hepes·KOH, pH6.5, 2mM EDTA, 15% sucrose, 1 mM DTT, 0.2mM PMSF, 1% protease inhibitors [Sigma]). Cells were disrupted in a blender with short bursts of 10 sec for a total of 1 min on ice. Cell lysate was filtered through double layer of miracloth and subjected to centrifugation at $10,000\times g$ for 10 min at 4°C . The supernatant was saved as the S10 protein fraction, and the pellet was discarded. The supernatant solution was centrifuged at $100,000\times g$ for 1 hour at 4°C to yield the S100 fraction and a membrane pellet that was resuspended in extraction buffer at 1/10 of the starting volume and labeled as the P100 fraction.

Solubilization of microsomal membrane proteins

A P100 microsomal fraction was isolated from either 5-week-old hydroponically grown Arabidopsis above-ground tissues or from 4 to 5-day-old Arabidopsis suspension cultured cells. Equal amounts of P100 microsomal protein were resuspended in extraction

buffer (50mM Hepes·KOH, pH6.5, 2mM EDTA, 15% sucrose, 1 mM DTT, 0.2mM PMSF, 1% protease inhibitors [Sigma]) and incubated with equal volume of the same buffer containing 4M Urea, 2M NaCl, 0.2M Na₂CO₃, 0.4% Triton X-100, 0.4% SDS or extraction buffer alone for 30 minutes on ice. After treatment all solutions were centrifuged at 100,000×g for 1 hour at 4°C. Supernatants were saved and the pellets were resuspended in the same volume of extraction buffer. Equal volumes of each fraction were used for SDS-PAGE and immunoblotting.

Sucrose density gradient fractionation of microsomal membranes

The S10 protein fraction isolated from Arabidopsis cultured cells was subjected to two sequential sucrose gradient fractionation steps. The first sucrose gradient was made in a SW28 centrifuge tube with 10 ml of extraction buffer containing 50% sucrose overlaid with 10 ml of extraction buffer containing 15% sucrose. S10 protein fraction was laid on top of the gradient and subjected to centrifugation of 100,000×g for 1 hour at 4°C. The interface (about 2 ml) between the two sucrose solutions was recovered and diluted with the same buffer without sucrose until the sucrose concentration reached between 25% and 30%. This diluted interface was subjected to a second centrifugation step. The second step used a linear gradient from 30% sucrose to 50% sucrose in the same extraction buffer in a SW40 centrifuge tube. About 2.5ml of the diluted interface from the first step was laid on top of the linear gradient and centrifuged at 100,000×g for 3 hours at 4°C. Fractions of about 800 µl each were collected with an Auto Dense-Flow fractionator (Labconco). Sucrose concentrations was determined with a refractometer (American Optical Corporation, Buffalo, NY).

Two phase partitioning

The two phase system developed by Larsson et al (1987) was used for the purification of plasma membranes. The crude microsomal membranes (P100 pellet) from suspension-cultured Arabidopsis cells were resuspended in buffer A (0.33 M sucrose, 3 mM KCl, 5 mM potassium phosphate at pH7.8, Protease Inhibitors [1:100, Sigma]) in 1/10 of the original volume. For every 3 g of this microsome solution 9 g of buffer B (buffer A plus 8.4% Dextran T500 and 8.4% PEG 3350) was added to make the final concentration of both Dextran and PEG to 6.3%. After inverting the tubes 30 times for mixing, the samples were centrifuged at 1,500×g for 5 minutes at 4°C in a swinging bucket rotor. The upper phase was collected and called the U1 fraction and the lower phase, the L1 fraction. Buffer C (buffer A plus 6.3% Dextran T500 and 6.3% PEG 3350) was made and mixed and allowed to sit at 4°C for overnight to separate into two phases. The U1 fraction was further extracted twice with an equal volume of the lower phase from buffer C to produce phases U2, L2', U3 and L3' sequentially. The L1 fraction was also further extracted twice with an equal volume of the upper phase from buffer C, to produce the U2', L2, U3' and L3 phases. Equal volumes of each phase or equal amounts of protein from each phase were used for SDS-PAGE and enzyme activity assays. Protein concentration was determined with Micro BCA kit (Pierce, Rockford, IL).

Preparation of Golgi rich microsomal membrane fractions

The centrifugation procedure developed by Buckeridge et al (1999) for maize was adopted for use with Arabidopsis. The S10 protein fraction was extracted from 4 to 5

days old cell suspension culture the same way as used for other applications except in a different buffer (84% sucrose [w/v], 20 mM Hepes·KOH, pH 7.0, 20 mM KCl, 5 mM EDTA, 5 mM EGTA, 10 mM DTT, Protease Inhibitors [1:100, Sigma]). The sucrose concentration in the S10 fraction was checked with a refractometer (American Optical Corporation, Buffalo, NY) and adjusted to around 40% sucrose (37~45%) using the same buffer containing no sucrose or 84% sucrose depending on the need. Sucrose gradient buffer contained 20 mM Hepes·KCl, pH7.0 and protease inhibitors (1:100, Sigma). For making the sucrose density gradient, 10 ml of S10 total protein with sucrose concentration adjusted was laid on top of 5 ml of gradient buffer containing 50% (w/v) sucrose in a SW28 centrifuge tube. On top of the sample, 8 ml of gradient buffer with 34% (w/v) sucrose, then 8 ml of 25% (w/v) sucrose in gradient buffer, and then 7 ml of 18% (w/v) sucrose in gradient buffer were laid on sequentially. About 2 ml of gradient buffer containing 9.5% (w/v) sucrose was used to make up the volume until the edge of the tube. The gradient was centrifuged at 100,000× g for 1.5 to 3 hours at 4°C. After centrifugation, the interface between layers with different sucrose concentrations were collected and designated as fraction 1, 2, 3, 4, and 5 from the top to the bottom of the gradient. According to the original protocol, developed and characterized in maize (Buckeridge et al., 1999), those five fractions are enriched with tonoplast, ER, Golgi, mitochondria, and plasma membrane, specifically. Here only fractions 3, 4 and 5 were further characterized and used for the AtCslD2 localization studies. The pellet fraction was resolubilized in the same buffer without sucrose. Protein concentrations were determined using the Micro BCA kit from PIERCE (Rockford, IL).

Expression of polypeptide P2 and P3 in E. coli cells

The DNA sequence encoding the first 272 amino acids of AtCslD2, fragment P2, was amplified from Arabidopsis genomic DNA with primers kee919 (5'-CCTACATATGGCATCTAATAAG-3') and kee921 (5'-TCATGAATTCTTGGGCCTCCAT-3'). The DNA sequence encoding the first 188 amino acids of AtCslD3, fragment P3, was amplified from Arabidopsis genomic DNA with primers kee920 (5'-TTAGCATATGGCGTCTAATAAT-3') and kee922 (5'-CTGCTTGTTGTTCTCGAGCAAA-3'). PCR products were inserted into expression plasmid pET28a via NdeI and EcoRI sites for DNA fragment encoding P2, and NdeI and XhoI sites for DNA fragment encoding P3. The identity constructs encoding peptide fragment P2 and P3 were confirmed by restriction digestion with NotI and sequencing. Peptide fragment P2 and P3 were expressed in BL21 (DE3) cells according to manufacturer's guide (pET system manual, Novagen, Madison, WI). Total soluble proteins were extracted and used for subsequent experiments.

Generation and purification of polyclonal antibodies

AtCslD2-specific peptide IQEPGRPPAGHSVKFAQ(C), corresponding to a region near the N-terminus (aa20~aa36), and AtCslD3-specific peptide (C)DAAEAERHQPPVSNSTFA (aa19~aa37) were synthesized and conjugated with keyhole limpet hemacyanin (KLH) for polyclonal antibody production in rabbits by Alpha Diagnostic International, Inc. (San Antonio, TX). Both polyclonal antibodies were affinity-purified using the SulfoLink Kit (PIERCE, Rockford, IL) according to the manufacturer's instruction. To prepare the affinity resin, one mg of either antigen peptide

with a Cys attached (lyophilized) was dissolved in 50 µl of DMSO plus 1 ml of coupling buffer supplied with the kit and attached onto SulfoLink coupling gel. One ml of the second bleed serum each from rabbit No. 6167 (against AtCslD2) and No. 6169 (against AtCslD3) was diluted 5 times before application to the SulfoLink affinity resin containing the specific peptides. The affinity-bound antibodies were eluted with 100 mM glycine buffer at pH2.5. Eluted antibodies were concentrated and the buffer was changed to PBS using the centrifugal filter device-Ultrafree (Millipore, Bedford, MA) with a cutoff size of 50 kDa. Sodium azide was added to the purified antibodies to a final concentration of 0.01%. Antibodies were placed at -20°C for long term storage and at 4°C for short term use.

Antigen competition assay

Equal volumes of antibodies to be analyzed were incubated at room temperature for 2 hours with variable quantities of *E. coli* total soluble protein extracts containing P2 or P3. After a centrifugation at 10,000×g for 10 minutes at 4°C, the supernatant was saved and used for immunoblotting.

SDS-PAGE and immunoblotting

All SDS-PAGE and immunoblotting procedures followed standard protocols (Harlow and Lane, 1988). Antibody against PMA2 (a *Nicotiana plumbaginifolia* plasma membrane H⁺-ATPase) was a gift of Dr. Marc Boutry. Antibodies against AtSYP61 (a Golgi marker), AtSYP21 (a PVC marker), AtELP (a TGN-PVC marker) and AtSEC12

(an ER marker) were gifts from Dr. Natasha Raikhel. Antibody against AtXT1 was generated by Dr. Ahmed Faik of our group.

Marker enzyme assays

The assay for β -glucan synthase II (callose synthase) activity was modified from existing protocols (White et al., 1993; Konishi et al., 2001). The reaction mixture contained 50 mM Hepes·KOH, pH7.0, 1 mM UDP-Glc, 5 mM CaCl_2 , 4.36 μM UDP- ^{14}C Glc (305.9 mCi/mmol). Reactions were carried out at room temperature for 45 min. Xyloglucan carrier (5 μl of a 1% solution) was added to each reaction before adding 750 μl of 70% ethanol to give a final concentration of 67% ethanol to stop the reactions. Reaction products were precipitated at room temperature for 30 minutes and washed three times with 70% ethanol by vortexing and precipitation at 12,000 g for 5 min. XyG fucosyltransferase activity assay was performed the same way as in chapter 2.

RESULTS

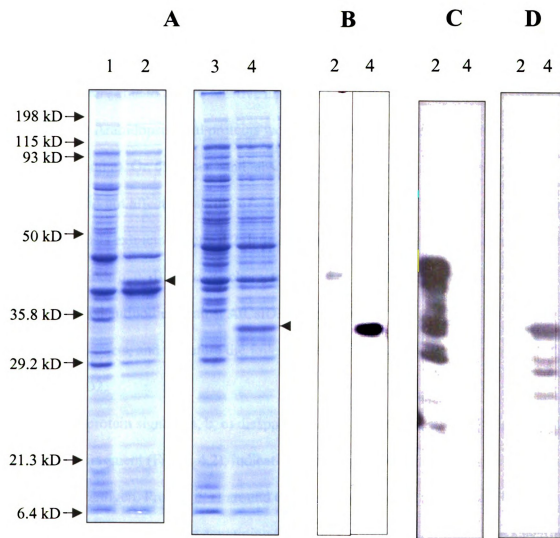
Generation, purification and characterization of antibodies against AtCslD2

Because AtCslD2 and AtCslD3 are the two most highly expressed members within the AtCslD gene family (see chapter 3), we sought to prepare antibodies against each of these two proteins. Short peptides of 18 aa and 20 aa, corresponding to a region near the N-terminus of AtCslD2 and AtCslD3, respectively, were chemically synthesized, coupled to a carrier protein and used as antigen to generate polyclonal antibodies. Both antibodies against AtCslD2 and D3 were affinity purified using an immobilized form of their corresponding peptides that had been used as antigen.

To characterize the antibodies, a polypeptide fragment P2 containing the N-terminal 272 amino acid from AtCslD2 and a polypeptide fragment P3 containing the N-terminal 188 amino acids from AtCslD3 were expressed in *E. coli*. Neither of the fragments contained any of the predicted transmembrane domains contained within the full-length protein. The expression of P2 and P3 in *E. coli* were confirmed by SDS-PAGE followed by Commassie blue staining (Figure 4.1A) and immunoblotting using antibodies against the His tag attached to the amino terminus of each expressed peptide (Figure 4.1B). The peptide antibodies against AtCslD2 and D3 were tested on the *E. coli* extracts containing fragment P2 or P3. Both antibodies were confirmed to be protein specific in that the antibodies against the AtCslD2 peptide recognized expressed AtCslD2 fragment P2 but not P3 that was derived from AtCslD3. Similarly antibodies against the AtCslD3 peptide recognized fragment P3 but not P2 (Figure 4.1C, D). Other proteins of smaller molecular weights were also detected on the immunoblots (Figure 4.1C, D). Those proteins might be just degradation products of fragments P2 or P3.

Figure 4.1: Expression and detection of peptides P2 and P3 in BL21 (DE3) cells. A:

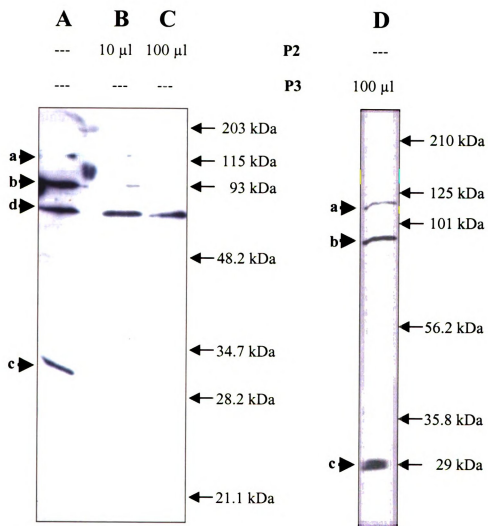
Total *E. coli* protein extracts were resolved on 12.5% SDS-PAGE and stained with Coomassie brilliant blue. Proteins were redissolved in SDS-PAGE loading buffer according to their cell cultures' OD600 values to give approximately equal protein concentrations. Equal volumes of extracts (20 μ l) from cells expressing P2 (1, 2) and P3 (3, 4) were loaded. Lanes 1,3: total protein extracts before induction; lanes 2, 4: total protein extracts after 3 hours induction. The induced peptide P2 and P3 are indicated by arrows. **B, C, D:** Immunoblots on *E. coli* extracts containing fragments P2 and P3 that were resolved on a 12.5% SDS-PAGE, using antibodies against 6 \times His tag (**B**); antibodies against AtCslD2 (**C**) and antibodies against AtCslD3 (**D**). Same amount of proteins were used as indicated in panel A.



Purified AtCslD2 antibodies recognized four proteins (designated a, b, c and d in Figure 4.2) in Arabidopsis protein extracts with protein “a” having the proper molecular size. To explore if these bands are specific for AtCslD2, an antigen competition assay was developed (Figure 4.2). In this assay, the purified antibodies against AtCslD2 were incubated with extracts from *E. coli* expressing fragment P2 or P3 before they were used for immunoblotting against Arabidopsis total proteins. *E. coli* extracts containing fragment P2 were able to absorb reactive antibodies so that no specific signal could be detected when Arabidopsis total proteins were probed with the absorbed serum (Figure 4.2, lane C, band a). On the other hand, absorption with *E. coli* extracts containing fragment P3 did not affect the ability of antibodies against AtCslD2 to recognize proteins from Arabidopsis extracts (Figure 4.2, lane D, band a). Other signals were also detected (Figure 4.2, bands b, c, d) and were characterized later. Similar absorption experiments with the purified antibodies against AtCslD3 did not identify a specific protein in the Arabidopsis extracts, and therefore the following experiments only used antibodies against AtCslD2.

Three protein signals (a, b, c) disappeared after antibody absorption using *E. coli* expressed P2 fragment (Figure 4.2), indicating that they all contained the same epitopes as the peptide antigen. Protein d, at around 65 kDa, was still detected after antibody absorption with *E. coli* proteins containing fragment P2, indicating it was a non-specific recognition by this antibody. In later experiments, this protein was not detected on immunoblots when fresher total protein samples or microsome membrane proteins were used and when the washing time during immunoblotting was extended. When Arabidopsis microsome membrane proteins were pelleted by centrifugation at 100,000×g

Figure 4.2: Specificity of AtCslD2 antibodies against Arabidopsis total protein extracts. Equal volumes (10 μ l) of antibodies against AtCslD2 were incubated with specified *E. coli* total protein extracts for 2 hours at room temperature and centrifuged at 10,000 \times g for 10 minutes before they were used for immunoblotting at a dilution of 1:1,000 against Arabidopsis total protein extracts. Antibody preparations were incubated with 100 μ l of total protein extracts from BL21 (DE3) culture expressing vector plasmid pET28a alone (**A**), 10 μ l (**B**) or 100 μ l (**C**) of total protein extracts from BL21 (DE3) culture expressing fragment P2 and 100 μ l of total protein extracts from BL21 (DE3) culture expressing fragment P3 (**D**). The *E. coli* protein extracts used here were the same as used in figure 4.1. Panels **A**, **B**, and **C** were from same gel containing 12.5% acrylamide whereas panel **D** was in a separate gel containing 10% acrylamide. The four major bands detected were designated as band a, b, c and d, respectively.



(P100 fraction), proteins a and c sedimented with microsomal membranes while protein b stayed in the soluble fraction (Figure 4.3A). Even though protein b showed similar behavior as protein a in the antibody absorption assay, its smaller size (~90 kDa) and fractionation with soluble proteins made it very unlikely to be AtCslD2, which has 8 predicted transmembrane domains. Furthermore, when Arabidopsis proteins recovered in the 10,000×g supernatant (S10 fraction) were fractionated by sucrose density gradient centrifugation, proteins a, b and c clearly behaved differently. Protein a peaked in fractions containing sucrose of 33% to 35% while protein b remained at the top of the gradient. Protein c peaked in fractions containing sucrose of ~21% indicating it was present in a different membrane system than protein a (data not shown). Finally, when Golgi rich membranes were prepared from Arabidopsis cell suspension cultures, protein a was the only one detected with the purified antibodies against AtCslD2 (Figure 4.3B). Therefore in purified Golgi rich membrane preparations this antibody specifically recognized a membrane protein with a molecular size of about 120 kDa.

AtCslD2 is an integral membrane protein

Sequence analysis predicted that AtCslD2 protein contains 8 transmembrane domains. After sequential centrifugation at 10,000×g and 100,000×g, the majority of AtCslD2 was detected in the P100 membrane fraction (Figure 4.3A), indicating AtCslD2 is associated with membranes. To investigate whether AtCslD2 is an integral membrane protein, microsomal membranes from the P100 fraction were treated with different reagents that affect the association of peripheral membrane proteins (Figure 4.4). AtCslD2 could not be removed from microsomal membranes by 2 M Urea, 1 M NaCl,

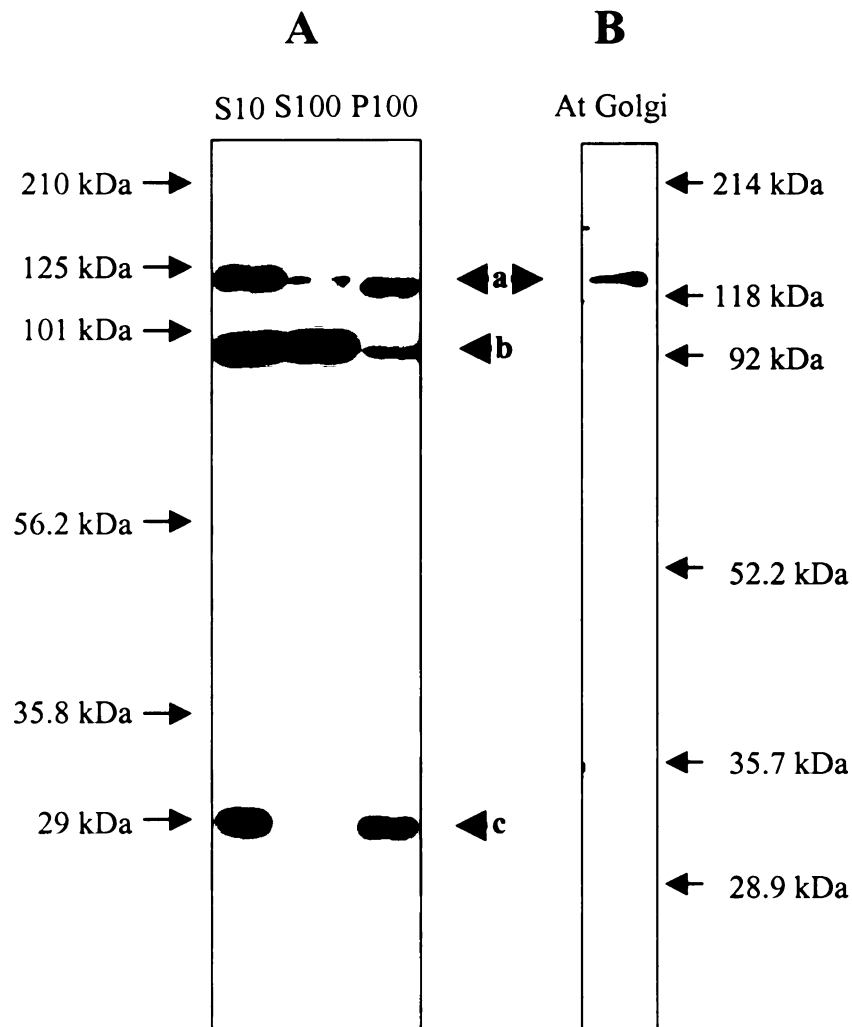


Figure 4.3: Immunoblotting using purified AtCslD2 antibodies against Arabidopsis crude membranes (A) and purified Golgi complexes (B). S10, total protein extracts after 10,000×g centrifugation; S100 and P100, soluble proteins and membrane pellets after 100,000×g centrifugation. Immunoblotting signals a, b and c are the same as indicated in figure 4.2.

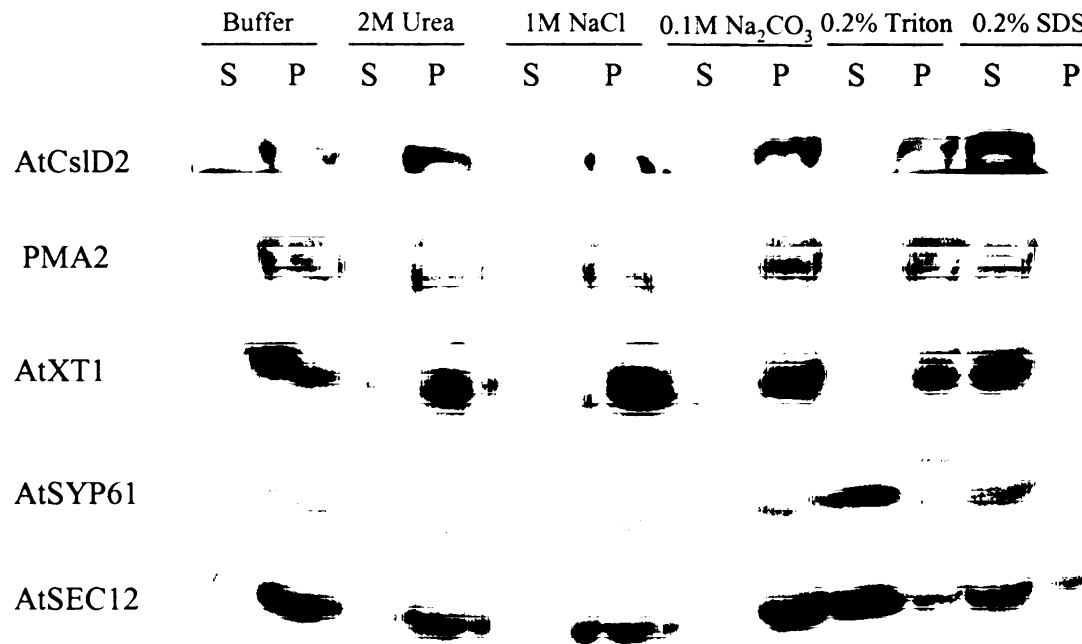


Figure 4.4: Solubilization of AtCslD2 proteins from Arabidopsis microsomal membranes with various reagents. Equal amounts of protein from the P100 fraction were incubated with buffer alone, or buffers containing 2 M Urea, 1 M NaCl, 0.1 M Na₂CO₃, 0.2% Triton X-100 or 0.2% SDS on ice for 30 min, and centrifuged again at 100,000×g for 1 hr. Pellets were resuspended in the same volume of extraction buffer as the supernatant. Equal volumes of each fraction were analyzed by SDS-PAGE and immunoblottings using antibodies against AtCslD2, plasma membrane marker PMA2, Golgi marker AtXT1 and AtSYP61 and ER marker AtSEC12. S, supernatant fractions; P, pellet fractions.

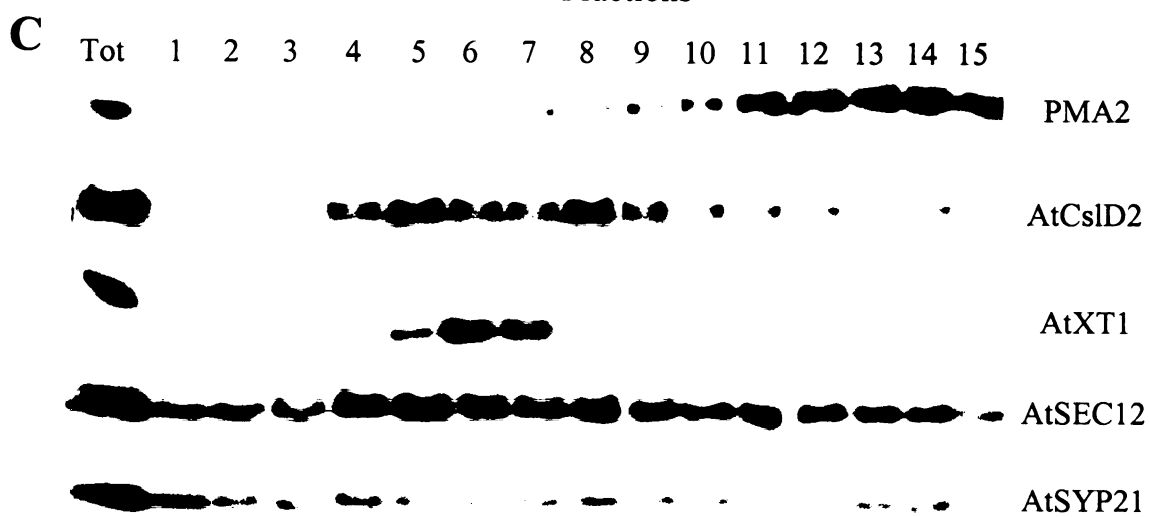
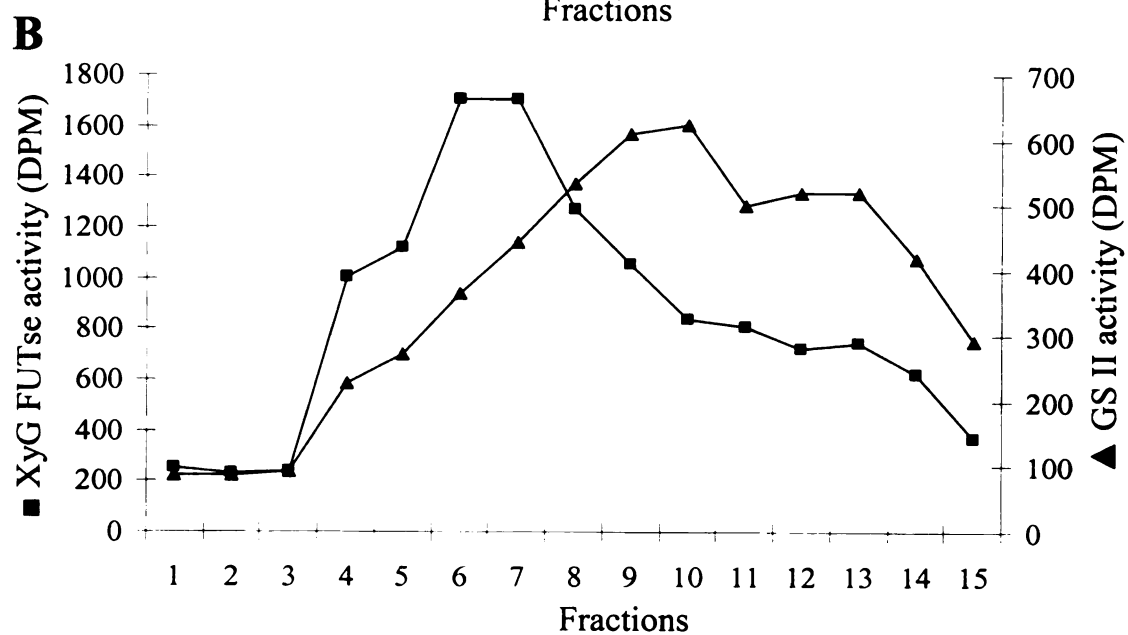
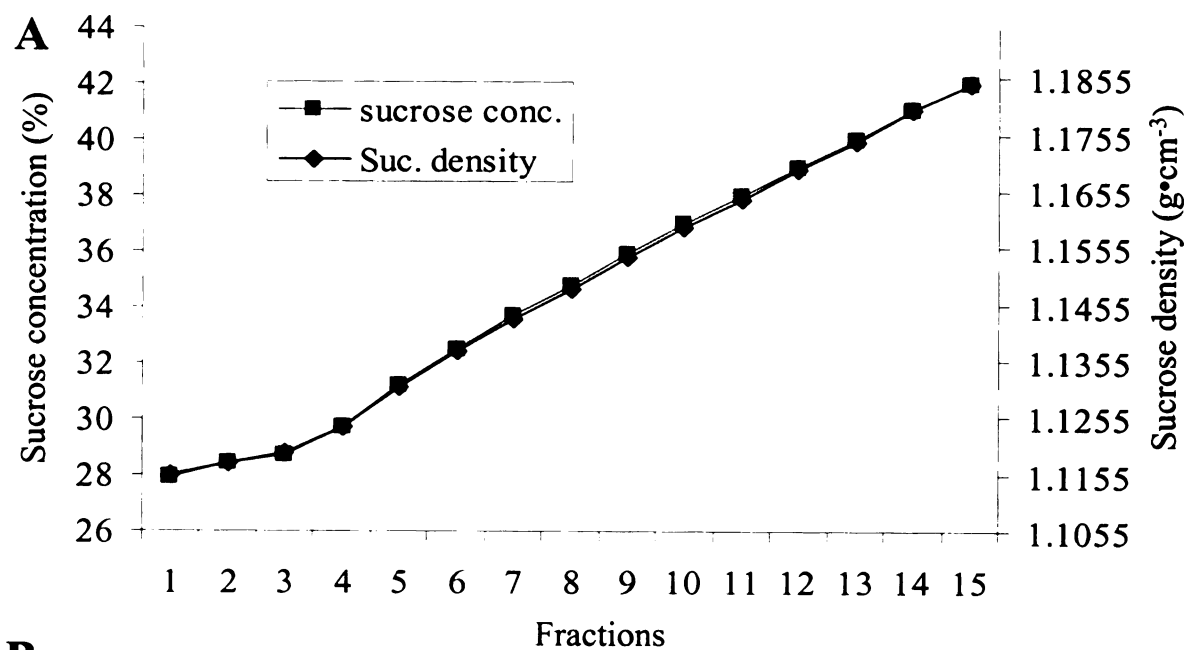
0.1 M Na₂CO₃ or 0.2% Triton X-100, which can dissociate peripheral membrane proteins. Only 0.2% SDS completely solubilized AtCslD2 from the microsomal membranes, indicating that AtCslD2 is an integral membrane protein.

Several control proteins were monitored to check whether the fractionation experiments yielded the expected results. PMA2 is a plasma membrane H⁺-ATPase with multiple transmembrane domains and a topology similar to AtCslD2, four transmembrane domains near the N-terminus and six close to the C-terminus (Morsomme et al., 1998). PMA2 was also only removed by 0.2% SDS and behaved exactly like AtCslD2 during these treatments. AtXT1 is predicted to be a type II integral membrane protein. It was only completely solubilized by 0.2% SDS, but trace amounts of AtXT1 were also solubilized by all the other reagents used, except with the buffer alone, indicating that AtXT1 is also an integral membrane protein but might not associated with the membranes as tightly as AtCslD2 or PMA2. AtSEC12 is an ER-associated integral membrane protein that could only be removed from membranes by nonionic or ionic detergents but not by other treatments such as urea, salt or alkaline conditions (Bar-Peled and Raikhel, 1997). The behavior of AtSEC12 (Figure 4.4) was the same as observed before (Bar-Peled and Raikhel, 1997) and served as a nice control. AtSEC12 also demonstrated a looser integration with the membranes, because, in addition to nearly complete solubilization by 0.2% SDS, AtSEC12 were also largely solubilized by 0.2% Triton X-100. AtSYP61 is a trans-Golgi network (TGN) protein with a single transmembrane domain near its C-terminus. It also showed a weaker association with membranes compared with AtCslD2 or PMA2, as AtSYP61 was also removed from the membrane by 0.2% Triton X-100 (Figure 4.4).

AtCslD2 migrates differently from a plasma membrane marker PMA2 during linear sucrose gradient centrifugation

Sucrose density gradient centrifugation was employed in an attempt to resolve different membranes such as plasma membrane, ER, Golgi, and mitochondria. As a first step of enrichment, the S10 protein fraction from Arabidopsis suspension cultured cells was subjected to a sucrose step gradient of 15% and 50%. The microsomes from the interface between 15% and 50% sucrose were recovered and further fractionated on a linear sucrose density gradient from 30% to 50%. The range of 30% to 50% was picked because it produced a gradient covering the range of densities for most endomembrane organelles. After centrifugation the sucrose density distribution was nearly linear (Figure 4.5A). XyG fucosyltransferase activity peaked in fraction 6 and 7 that contain 32% to 34% sucrose (Figure 4.5B). Immunoblotting demonstrated that AtXT1 was detected in the same fractions (Figure 4.5C), leading to the conclusion that Golgi membranes were located in these fractions. AtCslD2 was distributed most abundantly in fractions 5 to 8 that contain 31% to 35% of sucrose (Figure 4.5C). Therefore the conclusion was made that AtCslD2 was localized in the Golgi complex, but had a broader distribution than XyG fucosyltransferase and xylosyltransferase. On the other hand the plasma membrane marker PMA2 was distributed toward the bottom of the gradient among fractions 11 to 14 containing 38% to 41% sucrose (Figure 4.5C). The distribution of PMA2 detected by immunoblotting matched with the second peak of the GSII activity distribution in the gradient. GS II activity peaked twice in the gradient with its first peak at fractions 9 and

Figure 4.5: Migration of AtCslD2 and selected marker proteins on a linear sucrose density gradient. S10 fraction proteins from 4 to 5-day-old Arabidopsis cultured cells were placed on top of a sucrose step gradient of 15% and 50%. After centrifugation at 100,000×g for 1 hour, the interface was collected and its sucrose content was diluted to between 25% and 35%, then loaded on a linear sucrose gradient from 30% to 50%. Fractions of 0.8 ml were collected after centrifugation at 100,000×g for three hours. Aliquots of each fractions were used for enzyme activity assays, or SDS-PAGE followed by immunoblotting with various antibodies. **A:** Sucrose concentration of each fraction; **B:** Enzyme activity assays for XyG fucosyltransferase and GS II; **C:** Immunodetection of AtCslD2 and marker proteins PMA2 (plasma membrane), AtXT1 (Golgi), AtSEC12 (ER) and AtSYP21 (PVC).



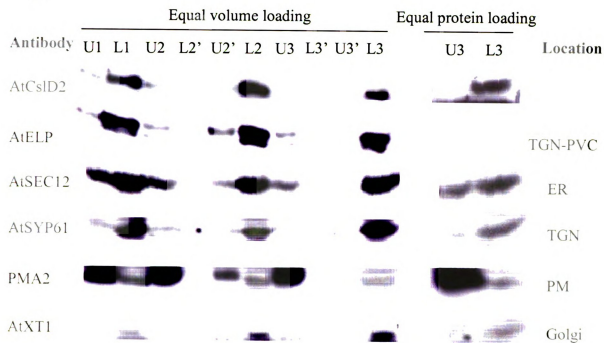
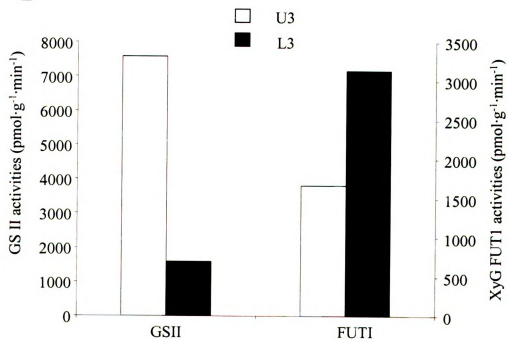
10 containing 35% to 37% sucrose. This could result from the presence of multiple enzyme activities that catalyze the polymerization of UDP-glucose.

AtCslD2 is not a plasma membrane protein as revealed by two-phase partitioning

Because density gradient centrifugation was not definitively conclusive with respect to the localization of AtCslD2, an independent approach to address this problem was sought. The aqueous two-phase partitioning method (Figure 4.6) enriches the plasma membrane in the upper phase and most other cellular membranes in the lower phase. Three consecutive partitioning steps were employed. The upper and lower phase U3 and L3 from the third partitioning were analyzed for XyG fucosyltransferase and GS II activity to confirm the effect of partitioning (Figure 4.6 B). The lower phase L3 showed only about one fifth the level of GSII activity compared with the upper phase U3 (Figure 4.6B), indicating that highly enriched plasma membrane fraction was obtained. All phases then were analyzed by immunoblotting to locate AtCslD2 protein, the Golgi marker protein AtXT1, TGN marker protein SYP61, TGN-PVC marker protein AtELP, plasma membrane marker protein PMA2, and ER marker protein AtSEC12. At the end of the third partitioning AtCslD2 was found primarily in the lower phase, which also contained markers derived from ER, Golgi and TGN, while the plasma membrane marker, PMA2, partitioned predominantly into the upper phase (Figure 4.6). From these observations, it was concluded that AtCslD2 is not localized in the plasma membrane.

AtCslD2 protein is localized at Golgi rich vesicles during floatation sucrose gradient centrifugation

Figure 4.6: Two-phase partitioning of Arabidopsis microsomal membranes. The S10 protein fraction prepared from Arabidopsis suspension cultured cells was centrifuged at 100,000×g for 1 hr to yield the microsomal membranes. The microsomal membranes were then partitioned three times in buffers contained 6.2% Dextran T500 and 6.2% PEG 3350 (Materials and Methods). **A.** Aliquots of equal volume from each fraction were resolved in SDS-PAGE and transferred to PVDF membrane for immunoblotting with various antibodies as probes. Equal amount of protein were also taken from U3 and L3 fractions for similar immunoblottings. Un and Ln (n=1, 2 or 3) fractions are the upper and lower phases after each partitioning. The experimental procedure was explained in the Materials and Methods. **B.** The specific activity of GSII and XyG fucosyltransferase (FUT1) in fractions U3 (white blocks) and L3 (black blocks).

A**B**

As a third method to investigate the location of AtCslD2, microsome membranes were isolated from Arabidopsis suspension cultured cells and fractionated via flotation on a sucrose step gradient (Figure 4.7A). The enrichment of Golgi vesicles and plasma membrane was evaluated by XyG fucosyltransferase and GS II activity assays respectively (Table 4.1). The specific activity of XyG fucosyltransferase in the Golgi-rich fraction (fraction 3) had been enriched more than 130 times compared to the starting membrane material (Table 4.1). Fraction 5 contained highly purified plasma membranes, showing only 5% the level of specific activity for XyG fucosyltransferase relative to fraction 3. At the same time the GS II activity had almost equal distribution between fraction 5 (plasma membrane enriched) and fraction 4 (Table 4.1). The purified Golgi membranes still showed some incorporation of radio labeled UDP-glucose during GS II activity assay (Table 4.1).

The GSII activity recorded for fraction 3 may not reflect the true GS II enzyme activity, because when the same reaction was carried out for 15 and 45 minutes, the radiolabel incorporation did not increase as expected (data not shown). During the same assay with other fractions, the incorporation of radio-labeled UDP-glucose increased significantly when assayed for 45 min instead of 15 min. Immunoblotting indicated that Golgi marker proteins AtSYP61 and AtXT1 were almost exclusively found in fraction 3 (Figure 4.7B), indicating that fraction 3 was highly enriched in Golgi vesicles. The plasma membrane marker protein PMA2 was also detected in fractions 3 and 4, although the majority of it was detected in the plasma membrane rich fraction (fraction 5, Figure 4.7B).

Almost equal amount of GS II activities were detected in fraction 4 and 5 (Table

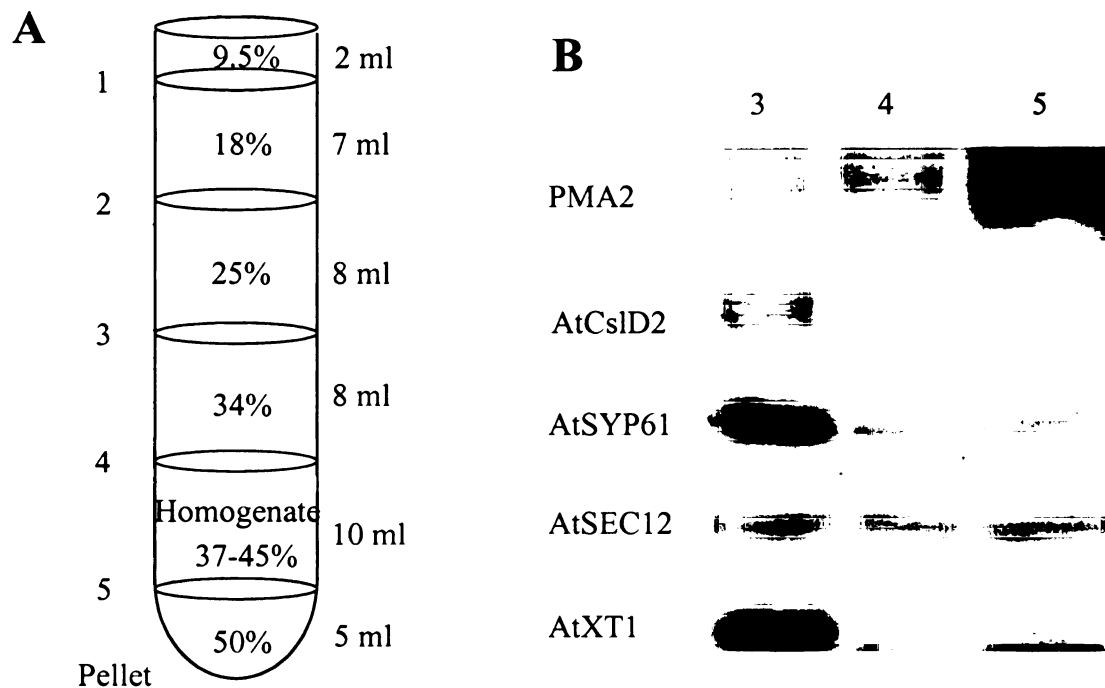


Figure 4.7 Fractionation of microsomal vesicles by floatation centrifugation on a sucrose step gradient. S10 protein fraction isolated from Arabidopsis 5 day-old suspension cultured cells was adjusted to contain sucrose of around 40% (37-45%) and laid on top of the 50% sucrose cushion. On top of the sample, buffers containing 34%, 25%, 18% and 9.5% of sucrose were sequentially loaded (**A**). The gradient was centrifuged at 100,000×g for 3 hours and the membranes present at the interfaces between different sucrose concentrations were collected. Equal amount of proteins from fraction 3, 4 and 5 were resolved on SDS-PAGE and transferred onto PVDF membranes for immunoblottings with different antibodies against selected marker proteins (**B**). Data shown in this figure is representative of three different experiments.

Table 4.1: Specific activity of XyG fucosyltransferase and GSII for membrane vesicles fractions isolated from sucrose step gradient. Gradient was described in Figure 4.7. Assays were carried out according to Materials and Methods. These data are representative for three different experiments with similar results.

	FUTase activity ($\text{pmol}\cdot\text{g}^{-1}\cdot\text{min}^{-1}$)	GSII activity ($\text{pmol}\cdot\text{g}^{-1}\cdot\text{min}^{-1}$)	Protein (mg/ml)	Volume (ml)
S10	1552	380	14.67	10
1	0	0	0.11	1.5
2	0	0	0.09	0.2
3	208825	443	0.43	0.4
4	30385	1602	3.75	1.1
5	10684	1450	4.07	1.6
Pellet	0	306	5.57	2

4.1), while the majority of PMA2 proteins were found in fraction 5 by immunoblotting (Figure 4.7 B). This inconsistency between the two plasma membrane markers was also observed during the sucrose density linear gradient (Figure 4.5) where GSII activity peaked twice in different fractions while PMA2 proteins were immuno-localized in mainly those fractions showing the second peak of GSII activities (Figure 4.5). This observation may indicate the presence of more than one enzyme that shows activity in the GSII assay.

DISCUSSION

Three experimental procedures were used to investigate the localization of AtCslD2 proteins. Observations from those experiments led to the conclusion that AtCslD2 proteins are localized in Arabidopsis Golgi membranes. Firstly, AtCslD2 was detected in microsomal membrane fractions different from the plasma membrane marker protein, PMA2, during linear sucrose density gradient fractionation. The fractions that contained AtCslD2 proteins also showed the highest XyG fucosyltransferase activity and the presence of AtXT1, the XyG xylosyltransferase. These observations are consistent with a Golgi localization for AtCslD2. Secondly, during an aqueous two phase partitioning, AtCslD2 partitioned into the lower phase which contained highly enriched XyG fucosyltransferase activity and most of the cellular organelles except the plasma membrane, while the plasma membrane marker PMA2 partitioned into the upper phases together with most of the GSII activities. Again the AtXT1 co-partitioned with AtCslD2 into the lower phase. Thirdly, when the microsomal membranes were fractionated by sucrose density step gradient floatation centrifugation, AtCslD2 was detected in the fraction rich in Golgi vesicles, as evidenced by marker proteins AtSYP61 and AtXT1 and XyG fucosyltransferase activity, while most of plasma membrane marker PMA2 was detected in the fraction rich in plasma membranes. When taken individually, none of above observations could convincingly support a Golgi localization of AtCslD2. However, collectively these three observations provide compelling evidence for a Golgi localization of AtCslD2 proteins.

Electron microscopic (EM) localization studies would provide confirmation for the conclusions described above. However, the purified antibody against AtCslD2 still

recognized a soluble protein and a smaller membrane protein during immunoblotting (Figure 4.2). These cross-reactive proteins would cause problems during analysis by EM.

AtCslD2's localization at the Golgi complex is contrary to a previous speculation of a plasma membrane localization (Doblin et al., 2001) or evidence supporting a ER localization (Favery et al., 2001). The prediction of plasma membrane localization of AtCslD protein was based on the speculation that NaCslD1 was a tissue-specific cellulose synthase (Doblin et al., 2001). NaCslD1 was concluded to be a cellulose synthase based on the fact that CslD proteins contain the D,D,D,QXXRW motif, similar transmembrane domain structures, and fairly high sequence identities with CesA proteins, and the observation of specific expression of NaCslD1 in pollen tubes of *Nicotiana alata* (Doblin et al., 2001). A single CslD gene (NaCslD1) and a single CesA gene (NaCesA1) were detected by RT-PCR reactions in *Nicotiana alata* pollen tubes. While NaCesA1 was detected to be expressed weakly in many other tissues, it is not detected in the male gametophyte (pollen or anther) or in vitro cultured pollen tubes (Doblin et al., 2001). However NaCslD1 was only expressed in male gametophyte tissues after pollen mitosis and in vitro cultured pollen tubes at fairly high levels (Doblin et al., 2001). The authors therefore concluded that NaCslD1 was a cellulose synthase based on the assumption that the high cellulose content in the pollen tubes should have a high expression of cellulose synthase gene. In this case NaCslD1 seemed to be the only candidate (Doblin et al., 2001). Our data however, strongly support a Golgi localization of AtCslD2, and therefore we conclude that AtCslD2 is not a cellulose synthase.

The localization of AtCslD3 at ER came from the observation that the expression of a AtCslD3-GFP fusion protein under the control of constitutive 35S promoter in

Nicotiana benthamiana leaf cells led to GFP appearance in the endoplasmic reticulum (Favery et al., 2001). However, high level expression of an integral membrane protein directed to the secretory pathway could congest the pathway and cause the protein to show up in all cellular compartments along the secretory pathway. For example, a GFP protein fused to the signal anchor sequence of a human galactosyltransferase that was delivered to the Golgi apparatus showed up mostly in the ER as fusiform bodies and only weakly in the Golgi (Hawes et al., 2001).

It is possible that CslD1, D2 and D3 have different locations and different functions as well, and the conclusions drawn from the localization studies described above might all be valid. However the fairly high sequence identity among AtCslD1, D2 and D3 proteins, from 66% to 88%, suggests that they are very likely to have similar biochemical functions. Therefore other AtCslD proteins may be located on the Golgi apparatus just as AtCslD2 is.

AtCslD proteins are therefore not likely cellulose synthases or callose synthases that are localized at the plasma membranes. All AtCslD proteins contain the D,D,D,QxxRW motif indicative of processive glycosyltransferases (Saxena et al., 1995; Richmond and Somerville, 2000) and belong to the family 2 of the inverting nucleotide-diphospho-sugar glycosyltransferases that synthesize repeating β -glycosyl unit structures (Campbell et al., 1997; Richmond and Somerville, 2001). Therefore AtCslD proteins could be responsible for the backbone synthesis of hemicelluloses such as xyloglucan, xylan, glucomannan, mannan and galactomannan, or galactan side chains that have β -(1,4)-linkages on their backbones found on pectin, or AGPs etc.

AtCslD2 behaved very similarly to the plasma membrane marker PMA2 in the membrane stripping experiments, showing similar difficulty to be solubilized with various reagents. This supports the hypothesis of a similar membrane topology as PMA2, which is predicted to have four transmembrane domains near the N-terminus and six close to the C-terminus (Morsomme et al., 1998). AtCslD2 is predicted to have two transmembrane domains near the N-terminus and also six close to the C-terminus. AtCslD2 is the first type III transmembrane protein localized in the Golgi complex (Singer, 1990).

The purified antibody against AtCslD2 is a valuable molecular tool that will be useful in future studies. The antigen for this antibody is located near the N-terminus of the protein. When combined with antibodies against other regions, the topology of AtCslD2 in the Golgi membrane could be examined. This topology study would eventually tell if the C-terminal catalytic domain faces the Golgi lumen or the cytosol. The different topology of AtCslD proteins might suggest a very different mechanism of action. A cytosol-facing AtCslD might utilize substrate present in the cytosol, transfer them across the Golgi membrane, and incorporate them into the product in the Golgi lumen. This enzyme mechanism is very similar to that of cellulose synthases that localize at the plasma membrane and incorporate glucose from the cytosol side into cellulose chains outside of the cell. On the other hand if the catalytic domain of AtCslD is facing the Golgi lumen, AtCslD may catalyze reactions similarly to other glycosyltransferases, utilizing substrate and transferring it into product at the same side of the Golgi membranes.

REFERENCES

- Albertsson, P.-A.** (1977). "Separation of particles and macromolecules by phase partition." *Endeavour, new series* **1** (2): 69-74.
- Axelos, M., Curie, C., Mazzolini, L., Bardet, C. and Lescure, B.** (1992). "A protocol for transient gene expression in *Arabidopsis thaliana* protoplasts isolated from cell-suspension cultures." *Plant Physiol. Biochem.* **30** (1): 123-128.
- Bar-Peled, M. and Raikhel, N. V.** (1997). "Characterization of AtSEC12 and AtSAR1." *Plant Physiol.* **114**: 315-324.
- Baydoun, E. A. H., Abdel, M. R. M., Dani, D., Rizk, S. E. and Brett, C. T.** (2001). "Galactosyl- and fucosyltransferases in etiolated pea epicotyls: Product identification and sub-cellular localisation." *J. Plant Physiol.* **158** (2): 145-150.
- Benhamou, N.** (1995). "Immunocytochemistry of plant defense mechanisms induced upon microbial attack." *Micros. Res. Tech.* **31**: 63-78.
- Bolwell, G. P.** (1993). "Dynamic aspects of the plant extracellular matrix." *Int. Rev. Cytol.* **146**: 261-323.
- Brown, R. M. J. and Montezinos, D.** (1976). "Cellulose microfibrils: visualization of biosynthetic and oriented complexes in association with the plasma membrane." *Proc. Natl Acad. Sci. USA* **73**: 143-147.
- Brummell, D. A., Camirand, A. and Maclachlan, G. A.** (1990). "Differential distribution of xyloglucan glycosyltransferases in pea Golgi dictyosomes and secretory vesicles." *J. Cell Sci.* **96** (4): 705-710.
- Buckeridge, M. S., Vergara, C. E. and Carpita, N. C.** (1999). "The mechanism of synthesis of a mixed-linkage (1-3),(1-4) β -D-Glucan in maize. Evidence for multiple sites of glucosyl transfer in the synthase complex." *Plant Physiol.* **120**: 1105-1116.
- Campbell, J. A., Davies, G. J., Bulone, V. and Henrissat, B.** (1997). "A classification of nucleotide-diphospho-sugar glycosyltransferases based on amino acid sequence similarities." *Biochem. J.* **326**: 929-939.
- Delmer, D. P. and Stone, B. A.** (1988). "Biosynthesis of plant cell walls." *The Biochemistry of Plants. J. Priess*, New York, Academic Press Inc. **14**: 373-421.
- Doblin, M. S., Melis, L. D., Newbigin, E., Bacic, A. and Read, S. M.** (2001). "Pollen tubes of *Nicotiana glauca* express two genes from different beta-glucan synthase families." *Plant Physiol.* **125**: 2040-2052.

- Edwards, M. E., Dickson, C. A., Chengappa, S., Sidebottom, C., Gidley, M. J. and Reid, J. S. G.** (1999). "Molecular characterisation of a membrane-bound galactosyltransferase of plant cell wall matrix polysaccharide biosynthesis." *Plant J.* **19**: 691-697.
- Faik, A., Bar-Peled, M., DeRocher, A. E., Zeng, W., Perrin, R. M., Wilkerson, C., Raikhel, N. V. and Keegstra, K.** (2000). "Biochemical characterization and molecular cloning of an alpha-1,2-fucosyltransferase that catalyzes the last step of cell wall xyloglucan biosynthesis in pea." *J. Biol. Chem.* **275** (20): 15082-15089.
- Faik, A., Price, N. J., Raikhel, N. V. and Keegstra, K.** (2002). "An Arabidopsis gene encoding an alpha-xylosyltransferase involved in xyloglucan biosynthesis." *Proc. Natl Acad. Sci. USA* **99** (11): 7797-7802.
- Favery, B., Ryan, E., Foreman, J., Linstead, P., Boudonck, K., Steer, M., Shaw, P. and Dolan, L.** (2001). "KOJAK encodes a cellulose synthase-like protein required for root hair cell morphogenesis in *Arabidopsis*." *Gene. Dev.* **15**: 79-89.
- Fredrikson, K., Kjellbom, P. and Larsson, C.** (1991). "Isolation and polypeptide composition of 1,3-beta-glucan synthase from plasma membranes of *Brassica oleracea*." *Physiol. Plant.* **81**: 289-294.
- Gibeaut, D. M., Hulett, J., Cramer, G. R. and Seemann, J. R.** (1997). "Maximal biomass of *Arabidopsis thaliana* using a simple, low-maintenance hydroponic method and favorable environmental conditions." *Plant Physiol.* **115**: 317-319.
- Handford, M. G., Baldwin, T. C., Goubet, F., Prime, T. A., Miles, J., Yu, X. and Dupree, P.** (2003). "Localisation and characterisation of cell wall mannan polysaccharides in *Arabidopsis thaliana*." *Planta* **217** (3): 1073-1079.
- Harlow, E. and Lane, D.** (1988). Antibodies, a laboratory manual. Cold Spring Harbor Laboratory.
- Hawes, C., Saint-Jore, C., Martin, B. and Zheng, H.-Q.** (2001). "ER confirmed as the location of mystery organelles in *Arabidopsis* plants expressing GFP!" *Trends Plant Sci.* **6** (6): 245-246.
- Horisberger, M. and Rouvet-Vauthey, M.** (1985). "Cell wall architecture of the fission yeast *Schizosaccharomyces pombe*." *Experientia* **41**: 748-750.
- Horisberger, M., Rouvet-Vauthey, M., Richli, U. and Farr, D. A.** (1985). "Cell wall architecture of the halophilic yeast *Saccharomyces rouxii*. An immunocytochemical study." *Eur. J. Cell Biol.* **37**: 70-77.
- Hotchkiss, A.** (1989). "Cellulose biosynthesis in plant cell wall polymers: biogenesis and biodegradation". N. G. a. P. Lewis, M. G., American Chemical Society: 232-247.

Kauss, H. (1987). "Some aspects of calcium-dependent regulation in plant metabolism." *Annu. Rev. Plant Physiol.* **38**: 47-72.

Kimura, S., Laosinchai, W., Itoh, T., Cui, X., Linder, C. R. and Brown, R. M. J. (1999). "Immunogold labeling of resette terminal cellulose-synthesizing complexes in hte vascular plant *vigna angularis*." *Plant Cell* **11**: 2075-2085.

Konishi, T., Nakai, T., Sakai, F. and Hayashi, T. (2001). "Formation of callose from sucrose in cotton fiber microsomal membranes." *J. Wood Sci.* **47**: 331-335.

Larsson, C., Widell, S. and Kjellbom, P. (1987). "Preparation of high purify plasma membranes." *Methods Enzymol.* **148**: 558-568.

Latge, J. P., Cole, G. T., Horisberger, M. and Prevost, M. G. (1986). "Ultrastructure and chemical composition of the ballistospore wall of *Conidiobolus obscurus*." *Exp. Mycol.* **10**: 99-113.

Lu, S. X. and Hrabak, E. M. (2002). "An Arabidopsis calcium-depentend protein kinase is associated with the endoplasmic reticulum." *Plant Physiol.* **128**: 1008-1021.

Lynch, M. A. and Staehelin, L. A. (1992). "Domain-specific and cell type-specific localization of two types of cell wall matrix polysaccharides in the clover root tip." *J. Cell Biol.* **118** (2): 467-479.

Madson, M., Dunand, C., Li, X., Verma, R., Vanzin, G. F., Caplan, J., Shoue, D. A., Carpita, N. C. and Reiter, W.-D. (2003). "The MUR3 gene of Arabidopsis encodes a xyloglucan galactosyltransferase that is evolutionarily related to animal exostosins." *Plant Cell* **15**: 1662-1670.

Meikle, P. J., Bonig, I., Hoogenraad, N. J., Clarke, A. E. and Stone, B. A. (1991). "The location of (1-3)-beta-glucans in the walls of pollen tubes of *Nicotiana alata* using a (1-3)-beta-glucan-specific monoclonal antibody." *Planta* **185**: 1-8.

Mizuta, S. and Brown, R. M. J. (1992). "High resolution analysis of the formation of cellulose synthesizing complexes in *Vaucheria hamata*." *Protoplasma* **166**: 187-199.

Moore, P. J., Swords, K. M. M., Lynch, M. A. and Staehelin, L. A. (1991). "Spatial organization of the assembly pathways of glycoproteins and complex polysaccharides in the Golgi apparatus of plants." *J. Cell Biol.* **112** (4): 589-602.

Morsomme, P., Dambly, S., Maudoux, O. and Boutry, M. (1998). "Single point mutations distributed in 10 soluble and membrane regions of the *Nicotiana plumbaginifolia* plasma membrane PMA2 H⁺-ATPase activate the enzyme and modify the structure of the C-terminal region." *J. Biol. Chem.* **273**: 34837-34842.

- Mueller, S. C. and Brown, R. M. J.** (1980). "Evidence for an intramembranous component associated with a cellulose microfibril synthesizing complex in higher plants." *J. Cell Biol.* **84**: 315-326.
- Mueller, S. C., Brown, R. M. J. and Scott, T. K.** (1976). "Cellulosic microfibrils: nascent stages of synthesis in a higher plant cell." *Science* **194**: 949-951.
- Northcote, D. H., Davey, R. and Lay, J.** (1989). "Use of antisera to localise callose, xylan and arabinogalactan in the cell plate, primary and secondary walls of plant cells." *Planta* **178**: 353-366.
- Northcote, D. H., Davey, R. and Lay, J.** (1989). "Use of Antisera to Localize Callose Xylan and Arabinogalactan in the Cell-Plate Primary and Secondary Walls of Plant Cells." *Planta* **178** (3): 353-366.
- Perrin, R., Wilkerson, C. and Keegstra, K.** (2001). "Golgi enzymes that synthesize plant cell wall polysaccharides: finding and evaluating candidates in the genome era." *Plant Mol. Biol.* **47**: 115-130.
- Perrin, R. M., DeRocher, A. E., Bar-Peled, M., Zeng, W., Norambuena, L., Orellana, A., Raikhel, N. V. and Keegstra, K.** (1999). "Xyloglucan fucosyltransferase, an enzyme involved in plant cell wall biosynthesis." *Science* **284** (5422): 1976-1979.
- Porchia, A. C., Sorensen, S. O. and Scheller, H. V.** (2002). "Arabinoxylan biosynthesis in wheat. Characterization of arabinosyltransferase activity in Golgi membranes." *Plant Physiol.* **130**: 432-441.
- Richmond, T. A. and Somerville, C. R.** (2000). "The cellulose synthase superfamily." *Plant Physiol.* **124**: 495-498.
- Richmond, T. A. and Somerville, C. R.** (2001). "Integrative approaches to determining Csl function." *Plant Mol. Biol.* **47**: 131-143.
- Rudolph, U., Gross, H. and Schnepf, E.** (1989). "Investigation of the turnover of the putative cellulose-synthesizing particle 'rosettes' within the plasma membrane of *Funaria hygrometrica* protonema cells." *Protoplasma* **148**: 57-69.
- Saxena, I. M., Brown, R. M. J., Fevre, M., Geremia, R. A. and Henrissat, B.** (1995). "Multidomain architecture of beta-glycosyltransferases: implications for mechanism of action." *J. Bacteriol.* **177**: 1419-1424.
- Sherrier, D. J. and Vandenbosch, K. A.** (1994). "Secretion of cell wall polysaccharides in *Vicia* root hairs." *Plant J.* **5** (2): 185-195.
- Singer, S. J.** (1990). "The structure and insertion of integral proteins in membranes." *Annu. Rev. Cell Biol.* **6**: 247-296.

Staehelin, L. A. and Moore, I. (1995). "The Plant Golgi Apparatus: structure, functional organization and trafficking mechanisms." *Annu. Rev. Plant Physiol. Plant Mol. Biol.* **46**: 261-288.

Turner, A., Bacic, A., Harris, P. J. and Read, S. M. (1998). "Membrane fractionation and enrichment of callose synthase from pollen tubes of *Nicotiana alata* Link et Otto." *Planta* **205**: 380-388.

White, A. R., Xin, Y. and Pezeshk, V. (1993). "Xyloglucan glucosyltransferase in Golgi membranes from *Pisum sativum* (pea)." *Biochem. J.* **294** (1): 231-238.

Widell, S. and Larsson, C. (1990). "A critical evaluation of markers used in plasma membrane purification." *The Plant Plasma Membrane: Structure, Function and Molecular Biology*. C. a. M. Larsson, I. M., Berlin, Springer-Verlag: 16-43.

Zaar, K. (1979). "Visualization of pores (export sites) correlated with cellulose production in the envelope of the green negative bacterium *Acetobacter xylinum*." *J. Cell Biol.* **80**: 773-777.

Zhang, G. F. and Staehelin, L. A. (1992). "Functional compartmentation of the Golgi apparatus of plant cells: immunocytochemical analysis of high-pressure frozen and freeze-substituted sycamore maple suspension culture cells." *Plant Physiol.* **99** (3): 1070-1083.

CHAPTER 5

Generation and Characterization of RNAi Transgenic Plants for AtCslD Genes

ABSTRACT

Among all AtCsl protein families, AtCslD proteins have the highest sequence identity with cellulose synthases. AtCslD proteins are also similar in size to AtCesA proteins and possess the motifs specific for β -processive glycosyltransferases. In the previous chapter, AtCslD2 proteins were shown to be localized in the Golgi complex and therefore are likely enzymes involved in the cell wall matrix polysaccharide biosynthesis. However, the biochemical functions of AtCslD proteins are still unknown. Here a reverse genetic approach was taken to determine the biosynthesis of which wall polysaccharide is the AtCslD proteins involved in. Studies on mutants of single AtCslD genes, including the root hair loss mutant *kjk* (*AtCslD3*), so far have not yielded a direct link between AtCslD proteins and biosynthesis of a specific cell wall polysaccharide. Therefore a RNAi approach was used to generate transgenic plant that would possibly have suppressed expression of multiple AtCslD genes. The goal was to define visible phenotypes and to establish a connection between the function of AtCslD proteins and the presence of a certain polysaccharide. Transgenic plants containing RNAi constructs targeting AtCslD genes showed deformed cotyledons, dwarfed adult plants, and shortened roots with more branches. However the transcript suppression was only clearly seen in cotyledons, and there was no clear alterations in sugar composition that could be associated with transcript suppression. Therefore the exact biochemical functions of AtCslD proteins still could not be determined.

INTRODUCTION

AtCsl proteins are proposed to be involved in the biosynthesis of glycans that form the backbones of various hemicellulosic polysaccharides, because of their sequence similarities with AtCesA proteins (see chapter 3). Among all AtCsl proteins, the AtCslD family showed the highest sequence identity with AtCesA proteins (see chapter 3). Results from the previous chapter also showed that AtCslD2 proteins are localized in the Golgi complex instead of the plasma membrane and therefore AtCslD genes do not likely encode cellulose synthase or callose synthase (see chapter 4). Due to the chemical structure similarity shared by the XyG backbone and cellulose, AtCslD genes have become the most likely candidates for encoding the XyG backbone glucan synthase. Therefore the goal of this chapter is to determine the function of AtCslD genes.

The functional studies of AtCsl genes are still in the initial stages. In an effort to identify genes involved in the synthesis of β -glucans in *Nicotiana alata* pollen tubes, a CslD cDNA was isolated as well as a CesA cDNA (Doblin et al., 2001). This NaCslD1 gene was expressed abundantly in male gametophyte tissues, in mature pollen and in growing pollen tubes, while the NaCesA1 was not expressed in the male gametophyte (pollen or anthers) at any stage of development (Doblin et al., 2001). Given the existence of large amounts of cellulose, NaCslD1 was proposed to be a male gametophyte specific cellulose synthase (Doblin et al., 2001).

Among all cell wall polysaccharides, only cellulose and callose are synthesized at the plasma membrane and directly incorporated into the wall, while all other polysaccharides are synthesized in the Golgi complex and then transported to the cell surface for their incorporation into the wall (Delmer and Stone, 1988). AtCslD2, however,

was localized at the Golgi instead of the plasma membrane according to studies described in chapter 4. Therefore a non-cellulosic function was proposed for AtCslD2. It seems reasonable to extend this hypothesis to all members of the CslD family of proteins. While this hypothesis is contrary to the one of Doblin et al. (2001) that CslD proteins are involved in cellulose synthesis, it still does not provide a specific function for them. I am therefore interested in further determining the biochemical functions of AtCslD proteins. At this time activity assays for cellulose synthase and XyG backbone synthase, the two mostly likely enzymes that AtCslD genes may encode, are both unavailable. Therefore I decided to employ a genetic approach.

Genetics has played a critical role and been very successful in illustrating the functions of genes involved in cell wall biosynthesis. The most prominent cases are the characterizations of mutant plants that have led to identification of the cellulose synthase genes. So far six of the 10 AtCesA genes, including AtCesA1, 3, 4, 6, 7, 8, have been confirmed to encode cellulose synthase catalytic subunits (Arioli et al., 1998; Taylor et al., 1999; Fagard et al., 2000; Taylor et al., 2000; Scheible et al., 2001; Burn et al., 2002; Desprez et al., 2002; Zhong et al., 2003). All of the functional confirmations for these AtCesA genes were accomplished through the characterizations of mutants identified through forward genetics (*AtCesA1: rsw1*; *AtCesA3: ixr1*; *AtCesA6: procuste1, ixr2*; *AtCesA7: irx3*; *AtCesA8: irx1*). These AtCesA mutants all showed decreased cellulose content in their cell walls, disrupted wall structures, and altered plant morphologies. The functions of AtCesA1 and A3 were also confirmed through the characterizations of antisense plants generated through reverse genetics (Burn et al., 2002)

Genetic studies also have been very successful to define the functions of a few genes involved in the biosynthesis of matrix polysaccharides. Examples include the identification of the XyG fucosyltransferase gene *AtFut1 (mur2)* (Vanzin et al., 2002), XyG galactosyltransferase gene *AtGalT (mur3)* (Madson et al., 2003), a RGII glucuronyltransferase gene (*NpGUT1*) (Iwai et al., 2002), and a HGA glycosyltransferase (*qual1*) (Bouton et al., 2002). In all cases, careful phenotypic and morphological analyses have revealed the absence of a particular sugar linkage from a specific matrix polysaccharide, which then led to functional propositions for the specific mutated genes. In the cases of identification of *AtFut1* and *AtGalT*, genetic approaches were used in combination with biochemical approaches by expressing the cDNAs in *Pichia pastoris* to obtain specific enzyme activities (Perrin et al., 1999; Madson et al., 2003).

However the genetic studies for *AtCsl* genes have not been as successful. So far, mutation in only three *AtCsl* genes yielded specific phenotypes. They are a T-DNA insertion mutant of *AtCslA9, rat4* (Zhu et al., 2003), a transposon insertion line of *AtCslA7* (Goubet et al., 2003), and a *AtCslD3* mutant *kojak (kjk)* (Favery et al., 2001; Wang et al., 2001). The *rat4* plants showed less than one fourth of crown gall formation compared with wild type plants when their roots were infected with *Agrobacterium tumefaciens* A208, as well as decreased lateral roots (Zhu et al., 2003). *AtCslA7* plants showed recessive embryo lethality and impaired pollen tube growth (Goubet et al., 2003). *kjk* plants showed impaired root hair growth with the root hairs ruptured soon after initiation, giving rise to a bald phenotype for the roots (Favery et al., 2001). However none of the mutations has been linked to changes in a specific sugar linkage within a specific cell wall polysaccharide and therefore the functions of these genes could not be

deduced. At the same time mutant plants with defects in other AtCsl genes, including AtCslC4, AtCslG1 and AtCslB5, did not show any visible phenotypes or detectable changes in cell wall sugar composition (Richmond and Somerville, 2001). This could be due to gene redundancy because the presence of multiple members in most AtCsl gene families supply redundant functions. Therefore it seems the loss-of-function in multiple genes in the same AtCsl gene family is necessary to see phenotypic defects. As the effect of knock-out mutations of AtCsl genes is being determined by Chris Somerville's group as part of a 2010 project (personal communication), I decide to pursue the genetic studies of AtCslD genes using the RNAi approach. My goal was to generate transgenic plants showing suppressed expression of more than one AtCslD gene, leading to more easily detectable morphological phenotypes.

RNA interference (RNAi) is a post transcriptional gene silencing phenomenon induced by double-stranded RNA (dsRNA) that is found in fungi, plants, and animals, including mammals (Bosher and Labouesse, 2000). The dsRNA can be a replication intermediate of many viruses, can be produced by the transcription of inverted repeat transgenes, or can be synthesized in vitro biochemically and delivered into cells (Voinnet, 2003). The dsRNA molecules are recognized as aberrant RNAs and degraded to 21-26 nucleotide RNA duplexes, called short interference RNAs (siRNAs), by a dsRNA specific endonuclease called Dicer (Bernstein et al., 2001; Billy et al., 2001; Grishok et al., 2001; Ketting et al., 2001). Dicer family proteins usually contain putative RNA helicase, PAZ, RNase III, and dsRNA binding domains. The RNase III domain is thought to cleave the dsRNA into siRNAs to mediate the RNAi response. In plants, there are two distinct classes of siRNAs of 21 nt and 25 nt as found in tobacco, Arabidopsis and wheat

extracts (Hamilton et al., 2002; Tang et al., 2003; Voinnet, 2003). These two classes of siRNAs in plants are probably generated by two different Dicer proteins (Tang et al., 2003; Voinnet, 2003). The siRNAs then are incorporated into a RNA-induced silencing complex (RISC). This RISC, through base pairing, mediates the specific cleavage of target RNAs at sequences with extensive complementarities to the siRNAs (Hammond et al., 2000; Hammond et al., 2001; Hutvagner and Zamore, 2002; Martinez et al., 2002). The large fragments resulted from the endonuclease cleavage of the target mRNAs then are degraded by the general RNA degradation machineries with conventional exonucleases (Han and Grierson, 2002).

One of the advantages of RNAi technique is that the siRNA can also induce the degradation of RNA molecules other than the immediate target as long as these RNA molecules show sufficient sequence identity with the immediate target RNA (Bosher and Labouesse, 2000; Parrish et al., 2000). Another advantage, especially for plants, is that when transformed with a construct whose transcripts form hairpins, a series of independent lines will be generated with different degrees of phenotypes and different degrees of mRNA suppression (Helliwell et al., 2002; Stoutjesdijk et al., 2002; Waterhouse and Helliwell, 2003). This feature of the RNAi approach will guarantee that some transgenic plants with partial RNA suppression and partial phenotypes will be available in case a knockout mutant is lethal.

Six RNAi constructs, including two targeting AtCslD genes, and other four targeting AtCsl genes of other AtCsl subfamilies were generated and introduced into Arabidopsis plants, together with the vector control construct. It turned out that only the two constructs targeting AtCslD genes showed obvious phenotypes. Therefore transgenic

plants containing other constructs served as controls, along with the vector alone construct. The transgenic plants with suppressed AtCslD transcripts showed deformed cotyledons, shortened adult plants and roots, and weakened cell adherence among cotyledon cells. These phenotypic characterizations suggested that AtCslD proteins are developmentally important and might be involved in cell-cell adherence. However, biochemical analyses of wall materials from the transgenic plants were not conclusive, therefore the connection between the function of AtCslD genes and the biosynthesis of a particular wall polysaccharide still could not be established.

MATERIALS AND METHODS

Arabidopsis transformation and screening

The Columbia ecotype of *Arabidopsis* was used for all experiments. *Arabidopsis* transformation was accomplished using the floral dip method (Clough and Bent, 1998). *Agrobacterium* GV3101 containing binary plasmid pCAMBIA3300 (Basta resistant) carrying RNAi constructs were cultured overnight in 5 ml of LB medium with 34 µg/ml Rifampicin, 25 µg/ml Gentamycin and 25 µg/ml Kanamycin. A large culture of 500 ml then was inoculated with a 1:100 dilution of the overnight culture and allowed to grow for 16 to 20 hours until the cultures reached stationary phase. *Agrobacterium* cells were collected by centrifugation at 10,000×g at 4°C for 5 minutes, and resuspended in 5.0% sucrose solution containing 0.05% (i.e. 500µl/L) Silwet L-77 (LEHLE SEEDS, Round Rock, TX) to give a final OD600 of around 0.8. *Arabidopsis* plants growing in mesh covered pots at about 4 weeks old with many opened flowers were dipped in the *Agrobacterium* solution for 3 to 5 seconds. Pots with transformed *Arabidopsis* plants were covered with saran wrap and stored on their side overnight in the dark. Seeds were collected from transformed plants about 4 weeks later and labeled as the T1 generation.

Arabidopsis seeds were sterilized and grown in MS medium according to Fitzpatrick and Keegstra (2001). Transgenic seeds were screened on MS medium (plus 1% sucrose) containing 10 µg/ml Basta (Crescent Chemical, Islandia, NY) and 500 µg/ml Carbenicillin (Invitrogen, Carlsbad, CA). Antibiotic resistant plants were picked at day 4 to 6 and moved to new MS plates for root measurement or other phenotype studies. When the transgenic seeds were planted directly in soil, screening was achieved after seed germination by feeding or spraying with water containing 100 µg/ml Basta.

Genomic DNA preparation

Arabidopsis rosette leaves were ground in liquid nitrogen; the powder was resuspended in CTAB solution (AutoGen, AG00121) and incubated in 65°C for 1 hour. Genomic DNA was then extracted using the AutoGenprep 240 (Genomics Facility, Michigan State University). The dried genomic DNA was resuspended in water and extracted with phenol-chloroform.

RNA preparation

Total RNA was prepared from various tissues using TRIzol Reagent (Invitrogen, Carlsbad, CA) according to the manufacturer's instructions and treated with DNase I (Roche, 776785, Mannheim, Germany) according to the instructions. After determining the concentration of RNA, all samples were stored at -80°C.

PCR and RT-PCR reactions

All PCR reactions were carried out in a thermocycler PTC-200 (MJ Research, Waltham, MA). One step RT-PCR reactions used the Superscript One-Step RT-PCR with Platinum Taq (Invitrogen, Carlsbad, CA) according to the instructions. Two step RT-PCR reactions used the Superscript II RNase H⁻ Reverse Transcriptase (Invitrogen, Carlsbad, CA) according to instructions, and Taq polymerase (Roche, Indianapolis, IN) for the following PCR reactions.

Generation of RNAi constructs

An intermediate cloning vector named pGEM-GUS was engineered from pGEM-7Zf(+) (Promega, Madison, WI) by inserting between its SmaI and Csp45I sites a 1.1 kb GUS gene fragment released from vector plasmid pBI121 (Clontech, Palo Alto, CA). DNA fragments for each RNAi construct then were inserted into pGEM-GUS at both ends of the GUS-SmaI-Csp45I fragment in opposite directions utilizing enzyme recognition sites XhoI, EcoRI or KpnI in the T7 end and BamHI, HindIII or ClaI in the SP6 end. All plasmid engineering was carried in *E. coli* cells DH5 α or JM101 (Promega, Madison, WI). The sequences of constructs were confirmed by restriction digestion and sequencing (Genomics Facility, Michigan State University). The finished RNAi constructs and the GUS fragment control were released by restriction digestion with XbaI and SacI, and inserted into binary vectors pCambia3300 (Basta⁺), pCambia1300 (Hygromycin⁺), or pBI121 (Kanamycin⁺) for different antibiotic resistances. All three vectors contain 35S promoters for the transcription of the construct gene fragments. Constructs in binary vectors were introduced into *Agrobacterium* competent cells GV3101 (pMP90). Plasmids were isolated from *Agrobacterium* and transformed back into DH5 α competent cells to confirm the constructs in GV3101 (pMP90) cells. Finally *Agrobacterium* containing the RNAi constructs and control construct were used to transform *Arabidopsis* Columbia plants.

Sugar composition analysis by gas chromatography

Cell wall monosaccharides were analyzed as alditol acetates after acid hydrolysis (Blakeney et al., 1983; Reiter et al., 1993). Plant tissues were washed twice in 1ml of 70% ethanol at 70°C, 1ml of acetone at room temperature for 5 min, and dried. The dried

samples were hydrolyzed with 250 μ l of 1 M H_2SO_4 at 121°C for 1 hour. 100 μ g inositol was added as control. The resulting sugars were reduced to alditols by adding 100 μ l of 9 M ammonium hydroxide and then 1 ml of 2% (w/v) sodium borohydride (NaBH_4) in dimethyl sulfoxide, and incubated at 40°C for 90 min. The remaining borohydride was destroyed by adding 250 μ l of acetic acid to each sample. The alditols were converted into alditol acetates by adding 250 μ l of 1-methylimidazole followed by 4 ml of acetic anhydride. Finally 8 ml of water was added in each sample to destroy excess acetic anhydride. After the samples cooled to room temperature, 2 ml of dichloromethane (CH_2Cl_2) were added into each tube to partition the alditol acetates. After sitting at 4°C for 2 hours, the dichloromethane phase was recovered. For alditol acetates separation, an Agilent 6890 series GC system fitted with an Agilent DB-225 capillary column (Agilent, Palo Alto, CA) and a flame ionization detection GC ChemStation software (Agilent) was used for quantitation. The temperature program used was 1 min at 160°C; 20°C min^{-1} to 200°C; hold for 5 min; 20°C min^{-1} to 240°C; hold for 11.5 min.

Microscopy

For light microscopy, tissues were fixed in 2.5% glutaraldehyde and 2.0% paraformaldehyde in 0.1 M phosphate buffer (pH 7.4) overnight and washed with 0.1 M phosphate buffer (pH 7.4) three times for 20 min each. Samples then were incubated in 0.1 M phosphate buffer (pH 7.4) with 1% osmium tetroxide overnight at 4°C and washed three times for 20 min each with phosphate buffer. After dehydration samples were infiltrated in Poly/Bed 812 resin and embedded in silicone molds and polymerized for 2

days at 60°C. Samples were then sectioned and stained with different dyes and observed under light microscope.

For scanning EM, tissues were fixed in 4% glutaraldehyde in 0.1 M phosphate buffer (pH 7.4) for 3 hours at 4°C and dehydrated. Samples then were dried at critical point in a Balzers Critical Point Dryer using liquid carbon dioxide as the transitional fluid, and mounted on aluminum stubs using adhesive tabs. Samples then were coated with 20 nm thick gold in an Emscope Sputter Coater model SC 500 purged with argon gas. The samples were examined in a JEOL 6400 V SEM (Japan Electron Optics Limited).

RESULTS

Generation of RNAi constructs

It was reported in *C. elegans* that RNAi constructs of less than 100 bp long still could induce gene silencing effectively, but the silencing effect increased with longer constructs (Parrish et al., 2000). At the time when this work began, the shortest RNAi construct reported to show gene silencing in Arabidopsis was 288 bp long (Chuang and Meyerowitz, 2000). Therefore, 280 bp was chosen to be the lower limit for the construct length. On the other hand it was reported that dsRNA produced by RNAi construct could induce the silencing of related but not identical genes that share significant overall homology and uninterrupted segments of significant length, probably more than 30 bp (Sharp, 2001). Therefore during the design of RNAi constructs targeting various AtCsl genes, I decided to choose construct fragments sharing an identity of 80% or more, with as many as possible of the other gene members within the same AtCsl family. The rationale was that this strategy would provide the best chance for these RNAi constructs to induce the suppression of more than one target gene.

Without any conclusive support for a specific function for any AtCsl genes, I started with making RNAi constructs targeting genes of each AtCsl family, except for AtCslA. AtCslA genes do not share more than 81% identity between any two of them. In addition, more work needs to be done to confirm the re-annotated sequences (data not shown and chapter 3). Using these criteria, six constructs were generated and designated as D1235f3, D23f2, B123456f3, C58f5, E1f1 and G123f3. The first letter in their names represents the AtCsl family. The numbers after the letter represent the genes within that family showing more than 80% overall identity with the specific construct. The letter “f”

designates “from”. The last number represents the gene member in that particular AtCsl family was used as PCR or RT-PCR template for amplification of the RNAi construct.

The construct length, the restriction enzyme recognition sites designed at the end of primers, the main parameters of PCR or RT-PCR for the construct amplification, and the primers sequences are all listed in Table 5.1. The primers used for PCR reactions to confirm the existences of RNAi constructs in transgenic plants are listed in Table 5.2. The gene specific primers used to test the suppression of target gene transcripts are listed in Table 5.3.

Six RNAi constructs were generated that should produce hairpin RNAs after transcription (Figure 5.1). Two of them, D1235f3 and D23f2, target AtCslD genes, while the other four, B123456f3, C58f5, E1f1 and G123f3, target genes of other AtCsl families. An empty vector control was also generated with only a fragment of GUS gene that is used as the center loop region for all constructs (Figure 5.1). Later on it was found that the transgenic plants containing construct B123456f3, C58f5, E1f1, or G123f3 did not show any obvious phenotypes and therefore they also were used as controls.

The 280 bp DNA fragment of construct D1235f3 was generated by PCR reactions using AtCslD3 as template (Table 5.1). This fragment is derived from the most conserved region throughout the whole AtCslD family and shows more than 80% sequence identity with the counterpart regions of AtCslD1, 2, and 5 (Figure 5.2). This DNA fragment contains uninterrupted identical sequence segments of 24 bp compared with AtCslD1, D2, and D4, 26 bp with D5 and 14 bp with D6 (Figure 5.2). Therefore, it was interesting to see after the construct D1235f3 was introduced into plants which AtCslD genes might be suppressed. The 380 bp DNA fragment of construct D23f2 was generated using the

Table 5.1: Design of RNAi constructs targeting different AtCsl genes and primers

used to create them. Each construct was amplified by PCR or RT-PCR reactions twice with two sets of primers having different restriction enzyme recognition sites at their ends. The two DNA fragments were then inserted into the cloning intermediate vector plasmid pGEM-GUS utilizing the enzyme recognition sites introduced by the primers.

Construct (length)	Restriction sites used	Reaction	Primers	Primer sequences
D1235f3 (280 bp)	XhoI	PCR, 60°C	kee546	5' TCTTGTCTATGTTTCCCTCGAGAAGCGACCG 3'
	EcoRI		kee547	5' CCCATGAATTCATCAAGTGCTCTCATGTTTACA 3'
	BamHI	PCR, 55°C	kee558	5' CGTGAGAAGGATCCGGGTATG 3'
	Clal		kee532	5' ATCAACCCATCGATAGCTCTCAT 3'
D23f2 (380 bp)	XhoI	PCR, 55°C	kee548	5' AAGCCACCTCGAGATGAACCAC 3'
	KpnI		kee560	5' ACCGGTACCATAAGCCCATCAACT 3'
	BamHI	PCR, 55°C	kee550	5' ACCTAGTGAGGATCCACTACAC 3'
	Clal		kee561	5' ACCGGATCGATAAGCCCATCAACT 3'
B123456f3 (330 bp)	XhoI	RT-PCR, 50°C	kee521	5' GAAGATTTCTCGAGTACAAAACC 3'
	KpnI		kee523	5' TTCGTCGGCGGTACCATCATAGAAC 3'
	BamHI	RT-PCR, 50°C	kee522	5' AAGATTTCTCGGATCCAAAACCAAA 3'
	HindIII		kee524	5' GTCGCGGTTAGAAGCTTAGAACTCTT 3'
C58f5 (710 bp)	KpnI	RT-PCR, 50°C	kee525	5' CCAAATGGTACCAAAAGGGAGT 3'
	XhoI		kee527	5' AGGGAGCTCGAGCTTCTGGAA 3'
	Clal	RT-PCR, 45°C	kee526	5' TTGCCAAATCGATCCAAAAGGGA 3'
	HindIII		kee528	5' AGGGAGGTAAGCTTCTGGAACA 3'
E1f1 (530 bp)	XhoI	PCR, 55°C	kee559	5' GTCTCGAGGTCGTGGTTTATTC 3'
	KpnI		kee556	5' AAACAGGTACCGGCAGATAAAG 3'
	HindIII	PCR, 60°C	kee555	5' GGTCTCAAGCTTGTGGTTTATTC 3'
	Clal		kee557	5' TACAAAATCGATAAACAGGTACAG 3'
G123f3 (540 bp)	XhoI	PCR, 55°C	kee533	5' CACAACCCTCGAGACGTGTCAT 3'
	EcoRI		kee535	5' CATCTTGAATTCTCAGCTTCA 3'
	HindIII	PCR, 50°C	kee534	5' GGCGACACAAGCTTCCACACGTG 3'
	Clal		kee536	5' GTACATCATATCGATATTTTCAGC 3'

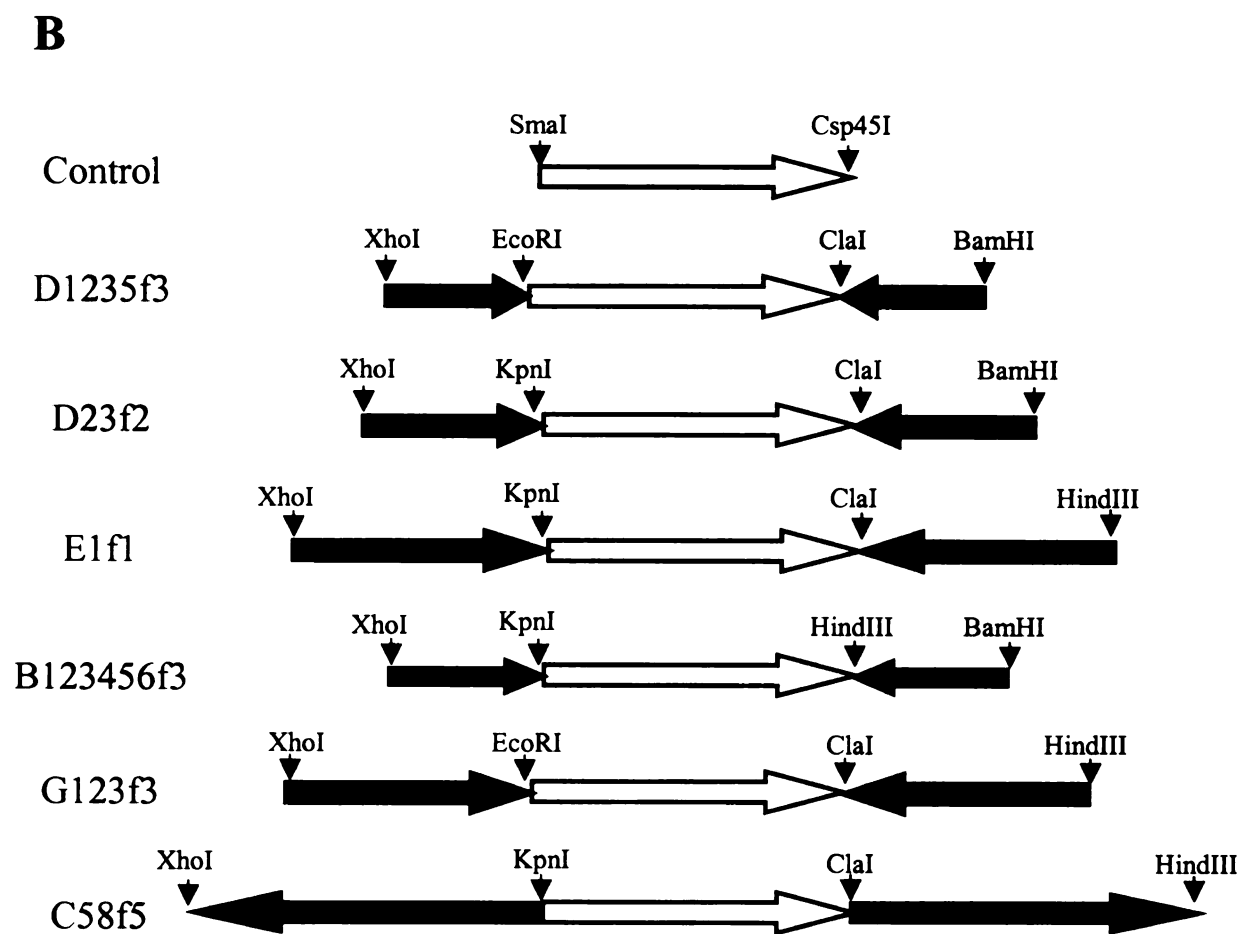
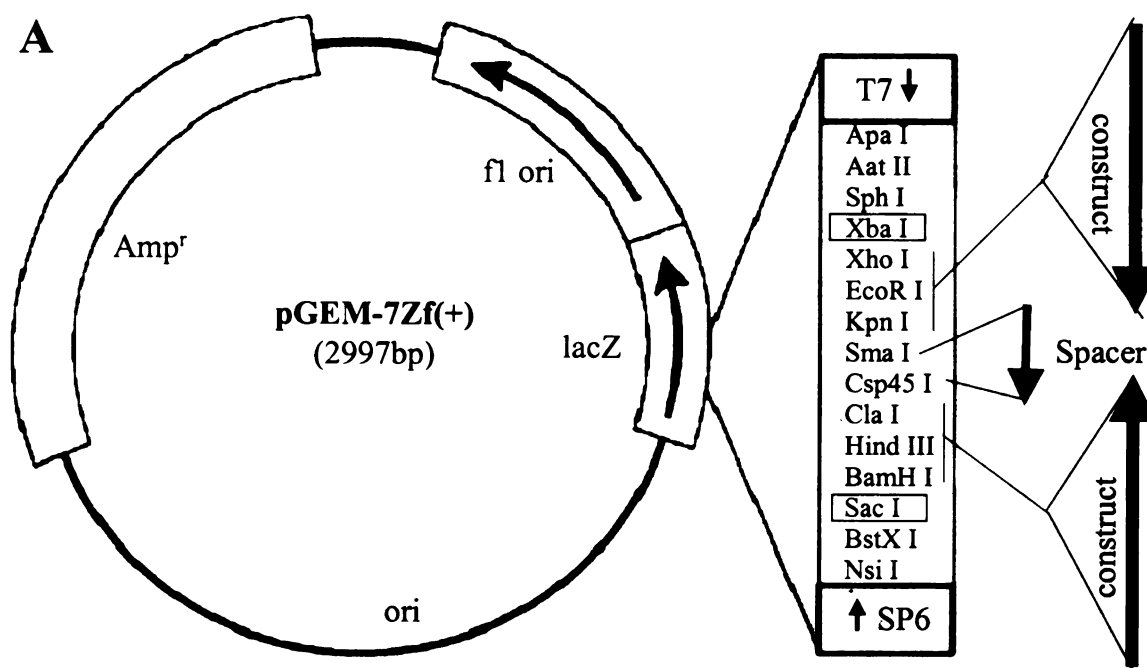
Table 5.2: Primers used for PCR reactions to confirm the existence of constructs in transgenic plants.

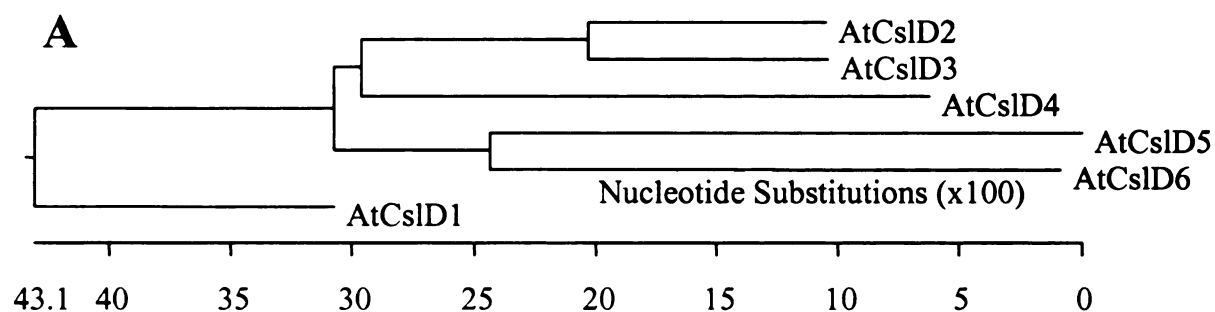
Primer	Specificity	Sequence
Kee578 (C1)	Spacer	5' TGTTACGTCCTGTAGAAACCC 3'
Kee579 (C2)	Spacer	5' CCAGTTCAGTTCGTTGTTTAC 3'
Kee581 (C4)	Spacer	5' AACCACAAACCGTTCTACTTT 3'
Kee582 (b1)	B123456f3	5' AAGAGTGTGTCAGGGTTGATGAC 3'
Kee587 (e1)	E1f1	5' AGATTTGAAAACAATGGGGAT 3'
Kee550 (d2)	D23f2	5' ACCTAGTGAGGATCCACTACAC 3'
Kee727 (d3)	D1235f3	5' CATATACAACCTCTCAAGGTTTA 3'

Table 5.3: Primers used for RT-PCR reactions to confirm the suppression of transcripts. RT-PCR reactions were carried in two steps using the Oligo-dT primer for the reverse transcription reactions. All cDNAs were treated with RNase and used as template for PCR reactions with gene specific primers. “+”: the downstream primer kee625 comes from the 3’ UTR region of AtCslD3.

Gene	Primers	Primer sequences
CytC	LM432	5' GGAATCTACTGCGCCTAAGT 3'
	LM433	5' GCCTCAGAAAATCAAATGTACT 3'
AtCslE01	Kee592	5' TTATGGACACGATTAAGAAGC 3'
	Kee593	5' ACAGGTACAGGCAGATAAAGC 3'
AtCslD2	Kee620	5' TCTCCTTCACGCTCACGAGT 3'
	Kee621	5' TTTGACAAGAAAGAAATCAACCT 3'
AtCslD3+	Kee624	5' CTCACTTAGCCGCGGTTATC 3'
	Kee625	5' GGCCAAAATGTGTCTCCATC 3'
AtCslD5	Kee616	5' CTCAGCTTTTGGGTGCTTTG 3'
	Kee617	5' AACTTTCATGCCTTGTACCAC 3'
AtCslD1	Kee1197	5' GCATCACCGTAACCCTAACCC 3'
	Kee1198	5' TAAGCGGCATGATGAATAAGCCT 3'
AtCslD4	Kee1199	5' TCTTATGATCACCATTTGTTTGATT 3'
	Kee1200	5' TATTATGTTACCATTTGCTATCAC 3'
AtCslD6	Kee1201	5' AAGCCGCAAACCGCTTGATTTCG 3'
	Kee1202	5' CCGTCCTACAAACCGCGAAAAGT 3'

Figure 5.1: Design of RNAi constructs for AtCsl genes. **A.** Recombinant plasmid construction scheme. A 1.1 kb fragment of the GUS gene coding region from vector plasmid pBI121 was inserted into plasmid pGEM-7Zf through restriction sites SmaI and Csp45I, and used as the spacer loop region for all RNAi constructs. PCR amplified DNA fragments from various AtCsl genes were inserted into both ends of the spacer fragment in opposite directions to give rise to RNAi constructs through restriction sites for XhoI, EcoRI, or KpnI and ClaI, HindIII, or BamHI. RNAi constructs were released from pGEM-7Zf via XbaI and SacI and introduced into binary vectors pBI121, pCambia3300, or pCambia 3100 for Arabidopsis transformation. **B.** RNAi constructs including six of them targeting different AtCsl genes and a control construct containing only the spacer fragment. Open arrows represent the spacer fragment derived from the GUS gene, and the filled arrows represent DNA fragments amplified from various AtCsl genes. The arrows point from 5' end to the 3' end of all DNA fragments. Restriction sites used for plasmid construction are indicated.





B

D1235f3	D1	D2	D3	D4	D5	D6
Identity	81.47%	87.76%	100%	76.22%	83.22%	75.87%
Uninterrupted identical sequence match	24 bp × 1 14 bp × 1	24 bp × 1 23 bp × 1 20 bp × 1 18 bp × 1 17 bp × 1	286bp × 1	24 bp × 1 14 bp × 1	26 bp × 1 20 bp × 1 18 bp × 1 17 bp × 1 14 bp × 2	14 bp × 1

D23f2	D1	D2	D3	D4	D5	D6
Identity	72.21%	100%	85.6%	73.25%	73.91%	74.23%
Uninterrupted identical sequence match	17 bp × 1	382 bp × 1	24 bp × 1 23 bp × 1 20 bp × 1 18 bp × 1 17 bp × 1 14 bp × 1	17 bp × 1 14 bp × 2	20 bp × 2	15 bp × 1 14 bp × 3

Figure 5.2: Sequence similarities between RNAi construct D1235f3, D23f2 and AtCslD genes. **A.** Alignment of AtCslD cDNA sequences by the Multialign program of DNASTar (Madison, WI). **B.** Sequence identities shared by RNAi constructs D1235f3, D23f2 with the counterpart regions of each AtCslD cDNA sequence; and the frequencies of uninterrupted identical sequence strings.

sequence of AtCslD2 (Table 5.1). This fragment from AtCslD2 contains the whole region that is contained in the D1235f3 construct plus extra sequence on each end. It shows more than 80% identity with AtCslD3 (Figure 5.2). The longest uninterrupted stretch of identities that D23f2 DNA fragment showed with its counterparts from AtCslD1, 4, 5, 6 are 20 bp and shorter (Figure 5.2); therefore plants transformed with D23f2 construct are unlikely to show mRNA suppression of AtCslD1, 4, 5 and 6. The DNA fragment for construct B123456f3 was amplified from AtCslB3 at the most conserved region throughout the AtCslB family and shows more than 80% identity with its counterparts from all other AtCslB genes. The same is true for construct G123f3. The DNA fragment of C58f5 is only conserved in AtCslC5 and C8 and did not show much identity with other AtCslC genes. E1f1 was amplified from the only member of AtCslE family at a region showed low identity with AtCsl genes of other families (data not shown).

Generation of transgenic plants containing AtCsl RNAi constructs

All six RNAi constructs that targeted AtCsl genes and the control construct containing only the spacer segment were introduced into Arabidopsis individually (Figure 5.3). After transformation, plants were allowed to grow under normal conditions and seeds were collected after about 4 weeks when the plants had matured. These T1 generation seeds were germinated on MS plates with Basta for selection. The Basta resistance gene is carried on the transformation vector. Genomic DNA was prepared from rosette leaves of T1 plants that survived screening on antibiotics; the DNA was used to confirm the presence of various constructs. The presence of the spacer segment in the constructs was confirmed by PCR reactions using two specific primers C1 and C2

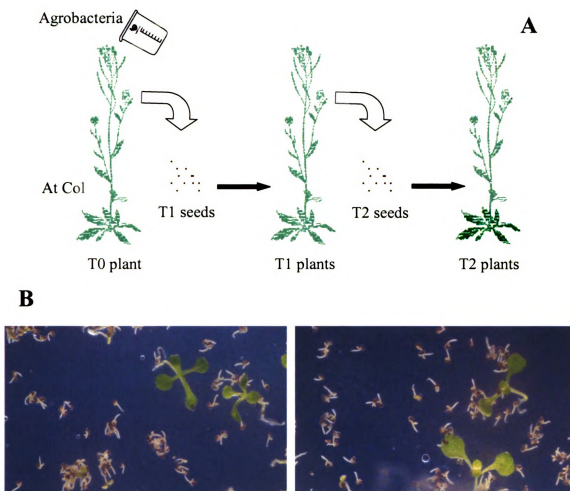


Figure 5.3: Transformation and screening of RNAi plants. Arabidopsis plants were transformed by flower dipping method (Clough and Bent, 1998). T1 seeds were germinated in MS agar plates with 500 $\mu\text{g/ml}$ Carbenicillin and 10 $\mu\text{g/ml}$ Basta, or in soil directly with 100 $\mu\text{g/ml}$ Basta. Plants survived the Basta screening were selected after 4-6 days and transferred to new plates for phenotype observation. They were transferred to soil after another 9 days. T2 seeds were collected from individual T1 plants and screened the same way as for T1 seeds. **A.** Flow chart of transformation and screening procedure. **B.** Part of a screening plate for T1 plants carrying construt D1235f3 at 10 days old, showing a couple of antibiotic resistant plants survived and most of other plants died right after germination.

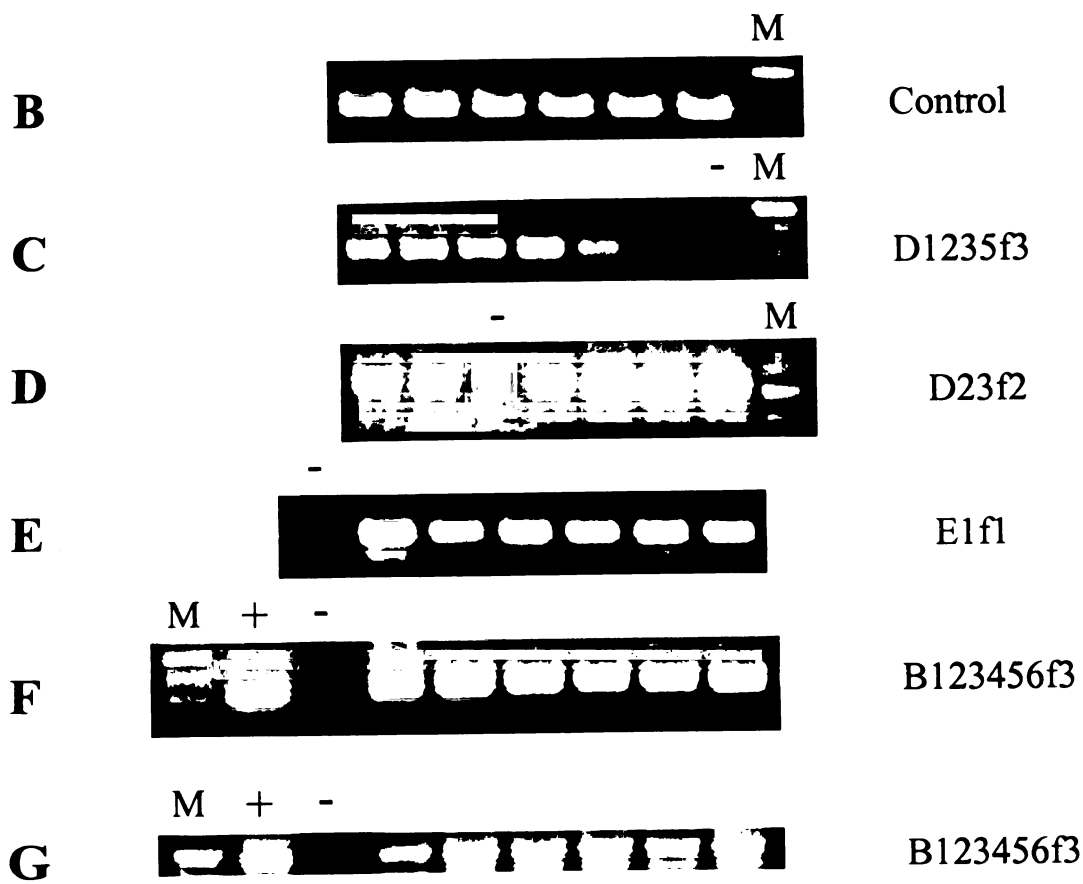
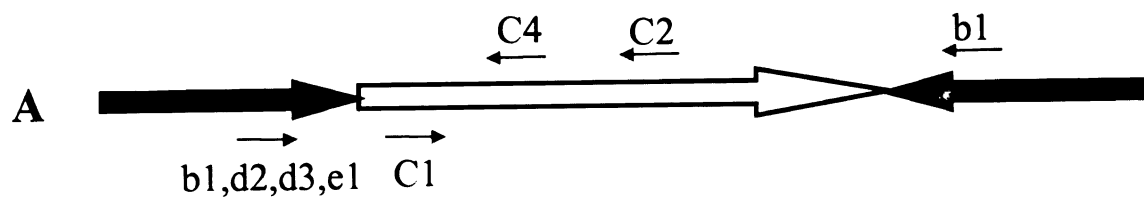
(Figure 5.4). The presence of construct B123456f3 was confirmed by two different PCR reactions using spacer-fragment-specific primer C4 and B123456f3 specific primer b1, or using B123456f3 specific primer b1 alone (Figure 5.4). The DNA fragment amplified with spacer-fragment-specific primers would confirm the presence of the central loop region of the constructs, while the PCR reaction using just one primer that is B123456f3 specific would not only confirm the presence of this construct but also confirm the structure of the construct, showing head to head arrangement of the same DNA fragment in the construct (Figure 5.4). The presences of RNAi constructs D23f2, D1235f3 and E1f1 were all confirmed by PCR reactions using construct specific primers d2, d3, and e1 respectively with a spacer-fragment-specific primer C4 (Figure 5.4). More than 25 independent transgenic plants were examined for each RNAi construct. All transgenic plants that were positive during antibiotic screening showed the presence of a corresponding construct.

RNAi transgenic plants containing construct D1235f3 or D23f2 show deformed cotyledons and reduced adhesion of cotyledon cells

T1 seeds from transgenic Arabidopsis plants transformed with RNAi constructs were screened on MS medium plates containing Basta. The screening procedure is summarized in Figure 5.3. At 4 to 6 days old, a cotyledon deformation phenotype was observed from some T1 seedlings (Figure 5.5). The phenotype was recorded as “strong”, “intermediate II”, “intermediate I”, or “normal” according to the degree of cotyledon deformation. Collectively about 50% of the T1 transgenic plants containing construct D1235f3 showed cotyledon deformation of different degrees, and about 21% of the T1

Figure 5.4: Determination of the presence of RNAi constructs in transgenic plants.

All T1 transgenic plants that survived antibiotic screening were confirmed to **contain** the appropriate constructs by PCR reactions using construct specific primers. At least **25** independent transgenic plants were tested for each construct. Data shown here is **results** from only six plants for each construct. RNA samples for F and G are from the **same** six transgenic plants. "M" is DNA molecular size marker, "+" are positive controls **using** construct plasmid DNA as PCR reaction template. "-" are negative controls using **RNA** prepared from wild type plants that were grown under similar conditions. **A: Positioning** of construct specific primers used for PCR reactions. C1, C2 and C4 are primers **specific** for the spacer fragment used as the central loop of RNAi constructs. C1 and C2 are **used** for PCR reactions confirming the presence of the spacer fragment. C4 is used in combination with construct specific primers b1, d2, d3 and e1 for B123456f3, D23f2, D1235f3 and E1f1 respectively. Sequences of all primers are listed in Table 5.2. **B: PCR** reactions using primers C1 and C2 for RNAi plants containing the spacer control construct. **C-F:** PCR reactions using primer C4 combined with primer d3 (**C**), d2 (**D**), e1 (**E**) and b1 (**F**) to confirm the presence of construct D1235f3, D23f2, E1f1 and B123456f3 respectively. **G:** PCR reactions using primer b1 only to confirm the **presence** of construct B123456f3.



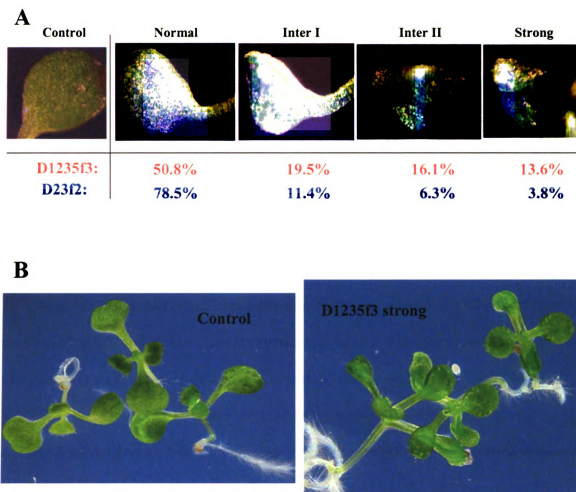


Figure 5.5: Cotyledon deformation phenotype of transgenic plants carrying construct D1235f3 or D23f2. Cotyledons were taken from T1 plants at 7 days old growing on MS-Basta plates. **A.** Cotyledons from 7-day-old T1 plants containing RNAi construct spacer control (Control), D1235f3, or D23f2 that showed different degrees of cotyledon deformation (Normal, Inter I, Inter II, and Strong). Numbers listed are the percentages of T1 plants showing different degrees of cotyledon deformation for D1235f3 and D23f2 lines. **B.** Representative T2 plants of 7 days old on screening plates, showing normal cotyledons in control plants and strongly deformed cotyledons of D1235f3 strong lines.

transgenic plants containing construct D23f2 showed cotyledon deformations (Figure 5.5). T1 plants containing construct D1235f3 not only have more seedlings showing cotyledon deformation, but also showed a more severe degree of deformation compared to plants containing D23f2. While 13.6% of T1 plants containing D1235f3 showed strongly deformed cotyledons, this number for T1 plants containing construct D23f2 is only 3.8% (Figure 5.5). In contrast, T1 transgenic plants containing the control construct or constructs targeting AtCsl genes of other families did not show this phenotype (Figure 5.5 and data not shown).

The introduction of all six constructs into *Arabidopsis* was repeated at least three more times by different transformation experiments. In each case, the same cotyledon deformation phenotypes were observed with only plants carrying construct D1235f3 and D23f2. The percentages of T1 plants showing the phenotype are also similar to what obtained from the first screening. In one case, the construct D1235f3 was introduced into *Arabidopsis* plants in ten separate transformation experiments. The T1 generations from these 10 plants all showed similar cotyledon deformation phenotype and similar percentage of offspring that showed the phenotype. At the same time the control experiment containing the construct with a GUS fragment spacer consistently showed no cotyledon deformation.

When observed by SEM, the abaxial side of deformed cotyledons showed distorted epidermal cells protruding from the surface, compared with cotyledons from either control line or T1 plants showing normal cotyledons (Figure 5.6).

Transverse sections of cotyledons of normal, intermediate and strong deformation were compared with those from control plants. The number of cell layers were not altered

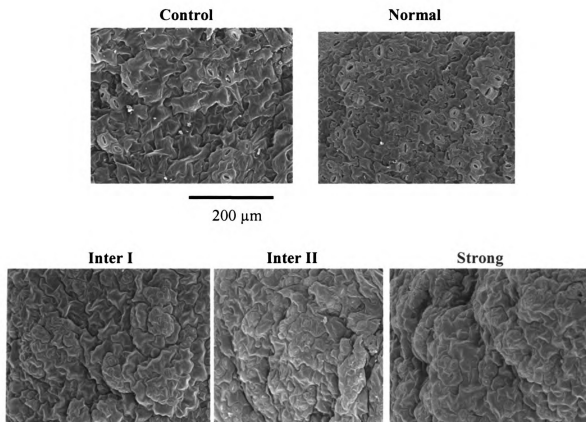


Figure 5.6: Abaxial side of cotyledons from T2 RNAi plants. Cotyledons were selected from 12-day-old plants grown on MS-Basta plates containing the control construct (Control), or construct D1235f3 showing different degree of cotyledon deformation (Normal, Inter I, Inter II and Strong). Samples were fixed in 4% glutaraldehyde, dehydrated in ethanol series and critical point dried using liquid carbon dioxide as the transitional fluid. After mounted on aluminum stubs using adhesive tabs, samples were coated with gold (20nm thick) and examined in a JEOL 6400V SEM.

for cotyledons that are deformed (Figure 5.7). The vascular tissue also seemed unaffected by the cotyledon phenotype (Figure 5.7). However, while the cells in control and normal cotyledons did not show any lack of adhesion between each other, the cells in deformed cotyledons displayed big gaps and were greatly detached from each other (Figure 5.7). Furthermore, the cells in deformed cotyledons are more rounded compared with cells from control or normal cotyledons (Figure 5.7). There seemed to be a correlation between the degree of abnormality of cell adhesion and cell shape and the degree of cotyledon deformation. However, a cause-and-effect relationship between them could not be established, although the distortion of epidermal cells visible in deformed cotyledons likely resulted from more airspace between cells.

D1235f3 transgenic plants showing deformed cotyledons have corresponding suppression of AtCslD gene transcripts

The levels of AtCslD transcripts were tested by RT-PCR reactions using gene specific primers (Figure 5.8). The initial efforts to detect the suppression of AtCslD expression used total RNA extracted from cauline leaves from D1235f3 T1 plants that had been germinated on plates and transferred to soil at 6 days old and grown for another 4 weeks. Among 58 D1235f3 T1 plants tested, 18 showed strongly deformed cotyledons. However only a few showed possible weak suppression of transcript levels for AtCslD3 (Figure 5.8A). The transcript abundance of a cytochrome C gene was used as a unrelated control, and that of AtCslE1 was used as a control to show that the expression of a AtCsl gene with low sequence identity with the RNAi construct was not suppressed (Figure 5.8).

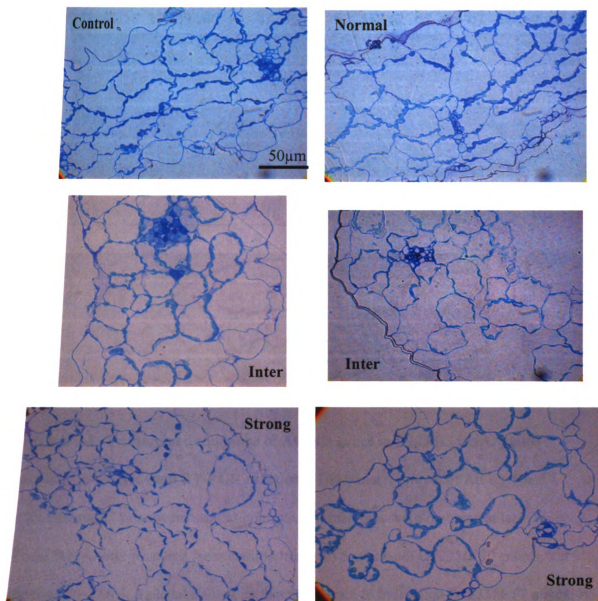


Figure 5.7: Cells within deformed cotyledons of D1235f3 plants showed less adherence. Cotyledons of T2 D1235f3 plants at 12 days old were fixed in 2.5% glutaraldehyde and 2% paraformaldehyde, infiltrated in Poly/Bed 812 resin and embedded in silicone molds, and sectioned. Sections were observed under light microscope after Toluidine Blue staining.

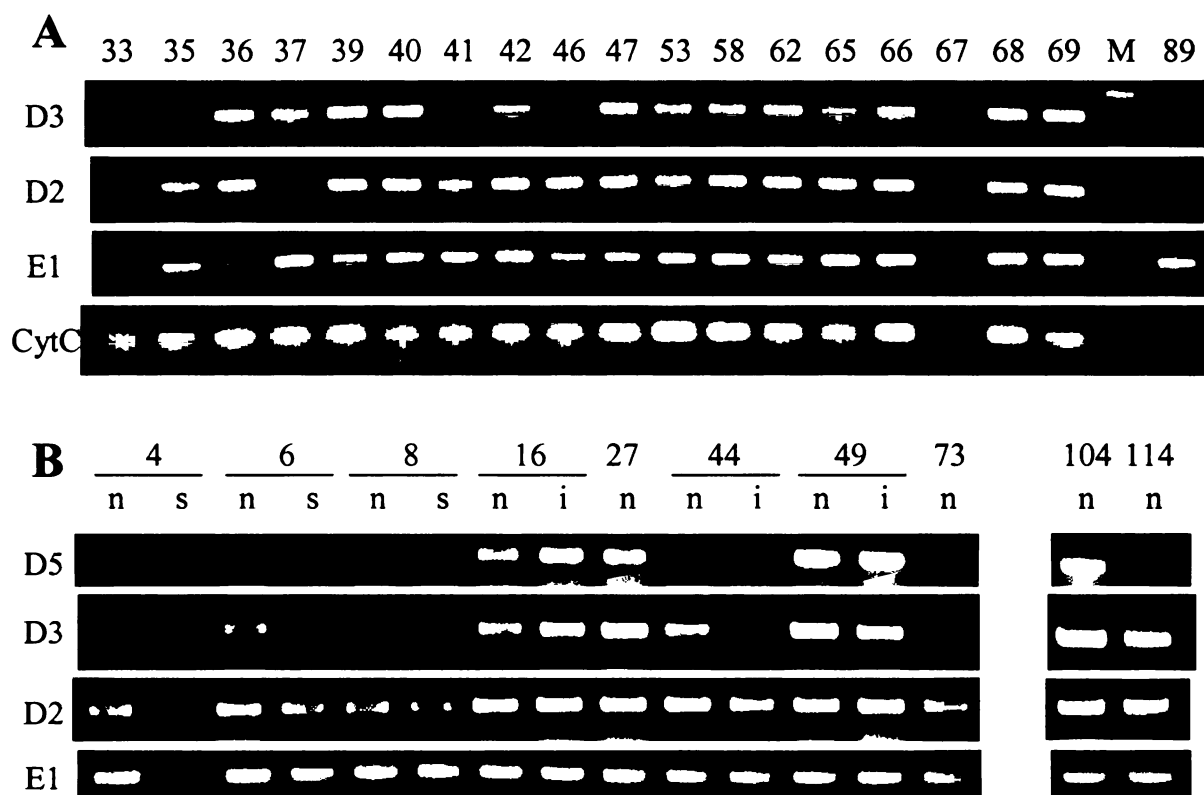


Figure 5.8: Transcript abundance of AtCslD genes in D1235f3 RNAi plants examined by two-step RT-PCR reactions. The transcript level of AtCslE1 and a cytochrome C gene were used as controls. All reactions were repeated at least twice. **A.** Total RNA was prepared from cauline leaves of 5-week-old D1235f3 T1 plants. “M” represents DNA molecular markers. Numbers refer to individual D1235f3 T1 plants. **B.** Total RNA was prepared from pooled cotyledons of 12-day-old T2 siblings showing similar cotyledon phenotypes on MS plates. Numbers refer to their T1 parent plants. “n”, “ii” and “s” represent pooled T2 siblings showing “normal”, “intermediate” and “strong” cotyledon deformations. In the T1 generation, plants No. 4, 6 and 8 showed strongly deformed cotyledons, No. 16, 44 and 49 showed intermediate cotyledon deformation, while No. 27 and 73 had normal cotyledons. Plant No. 104 and 114 are control lines.

The expression of the cytochrome C gene and AtCslE1 were found to be similar in all T1 plants tested (data not shown and Figure 5.8).

Because the suppression of AtCslD genes was not always found in adult T1 plants (Figure 5.8A), I reasoned that the molecular phenotype could be absent in tissues that had normal morphology. Therefore, the expression of AtCslD genes was examined in the cotyledons where the morphological phenotype was present. Total RNA was extracted from cotyledons of 12-day-old plate-grown T2 plants. Cotyledons from 10 to 15 T2 plants showing similar cotyledon deformation phenotype and coming from the same parent plant were pooled together. In this case, both AtCslD3 and D5 were suppressed in strongly deformed cotyledons (Figure 5.8B). Other AtCslD genes did not show any suppression of their expressions. In summary the suppression of target transcripts could be detected in deformed cotyledons but not in normal cotyledons or cauline leaves.

The sequence of RNAi construct D1235f3 was based on AtCslD3. It showed the highest identity of 87.8% with D2 among all AtCslD genes (Figure 5.2B). However the messenger suppression of AtCslD2 was not detected for all cotyledon-deformation-strong lines tested (Figure 5.8). On the other hand, AtCslD5 shows the second highest identity with D1235f3 of 83.2% and the maximum length of the uninterrupted sequence match between them is 26 bp, which is longer than the 24 bp shown between construct D1235f3 and AtCslD2 (Figure 5.2B). Since AtCslD5 was clearly suppressed in the strong cotyledon lines that also had AtCslD3 suppression, it seemed like uninterrupted sequence match is more important than the overall sequence match. This result makes sense considering the siRNA are usual 21-25 bp long.

D1235f3 transgenic plants showing deformed cotyledons also produced dwarfed adult plants and shortened roots with more branching

It was observed that T1 plants containing RNAi construct D1235f3 have shorter roots compared to T1 plants containing other constructs or control construct containing only the spacer fragment (Figure 5.9). When grown side by side on vertical plates, the average root length of D1235f3 T1 plants was significantly less than control plants (Figure 5.9).

When the root length was compared among D1235f3 T1 plants with different degrees of cotyledon deformation, it was found that those plants showing strong cotyledon deformation had the shortest roots and the plants showing normal cotyledons had the longest roots (Figure 5.10). Thus, reduced root elongation seemed to be correlated with cotyledon deformation.

Plants with strong cotyledon deformation not only showed root shortening, but also showed more root branching (Figure 5.11). Among D1235f3 T1 plants having strongly deformed cotyledons, 54.5% showed root branching. Among D1235f3 T1 plants showing normal cotyledons, only 23.9% had root branching. Taken together, 37% of D1235f3 T1 plants showed some root branching. The root branching observed in control lines and other RNAi lines was always less than 10%. However, the presence of this root branching phenotype did not match exactly the cotyledon deformation or root shortening phenotypes. The cotyledon normal D1235f3 T1 plants did not show root shortening (Figure 5.9, 5.10) compared with control plants, but still showed the root branching phenotype, although to a lesser degree than the plants with strongly deformed cotyledons (Figure 5.11). Therefore, the root branching seems to be affected more easily by the

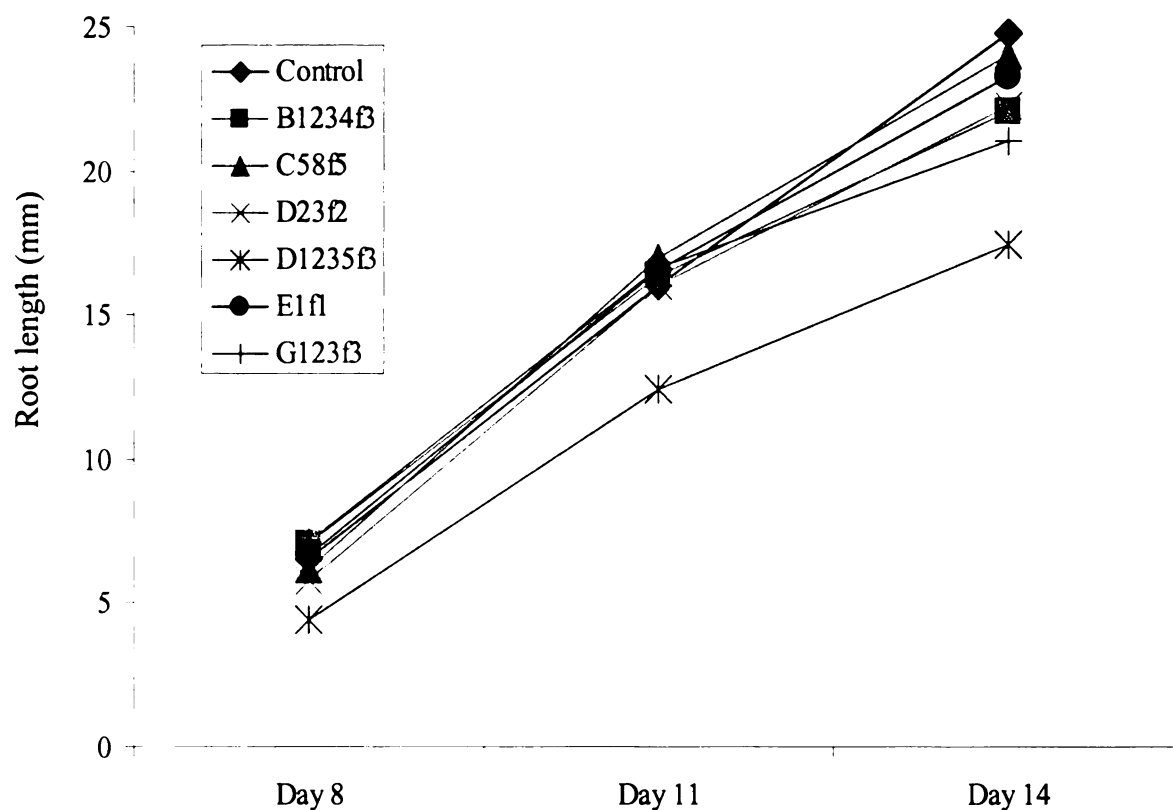


Figure 5.9: Root length of T1 transgenic plants containing RNAi constructs Control, B123456f3, C58f5, D23f2, D1235f3, E1f1 and G123f3. T1 seeds were screened on MS plates containing 10 $\mu\text{g/ml}$ Basta and 500 $\mu\text{g/ml}$ Carbenicillin. Basta-positive plants were transferred to new plates at 5 days old and grown vertically. Root length were recorded at the time points indicated. The numbers are averages of 75 T1 plants for construct D23f2, 100 T1 plants for construct D1235f3, and 50 T1 plants for each other construct.

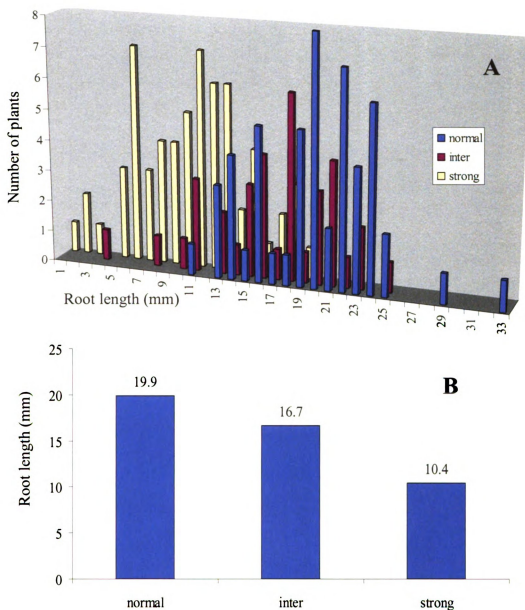
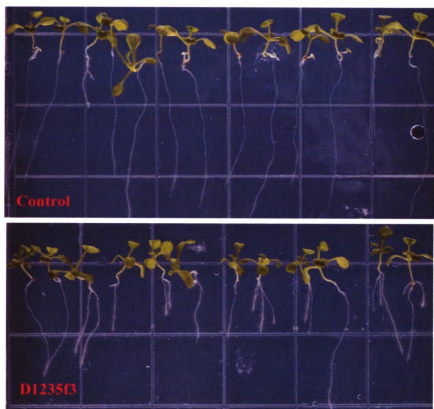
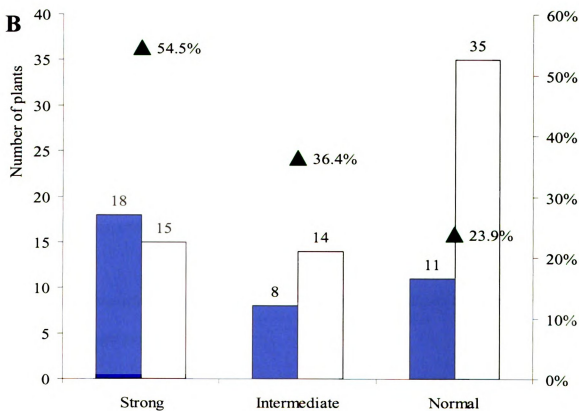


Figure 5.10: Root length of T1 plants containing construct D1235f3. 149 Basta resistant T1 plants were picked from screening plates and transferred to vertical plates at 5 days old. These plants were grouped as “normal”, “inter” and “strong” according to the degree of their cotyledon deformation. Root length was measured at age 14 days. **A.** Numbers of plants that have a specific root length for plant groups “normal”, “inter” and “strong”. **B.** Average root length for D1235f3 T1 plants showing normal, intermediate and strong deformed cotyledons.

Figure 5.11: T1 plants containing construct D1235f3 showing deformed cotyledons also showed more branched roots. About 100 positive transgenic D1235f3 RNAi lines screened from MS plate with antibiotics were picked and transferred at day 6 to new plates for vertical growth. Cotyledon deformation and root branching were recorded at day 14. **A.** T1 plants containing the control or D1235f3 RNAi construct on vertical MS plates at 14 days old. **B.** Numbers of D1235f3 T1 plants showing deformed cotyledons and branching or non-branching roots. Filled bars represent the numbers of plants showing branched roots, unfilled bars are the numbers of plants show unbranched roots. Filled triangles are percentages of plants showing branched roots among the plants in each category of cotyledon deformation.

A**B**

presence of RNAi construct D1235f3 than other processes such as cotyledon development or root elongation. The mechanism behind this observation could not be established from these experiments.

Plant development also was altered by the presence of RNAi construct D1235f3. The T1 plants showing strong cotyledon deformation were also smaller in overall size and shorter in plant height (Figure 5.12). At six weeks of age, the D1235f3 T1 plants showed a very good correlation between their overall size and the cotyledon deformation phenotypes recorded at day 6. Plants with more severely deformed cotyledons were smaller in size at age 6 weeks (Figure 5.12). It was also noted that D1235f3 T1 plants with strong cotyledon deformation and small overall size yielded fewer seeds (data not shown).

T2 plants with strong cotyledon deformation phenotypes also showed dwarfed adult plants as with the T1 parent plants (Figure 5.13). Twenty T2 plants from a T1 plant with strong cotyledon deformation were picked up and transferred to soil. Ten of them showed strong cotyledon deformation and the other ten showed normal cotyledons. At six weeks, the seedlings with strong cotyledon deformation were much smaller than those with normal cotyledons (Figure 5.13).

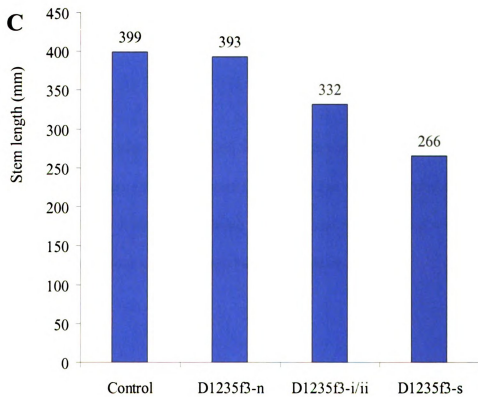
Despite the phenotypes observed for roots and whole seedlings, we have not yet looked at the suppression of AtCslD transcripts in either roots or bolting hypocotyls.

Cotyledon deformation is inheritable for D1235f3 transgenic plants but weakens when passed to the next generation

Figure 5.12: D1235f3 T1 plants had deformed cotyledons also yielded dwarfed adult plants. **A.** Typical 6-week-old D1235f3 T1 plants with different degrees of cotyledon deformation. Plants were germinated on MS plates with antibiotics and transferred to soil at 14 days old. **B.** Cotyledon deformation phenotype of plants shown in A. “s”, “ii”, “i” and “n” represent cotyledon deformation phenotype of strong, intermediate II, intermediate I and normal. **C.** Stem length of mature plants. About 50 Control and 100 D1235f3 T1 plants were selected from MS screening plates at 14 days old and transferred to soil. Stem length was measured when plants matured, but before seed collection. Plants were grouped according to their degree of cotyledon deformation as recorded at 6 days old on screening plates. Numbers shown are the averages.

A**B**

s	s	s	s
ii	ii	ii	ii
n	i	i	i
n	n	n	n



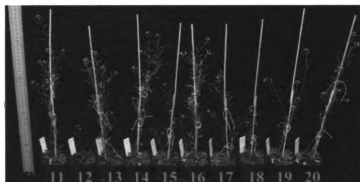


Figure 5.13: Adult T2 plants containing RNAi construct D1235f3 at 6 weeks. All plants were derived from a single T1 plant D1235f3-4 that showed strong cotyledon deformation. Seedlings 1-10 showed strong cotyledon deformation, and seedlings 11-20 showed normal cotyledons when observed at 6 days old on MS plate.

D1235f3 T1 plants with different degrees of cotyledon deformation were selfed to monitor the inheritance of cotyledon deformation phenotype. From a typical T1 screening experiment for plants containing construct D1235f3, 118 antibiotic resistant T1 plants were selected. Approximately 50 T2 seeds derived from each of the 12 strong, 14 intermediate ii, 16 intermediate i, and 19 normal cotyledon T1 plants were germinated the same way as for T1 seeds. When the cotyledons of these T2 plants were examined, all of the offspring from the parents with strong or intermediate cotyledon deformation showed phenotype segregation or phenotype disappearance (Table 5.4). Out of the 12 strong T1 lines, T2 progenies from 4 of them showed strong, intermediate, and normal cotyledons in different siblings (Table 5.4); T2 progenies from 6 other T1 lines showed only intermediate and normal cotyledons, while the 2 other T1 lines totally lost the cotyledon deformation phenotype at the T2 generation (Table 5.4). Similar phenotype weakening and segregation was also observed for those 20 intermediate cotyledon T1 lines (Table 5.4). At the same time, T1 plants that did not show any cotyledon deformation did not show any deformation in their progenies (Table 5.4). Therefore the cotyledon deformation phenotype can be passed to the next generation together with the antibiotic markers, but the phenotype weakens and segregates.

In order to determine the number of transgenes inserted in D1235f3 T1 plants and to find out if the inheritance of cotyledon deformation phenotype follows Mendelian genetics, the numbers of T2 progenies that are Basta resistant (alive on screening plates) or sensitive (died right after germination on screening plates) were recorded for individual T1 parents (Table 5.5). Surprisingly, the ratios of Basta resistant to Basta sensitive plants were always high among T2 progenies coming from parents with strong

Table 5.4: Summary of the inheritance of cotyledon deformation phenotype from T1 to T2 generation for D1235f3 RNAi lines. The cotyledon deformation phenotypes of T2 offspring from 12 strong, 15 intermediate and 10 normal T1 lines were tested.

T1 cotyledon phenotype	Number of T1 plants tested	Number of T1 plants whose T2 offsprings showed cotyledon phenotype as:		
		s, i, or n	i, or n	n
s	12	4	6	2
ii	14		12	2
i	16		8	8
n	19			19

Table 5.5: Inheritance and segregation of cotyledon deformation phenotype and Basta resistance marker for D1235f3 RNAi plants. T1 plants were selected from an antibiotic screening plate and their cotyledon deformation phenotype were recorded at 6 days old. T2 seeds from each T1 plant were germinated on MS plates the same way as for T1 plants. T2 plants with different cotyledon phenotype were counted. Seeds that died short after germination were counted as dead plants (as in Figure 5.3B).

T1 plants			T2 plants				
plant no.	cotyledon	n	i	s	died	alive/dead	
3	s	10	3	0	2	13/2	
4	s	39	20	27	3	86/3	
5	s	55	2	0	2	57/2	
6	s	13	10	13	0	36/0	
8	s	38	0	19	2	57/2	
9	s	39	0	0	0	39/0	
10	s	45	0	0	2	45/2	
11	s	37	1	0	0	38/0	
12	s	4	10	0	1	14/1	
13	s	41	3	0	0	44/0	
14	s	18	24	0	3	42/3	
16	s	10	14	4	14	28/14	
18	ii	13	16	0	9	29/9	
19	ii	13	5	0	1	18/1	
21	ii	41	6	0	11	47/11	
22	ii	22	2	0	1	24/1	
23	ii	2	22	0	6	24/6	
26	ii	18	7	0	1	25/1	
27	ii	13	8	0	9	21/9	
28	ii	21	15	0	2	36/2	
29	ii	6	14	0	4	20/4	
30	ii	26	0	0	12	26/12	
31	ii	23	9	0	9	32/9	
32	ii	18	12	0	2	30/2	
33	ii	36	4	0	0	40/0	
34	ii	43	0	0	0	43/0	
2	i	35	10	0	6	45/6	
39	i	20	5	0	9	25/9	
40	i	9	16	0	3	25/3	
41	i	17	0	0	9	17/9	
42	i	44	0	0	2	44/2	
43	i	33	0	0	8	33/8	
44	i	20	12	0	13	32/13	
45	i	31	0	0	8	31/8	
46	i	11	21	0	9	32/9	
47	i	38	0	0	2	38/2	
48	i	55	0	0	3	55/3	
49	i	19	22	0	0	41/0	
50	i	19	16	0	12	35/12	
51	i	18	0	0	10	18/10	
52	i	7	0	0	25	7/25	
54	i	24	13	0	0	37/0	
60	n	14	0	0	4	14/4	
61	n	30	0	0	10	30/10	
62	n	12	0	0	5	12/5	
63	n	17	0	0	3	17/3	
64	n	15	0	0	6	15/6	
65	n	27	0	0	5	27/5	
66	n	31	0	0	11	31/11	

cotyledon deformation (Table 5.5). On the other hand, the ratios of Basta resistant to sensitive T2 siblings from parents with normal cotyledons were significantly lower and much closer to the 3:1 ratio expected for a single gene inheritance (Table 5.5). It seemed like the presence of multiple copies of RNAi construct is necessary to maintain the cotyledon deformation phenotype, or in other words, to maintain a RNAi effect.

In order to determine if the cotyledon deformation phenotype can be inherited past two generations, more than 50 independent T1 D1235f3 plants showing strong cotyledon deformations were self-fertilized until the T4 generation. Overall the number of plants with deformed cotyledons decreased from generation to generation but still followed the rule that only parents with strong cotyledon deformation produced offspring with the strong phenotype. The offspring from most of the lines with strong cotyledon deformation at the T1 generation completely lost the cotyledon phenotype by the T4 generation. Only a few plants with strong cotyledon deformation at the T1 generation kept the same phenotype until the T4 generation. T1 plants 4 and 8, that showed strong transcripts suppression of AtCslD3 and D5 (Figure 5.8), are two that still displayed this phenotype in the T4 generation.

To see if a phenotypically stable transgenic RNAi line with a single transgene insert could be identified, T1 seeds from different transformation experiments were screened again and again. During one of the last screening experiments for D1235f3 T1 plants, 12 T1 lines showed strongly deformed cotyledons. When these 12 lines were passed to the T2 generation, one of them, number 94, not only showed perfect 3:1 ratio between Basta resistant and sensitive siblings, but also showed strongly deformed cotyledons in all the T2 offspring with Basta resistance. This seemed a rare event

considering the numbers of T1 plants that have been tested. This particular line is still being tested for the inheritance of the cotyledon deformation phenotype and the transgene segregation. One possible explanation for this particular T1 line is that a single D1235f3 RNAi construct was inserted into a transcriptional hot spot and therefore the dsRNA transcript level was high enough to induce the RNAi effect, which in many of the other lines was induced by the transcription of multiple copies of the inserts in the genome.

D1235f3 RNAi transgenic plants did not show clear alteration in cell wall sugar composition

To see if the monosaccharide content of the wall materials from D1235f3 lines have been altered, cell wall material was prepared and analyzed for sugar content. The alditol acetate forms of sugars were examined by gas chromatography. When the wall materials were prepared from rosette leaves of different T1 D1235f3 plants, none of the monosaccharide content was significantly different from controls (Figure 5.14).

Four strong T1 lines, whose offspring at T4 generation still showed some cotyledon deformation, were selected for cell wall monosaccharide analysis. Young seedlings of 12 days old from T2 siblings of these 4 lines were pooled together for preparation of cell wall material. The sugar composition of these cell walls is shown in Figure 5.15. Although the glucose content of the seedlings with strong cotyledon deformation was always less than that with normal cotyledons (Figure 5.15A), the numbers are not statistically significant (Figure 5.15B). Besides, the glucose content is the most difficult to compare due to its widespread presence in various macromolecules and the contribution from residual starch (Figure 5.15).

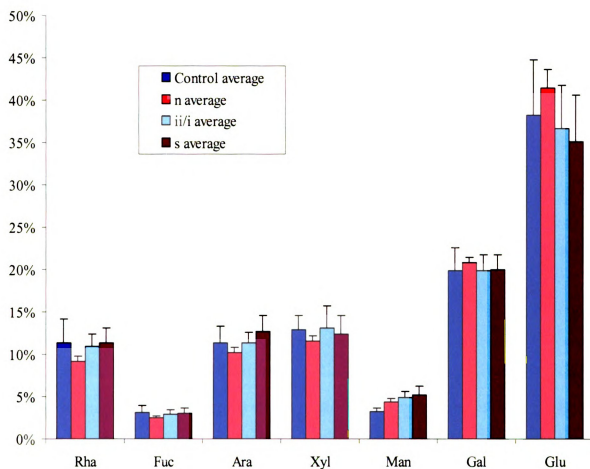
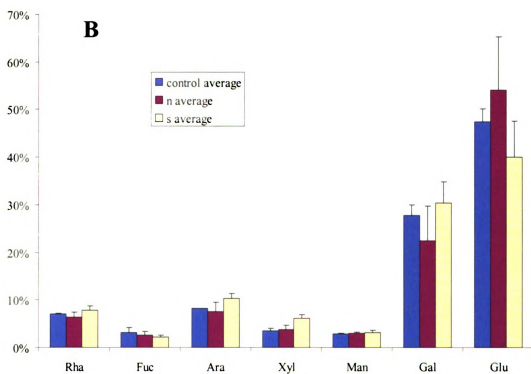
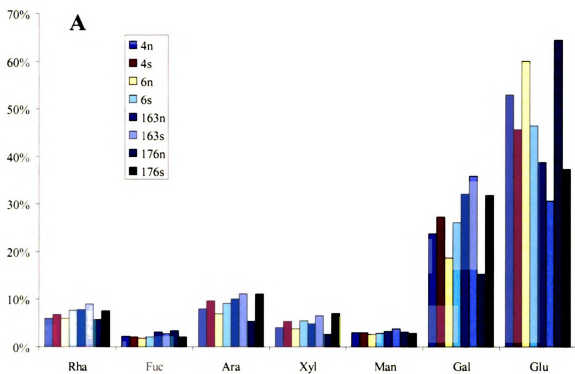


Figure 5.14: Cell wall sugar composition of rosette leaves from T1 D1235f3 plants showing different cotyledon deformation. All plants were from the same screening plate. Samples included 4 Control, 5 cotyledon normal, 8 intermediate, and 15 strong lines. Bars represent average values for each cotyledon category with standard deviation. Cell wall preparation, treatment, and measurement of the sugar composition were described in Materials and Methods.

Figure 5.15: Sugar composition analysis for T2 plants of D1235f3 RNAi lines. Walls were prepared from 5 to 10 T2 sibling plants at 12 days old that showed the same strong (s) or normal (n) cotyledon phenotype. T1 lines 4, 6, 163, and 176 showed strong cotyledon deformation. Control includes two lines of plants containing spacer loop only construct. They are processed the same way as for D1235f3 plants. **A.** Relative sugar contents of individual lines. **B.** Average sugar contents for seedlings from **A** that showed strong (s) or normal (n) cotyledon phenotypes. Standard deviations are included.



Due to the limitation on tissue availability, wall material fractionation was not feasible and therefore I could not determine whether the amount of any particular polysaccharide was altered by the introduction of the RNAi construct.

DISCUSSION

RNAi methodology was used to generate transgenic *Arabidopsis* plants with decreased expression of AtCslD genes, trying to shed some lights on the biochemical functions of AtCslD proteins. A couple of interesting observations were made for the RNAi plants that contain construct D1235f3 and showed suppression of AtCslD3 and AtCslD5 expressions. These include deformed cotyledons and weakened cell cell adhesion within cotyledons, shortened roots with more branches, and dwarfed adult plants. These morphological alterations resulted from the presence of the RNAi construct indicating that AtCslD proteins have an important function during plant growth and development.

However, no biochemical function could be proposed for the AtCslD proteins because the cell wall sugar composition analysis did not reveal significant difference. Cell wall monosaccharide composition analysis has been successfully used during mutant plant characterization to connect the function of a gene with the altered content of a specific sugar in the wall, and in turn suggesting possible biochemical functions for the protein encoded by the particular gene (Bouton et al., 2002; Iwai et al., 2002; Vanzin et al., 2002; Madson et al., 2003). In our case, the monosaccharide composition assay was made more difficult by the fact that glucose is the sugar most likely to be affected by the presence of RNAi constructs targeting AtCslD genes. AtCslD genes have fairly high degree of identity with AtCesA proteins at 39% to 46% (Table 3.3). They also share very similar protein structure with common protein motifs and similar transmembrane domain organizations (Chapter 3). Therefore AtCslD proteins might have very similar enzymatic mechanisms with AtCesA proteins, i.e. using UDP-glucose as substrate and incorporate

β -linked glucans. Glucose however has been notoriously difficult to measure among cell wall monosaccharides because of its widespread presence among different wall polysaccharides. Glucose could also be obtained during wall material preparation as contaminant from other molecules, such as starch. One way to circumvent the problem imposed by analyzing wall glucose content is to analyze the amount of major wall polysaccharides directly. A decrease of a certain polysaccharide or a certain sugar moiety within a particular polysaccharide would provide hints for the biochemical functions of the proteins encoded by the suppressed gene(s). However, limited tissue availability has prevented this approach because a stable transgenic line with a strong phenotype was not yet established.

The RNAi methodology was still in its infancy when I started the work described in this chapter. My data obtained using this technology also revealed some questions regarding how the RNAi method works in plants, especially the maintenance and inheritance of the phenotypes induced by RNAi constructs.

Suppressed expression of multiple genes seems necessary to obtain a visible phenotype when the gene in question is part of a family and other family members supply redundant functions. This seems to be true for the families within AtCsl super family. One piece of evidence comes from the observation that single knock-out mutants of AtCslC4, AtCslG1 and AtCslB5 did not show any visible phenotypes or detectable cell wall sugar composition alteration (Richmond and Somerville, 2001). Functional gene redundancy might also play a role when using the RNAi approach to suppress gene expressions. In my study the tissue deformation phenotype was only observed for the cotyledons where both AtCslD3 and AtCslD5 were suppressed. For other tissues that did

not show deformation phenotype it was likely that the suppression of multiple AtCslD genes did not happen. That was certainly the case for the cauline leaves.

Suppression of AtCslD genes other than D3 and D5 was not detected, which might be the reason that no more profound phenotype was observed for the RNAi plants. This could be caused by the overall low sequence identities shared by the construct D1235f3 with other D members, or because there are not enough sufficiently long uninterrupted stretches of identity. As indicated in Figure 5.2B, AtCslD5 shares the highest uninterrupted sequence identity of 26 bp with construct D1235f3, and none of the other AtCslD members showed uninterrupted sequence identity of more than 24 bp with the construct D1235f3.

The root hair disappearance phenotype presented by the AtCslD3 mutant *kojak* was not observed in any RNAi plants, even with the RNAi construct D235f3 that is immediately targeting the same gene. One possible explanation is that the RNAi approach does not completely suppress the expression of a gene whereas many conventional mutants are complete nulls. Another possible explanation is that the promoter used for the RNAi approach does not provide sufficiently high expression in root hair cells to express the null phenotype in these cells.

Another possibility for not seeing more severe phenotypes could be that when more complete suppression of multiple AtCslD genes occurred, it led to lethality to the transgenic plants that died during the screening. Indeed, some of the transgenic plants containing the RNAi construct D1235f3 showed deformed true leaves but died on screening plates shortly after the appearance of the true leaves.

The major phenotype for RNAi plants containing construct D1235f3, cotyledon deformation, was identified as a series from weak to strong. The presence of T1 plants with different degrees of phenotype was also observed in other cases using RNAi approach and was regarded as one of the unique features and advantages for this approach. Almost all T1 plants with strong phenotype had multiple transgene insertions revealed by the fact that the segregation ratios for the antibiotic marker are much higher than 3:1. In contrast, T1 plants without a phenotype showed ratios much closer to 3:1. It seems that multiple copies of transgenes are needed to maintain the phenotype caused by the RNAi construct, or in fact a concentration threshold of the RNAi construct transcript has to be reached in order to induce a RNAi effect. The cotyledon deformation phenotype was inherited up to the T4 generation but kept weakening and segregating. A possible explanation for this is that the segregation of inserts diluted the concentration of the dsRNA transcribed from the RNAi construct from generation to generation, and therefore a weaker and weaker RNAi effect was observed. When the concentration of dsRNA transcripts becomes below the concentration threshold, the phenotypes caused by the RNAi effect disappeared. The phenotype drifting and weakening or even reversion sometimes for the RNAi approach has also been noticed by other groups as well (Dr. Jen Sheen, Dr. Jiankang Zhu, personal communications).

Among those cases where the RNAi approach has been successfully used in plants to study gene function (Chuang and Meyerowitz, 2000; Smith et al., 2000; Escobar et al., 2001; Wesley et al., 2001; Klahre et al., 2002; Stoutjesdijk et al., 2002), only two of them provided more detailed descriptions of the most important features of RNAi approach in plants, namely the appearance of phenotypes, the suppression of target

transcripts and the inheritance of phenotypes (Chuang and Meyerowitz, 2000; Stoutjesdijk et al., 2002). Chuang and Meyerowitz (2000) used RNAi constructs to reproduce the knock out phenotypes for four genes that are involved in flower development. The same phenotypes as with knock out mutants were recorded but in a series from weak to strong as observed for the cotyledon deformation phenotype in my case. In situ hybridizations indicated correlated transcripts suppression levels with phenotypes. However 100% suppression of transcripts was not achieved as seen from the weak in situ hybridization signals shown in strong lines.

Stoutjesdijk et al (2002) used RNAi constructs to successfully suppress the expression of the FAD2 Δ 12-desaturase gene in Arabidopsis seeds. Suppression of target transcripts was not examined but the oleic desaturation proportion (ODP) controlled mainly by the enzyme encoded by this gene was examined to monitor the RNAi effect. This molecular phenotype also covered a gradient from weak to strong in the T1 generation. It was found that a couple of T1 lines with the most severe phenotypes all contained multiple transgene insertions revealed by DNA blottings. Similar phenomena was observed in my study as well as described earlier.

In both cases, the phenotype segregation in T2 and possibly later generations was not addressed in detail. However, at least one “good” line was identified to have just a single transgene insert and the phenotypes were stably inherited to at least T2 (Chuang and Meyerowitz, 2000) and T5 (Stoutjesdijk et al., 2002) generations. However, they did not report how many T1 lines needed to be screened to find a “good” line. It was possible that those a few “good” T1 lines are rare events that had the transgenes inserted into transcriptional super active regions of the genome and therefore could produce high

concentrations of dsRNAs that in other T1 lines needed multiple transgene insertions to obtain, to induce the RNAi effect. Toward the end of my studies one such “good” line was identified after monitoring the inheritance of more than 100 T1 lines with strong cotyledon deformation phenotype. This particular line showed a perfect 3:1 ratio for the selection marker and all of its T2 offspring showed the same strong phenotype. This particular line, once established, could be very useful for analyzing the proportions of cell wall polysaccharides. If this data could be obtained, it might provide a specific hypothesis regarding the biochemical functions of AtCslD proteins.

The study described in this chapter began when the mechanism of RNAi approach was still not well understood. Consequently, the strategies needed to consistently suppress gene expression were not well understood. Given the results described in this chapter and the new knowledge about the RNAi approach, if someone were to start over again, a couple of modifications should be made to more successfully suppress the expression of AtCslD genes. First, the intron containing RNAi vector, pHANNIBAL should be used instead of the homemade vector containing a GUS fragment as loop region. Intron containing RNAi constructs generally produce 90% to 100% of independent transgenic plants showing the silencing effect, while RNAi constructs with other DNA fragment as the loop region are only about 60% effective (Smith et al., 2000; Wesley et al., 2001). Second, the DNA fragment selected from AtCslD3 for the RNAi construct should not only have high overall sequence identity, but also should have long uninterrupted regions of sequence identity. Third, after identifying the major visible phenotype for the transgenic plants containing the corresponding RNAi construct, the

first priority should be selecting some stable lines with a single transgene insert and put all efforts of phenotype characterizations on those lines.

Another alternative for pursuing a reverse genetic approach to identify AtCslD functions would be to utilize the traditional knock out mutants. Stable knock out mutant plants will make detailed cell wall polysaccharide and sugar composition analyses possible. If gene redundancy becomes a concern, mutant plants with multiple AtCslD genes knocked out can be generated by crossing the single knock out mutants, because the six AtCslD genes are located on five different chromosomes (Figure 3.2).

REFERENCES

- Arioli, T., Peng, L., Betzner, A. S., Burn, J., Wittke, W., Herth, W., Camilleri, C., Hofte, H., Plazinski, J. and Birch, R.** (1998). "Molecular analysis of cellulose biosynthesis in *Arabidopsis*." *Science* **279**: 717-720.
- Bernstein, E., Caudy, A. A., Hammond, S. M. and Hannon, G. J.** (2001). "Role for a bidentate ribonuclease in the initiation step of RNA interference." *Nature* **409**: 363-366.
- Billy, E., Brondani, V., Zhang, H., Muller, U. and Filipowicz, W.** (2001). "Specific interference with gene expression induced by long, double-stranded RNA in mouse embryonal teratocarcinoma cell lines." *Proc. Natl Acad. Sci. USA* **98**: 14428-14433.
- Blakeney, A. B., Harris, P. J., Henry, R. J. and Stone, B. A.** (1983). "A simple and rapid preparation of alditol acetates for monosaccharide analysis." *Carbohydr. Res.* **113**: 291-299.
- Bosher, J. M. and Labouesse, M.** (2000). "RNA interference: genetic wand and genetic watchdog." *Nat. Cell Biol.* **2**: E31-E36.
- Bouton, S., Leboeuf, E., Mouille, G., Leydecker, M.-T., Talbotec, J., Granier, F., Lahaye, M., Hofte, H. and Truong, H.-N.** (2002). "*QUASIMODO1* encodes a putative membrane-bound glycosyltransferase required for normal pectin synthesis and cell adhesion in *Arabidopsis*." *Plant Cell* **14**: 2577-2590.
- Burn, J., Hocart, C. H., Birch, R. J., Cork, A. C. and Williamson, R. E.** (2002). "Functional analysis of the cellulose synthase genes *CesA1*, *CesA2*, *CesA3* in *Arabidopsis*." *Plant Physiol.* **129**: 797-807.
- Chuang, C. H. and Meyerowitz, E. M.** (2000). "Specific and heritable genetic interference by double-stranded RNA in *Arabidopsis thaliana*." *Proc. Natl Acad. Sci. USA* **97**: 4985-4990.
- Clough, S. J. and Bent, A. F.** (1998). "Floral dip: a simplified method for *Agrobacterium*-mediated transformation of *Arabidopsis thaliana*." *Plant J.* **16** (6): 735-743.
- Delmer, D. P. and Stone, B. A.** (1988). "Biosynthesis of plant cell walls." *The Biochemistry of Plants*. J. Priess, New York, Academic Press Inc. **14**: 373-421.
- Desprez, T., Vernhettes, S., Fagard, M., Refregier, G., Desnos, T., Aletti, E., Py, N., Pelletier, S. and Hofte, H.** (2002). "Resistance against herbicide isoxaben and cellulose deficiency caused by distinct mutations in same cellulose synthase isoform CESA6." *Plant Physiol.* **128**: 482-490.

- Doblin, M. S., Melis, L. D., Newbigin, E., Bacic, A. and Read, S. M.** (2001). "Pollen tubes of *Nicotiana glauca* express two genes from different beta-glucan synthase families." *Plant Physiol.* **125**: 2040-2052.
- Escobar, M. A., Civerolo, E. L., Summerfelt, K. R. and Dandekar, A. M.** (2001). "RNAi-mediated oncogene silencing confers resistance to crown gall tumorigenesis." *Proc. Natl Acad. Sci. USA* **98** (23): 13437-13442.
- Fagard, M., Desnos, T., Desprez, T., Goubet, F., Refregier, G., Mouille, G., McCann, M., Rayon, C., Vernhettes, S. and Hofte, H.** (2000). "*PROCUSTE1* encodes a cellulose synthase required for normal cell elongation specifically in roots and dark-grown hypocotyls of *Arabidopsis*." *Plant Cell* **12**: 2409-2432.
- Favery, B., Ryan, E., Foreman, J., Linstead, P., Boudonck, K., Steer, M., Shaw, P. and Dolan, L.** (2001). "*KOJAK* encodes a cellulose synthase-like protein required for root hair cell morphogenesis in *Arabidopsis*." *Gene. Dev.* **15**: 79-89.
- Goubet, F., Misrahi, A., Park, S. K., Zhang, Z., Twell, D. and Dupree, P.** (2003). "AtCSLA7, a cellulose synthase-like putative glycosyltransferase, is important for pollen tube growth and embryogenesis in *Arabidopsis*." *Plant Physiol.* **131**: 547-557.
- Grishok, A., Pasquinelli, A. E., Conte, D., Li, N., Parrish, S., Ha, I., Baillie, D. L., Fire, A., Ruvkun, G. and Mello, C. C.** (2001). "Genes and mechanisms related to RNA interference regulate expression of the small temporal RNAs that control *C. elegans* developmental timing." *Cell* **106** (23-34).
- Hamilton, A., Voinnet, O., Chappell, L. and Baulcombe, D.** (2002). "Two classes of short interfering RNA in RNA silencing." *EMBO J.* **21**: 4671-4679.
- Hammond, S. M., Bernstein, E., Beach, D. and Hannon, G. J.** (2000). "An RNA-directed nuclease mediates post-transcriptional gene silencing in *Drosophila* cells." *Nature* **404**: 293-296.
- Hammond, S. M., Boettcher, S., Caudy, A. A., Kobayashi, R. and Hannon, G. J.** (2001). "Argonaute2, a link between genetic and biochemical analyses of RNAi." *Science* **293**: 1146-1150.
- Han, Y. and Grierson, D.** (2002). "Relationship between small antisense RNAs and aberrant RNAs associated with sense transgene mediated gene silencing in tomato." *Plant J.* **29** (4): 509-519.
- Helliwell, C. A., Wesley, S. V., Wielopolska, A. J. and Waterhouse, P. M.** (2002). "High throughput vectors for efficient gene silencing in plants." *Funct. Plant Biol.* **29**: 1217-1225.

- Hutvagner, G. and Zamore, P. D.** (2002). "A microRNA in a multiple-turnover RNAi enzyme complex." *Science* **297**: 2056-2060.
- Iwai, H., Masaoka, N., Ishii, T. and Satoh, S.** (2002). "A pectin glucuronyltransferase gene is essential for intercellular attachment in the plant meristem." *Proc. Natl Acad. Sci. USA* **99** (25): 16319-16324.
- Ketting, R. F., Fischer, S. E., Bernstein, E., Sijen, T., Hannon, G. J. and Plasterk, R. H.** (2001). "Dicer functions in RNA interference and in synthesis of small RNA involved in developmental timing in *C. elegans*." *Genes & Dev.* **15**: 2654-2659.
- Klahre, U., Crete, P., Leuenberger, S. A., Iglesias, V. A. and Meins, F. J.** (2002). "High molecular weight RNAs and small interfering RNAs induce systemic posttranscriptional gene silencing in plants." *Proc. Natl Acad. Sci. USA* **99** (18): 11981-11986.
- Madson, M., Dunand, C., Li, X., Verma, R., Vanzin, G. F., Caplan, J., Shoue, D. A., Carpita, N. C. and Reiter, W.-D.** (2003). "The MUR3 gene of Arabidopsis encodes a xyloglucan galactosyltransferase that is evolutionarily related to animal exostosins." *Plant Cell* **15**: 1662-1670.
- Martinez, J., Patkaniowska, A., Urlaub, H., Luhrmann, R. and Tuschl, T.** (2002). "Single-stranded antisense siRNAs guide target RNA cleavage in RNAi." *Cell* **110**: 563.
- Parrish, S., Fleenor, J., Xu, S., Mello, C. and Fire, A.** (2000). "Functional anatomy of a dsRNA trigger: differential requirement for the two trigger strands in RNA interference." *Mol. Cell* **6**: 1077-1087.
- Perrin, R. M., DeRocher, A. E., Bar-Peled, M., Zeng, W., Norambuena, L., Orellana, A., Raikhel, N. V. and Keegstra, K.** (1999). "Xyloglucan fucosyltransferase, an enzyme involved in plant cell wall biosynthesis." *Science* **284** (5422): 1976-1979.
- Reiter, W. D., Chapple, C. C. S. and Somerville, C. R.** (1993). "Altered growth and cell walls in a fucose-deficient mutant of *Arabidopsis*." *Science* **261**: 1032-1035.
- Richmond, T. A. and Somerville, C. R.** (2001). "Integrative approaches to determining Csl function." *Plant Mol. Biol.* **47**: 131-143.
- Scheible, W.-R., Eshed, R., Richmond, T. A., Delmer, D. and Somerville, C. R.** (2001). "Modifications of cellulose synthase confer resistance to isoxaben and thiazolidinone herbicides in Arabidopsis *Ixr1* mutants." *Proc. Natl Acad. Sci. USA* **98** (18): 10079-10084.
- Sharp, P. A.** (2001). "RNA interference - 2001." *Genes & Dev.* **15**: 485-490.

Smith, N. A., Singh, S. P., Wang, M. B., Stoutjesdijk, P. A., Green, A. G. and Waterhouse, P. M. (2000). "Total silencing by intron-spliced hairpin RNAs." *Nature* **407**: 319-320.

Stoutjesdijk, P. A., Singh, S. P., Liu, Q., Hurlstone, C. J., Waterhouse, P. M. and Green, A. G. (2002). "hpRNA-mediated targeting of the Arabidopsis FAD2 gene gives highly efficient and stable silencing." *Plant Physiol.* **129**: 1723-1731.

Tang, G., Reinhart, B. J., Bartel, D. P. and Zamore, P. D. (2003). "A biochemical framework for RNA silencing in plants." *Genes & Dev.* **17**: 49-63.

Taylor, N. G., Laurie, S. and Truner, S. R. (2000). "Multiple cellulose synthase catalytic subunits are required for cellulose synthesis in Arabidopsis." *Plant Cell* **12**: 2529-2539.

Taylor, N. G., Scheible, W.-R., Cutler, S., Somerville, C. R. and Turner, S. R. (1999). "The irregular xylem3 locus of Arabidopsis encodes a cellulose synthase required for secondary cell wall synthesis." *Plant Cell* **11**: 769-779.

Vanzin, G. F., Madson, M., Carpita, N. C., Raikhel, N. V., Keegstra, K. and Reiter, W. D. (2002). "The *mur2* mutant of Arabidopsis thaliana lacks fucosylated xyloglucan because of a lesion in fucosyltransferase AtFUT1." *Proc. Natl Acad. Sci. USA* **99** (5): 3340-3345.

Voinnet, O. (2003). "RNA silencing bridging the gaps in wheat extracts." *Trends Plant Sci.* **8** (7): 307-309.

Wang, X., Cnops, G., Vanderhaeghen, R., Block, S. D., Montagu, M. V. and Lijsebettens, M. V. (2001). "*AtCSLD3*, a cellulose synthase-like gene important for root hair growth in Arabidopsis." *Plant Physiol.* **126**: 575-586.

Waterhouse, P. M. and Helliwell, C. A. (2003). "Exploring plant genomes by RNA-induced gene silencing." *Nat. Rev. Genet.* **4**: 29-38.

Wesley, S. V., Helliwell, C. A., Smith, N. A., Wang, M. B., Rouse, D. T., Liu, Q., Gooding, P. S., Singh, S. P., Abbott, D., Stoutjesdijk, P. A., Robinson, S. P., Gleave, A. P., Green, A. G. and Waterhouse, P. M. (2001). "Construct design for efficient, effective and high throughput gene silencing in plants." *Plant J.* **27** (6): 581-590.

Zhong, R., Morrison III, W. H., Freshour, G. D., Hahn, M. G. and Ye, Z.-H. (2003). "Expression of a mutant form of cellulose synthase *AtCesA7* causes dominant negative effect on cellulose biosynthesis." *Plant Physiol.* **132**: 786-795.

Zhu, Y., Nam, J., Humara, J. M., Mysore, K. S., Lee, L. Y., Cao, H., Valentine, L., Li, J., Kaiser, A. D., Kopecky, A. L., Hwang, H. H., Bhattacharjee, S., Rao, P. K., Tzfira, T., Rajagopal, J., Yi, H., Veena, Yadav, B. S., Crane, Y. M., Lin, K., Larcher,

Y., Gelvin, M. J., Knue, M., Ramos, C., Zhao, X., Davis, S. J., Kim, S. I., Ranjith-Kumar, C. T., Choi, Y. J., Hallan, V. K., Chattopadhyay, S., Sui, X., Ziemienowicz, A., Matthysse, A. G., Citovsky, V., Hohn, B. and Gelvin, S. B. (2003). "Identification of Arabidopsis *rat* mutants." *Plant Physiol.* **132 (2): 494-505.**